TECHNISCHE UNIVERSITÄT MÜNCHEN

TUM School of Life Sciences

Comprehensive characterization of the beer and brewing metabolome

Stefan Alexander Pieczonka

Vollständiger Abdruck der von der TUM School of Life Sciences der Technischen Universität München zur Erlangung des akademischen Grades eines

Doktors der Naturwissenschaften (Dr. rer. nat.)

genehmigten Dissertation.

Vorsitzende: Prof. Dr. Corinna Dawid

Prüfende der Dissertation:

1. Prof. Dr. Michael Rychlik
2. Prof. Dr. Wilfried Schwab
3. Prof. Dr. Régis Gougeon (Université de Bourgogne, Dijon)

Die Dissertation wurde am 27.12.2021 bei der Technischen Universität München eingereicht und durch die TUM School of Life Sciences am 10.05.2022 angenommen.

This page intentionally left blank

To my beloved and missed mother,
To my family, to my friends.

Acknowledgments

Almost four years of scientific research have been brought together in this thesis. An enriching time comes to an end with this work. I was able to learn from many wonderful people. Mindsets that have shaped me professionally, but also in my personal and social thinking. Therefore, I am all the more pleased that I can continue to work on great, progressive projects in such a helpful, inspiring, exceptional scientific environment.

An environment that first had to be defined. My first and very special thanks shall reach my supervisors Prof. Dr. Michael Rychlik and Prof. Dr. Philippe Schmitt-Kopplin. Making possible the novel research project, which now resulted in this thesis, was by no means a self-evident and straightforward matter. Between funding and supervision, between student practical courses and laboratory work, between teaching involvement and publications, between chair and research unit, there were quite a few issues to weigh. But those who think they have to choose between fish and meat forget that surf-and-turf is an attractive option as well. Without wanting to overstretch the image, we were able to show that PhD-theses in modern society can also be supervised by two “PhD-fathers”. I am very grateful that you had the necessary confidence in me to apply the flexibility and tread this path together. A path that I hope has not put too much strain on your scientific and friendly collaboration. In all this, the excellent professional and personal assistance should not be lost. The door was open for any affairs, in every regard. Thank you for the delighted discussions and creative ideas over the years that have filled this research project with life. Thank you for the freedom you gave me in my research and the guiding hand under which I was allowed to live it out.

A big thank you to all of my colleagues in both teams without whom this project would not have been possible. Even though I had to do a balancing act between two locations, I was welcomed as an integral part of the group in both. Thank you very much for welcoming me so well and for always giving me a helping hand. In you, I had outstanding colleagues in scientific discourse and friends at the same time. Many thanks to Jenny Uhl, Martina Daubmeier, Dr. Stefan Asam, Astrid Bösl and Anja Brinckmann for their support in all administrative matters, the small help in everyday life and for always being available. I want to thank Dr. Marianna Lucio for introducing me to the world of multivariate statistical analysis and for the exhaustive/exhausting work together on models and graphics. Many thanks to Dr. Michael Witting, Dr. Daniel Hemmler, Michelle Berger and Liesa Salzer for the introduction and handling of R-programming and LC-MS data treatment. I also thank Dr. Silke Heinzmann, Philippe Diederich and Dr. Norbert Hertkorn for broadening my horizon of NMR analysis. Many thanks to Dr. Basem Kanawati for the introduction to the FT-ICR-MS technology and Philippe Diederich and Jenny Uhl for troubleshooting regarding measurement automatization at long measurement nights. I thank Brigitte Look for her tireless work in providing technical assistance in the laboratory

and all colleagues, especially Dr. Franco Moritz and Dr. Daniel Hemmler, for many delightful discussions. Many thanks also to my chair-colleagues who have accompanied and endured me, in part, since the beginning of my Bachelor's studies. Your help with any administrative and organizational tasks was already then and is still very much appreciated. Many thanks to all of you for the amazing working atmosphere in the offices.
Many thanks to the whole team for the great and exuberant "beer-sampling conventions". More than 500 beers in total, hard to imagine without your help. But also the one or other drink outside the highly scientific sampling was appreciated very much.

Unfortunately, not all the time could be characterized by such beautiful exuberance. My very special and heartfelt thanks go to all the great colleagues and wonderful people who supported me and had my back during what was and will probably be the hardest year of my life. A not self-evident and extensive consideration of my supervisors Prof. Michael Rychlik and Prof. Philippe Schmitt-Kopplin made it possible that I still could continue this work. My special and emotional thanks go to Martina Daubmeier and Jenny Uhl for their emotional support, open ears and supportive phone calls during this time. Thanks to Leopold Weidner, who relieved me of numerous responsibilities. Thanks to all.

Finally, I would like to thank my family, who - voluntary or not - had to endure some controversial scientific discussions. I thank my father for his dedication and pleasure in helping me find scientific contacts and his expert advice in the field of brewing science. Many thanks to my whole family for your unconditional support and love, even in difficult times. Many thanks to my friends who inimitably understood how to clear my mind and enjoy all the other beautiful things in life. Most heartfelt thanks to my beloved and missed mother, to whom I owe where my path has led me.

Abstract

Beer is one of the oldest beverages of our civilization. The history of brewing science has produced numerous avant-garde developments and discoveries. The economic, cultural and social relevance of beer and brewing science has endured to this day. As a beverage that has accompanied mankind for thousands of years, its safety, quality and (molecular) characteristics have continuously been of considerable interest. Especially with the ever-increasing scale and technical ramifications of food supply networks, the food production process is becoming more complex to guide and more vulnerable to fraud. Considering the quality control and inspection of foodstuff, approaches that integrate and evaluate numerous analytical data ('big data') are of increasing importance. One of the major fields of the analytical spectrum that addresses this challenge, and under whose aegis this work stands, is the comprehensive analysis and molecular characterization of the metabolome – known as metabolomics.

The basis of this work is the combination of complementary analytical approaches, with a focus on (ultra)high-resolution mass spectrometric techniques. It opens the possibility to make visible and decompose the molecular diversity of what characterizes a beer. Mass spectrometric methods, statistical and molecular network data analysis strategies were developed to utilize the unrivaled mass resolution and accuracy associated with high-field Fourier transform ion cyclotron mass spectrometry (FT-ICR-MS). The view into a comprehensive and holistic overall picture of beer's molecular composition and complexity has been integrated into the field of brewing science as a novelty. It was made possible to unravel numerous deep molecular profiles of different brewing raw materials and process parameters. By complementary liquid chromatography-coupled time of flight mass spectrometry (UPLC-ToF-MS), the FT-ICR-MS-based compositional information and networks were confirmed. The dimension of isomer separation and compound identification could be addressed. The potential of this methodology for basic research of the complex brewing process, process guidance and quality control is highlighted in this thesis.

The intrinsic metabolite signatures associated with the brewing styles of different beers were uncovered and visualized in van Krevelen diagrams and mass difference networks. Statistical data analysis (HCA, PCA, PLS) revealed the molecular similarities between beers of the same type of brewing, including molecular fingerprints of individual breweries. The diverse selection of the up-and-coming 'craft beers' finds its common ground in the cold hopping process and the previously hidden large number of the associated highly oxygenated hop compounds. Wheat beers derive their particular compositional characteristics from the eponymous raw material. A network of potential phytoanticipine secondary metabolites of wheat, namely benoxazinone derivatives, showed a molecular imprint specific for the wheat grain. Several compounds of this group, including hitherto unknowns, were identified in the beer matrix.

Based on the ability of FT-ICR-MS to comprehensively detect composition signatures, the complex Maillard reaction was tackled. Thousands of unambiguous molecular formulae were assigned to respective mass signals. The compositional space of Maillard reaction-derived compounds could be identified as one of the driving forces of beer's molecular diversity, leading to key compositional changes. The molecular signature of the reaction of amino compounds and carbonyls pervades over 2,800 (40%) of all resolved small molecules. Their shared systematic nature was made visible. Validated by an experimental Maillard reaction model system, the major typical compositional changes were investigated by mass difference network analysis. Molecular networking resulted in general reaction sequences that were assigned to successive Maillard intermediate phase reactions by shortest path analysis. These findings contribute to a better understanding of the complex molecular processes involved in the Maillard reaction and might be a starting point for potential process development and quality control in both the malting and brewing industry.

Against the background of the historical German Purity Law, the influence of corn and rice starch sources on the metabolic signature of the final beer product was investigated. Utilizing the holistic analytical approach, both polar and non-polar metabolites were traced back to the respective starch sources and set into relation by molecular networking. The few corn-specific compounds in beer described in the 1990s could be confirmed. Those secondary metabolites were embedded in molecular networks that offer a whole compositional signature of related molecules for the grain adjunct. Further potential analytical markers of the lipid compound class were described. Such a compositional pattern that indicates plant secondary metabolites was found accordingly also for rice as a starch source. Ultimately, the aspartic acid conjugate of N-β-D-glucopyronosyl-indol-3-acetic acid represents an identified potential marker for the hitherto unknown molecular signature of rice in beer. The majority of decisive compounds, screened in foodstuff, were already found in the corresponding raw materials and survive the entire brewing process.

These investigations built a deep base of knowledge about the beer's metabolome. The characteristic chemical profiles made it possible to describe and trace the nature of a 130-year-old historical beer. The beer, dated to the German Empire era, was recently found in northern Germany. Its chemical composition represents a unique source of brewing culture at the end of the 19th century when pioneer innovations laid the foundations for modern industrial brewing. Complementary analytical approaches, including comprehensive metabolite profiling by means of DI-FT-ICR-MS, LC-ToF-MS, and NMR, revealed its compositional profile and unprecedented good storage condition. By chemometric comparison with 400 modern brews, metabolite profiles and markers allowed to conclude a typical lager beer which was brewed according to the Bavarian Purity Law applicable at that time. It was subject to bottom-fermentation even though industrial production with accordant yeasts was still under early development. Further critical production steps of the brewing process could be recreated. Technological aspects of the brewing culture in the late 19th century like grain and wort processing left molecular imprints visible in the beer's metabolome. Both the efficient germ removal and optimization of

wort’s pH by lactic acidification were not yet established. An exhaustive filtration process enabled long-term storage without microbial spoilage. Lacking disrupting biochemical influences, the beer represents a unique source of decades of persistent chemical alterations in such a sealed mixture of organic complexity. Ravages of time lead to oxidative polyphenol sedimentation, an unknown diversity of oxidized hop bitter acid derivatives and concentrations of Maillard reaction markers like HMF and furfural far exceeding what previous brewing literature described.

Zusammenfassung

Bier ist eines der ältesten Getränke unserer Zivilisation. Die Geschichte seiner Erforschung hat zahlreiche avantgardistische Entdeckungen und Entwicklungen hervorgebracht. Der wirtschaftliche, soziale und kulturelle Wert des Bieres und der Brauforschung hat bis heute Bestand. Die Menschheit über tausende Jahre hinweg begleitend, sind seine Qualität und (molekulare) Charakteristik von entscheidender Bedeutung. Gerade mit dem stetig steigenden Maßstab der Lebensmittelproduktion und der Verflechtung von Versorgungsnetzwerken wird das Steuern der Lebensmittelproduktion immer komplexer und anfälliger für Betrugsversuche. Im Hinblick auf die Qualitätskontrolle von Lebensmitteln gewinnen Ansätze, die zahlreiche analytische Daten integrieren und auswerten (‘big data‘), zunehmend an Bedeutung. Eines der großen Felder des analytischen Spektrums, das diese Herausforderung angeht und unter dessen Stern diese Arbeit steht, ist die molekulare Charakterisierung und umfassende, holistische Analyse des Metaboloms – bekannt als Metabolomik.

Die Grundlage dieser Arbeit bildet die Kombination von komplementären analytischen Methoden, mit dem Fokus auf (ultra)hochauflösende massenspektrometrische Techniken. Sie ermöglicht es, die molekulare Vielfalt dessen, was das Bier ausmacht, sichtbar zu machen und zu beschreiben. Dabei wurden massenspektrometrische und statistische Methoden sowie Strategien zur Analyse molekularer Netzwerke entwickelt, um die Massenauflösung und -genauigkeit der Hochfeld-Fourier-Transformations-Ionenzyklotron-Massenspektrometrie (FT-ICR-MS) nutzbar zu machen. Der Blick auf ein erschöpfendes und holistisches Gesamtbild der molekularen Zusammensetzung und Komplexität wurde in dem Feld der Brauforschung etabliert. So war es möglich zahlreiche metabolische Profile verschiedener Braurohstoffe und -parameter aufzuklären und damit ihren Einfluss auf das Endprodukt. Durch komplementäre Flugzeit-Massenspektrometrie, gekoppelt mit Flüssigkeitschromatographie, (UPLC-ToF-MS) konnten die gefundenen FT-ICR-MS-basierten molekularen Netzwerke bestätigt werden, die Dimension der Isomerentrennung und der Strukturidentifizierung ergänzt werden. Das Potenzial dieser Methodik für die Grundlagenforschung des komplexen Brauprozesses, seiner Steuerung und Qualitätskontrolle konnte aufgezeigt werden.

Die intrinsische molekulare Signatur, die mit den Brauweisen verschiedener Biersorten einhergehen, konnte aufgedeckt und durch Visualisierung der Metabolomdaten in van Krevelen Diagrammen und Massendifferenznetzwerken sichtbar gemacht werden. Durch statistische Datenanalyse (HCA, PCA, OPLS) konnten die Gemeinsamkeiten der Biere gleicher Brauart herausgearbeitet werden, bis hin zu molekularen Fingerabdrücken einzelner Brauereien. Die Vielfalt der aufstrebenden ‘Craftbiere‘ findet im Kalthopfungsprozess und der bislang unentdeckten Vielzahl der damit einhergehenden hochoxigenierten Hopfenbestandteile ihre Gemeinsamkeit. Weizenbiere beziehen ihre besondere

molekulare Charakteristik von ihrem namensgebenden Rohstoff. Ein Netzwerk aus potentiellen Sekundärmetaboliten des Weizens (Phytoanticipine), namentlich Benzoxazinon-Derivate, zeigte sich als charakteristisch. Einige dieser Verbindungen, einschließlich bislang unbekannten, konnten in der Biermatrix identifiziert werden.

Basierend auf der Eigenschaft der FT-ICR-MS, Signaturen von molekularen Zusammensetzungen umfassend zu detektieren, wurde die komplexe Maillard-Reaktion untersucht. Tausenden Massensignalen konnten eindeutige Summenformeln zugeordnet werden. Die Maillard-Reaktion, die zu bedeutenden Veränderungen der molekularen Zusammensetzung des Bieres führt, konnten als treibende Kraft für die molekulare Diversität des Bieres herausgestellt werden. Die systematische Natur dieser Reaktionsprodukte, deren spezifische Signatur über 2.800 (40%) aller kleinen Moleküle des Bieres einschließen, wurde sichtbar gemacht. Durch ein experimentelles Maillard-Reaktions-Model validiert, wurden die wesentlichen Änderungen in der molekularen Zusammensetzung analysiert. Molekulare Netzwerke zeigten allgemeine Reaktionssequenzen auf, die durch die Bestimmung der kürzesten Pfade in aufeinanderfolgende Reaktionen der Maillard-Zwischenphase zugeordnet wurden. Diese Erkenntnisse tragen zu einem besseren Verständnis der komplexen molekularen Prozesse bei, die an der Maillard-Reaktion beteiligt sind. Sie sind ein potenzieller Ausgangspunkt für eine Weiterentwicklung von Prozessschritten und Qualitätskontrolle in der Mälz- und Brauindustrie.

Vor dem Hintergrund des historischen Deutschen Reinheitsgebots wurden der Einfluss von Mais und Reis als Stärkequelle auf die Signatur des Biermetaboloms untersucht. Den holistischen analytischen Ansatz nutzend konnten sowohl polare als auch unpolare Metabolite auf die entsprechenden Stärkequellen zurückgeführt und ihre strukturelle Ähnlichkeit über molekulare Netzwerke beschrieben werden. Die wenigen bekannten Mais-spezifische Verbindungen im Bier, die in den 1990er Jahren beschrieben wurden, konnten bestätigt werden. Diese Sekundärmetabolite wurden in molekularen Netzwerken eingebunden und bildeten damit einen Teil einer umfassenden molekularen Signatur von verwandten Verbindungen des Getreides. Als Lipide klassifizierte Bestandteile wurden als weitere potenzielle analytische Marker beschrieben. Ein solcher molekularer Fingerabdruck, der Pflanzensekundärmetabolite umfasst, wurde ebenso für Reis als Stärkequelle gefunden. Letztlich wurde das Asparaginsäure-Konjugat der N-β-D-Glucopyronosyl-indol-3-Essigsäure als potenzielle Markerverbindung für die bislang unbekannte molekulare Signatur von Reis in Bier gefunden. Der Großteil aller beschriebenen Verbindungen wurde bei der Analyse von weiteren Lebensmitteln bereits in den entsprechenden Rohstoffen gefunden.

Diese Untersuchungen bildeten eine fundierte Wissensgrundlage über das Metabolom des Bieres. Die grundlegenden charakteristischen chemischen Profile ermöglichten es, die Natur eines historischen über 130 Jahre alten Bieres zu beschreiben und zurückzuverfolgen. Dieses Bier, das aus der Deutschen Kaiserzeit stammt, wurde in Lübbecke im Norden Deutschlands gefunden. Seine chemische Zusammensetzung stellt eine einzigartige Quelle der Braukultur im späten 19.

Jahrhundert dar, als Erfindungen von Pionieren die Grundlage des industriellen Brauens legten. Komplementäre analytische Methoden wie DI-FT-ICR-MS, LC-ToF-MS und NMR enthüllten seine molekulare Zusammensetzung und beispiellos guten Lagerzustand. Der chemometrische Vergleich mit 400 modernen Bieren zeigte die Signatur eines typischen Lagerbieres auf, das nach dem damals gültigen Reinheitsgebot gebraut wurde. Das Bier wurde durch untergärige Fermentation hergestellt, zu einer Zeit, in der das industrielle Brauen mit entsprechenden Hefen in seinen Anfängen stand. Weitere Produktionsschritte des Brauprozesses konnten nachverfolgt werden. Technologische Aspekte des 19. Jahrhunderts wie die Getreideverarbeitung und Würzebereitung hinterließen molekulare Abdrücke im Biermetabolom. Sowohl die effiziente Entfernung des Keimlings, als auch die Optimierung des pH-Wertes der Würze durch laktische Ansäuerung waren noch nicht etabliert. Ein umfassender Filtrationsprozess ermöglichte die lange Lagerzeit ohne mikrobiellen Befall. Ohne diese biochemischen Einflüsse stellt das historische Bier eine einzigartige Quelle hinsichtlich Jahrzehnte lang ablaufender chemischer Veränderungen in einem solchen versiegelten Gemisch molekularer Komplexität dar. Der Zahn der Zeit resultierte in der oxidativen Ablagerung von Polyphenolen, einer bislang unbekannten Vielfalt an oxidierten Hopfenbittersäurederivaten und Konzentrationen von Maillard-Reaktionsprodukten wie HMF und Furfural, die weit über das hinausgehen, was in der bisherigen Brauliteratur beschrieben wurde.

Table of Contents

Scientific Communications

Publications

Chapter 1: Pieczonka, S.A., Rychlik, M., Schmitt-Kopplin, P. Metabolomics in brewing research. In Comprehensive Foodomics 1st Vol. (edited by Cifuentes, A.) Chapter 2.08, 116-128 (Elsevier, 2021)
The publication is one component of the General Introduction and Analytical Approach section.

Chapter 2: Pieczonka, S.A., Lucio, M., Rychlik, M., Schmitt-Kopplin, P. Decomposing the complexity of brewing. Nature Partner Journal Science of Food 4 (11), 1-10 (2020)

Chapter 3: Pieczonka, S.A., Hemmler, D., Moritz, F., Lucio, M., Zarnkow, M., Jacob, F., Rychlik, M., Schmitt-Kopplin, P. Hidden in its color: A molecular-level analysis of the beer's Maillard reaction network. Food Chemistry 361 (130112), 1-9 (2021)

Chapter 4: Pieczonka, S. A., Paravicini, S., Rychlik, M., Schmitt-Kopplin, P. On the trail of the German Purity Law: Distinguishing the metabolic signatures of wheat, corn and rice in beer. Frontiers in Chemistry: Analytical Chemistry 9 (715372), 1-12 (2021)

Chapter 5: Pieczonka, S. A., Zarnkow, M., Diederich, P., Hutzler, M., Weber, N., Jacob, F., Rychlik, M., Schmitt-Kopplin, P. Archeochemistry reveals the first steps into modern industrial brewing. Nature Scientific Reports 12 (9251), 1-15 (2022)

Oral presentations

17. Rohstoffseminar Weihenstephan 2020, TUM School of Life Sciences, Brewing and Beverage Technology, Freising. Title: Metabolomik und die Komplexität der Brauens. Eine ganzheiltiche Betrachtung.

49. Deutscher Lebensmittelchemikertag 2021, Gesellschaft Deutscher Chemiker, Wuppertal. Title: Das Maillard-Reaktionsnetzwerk des Bieres auf molekularer Ebene. (digital)

38th European Brewery Convention Congress, 2022, EBC, Madrid. Title: Can husk separation contribute to better beer quality?.

38th European Brewery Convention Congress, 2022, EBC, Madrid. Title: Archeochemistry reveals the first steps into modern industrial brewing.

Analytica Conference 2022, Gesellschaft Deutscher Chemiker, Munich. Title: Archeochemistry reveals the first steps into modern industrial brewing.

Poster presentations

FT-ICR-MS End User School 2018, EU-FT-ICR-MS network, Joensuu Finland. Title: The molecular complexity of brewing.

Doctoral Candidates Kick-Off Seminar 2019, Technical University of Munich, Raitenhaslach, Title: Die Komplexität des Brauens auf molekularer Ebene.

48. Deutscher Lebensmittelchemikertag 2019, Gesellschaft Deutscher Chemiker, Dresden. Title: Rapid metabolic profiling of diverse beer varieties by complementary (ultra)high resolution mass spectrometry techniques

FAPESP/BAYLAT (Fundação de Amparo à Pesquisa do Estado de São Paulo / Bayerisches Hochschulzentrum für Lateinamerika) Workshop 2019, Cooperation opportunities between Brazil and Germany, Global Bioeconomy Alliance, São Paulo Brazil, Title: Decomposing the molecular complexity of brewing.

Attention in the journalistic professional public (excerpt)

The Analytical Scientist, April 2021, Volume 96, pages 40-45, ‘The Dark Metabolome in Your Glass’ or
https://theanalyticalscientist.com/fields-applications/the-dark-metabolome-in-your-glass (24.03.2021)

Frontiers Science News, Press release August 10th 2021, ‘Tens of thousands of unique molecules detected in 467 beers from around the world’ or
https://blog.frontiersin.org/2021/08/10/frontiers-chemistry-chemical-complexity-beer-metabolomics/ (10.08.2021)

Current Trends in Mass Spectrometry, Newsletter October 26th 2021, ‘Profiling Metabolites in the Beer Matrix’ or
https://www.chromatographyonline.com/view/profiling-metabolites-in-the-beer-matrix (13.10.2021)

Gesellschaft Deutscher Chemiker (GDCh), Nachrichten aus der Chemie, Volume 69, page 98, November 2021, ‘Moleküle im Bier!’ or
https://doi.org/10.1002/nadc.20214119763 (01.11.2021)

Scientific American, Volume 325, issue 5, page 17, November 2021, ‘What’s Brewing in a Beer Is Startling Complexity - High-powered chemistry lets researchers trace a beer back to its ingredients’ or
https://www.scientificamerican.com/article/whats-brewing-in-a-beer-is-startling-complexity/ (01.11.2021)

Abbreviations

ACN	Acetonitrile
AI	Artificial intelligence
ANN	Artificial neuronal network
ANOVA	Analysis of variance
ASCA	ANOVA-simultaneous component analysis
APCI	Atmospheric pressure chemical ionization
APPI	Atmospheric pressure photo ionization
CAMOLA	Carbon module labeling
CDS	Calibrant delivery system
ChEBI	Chemical Entities of Biological Interest
CoA	Coenzyme A
CV	Cross validation
DART	Direct analysis in real time
DBE	Double-bond equivalents
DBE/C	Double-bond equivalents per carbon atom
DDA	Data dependent analysis
DDMP	2,3-Dihydro-3,5-dihydroxy-6-methyl-4(H)-pyran-4-one
DEV	Deutsches einheits Verfahren
DHBOA	Dihydroxybenzoxazinone
DI	Direct-infusion
DIBOA	N-hydroxy-HBOA
DMS	dimethyl sulfide
DNA	Deoxyribonucleic acid
DOM	Dissolved organic matter
EBC	European Brewery Convention
ESI	Electro spray ionization

FANCY	Functional analysis by co-responses in yeast
FI	Flow-injection
FID	Flame ionization detector
FooDB	Food database
FT-ICR	Fourier transform ion cyclotron resonance
Furaneol	4-Hydroxy-2,5-dimethyl-3(2H)-furanon
FWHM	Full width at half maximum
GC	Gas chromatography
GC x GC	Two-dimensional gas chromatography
GMP	Guanosinemonophosphate
GNPS	Global natural product social molecular networking
HBOA	Hydroxybenzoxazinone
H/C	Hydrogen-to-carbon ratio
HCA	Hierarchical cluster analysis
HMBOA	Hydroxymethoxybenzoxazinone
HMDB	Human Metabolome Database
HMF	5-Hydroxymethylfurfura
HSQC	Heteronuclear single quantum coherence
InChi	International chemical identifier
KEGG	Kyoto Encyclopedia of Genes and Genomes
KMD	Kendrick mass defect
LC	Liquid chromatography
LDA	Linear discriminant analysis
MALDI	Matrix-assisted laser desorption/ionization
MD	Mass difference
MDiM	Mass-difference map
MDiN	Mass-difference network
MEBAK	Mitteleuropäische Brautechnische Analysenkomission
MeOH	Methanol

MIB	Micro inoculum broth
MLP	Multilayer perceptron
MR	Maillard reaction
MRMS	Magnetic resonance mass spectrometry
(m)RNA	(Messenger) ribonucleic acid
MRP	Maillard reaction product
MRS	De Man, rogosa and Sharpe
MS	Mass spectrometry
MS^2	Tandem mass spectrometry
MSI	Metabolic standard initiative
MS/MS	Tandem mass spectrometry
MTA	5-Methylthioadenosine
m/z	Mass-to-charge ratio
NBB	Nachweis bierschädlicher Bakterien
NMR	Nuclear magnetic resonance
NNS	Non-linear nonparametric statistics
NOM	Natural organic matter
O2PLS	Two-way PLS
OPLS	Orthogonal PLS
O/C	Oxygen-to-carbon ratio
OSA	Orange serum agar
PCA	Principal component analysis (statistical context)
PCA	Plate count agar (microbiological context)
PCR	Polymerase chain reaction
PLS	Partial least squares or Projection to latent structures
ppb	Parts per billion
ppm	Parts per million
PSO	Particle swarm optimization
py	Pyrolysis

QC	Quality control
rDNA	Ribosomal DNA
RP	Reversed phase
RP	Resolving power
RT	Retention time
SCE	Space-charge effect
SICRIT	Soft ionization by chemical reaction in transfer
SI-units	The international system of units
SMILES	Simplified molecular input line entry specification
S/N	Signal-to-noise
TBA	2-Thiobarbituric acid
ToF	Time of flight
TOCSY	Total correlation spectroscopy
TPPI	Time-proportional phase incementation
TRACES	Trade control and expert system
TRS	Tryptic soy agar
TSP	Trimethylsilylpropanoic acid
U(H)PLC	Ultra-(high)-performance liquid chromatography
UV	Ultraviolet
Vis	Visible
VRBD	Violet red bile dextrose
WLD	Wallerstein differential medium
WLN	Wallerstein nutrient medium
YAG	Yeast extract glucose
YM	Yeast malt
YMDB	Yeast Metabolome Database
YPM	Yeast peptone mannitol

Chapter 1 |
General Introduction and Analytical Approach

1.1 Metabolomics

1.1.1 Origin and conceptuality

Origin. The origin of the comprehensive analysis of metabolites lies in the Metabolic Control Analysis (MCA) founded independently by Kacser and Burns [1] and Heinrich and Rapoport [2] in the 1970s. The control aspect referred to the enzymatic and catalytic regulation of metabolic fluxes and concentrations in biological systems. Enzyme activities were modulated by incremental small changes and the effect on either the metabolite fluxes or concentrations was determined. The specific Control Coefficients expressed the importance of one enzyme towards the regulation of a metabolic variable in vivo. Two decades ago, Oliver, et al. [3] then coined the term of the comprehensive analysis of the metabolome in a biological system. The focus of their work was on the relative concentration of metabolites as a function of the presence and expression of known genes. This reference to genetics already represented the first bridge to the nowadays numerous existing -omics techniques (e.g. genomics, transcriptomics, proteomics, lipidomics, fluxomics or foodomics). The evolving term of metabolomics described the identification and quantification of all metabolites in a given sample comprehensively [4]. The not to be mistaken field of metabonomics was founded as the analysis of metabolic reactions of living systems (rats) to pathophysiological stimuli (drugs) [5]. It focuses on the history of time-related metabolic changes in coordinated substrate channels and is traditionally connected to NMR-analytics.

Conceptuality. The analytical methods soon reached their limits when the strict definition of true metabolomics by Fiehn [4] was tried to be met: „The resolving power of the analytical method chosen must be high enough to maintain sensitivity, selectivity, matrix independence, and universal applicability". Even the sample preparation already harbors the risk of an intrinsic bias concerning physicochemical properties of the subset of metabolites accessible for analysis. A comprehensive implementation is difficult to guarantee. For this reason, further terms for the analysis of metabolites were subsequently developed, which are summarized in Table 1.1. When the analytical approach focuses on specific small molecules, all the others are incidental and extensive sample clean-ups are used to avoid interferences from accompanying compounds, the term targeted analysis was suggested. When aimed to measure a pre-defined group of biochemically characterized and interpreted

metabolites (as a subset of the metabolome) with great sensitivity, targeted metabolomics was established later [6]. Metabolite profiling deals with the analysis of defined compound classes as proxies for metabolic pathways. A high-throughput analytical approach that aims at classifying samples according to their origin or biological relevance is called metabolic fingerprinting. Identification or quantification of measured features is not required, even the resolution of all signals is not mandatory as well. Both the metabolic profiling and fingerprinting later are summarized as untargeted or non-targeted metabolomics [7,8]. Kell, et al. [9] introduced the term metabolic footprinting for the investigation of what a cell or system excretes under controlled conditions (exometabolome). The spectrum of accessible metabolites is therefore crucial for the definition of the analytical approach but as well is the level of characterization of the compounds. Regarding compound identification, the suggestions by the Metabolomics Standards Initiative around Sumner, et al. [10] prevailed in the metabolomics society. The authors differentiate between the levels (1) identified by two independent and orthogonal data sets relative to an authentic standard or a combination of MS (accurate mass, fragmentation pattern) and NMR (^{1}H, ^{13}C, 2D) data at minimum (2) putative annotations with regard to the spectral similarity in databases and libraries (3) putative characterized compound class upon characteristic physicochemical properties or specific signals (4) unknown. Whether all measured metabolites should be identified or only those that are of particular interest and crucial (e.g. biomarkers) is not fully described in the true metabolomics definition. However, a concept for identifying metabolites is mandatory for the analytical approach chosen. The term quantification could also be weighed up. Usually, it is connected to the specification of concentrations in SI-units but might include semi-quantitative data with regard to detector signal units in a stable analytical system as well.

Table 1.1 | Terms and definitions in the field of metabolome analysis [4,8,9].

(True) Metabolomics	Targeted Metabolomics
Identification and quantification of all metabolites in a biological sample comprehensively • avoid exclusion of any metabolite • well-conceived sample preparation • high-resolving, sensitive and universally applicable analytical method	Analysis of specific, selected, chemically characterized and biochemically annotated metabolites • extensive sample clean-up possible • (preferably) great sensitivity • identification and quantification
non-targeted Metabolomics	
Metabolite profiling	Metabolic fingerprinting / footprinting
Selected number of pre-defined metabolites as proxies for whole or intersecting pathways in a biological sample • sample clean-up specific to a chemical group (e.g. lipids, terpenes) possible • identification and quantification	Classification of samples according to their origin or biological relevance with focus on the intra-systemic (fingerprinting) or exometabolome (footprinting) • comprehensive feature detection • no identification or quantification • for diagnostic use in industry or clinical routines

Classification of DI-FT-ICR-MS. As elaborately discussed by Moritz, et al. [11], direct-infusion Fourier transform ion cyclotron resonance mass spectrometry (DI-FT-ICR-MS) surely enables to map the metabolome comprehensively by unrivaled mass resolution which comes with corresponding mass accuracy. Yet, it only provides semi-quantitative data and is somewhat susceptible to matrix effects. It would have to be coupled to separation techniques (which comes with a drastic decrease in performance [12]) to fulfill the definition of metabolic profiling. DI-FT-ICR-MS on its own consequently is located between metabolic profiling and fingerprinting. Precisely because the original concept of metabolomics presupposes a quantification and identification (concept of identification) of all analyzed small molecules, we avoided using it in the published research articles. Although the term metabolomics got softened over time and the strict definition is not consistently adhered to, we decided to use the more neutral terms of comprehensive metabolite profiling or characterization for the analytical approaches applied in this thesis' research. As of 2021, the Metabolomics Society generalizing refers to metabolomics as the "comprehensive characterization of the small molecule metabolites in biological systems" [13].

1.1.2 The metabolome: A holistic perspective on systems' function

Proteome research (1970s [14], term "proteomics" in 1994 [15]) and genome research (1970s [16], term "genomics" in 1986 [17]) developed much earlier than the rather young field of comprehensive metabolome analysis. In the early 1990s, the first chromosome sequence was completed [18] (S. cerevisiae) and DNA sequencing was able to define all the genes. It became evident that future research will move from gene to function rather than from function to gene. The -omics field most closely linked to genomics is transcriptomics [19]. It refers to the analysis of the complement of (m)RNA molecules in a biological system and forms the transition step from gene to protein. For the relation between genes and transcriptomes, a simple one-to-one equivalency is a justified assumption (not considering splicing phenomena). Such a straightforward link is not valid for the subsequent proteome due to post-translational processing and modifications. In the case of the metabolome, the context is even more complex. The synthesis and turnover of a single metabolite are determined by many genes. In the early stages of the -omics concept, the way from genotype to phenotype (Figure 1.1), where "DNA makes RNA makes protein", suddenly stopped at that level of macromolecules [20]. Yet, it is the metabolite profile that represents the direct and immediate link to systems function. The direct connection to phenotypes is the most important and most searched for property of the metabolome. Its potential to contribute to the understanding of the molecular complexity of living systems soon got recognized and embraced around the biological research community [4,21,22].

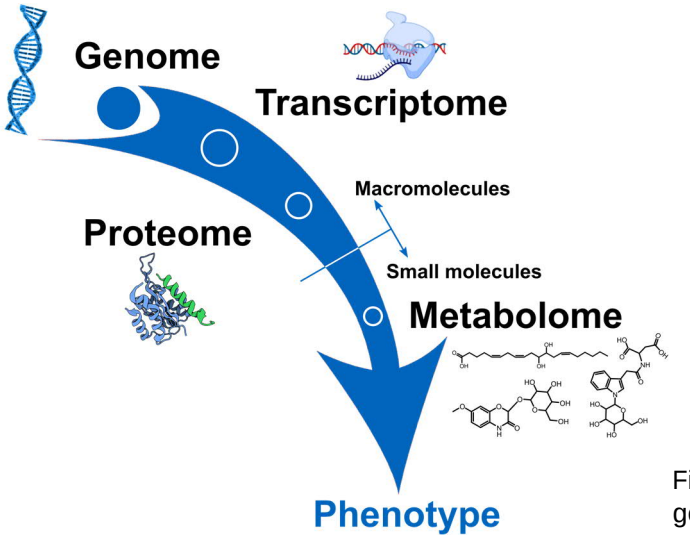

Figure 1.1 | From the genome to phenotypes.

With a metabolite typically being characterized as a molecule with less than 1,500 Da of mass [23], the field of metabolomics is not targeted at higher molecular mass biopolymers like polysaccharides, polypeptides/proteins, polynucleotides or lignins. The building blocks that form such functional and stability-giving macromolecules and the biosynthetic cycle of those are more so in the focus of the metabolomics approach. Apart from their importance to the primary metabolism, small molecules fulfill critical roles that are necessary for maintaining a living system. The regulation of a biological system is closely related to small signaling molecules and secondary metabolites. Metabolomics aims at resolving and setting in relation the extensive network of biochemical interactions the metabolome encompasses. Still, the ability to map and visualize all small molecules of just one given organism remains a vision for the future. Not considering side-streams and side products, the comparatively simple core carbohydrate metabolism comprises over 50 chemical compounds (mediated by over 100 enzymes) [24]. The mechanisms and interactions of all metabolites and their flow in the cycle become vastly complex when the connection points of the numerous compounds with other metabolic cycles and the secondary metabolism (with all its possible derivatives) are considered. In total, the diversity of the human and plant metabolome is expected to far exceed 100,000 and 200,000 metabolites respectively [25,26] (first thoughts stipulated around 600 for yeast [20]).

In a living biological environment, all the organisms involved exchange metabolites and interact, e.g. concerning food intake [27] and human microbiome [28]. The result is an enormously complex picture, which in its entirety leads to the accumulation and change of biomass. To envision the full complexity of the metabolic flux and dynamic balance gets almost intractably challenging when the interaction and cooperation of the observed organism with its surrounding biosystem and environment are included. As a part of the -omics techniques aiming to describe systems biology, metabolomics approaches lead to better understanding and characterization of biological systems from a holistic perspective. Because technical

limitations still exist and systems are extremely difficult to be described in all possible dynamics, metabolomics largely is applied to the description of individual metabolic reactions and the role of different pathways to certain stimuli and criteria (e.g. drugs, stress, environment, food, phenotypes and diseases). All those essential puzzle pieces eventually form the big picture.

1.1.3 Fields of application

Following the 'from gene to function'-concept, the first metabolome researches focused on the idea that the role of genes of unknown function should be elucidated by comparing the metabolomes of deletion mutants. This concept was established as the "guilt by association"-principle [29]. Such studies were carried out predominantly concerning yeast mutants analysis (FANCY, Functional analysis by co-responses in yeast [30,31]) before moving to the metabolites excreted to the growth media [32] (metabolic footprinting) by NMR analysis and bacterial cell [33] or foodstuff [34] specification utilizing DI-MS data (metabolic fingerprinting). The main important outcome of these studies was the proof of principle, opening the field of metabolomics to e.g. plant biologists [4,21,22] and medical research [35,36]. In their review articles, Kell and Oliver [20] and Alseekh and Fernie [25] describe the extensive developments that followed: Improving technologies and strategies like ^{13}C-labeling for flux-analysis [37], integrating community approaches [38], quality standards and comparison [10,39,40], uniform structural descriptors (SMILES [41], InChI [42]) , single-cell analysis [43], further automation [44], improvements in instrumental resolution [12], and in artificial intelligence (AI) implementation [45]. The concept of metabolomics paved its way into all fields of life sciences. Regardless of the field of application, metabolomic research shares one characteristic that reflects the holistic approach and may lead to the discovery of unexpected relations: It is focused on questions, not hypotheses.

Plant sciences. Probably the oldest field of the comprehensive analysis of small molecules is plant metabolomic studies. The world of the plant metabolome offers what presumably is the largest and most complex surface when a single organism is targeted. A comprehensive summary of strategies and achievements can be found elsewhere [46], yet a few targets of the numerous studies should be mentioned. The influence of the metabolome on plant or rather fruit/crop yield [47], quality [48] or shelf life [49] was examined. Questions were asked about new biochemical pathways [50] or the development and ripening process of fruits and crops [51]. Genotypes can be selected with regard to their nutritional composition [52,53] and stress tolerance [54,55] on basis of molecular descriptors. It opens many possibilities against the background of changing climates and therefore changing abiotic and biotic stresses. In addition to the climatic impact, the geographical sphere also has a significant influence on the metabolic composition of the plant [56,57]. This leads to another field of application, the environmental studies.

Environmental sciences. Environmental metabolomics deals with the comprehensive description of metabolites involved in the interactions of organisms within their environment or of the environmental system as a whole [58]. It ranges from understanding organismal responses to biotic or abiotic pressures to the holistic chemical description of an environmental system itself. Metabolic characteristics and regulatory reactions concerning special environmental conditions were well described for various organisms (within species) for low-temperature ecotypes [59], heat stress hardening [60], draught metabolic adaption [61], increasing salinization [62], food availability [63], toxicological concerns [64] or differing photoperiods [65]. Evolutionary developments led to special metabolic strategies, signatures and pathways [66] for extreme environmental conditions like acidity/alkalinity (pH 0-12.5) [67], salinity [68] (0-50 %) / water activity [69] ($a_w \approx 0.4$), temperatures [70] (-25°C-130°C), pressures [71] (> 125 MPa) or radiation [72] (11 kGy). In addition to describing the metabolome of individual adapted organisms (extremophiles), such special environments were also holistically characterized as a whole in their complex chemical composition, utilizing ultra-high-resolution techniques (Biogeochemistry) [73,74]. Biotic-biotic interactions in terms of competition [75] or herbivory activity [76] and necrotrophic [77] or biotrophic [78] pathogens are also assigned to environmental influences. Synergistic biotic systems as well influence the metabolome of the organisms involved between plants [79], insects [80], fungi [81] or bacteria [82]. Ultimately, environmental health, i.e. the monitoring of environmental influences on health or the development of diseases, is a topic of interest [83,84].

Health and medicine. In the field of health and medical research, metabolomics can evaluate the progress of diseases, select potential biomarkers, provide insights into underlying pathophysiology, offer (early) diagnostic platforms, and drive the search for new drugs and novel bioactive compounds [85]. Comprehensive metabolic approaches have the potential to identify metabolic pathways or individual biomarkers related to the disease under investigation. The global metabolite profile and homeostasis often mirror the physiological or pathological state of an organism. Utilizing a holistic approach, one can benefit from the data-driven and not hypothesis-driven findings [86]. Using metabolite profiling, the mitochondrial glycine biosynthetic pathway was assigned a key role in cancer cell proliferation, leading directly to implications for cancer therapy [87]. Metabolome analysis furthermore can contribute to the identification of cancer subtypes and grades based on tumor biology [88]. The actual etiology of Crohn's disease, an inflammatory bowel disease affecting the gastrointestinal tract, currently is unknown. Both host genetics and environmental factors play a role. In a twin study, the contribution of the gut microbiome to the patient's metabolic profile revealed several metabolites originating from different pathways as potential targets for disease monitoring, therapy and prevention [89]. Furthermore, drug discovery pipelines and high-throughput screenings benefit to a large extent from molecular level descriptors and similarity measures introduced by the metabolomics community [90]. Today, potential drug leads are characterized and compared by molecular modeling, molecular dynamics, their bioactivity, carrier binding or binding to active sites utilizing structure-activity relations and multiple cheminformatics tools [91]. Metabolomics nourishes the needed extensive chemical libraries and databases by the molecular

characterization of combinatorial chemistry mixtures [92] or natural sources of metabolic diversity. Whole ecosystems are screened as yet uninvestigated rich sources for natural products as bioactive compounds and potential novel drugs [93].

Food and nutrition. One aspect highly influencing human health and well-being is food intake and nutrition. The term foodomics was coined in 2009 by Alejandro Cifuentes [95] and describes the "application and integration of -omics technologies to improve consumer's well-being, health, and knowledge" (Figure 1.2).

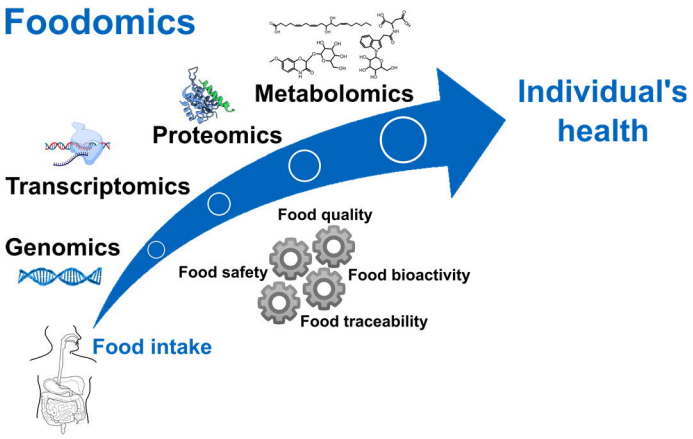

Figure 1.2 | Graphical representation of the foodomics integrative framework, adopted from Alvarez-Rivera, et al. [94].

Being one essential part of foodomics, metabolomics contributes to food quality (safety, utility, nutritional, sensory and ecological quality) and integrity. The demand for advanced analytical techniques in the field of food analysis has grown in parallel to highly industrialized food production and the consumers' concern about food integrity. Traditionally, a major goal of food analysis is to guarantee the safety of food in compliance with legislation. With the emerging resistance to pesticides and fungicides [96], agrochemical industries are in a predicament to develop novel and improved crop protection agents to avoid rot-related crop failures and health risks. Metabolomic studies investigating the mode-of-action of those bioactive compounds [97], the interaction of pathogens with crops [98] or unintended effects in genetically modified crops [99] can contribute to solving the global food issue. Targeted metabolite analysis, which can include several hundred components, ensures that the residues of protective agents do not exceed levels of health risk [100]. The 'knowledge' or 'confidence' aspect defining foodomic aims has gained in importance with the development of high-resolution analytical techniques and global food production. Metabolomics describes and explains the changes in food chemical composition that come with industrial food processing and that define consumers' gustatory experience [101,102]. Globalization certainly is a driving force for food traceability and integrity considerations including (1) fraudulent or deceptive practices, (2) the adulteration of food and (3) any other practices which may mislead the consumer [103,104]. Metabolomic studies can identify and quantify marker metabolites, find molecular differences in populations (discriminative) and create statistical models

to predict class memberships (predictive). ^{1}H-NMR profiling [105,106] is a comprehensive and rapid example, when compared to more traditional melissopalynology, to assess the quality, adulteration, the botanical and geographical origin of honey.

Foods that are highly affected by fraud attempts are edible oils. The adulteration of olive oil with rapeseed oil (denatured with aniline) caused hundreds of deaths and illnesses due to allergic syndromes [107]. Driven by such little farsighted criminal endeavors, there are numerous metabolomic approaches to assure oil authenticity, quality and safety today [108]. The melamine scandal of 2008 [109], where milk was thinned down with water and melamine was added to mimic the appropriate protein content, killed thousands of infants and raised awareness of the importance of food quality monitoring [110]. Among many others, wine [57,111], beer [112,113], tea [114,115], coffee [116,117], and meat [118] adulterations, quality, origin, and authenticity were characterized by GC-MS, DART-MS, LC-MS, DI-ToF-MS or DI-FT-ICR-MS. Closely linked to those food quality considerations are metabolomic studies concerning the influence of food intake and nutrition on health and well-being. Containing bioactive substances, our food has a significant effect on crucial metabolic pathways [119] and the global role and function of the gut microbiome [120]. The microbial communities in our gut exert a multitude of functions highly impacting human health and disease (risks). The imprint that food intake generates on the metabolite composition available to and generated by the gut microbiome was investigated by a variety of metabolomic studies [121] and combined -omic techniques [28]. Nutrimetabolomics [122] is an emerging field, yet a field in its infancy, aiming at the comprehensive characterization of dietary intake [123]. Decoding biomarkers for metabolic changes or personalized human food and lifestyle interventions for populations and patients are of interest. Overall, the exceedingly complex composition originating from biological organisms and (biological or chemical/technical) processing thereof, its economic, social and cultural relevance, its crucial impact on human health and influence on innumerable interfaces of a biological system (systems biology [124]) makes food and beverages a perfectly suitable matrix of interest for metabolomic studies.

1.1.4 Challenges and perspectives

Instrumentation and analytical approaches. What decisively distinguishes the metabolome from other targets of the -omics technologies is a lack of linear uniformity in the molecular structures to be examined. Genetic and transcriptome information consists of nucleotides. Proteins are made up of (modified) amino acid sequences. In contrast, metabolites cover a huge range of chemical structures. The analysis of the metabolome is particularly demanding due to the tremendous chemical diversity and physicochemical properties of metabolites. Celebrating its adulthood (18th birthday) and despite remarkable progress in this relatively short period, the comprehensive perception and subsequent identification of the molecular complexity that nature offers us remains a major task for the future. This goal is not ideological but enables a fundamental idea behind metabolomics: curiosity-driven hypothesis generation (instead of hypothesis testing) to find novel answers in unexpected places (Figure 1.3) [9]. In the case of mass spectrometry, molecule ionization, sensitivity, and resolution might be the key factors to make the chemical complexity of a system comprehensively visible. Considering the complementarity of the ESI, MALDI, APCI and APPI ionization techniques in both positive and negative ionization mode, the chemical space of metabolites is already well covered [126]; even if it should be mentioned that simultaneous use is still difficult to implement and specific molecules that are difficult to ionize (e.g. black carbon) can only be reached using special methods. Given the mass resolving power of high-field mass spectrometry, especially newest 21 Tesla FT-ICR-MS instruments, the mass resolution already seems to scratch the limit of what potentially is necessary to differentiate compositions [127]. Resolving molecular complexity in one mass dimension, however, lacks information about molecular identities. It will be interesting to observe whether classical separation techniques like liquid chromatography might be overtaken by advanced and cheminformatics-based mass fragmentation techniques like two-dimensional FT-ICR-MS [128]. It might be a combination of both that will make structural information by tandem-MS accessible (comparable to Data Independent-mass spectrometry [129]). The probably greatest instrumental challenge, therefore, is the sensitivity (with a corresponding dynamical range) that according to

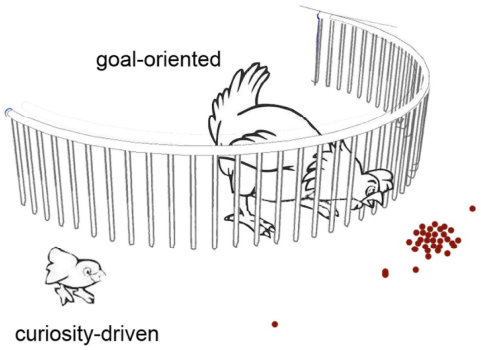

Figure 1.3 | Curiosity-driven research. This figure is adapted with permission from ©The Nobel Foundation 2005, Nobel Lecture of laureate Theodor W. Hänsch, Stockholm, Dec. 8, 2005 [125].

current developments is undergoing exponential growth [130]. Single-molecule analysis and imaging already is possible in specialized applications [131,132]. Awaiting these technical developments, systems' whole dynamics could be targeted in real-time instead of frozen-frames. Apparently opposite developments that look for the big picture in the small, such as single-cell analysis, are challenges for metabolite analysis of the future as well [133].

Challenges to tackle inside the metabolomics community. Regardless of technical developments, there are some challenges to tackle inside the metabolomics community. The standardization for experimental design, evaluation, validation and reporting is essential to be taken care of to make studies comparable and support the quality of metabolomics research. In 2005, with the backing of the Metabolomics Society, leading experts in the field gathered to form the Metabolomics Standards Initiative (MSI) [134]. Data repositories like MetaboLights [135] or Metabolomics Workbench [136] were created to make metabolomics data available to the community. The condition, or better, the assumption was that the MSI reporting standards (summarized by Goodacre [137]) are complied with. The disclosure of the analytical data enables studies to be retraced, proves their reproducibility and reveals comparative spectra for further studies or alternative advancing data treatment concepts. Yet, minimal reporting standards are often not met [138]. The metadata are of great importance against the background of advanced data treatment techniques and AI-guided data evaluation that aim at compound associations and identifications. Community-based open-access platforms like Global Natural Product Social Molecular Networking GNPS [139] have taken up the importance of making experimental data available (beyond the fragmentation spectrum of individual substances) and creating an infrastructure for sharing exploratory non-targeted analytics (2,034 metabolomic data sets and over 200,000 monthly accesses as of October 2021). The need to make metabolomics data publically available cannot be stressed too highly. The authors found that most studies annotate less than 10 % of all features even in the widely researched field of the human metabolome (2 % for all studies). Exemplifying the approach and by molecular networking of the community's shared data, the formation of novel bile acids was found to be initiated by changes of the microbiome in mice [140,141]. Spectral similarities of shared foodomics analytical data enhanced the understanding of human metabolomes as affected by nutrition [142]. In addition to efficient data structures and algorithms for searching databases, the use of artificial intelligence (AI) concepts can help to identify compounds. The retention time (and thus physicochemical properties) of compounds can be estimated [143] or molecules can be assigned to a sub-class, substructure or ultimately a molecular structure via specific fragmentation patterns (still being in its early phase of implementation) [144].

Artificial intelligence and future fields of application. "Progress in science depends on new techniques, new discoveries and new ideas, probably in that order" – Sydney Brenner, Nature, June 5, 1980 [145].

With the power of analytical instrumentation enhancing exponentially [130], a successful proof of concept and numerous applications of metabolomics all around in scientific literature, the field of new and far-reaching ideas is ready to be tackled. Depicting the whole metabolome comprehensively in big representative or clinical studies inherently comes with big datasets. The era of 'big data' has already found its way into many areas of life, yet the extensive data harvesting in analytical chemistry has not benefited sufficiently from existing chemometric tools. The group around A. Cifuentes [146] recognizes the "high level of experience and technical skills […] for software management and statistical data analysis" as one of the major challenges to tackle in metabolomics and foodomics research. Artificial intelligence (intelligent behavior of machines to create decision-making structures), machine learning (algorithms improving through experience) and deep learning (representation learning neural networks) are expected to highly increase the chemical (and metabolic) information we can obtain from chemical data [147]. It may bring us to not only see the analytical data as metabolite concentrations in a current state of the biological system but vision it as an information source for biological signaling that (cor-)respond to pathway dynamics. The power of AI in pattern recognition not only should be applied to analytical data of a steady-state, but also dynamic real-time and online analyses. Metabolic pathway dynamics prediction, however, is heavily reliant on the integration of other -omic tools (especially genomics, transcriptomics, proteomics) to metabolomics data against the background of enzyme-mediated processes. The integration of AI in analytical data sets on a global level is a crucial task and certainly will create future technologies and concepts. Following the thought of online analytics, health data (and thus meta-information about metabolite homeostasis) are already registered by so-called smartwatches. In the actual medical field, there are already wearable technologies to monitor diabetes patients' status [148]. Further development and integration of metabolite-analyzing sensory systems as a sort of early warning system in the daily routine of the human being is a future vision, but certainly not undisputed leaving questions about data handling and security open. Such medical systems, existing and future ones, in combination with AI data analysis have the potential to open up the field of personalized medicine, where therapies are tailored to the biological state of an individual [118].

In its today's shape, metabolomics has a key role as an approach to discover biomarkers within large diverse populations and translate them to cheaper and quicker methods (precision medicine) [149]. For highly targeted, yet not fully understood diseases like Parkinson's disease, research might need to get away from the idea of a healing marker molecule. Where whole systems of metabolic regulations are affected, whole pathways and dynamics need to be considered to make coherence analytically visible [150]. Personalized screenings could in the nearer future be part of a regular health check-up and finally contribute to or be the method for the early detection of diseases (when legitimate ethical, legal and social questions can be resolved and specific, sensitive and reproducible standards are established [85]). The influence of changing environmental, lifestyle or dietary influences on the human organism is summarized in the term of human exposome [151]. AI performed on large-scale studies and data integration of several comprehensive analytical

approaches (including metabolomics) can help to make such effects on the metabolome and microbiome visible.

Regarding the foodstuff itself, safety and authenticity profiling should be accompanied by the 'knowledge' part of foodomic aims. Food as an exceedingly complex mixture of chemical diversity still is not sufficiently characterized. The so-called "dark metabolome", small molecules of unknown structure, permeates a major part of the detectable signals in mass spectrometry. Barabasi, et al. [152] report the FooDB [153], a database representing the most comprehensive effort to integrate food composition, to record the presence of 26,625 distinct biochemicals in food. In contrast, Roullier-Gall, et al. [57] reported over 7,000 distinct mass signals (isomers not included) in wine alone. The overlap within FooDB was as few as 5 %. Process optimization can largely benefit from characterizing (and ideally identifying) such yet unknown metabolic profiles. Process control guided by AI might be an application. It is worth mentioning that such guiding signatures often do not consist of the volatile aromatic substances of the final end product but are determined to a particular extent by non-volatile chemical precursors. Integrating AI is still insufficiently pursued in both food research and industry and might strongly influence industrial food and beverage production in combination with online monitoring. Coming with the ever-increasing scale and complexity of food supply networks, the food production process is becoming more vulnerable to fraud and contamination. The analytical techniques to collect and analyze biological and chemical data within the extensive food chain are required to be rapid, robust, user-friendly, generally applicable and portable. The trend towards non-targeted analytical approaches already is visible. An integrated system of non-targeted analytics is far more difficult to circumvent especially when considering sophisticated fraud attempts with knowledge of testing programs [154,155]. Either spectroscopy, sensor chips or direct-infusion mass spectrometry seem the most suitable ones with the latter being far more comprehensive but still expensive and less mobile. A future perspective would combine predictive computing and the Internet of Things [156] to form whole system-based approaches that significantly reduce vulnerability to food fraud. A problem of systems requires system-level solutions [157].

1.2 Metabolomics in brewing research

The science of beer has a long history. As beer is one of the oldest beverages of our civilization the questions on quality control and product composition influencing its conservation and taste is integrating empirical knowledge over centuries. In the context of metabolomics, beer can be described as an exceedingly complex organic mixture in aqueous solution. The impact of the raw materials, the brewing process and aging on the molecular composition of beer has direct effects on its organoleptic perception and has been investigated using numerous analytical methods, which are resumed in this chapter. We also give an outlook on the use of a novel and powerful analytical approach in brewing research utilizing ultrahigh mass resolution, i.e, direct-infusion Fourier transform ion cyclotron mass spectrometry (DI-FT-ICR-MS), in the metabolome analysis of beer.

This review chapter has been published as Pieczonka, S. A., Rychlik, M. & Schmitt-Kopplin, P. Metabolomics in brewing research, in Comprehensive Foodomics Vol. 2 (ed A. Cifuentes) Chapter 2.08, 116-128, Copyright Elsevier (2021). It is reproduced with explicit permission. The last paragraph (Depicting the Molecular Complexity of Beer by Direct-Infusion Fourier Transform Ion Cyclotron Mass Spectrometry (DI-FT-ICR-MS) was left out due to overlap with Chapter 2. It can be found in the Supplementary section (Review Chapter A in Supplementary Chapter 1). The term FIA-FT-ICR-MS was exchanged due to uniform naming of the approach, with explicit permission. This contribution is integrated into the work as a dissertation-relevant publication.

Candidate's contributions: S.A.P. wrote, revised and approved the final book chapter. S.A.P. performed the literature research and article structuration.

1.2.1 Introduction

History of Beer and Signi**fi**cance of Brewing Research. Presumably, beer belongs to the oldest fermented beverage in the world [158,159]. Its distinction to the wine is not as obvious as the sensory impression might suggest. Such as wines, beers are fermented but not distilled drinks. Its carbohydrate source, on the contrary, is not fruit sugar (grapes), but starch. The historical importance of beer primarily can be attributed to its durability and bacteriostatic property. An analogy is, “what salt is to the meat, is alcohol and low pH-value to beer”. Thousands of years ago mankind commenced to purposefully produce durable beverages from domesticated cereals. During the emergence of brewing, the release of sugar from the long-chain carbohydrates was versatile. Initially, the amylase activity of human saliva (after chewing and spitting out of the grain) provided the mono-/disaccharides required for fermentation. In order to saccharify larger quantities, specialized species of barley and wheat were malted; cooked rice was superficially inoculated with mold or already fermented grain products such as bread were used. As starter culture yeast was added in form of ripe fruits, fruit juices or honey [160]. Nevertheless, the history of beer and beer analysis is by no means just a story of antiquity and tradition. It is a history of the progress of jurisprudence, technology and science. The Bavarian Purity Law of 1516, which stipulates only the ingredients barley, hops and water for beer, is regarded as a significative food legislation of the early modern period. It was written based on empirical knowledge to ensure the quality of the beer, the retention of valuable wheat and rye for the bakers and the preservation through antioxidant and antibacterial hops. The addition of spices and psychoactive ingredients such as opium poppy and belladonna were prohibited [161]. Although the concept and cultivation of yeast (Saccharomyces cerevisiae) were already known, it took more than 300 years before fermentation could be assigned to the metabolism of microorganisms instead of a purely chemical process. Furthermore, during his beer studies, Louis Pasteur discovered the first metabolic regulation by distinguishing aerobic and anaerobic conditions during fermentation [162]. We also owe the first isolated yeast cells and thus cultured yeasts to the brewing research [163]. This development paved the way for brewing using bottom-fermented yeasts, which are less susceptible to undesirable microorganisms such as Lactobacillus or Pediococcus due to low fermentation temperatures. The renunciation of the top-fermented brewing style was supported by another invention, which is indispensable today. Around that time, Carl von Linde developed the first commercial refrigeration unit to enable the fermenting cellars to be cooled [164]. The complexity of beer production and the exploration of fermentative, biochemical and purely chemistry-derived reactions still are significant research topics. The diversity of ingredients and the variability of processes continue to present key challenges to scientific research.

The Molecular Complexity of Brewing. Beer can be considered as a complex aqueous mixture in a continuum of volatile to semi-volatile and non-volatile molecules, to which its ingredients contribute as considerably as the brewing process itself. Even the ostensibly simplest, yet quantitatively most important ingredient - the

brewing water - has a significant impact on the metabolome of beer. Many breweries were built in the proximity of known springs. In addition to the numerous dissolved organic compounds [165], it is inorganic ions that guide the brewing process and thus the chemical composition of the beer. The water hardness, especially the Ca^{2+} concentration, is reported to protect α-amylase from early inactivation during mashing and to increase the hydrolysis reactions by lowering the pH-value closer to the optimum of β-amylase activity [166]. Thus, it has developed historically that the hard Munich water resources, which lead to intensive enzyme activity and thus high original wort content, resulted in a darker "Munich-type beer" with a more pronounced malt character and metabolome. Pale "Pilsner-type beers" with a greater focus on hop sensometabolites developed in regions with soft water. The selection of the hop variety, but also whether it is added as umbels, pellets or extract as well as the time of hopping is crucial for the molecular composition of beer, especially regarding its organoleptic properties. Isomerization reactions of hop α-acids during the boiling process lead to a focus on bitter sensometabolites, whereas adding hops at the end of the brewing process emphasizes the extraction of aroma compounds [167]. Generally, barley (Hordeum vulgare) and/or wheat (Triticum aestivum) are, besides water, the second most important ingredients in terms of quantity. The processes of grain malting (steeping, germination, kilning/roasting) lead to complex and diverse chemical reactions that are reflected in the beer's metabolome. The roasting of the carbohydrate source is a unique processing step, which notably lifts the molecular complexity of beer from that of wine. Recent studies showed that thousands of compounds are formed simply by heating one sugar and one amino acid, it can be anticipated that the complexity of the Maillard reaction in the malting and brewing process has not yet been fully explored [168]. Less common adjuncts like raw grains, triticale, spelt, emmer, rye, corn, sorghum or rice can also contribute to beer's composition with their abundance of phytometabolites. The fourth ingredient, the yeast, extends the diversity of the beer through varieties with unique or differently pronounced metabolic pathways during fermentation. Apart from its exometabolites, which lead to characteristic aromas, the yeast contributes to the molecular diversity when the beer is stored. Partially, unfiltered beers are refined by bottle-fermentation. Ultimately, yeast cells might undergo autolysis and release their metabolome, which leads to unwanted off-flavors [169]. Deterioration during beer storage can also take place through bacterial infection, oxidation or Maillard reactions. The entirety of all these raw materials and processes leads to a complex aqueous mixture of volatile and non-volatile compounds. Holistically oriented brewing research is aimed at decomposing this intricacy of brewing, which is only touched on here (Figure 1.4). Integrated approaches are needed, since food safety and quality control, the olfaction, taste and visual appearance, the optimization of brewing and malting parameters as well as the fundamental research into chemical and biochemical processes share one greater characteristic: they are by no means unidimensional, but multivariate in nature. For the most parts, the consideration of a single factor is not enough to account for complex behaviors. The overall perception of beer is affected by a variety of sensory impressions as the flavor (taste and olfaction), haze, color, foam and the astringent or sparkling mouth feeling contribute in a holistic way. In the 1970s chemometric data analysis found its way into malting science and beer

characterization through factor analysis of malt's trace elements, protein modification and degradation, the fermentation temperatures and volatile compounds [170,171]. The awareness of the multivariate connectivity of the multi-faceted brewing process formed the foundation from which the analysis and characterization of 'as-many-small-metabolites-as-possible' known as metabolomics developed.

Figure 1.4 | The molecular complexity and chemical diversity of beer originate from its raw materials and processing. Image sections (barrel, kettle) were obtained from 'Bayerischer Brauerbund e.V., München' under their explicit corresponding permission.

1.2.2 Metabolomics research in the field of brewing

Raw Material. Early publications on multivariate data analysis of beer date back to the late 1970s. The combined analysis of small molecules and other factors of brewing chemistry has been used to investigate the volatile composition of beer, applying gas chromatography and flame ionization [171]. It has been found that both the batch size of the brewing process as well as the yeast strain influence the composition of the measured fatty acids, esters and alcohols. In contrast, the location of the brewery site, which is related to less critical factors such as the technological parameters used and the brewing water, had only minor effects. The temperature during the fermentation process was found to be decisive for the composition of the aroma-active esters. The distribution of fatty acids - a factor that owes its variability, not just to the brewing process, but also to the yeast strains themselves - has been brought into focus with the same analytical methodology [172]. In general, diverse yeast strains can be differentiated by the analysis of their fatty acid profiles. Today being a part of lipidomics, this approach can be carried out comprehensively on modern instruments. Besides biological and microscopic test methods, instrumental analysis combined with multivariate data evaluation, therefore, enriches the methodological spectrum for quality analysis of the brewing raw materials. Timmins, et al. [173] contributed by receiving fingerprints of the whole brewing yeast organism with a pyrolysis mass spectrometry (py-MS) approach. This non-targeted approach allowed to depict the fundamental metabolic differences between lager and ale yeast strains that have already been predicted by genome studies. The used direct-infusion method, which offers a prompt analysis for quality control because it does not require a previous chromatographic separation, is used in the examination of the exometabolome of yeast. The varying footprint of the extracellular metabolites can be used to differentiate yeast strains. The direct-infusion of the yeast exometabolome into a ToF-mass spectrometer, though lacking highest resolution, in combination with a GC-MS analysis has proven to be a powerful approach for the non-targeted phenotyping of yeast strains [174]. Thus, yeast strains cannot be characterized solely on basis of their genome, but on basis of their specific metabolism. Hops, being the most characteristic beer raw material, has been subjected to metabolomic studies, as well. The characterization of hops regarding its aroma and authenticity plays an important role in the hop industry and thus brewing research. Comprehensive metabolomics approaches have been successfully used to characterize hop cone cultivars and hop extracts [175,176]. The combination of LC-ToF-MS, magnetic resonance spectrometry (^{1}H-NMR) and fast profiling through ultra-high-resolution mass spectrometry (FT-ICR-MS) reveals a comprehensive picture of hop metabolites. Primarily, known analytes such as hop bitter acids and fatty acids drove the differentiation between hop varieties and their extracts. Yet, the holistic approach additionally indicates the complexity of the previously unknown. Especially high-resolution mass spectrometry, whose power is tapped in the hop research mentioned before, can accomplish that. Furthermore, the compound class of proanthocyanidins, which is mainly composed of (epi-)catechin and (epi-)gallocatechin in di-, tri- and tetramers, have been shown to depict differences in

terms of the hop cultivation location and its variety by an LC-MS approach [177]. The signature of the territorial effects outweighs the influence of the vintage. The listed methods show the existence and importance of a multitude of small non-volatile molecules but have their limitation in more volatile compounds. The distinct complexity and high diversity of the metabolites that determine the hop aroma could be revealed utilizing gas chromatography. In a GC-MS approach, Stenroos and Siebert [178] could distinguish 117 peaks, of which monoterpenes have been identified in addition to volatile fatty acids. However, the characteristic variations in metabolic signature between different hop varieties originated from the unidentified features. Among those, the volatile profile of hops is consisting of alcohols, caryophyllenes, sesquiterpenes, carbonyls, ethers, esters and epoxides. This diversity can be used to characterize not only hop varieties but also different phenotypes. It was shown that the ratio of the aroma compounds is just as crucial as their absolute intensity, proving the necessity of multivariate data analysis. The aroma evaluation of 14 varieties with over 100 different genotypes showed that out of the 187 compounds detected and 87 identified by GC-FID, only very few were characteristic of hop varieties from non-European origin [179]. By showing that hops from America or China are richer in methyl decanoate, neryl acetate and α-copaene, the factor analysis of complex volatile signatures displays the possibility of an origin check. Compounds that negatively influence the overall aroma profile (off-flavors) such as curcumene, selinene, cymene or methyl octanoate also contributed to the specific character of the hop varieties regardless of their origin. A targeted metabolomics approach adds that European hop varieties feature more dominant sesquiterpenes such as humulene and farnesene, whereas the North American hops generally has a more pronounced profile of monoterpenes [180]. In the latter GC-MS-based study experimental hybrids were also analyzed in addition to commercial cultivars and thereby hop cultivation was addressed as an application for metabolomics. Besides the hop plant itself, further processing into pellets or CO_2-extracts with various essential oil fractions is crucial for the later aroma profile of the beer. While monoterpenes are dominant in the hop essential oil, sesquiterpenes are more frequently found in pellets and CO_2-extracts [181]. In comparison to hops, the aroma profile of the barley is substantially impacted by one undesirable compound: dimethyl sulfide (DMS). It is generated from the precursors S-methyl methionine and dimethyl sulfoxide during the thermal process of kilning and adversely affects the organoleptic properties of beer [182].

Organoleptic Perception. Besides aroma active molecules and compound classes mentioned above, the perception of the whole beer flavor clearly depends on multiple beer constituents producing multiple stimuli among our taste and olfactory receptors. This diversity is mirrored in a comprehensive analytical approach, including LC- and GC-MS, which revealed metabolite data for 5042 compounds in malt and 4568 compounds in beer respectively [183]. The analytical and sensory data were integrated by PCA and O2PLS models and revealed associations between flavor profiles in malts and beers. The fruity or corn chip flavor was correlated to the beer's purines, volatile ketones, amines and phenolics with malt lipids and saccharides also contributing. Still, it remains unclear whether the correlation of non-volatiles with sensory traits is due to their nature as aroma precursors or their influence on aroma

stability. In any case, it was shown that the diversity among different malts is reflected both in the chemical composition of the raw material itself and the characteristic sensory descriptions of the finished beer, which confirms the role of malt metabolites for the flavor and flavor stability of beer. Applying neuronal network data analysis on volatile patterns of Brazil lager beers enabled raw material specifications to be revealed in finished beer [184]. Antioxidative additives, preservatives and inadequate storage are characteristics reflected in the volatile profile of the dedicated beers and could be spotted through the data analysis approach based on artificial intelligence. The organoleptic description of those hop substances, which are important and characteristic components of beer flavor, was done using GC x GC-MS [185]. In the first step, it was shown by means of HCA that the genetic hierarchical cluster of hop varieties corresponds to the organoleptic tests carried out on the corresponding beers. Thereupon, a principal component analysis of the sensory impressions alongside the analytical data showed a correlation of over 300 volatiles with ester-like, herbal, spicy, citrusy, sylvan and floral aroma. Subsequently, it was possible to determine the 67 most significant components directly contributing to the aroma by means of GC-olfactometry and aroma extract dilution analysis. They range from terpenes to caryophyllenes and damascenones to ketones and epoxide structures. As a mixture in a certain composition, these compounds are able to reproduce the characteristic organoleptic impression of the hop varieties in beer. Nevertheless, all the remaining detected compounds may influence aroma or flavor in beer by synergistic or antagonistic effects with other coexisting compounds in beer or function as flavor precursors. Therefore, non-targeted analysis of hop volatiles has a twofold use. It gives brewers useful information on hop characteristics for designing and improving beer products. And, it provides hop culturists with ideas for desired varieties that should be developed.

Targeted metabolomic approaches, in contrast, focus on the bitter sensometabolites introduced by hops by means of LC-MS [186]. Monitoring of hop bitter acids across a large-scale brewing process showed the structure-specific reaction routes for their formation by hierarchical clustering. While prenylated flavonoids and β-acids (lupulones) are already poorly extracted from the hop umbel, it is the α-acids (humulones) which are merged with the wort. After the wort boiling, only 10 % of these compounds remain unchanged, whereby oxidation and isomerization products such as tricyclohumoles, humulinones and iso-α-acids are formed. By this approach, the extraction, oxidative degradation and reaction routes of bitter sensometabolites can be tracked throughout the induced process. Thus, metabolomics could offer the scientific basis for knowledge-based optimization of the beer's bitter taste by technological means. A similar approach was used to track the transformation of individual bitter compounds during beer storage by means of LC-MS/MS [187]. The onset of an undesirable harsh bitter aftertaste could be attributed to the evolution of lingering tasting tri- and tetracyclic derivatives. Based on their findings, as these compounds are generated by proton-catalyzed cyclization reactions, Intelmann, et al. [187] proposed the control of the initial pH-value to extend the shelf life of the desirable beer bitter taste. Due to the limited sensitivity for trace compounds, nuclear magnetic resonance spectroscopic studies focused on the

abundance of the major bitter humulones, but also associated changes of the purine metabolism of the yeast during the fermentation step depending on the hopping process [188]. The variety of all perceivable compounds, be it based on the diversity of hops, malt, yeast or originated from the brewing process, results in a complex sensory impression that we perceive as typical for beer beverages. With the abundance of beers commercially available, metabolomics-based design and control of a brewing process have been proven to be a successful way to meet new aroma and flavor requests of consumers [189]. By correlating sensory impressions and evaluations with the analysis of aroma active compounds, a beer was developed in order to specifically serve a market niche. Already in the 1990s, it could be shown that an non-targeted metabolomics and multi-variant approach enabled complex organoleptic processes to be mapped in analytical parameters and thus control the brewing process and the aroma of finished beer.

Molecular Characterization of Beer Types. The molecular signature of a beer is reflected in the less volatile metabolites, as well. Molecules of any volatility were analyzed using extracting ESI-MS, in which an N_2-gas flow is passed through the beer sample and the emerging aerosol is ionized with solvent [190]. By that, it was possible to describe metabolites, which are characteristic for different brewing styles and beer types like lager, Pilsner and wheat. In a more classic LC-ToF-MS approach, phenolic compounds, which originate from both hops and cereals, are identified to differ between the various chemical profiles of German Pilsner and Belgian Ale [191]. In this regard, pale beers show a different pattern in the composition of procyanidins and phenolic acids than beers brewed with darker malt, which is exposed to thermal influences to a greater extent [192]. Using direct-infusion mass spectrometry, the fingerprint of the sugar composition was used for quality control with regard to varying degrees of color and fermentation [193]. Metabolic differentiation of beer types uncovered by NMR spectroscopy is primarily based on the differences in the area of aromatic chemical shifts [194]. Next to phenolic and polyphenolic compositions, it is aromatic amino acids and nucleotides that constitute the chemical profile of lager compared to ale beers. A flow-injection ^{1}H-NMR approach accordingly attributes the differences in the metabolome signature between beers brewed with barley or wheat to their aromatic chemical space [195]. Additionally, beers exposed to deteriorations through bacterial contamination could be identified proving chemometric methods to be a rapid tool for quality control. The aliphatic composition of beer got into focus with regard to NMR-based differentiation of molecular profiles specific for brewing sites and elucidation of varying compositions of different batches within one brewery [196,197]. Metabolites deriving from the yeasts' tyrosine pathway and Ehrlich degradation like tyrosine, tyrosol and phenyl ethanol, which significantly drive the differentiation, indicate an influence of the fermentation parameters. The varying temperature sequences used by brewing sites during the mashing process are reflected in different enzyme activities and thus the composition of linear and branched carbohydrates. Furthermore, non-alcoholic beers were characterized by the presence of fermentable sugars such as glucose and maltose [198]. Mass spectrometric methods revealed specific sugar profiles [199] for alcohol-reduced beers (draft beers) and volatile patterns [200]. Fermentation-derived compounds as esters, alcohols and fatty acids were present in high quantities in alcohol-containing

beers. In contrast, volatiles that originate from the malting and roasting process - including pyrazines, pyrroles and furans - were found to be characteristic of low and alcohol-free beers. A very historic and traditional way of brewing is that of the Trappist beers. Originating in French monastery brew houses, it has spread in central Europe and is nowadays brewed especially in Belgium under strict criteria and requirements: The beer has to be brewed in a Trappist monastery under the monks' supervision, it should witness to business practices proper to a monastic way of life and is not a profit-making venture as all profit is donated (International Trappist Association, 2021). These specifications are reflected in a traditional and time-consuming brewing style. The European funding program TRACES reported on the challenge to describe this unique beer production method through instrumental analysis and enable authenticity control [201]. By means of GC-MS and DART-MS [113], the volatile pattern of over 120 of these traditional beers was analyzed. Chemometric analysis (PLS, LDA and ANN-MLP) was applied to the volatile patterns of a total of 265 beers. By dividing the batch into a training and test set, it was possible to predict a certain group of Trappist beers (100 %) and all Trappist certified beers against non-certified beers (93.3 %). The electron ionization provided access to highly volatile compounds like acetate esters, alcohols, aldehydes, free fatty acids and Maillard reaction products (furylethanone, furylmethanol), whereas the direct analysis in real-time ionization added organic acids, nucleotides, humulinones and sugars to the compositional space. A non-targeted LC-MS approach by Mattarucchi, et al. [112] focused on the successful O2PLS-recognition of the Trappist certified Rochefort beers, basing the analysis on a fingerprint level and leaving open the details about the different chemical compositions.

Beer Aging and Intake. The diversity and change of beers' complex molecular composition do not end with the finalized brewing process. Its staling process, the gradual change of beer over time, can be imitated through so-called 'forced aging'. The change of the volatile profile of beer when stored at 45 °C for 18 days can be tracked using principal component analysis of GC-MS data [202]. This approach enabled a rapid identification of the degree of deterioration affecting beer and the identification of specific compounds of relevance. With increasing storage time, well-established marker substances for the thermal impact on beer like HMF (5-hydroxymethylfurfural), furfural, diethyl succinate and the Strecker-degradation product phenylacetaldehyde were found. From the variety of metabolites analyzed, further components such as DDMP (2,3-dihydro-3,5-dihydroxy-6-methyl-4(H)-pyran-4-one) and hitherto unidentified compositions were proven to be aging-related. In addition to HMF formation, nuclear magnetic resonance spectroscopy showed an influence on the branching of dextrin's and on a plurality of organic acids [197]. Further studies that used a non-targeted LC-MS approach and different forced aging protocols showed the influence on the non-volatile fraction of beer staling. It influences the organoleptic perception not only through the release of aroma components from precursors but also through the changes in flavor-active compounds and their oxidation stability. A short-term storage trial including PCA of several aging steps shows that not only beer volatiles are affected, but also flavonoids, peptides and purines [203]. 5-MTA (5-methylthioadenosine), a sulfur-containing nucleoside deriving from the

yeast metabolome, was identified as a non-volatile oxidation and staling marker by the non-targeted approach and confirmed by further studies [204,205]. The type of hopping, including different plant content, particle size and dry hopping, could also be correlated to the flavor stability and thus decreasing 5-MTA concentration during aging [206]. The addition of antioxidant crowns or chelation agents (Fe^{2+}) against pro-oxidants could not be found to have an impact on the aging correlated metabolome. Metabolites from purine metabolism (deoxyguaniosine, deoxyadenosine and hypoxanthine) could be identified as the most characteristic non-volatile compounds for fresh beer. Besides the obvious influence of ethanol on the human organism, the molecular diversity of beer after its consumption can be tracked. Guerdeniz, et al. [207] developed an LC-MS approach on human urine and plasma to classify metabolites that are increased following beer intake into compounds originating from hops, wort, fermentation and human metabolism. A unique metabolic pattern reflecting the beer metabolome could be selected to establish a compliance biomarker model for the detection of beer intake. This includes metabolites originating from raw material (i.e., N-methyl tyramine sulfate and tricyclohumols) as well as compounds deriving from the brewing process (i.e., 2-ethyl malate and pyro-glutamyl proline). While utilizing a higher resolution mass spectrometric approach (LC-Orbitrap) a second study focused on differences of metabolite changes in urine, following the intake of alcoholic and non-alcoholic beer [208]. Humulinone, an oxidation product of humulone deriving from hops, and 2,3-dihydroxy-3-methylvaleric acid, a fatty acyl formed during fermentation, showed to be biomarkers for beer consumption overall. Against that, concentrations of metabolites related to the alcohol detoxification process such as ethyl sulfate, 2-phenylethanol and ethyl glucuronide only rose after consumption of alcohol-containing beer.

The overview of metabolomics research in the field of brewing science is finished by a summarizing table of literature references (Table A.1 in Supplementary Chapter 1).

1.3 Analytical approach

At the beginning of this introductory chapter, the origin of metabolomics and the conceptual classification of analytical approaches in the field of metabolome analysis were presented. The rationale for why the analysis of small molecules and their changes are of crucial interest has been highlighted with reference to numerous interdisciplinary fields of applications. In the following, the analytical approach applied in this thesis to comprehensively characterize the beer and brewing metabolome is presented. In addition to a deep understanding of the sophisticated analytical techniques used, the (statistic) evaluation and interpretation of data structures is an essential part.

1.3.1 Chemometrics

Studies in the field of comprehensive metabolome analysis usually generate an extensive set of data. The requirement that the analytical method should make as large a number of small molecules available as possible inevitably comes with the fact of large data matrices. Numerous measured features consequently have no intrinsic relevance concerning the actual question of interest. A key challenge, therefore, is to filter out the hidden information that the big picture of the analyzed metabolome offers. For this reason, the development of comprehensive metabolome analysis is closely linked to the improvement and expansion of chemometric tools [209]. Chemometrics is the application of statistical and mathematical analysis to the field of (analytical) chemistry [210]. It searches for molecular regularities and patterns to characterize, track and/or predict sample properties and make those interpretable. In general, two strategies can be distinguished when analyzing data matrices including thousands of variables from biological systems. The explanatory data analysis can reveal similarities of samples based on the multivariate spectral data without any pre-defined structure (unsupervised). The principal component analysis (PCA) processes and reduces the dimensionality of data sets via covariance and eigenvector analysis. It preserves the original relationships and thus can describe characteristic features for resulting clusters. Another possibility to display the natural (not pre-tagged) groupings of the samples is a dendrogram of the Hierarchical Cluster Analysis (HCA), based on the similarity of samples and sample clusters data.

In supervised classification modeling, a criterion of interest is pre-defined for each sample (sample class). When the number of variables (metabolite features) significantly exceeds the number of samples, as for most metabolomics researches, statistical models tend to lead to good classification by chance. This effect is known as overfitting [211]. Hence, careful statistical validation is necessary. The partial least squares regression or better, after Wold, et al. [212], projection to latent structures (PLS) finds the multidimensional direction in the space of metabolite data that explains the maximum variance for the given sample class distinction. Once a model is established

and validated, e.g. by the goodness of the fit (R^2) [213], the goodness of the prediction (Q^2) [214], further internal cross-validation like response permutation test [215] and CV-ANOVA [216] or external validation sets [217,218], unknown samples can be classified by prediction. However, standards of comparison and critical values for significance cannot be defined for these parameters in the context of metabolomics; they must always be viewed and questioned in their entirety (especially R^2 and Q^2). The probably most basic, yet crucial form of validation is to set in context the metabolic information on which the models are based. When analytical signals are characterized and not only regarded as unknown features, it allows to fathom the molecular nature of the statistical differentiation and relate it to findings of existing literature.

The orthogonal PLS analysis (OPLS) [219], as a modified form, is subject to the same restrictions. As a difference to PLS analysis, it divides the space of the explained variance into predictive and orthogonal model compartments. Identifying different sources of variability (predictive and uncorrelated) often leads to better interpretability of the statistical models [220,221]. The question of which of the two variants has the greater potential concerning metabolomics data is a topic of discussion. Mahadevan, et al. [222] assume that in the case of metabolomic data sets, where there is a significant divergence in the within-class variation, the OPLS might perform better. Tapp and Kemsley [223] one year later argue that because of intrinsic mathematical and conceptual reasons, “OPLS will never outperform PLS”. In the case of the data sets investigated in this thesis [224-228], both PLS and OPLS models share very similar statistical and validation parameters and carry the same metabolome information. The OPLS was preferred ultimately because the actual score plots are more stringently interpretable when visualized.

1.3.2 Direct-infusion Fourier transform ion cyclotron mass spectrometry (DI-FT-ICR-MS)

Schematic structure and components. The ultrahigh-resolution mass spectra were acquired on a Bruker solariX Ion Cyclotron Resonance Fourier Transform Mass Spectrometer (Bruker Daltonics GmbH, Bremen, Germany) equipped with a 12 Tesla superconducting magnet (Magnex Scientific Inc., Yarton, GB) and a APLOLO II ESI source (Bruker Daltonics GmbH, Bremen, Germany). The mass spectrometric technique is referred to as either Fourier transform ion cyclotron mass spectrometry (FT-ICR-MS) or magnetic resonance mass spectrometry (MRMS).

Like other mass spectrometers, the FT-ICR-MS can be coupled to numerous separation and ionization techniques. The most common is the flow-injection or direct-infusion analysis into a (nano-)electrospray ionization unit (Figure 1.5, 1). Utilizing high voltages between the metal capillary that carries the analyte solution and a counter electrode, charged aerosolic droplets are created. A heated carrier gas flow (N_2) induces the evaporation of the solvent and undissolved free molecular ions

are released through Coulomb-Explosion. Guided by the potential difference between sprayer capillary and the orifice, the ions are conducted into the MS-unit via a glass capillary (2). The ions are focused by the ion funnel (3) consisting of a series of stacked ring electrodes and guided into a quadrupole (4). In the quadrupole, ions of a specific mass range (m/z 100 to 1000) are brought onto stable trajectories by the applied electric field and are thus filtered. The collision cell (5) allows the collision-induced dissociation of specific ions into charged mass fragments. This option is oftentimes neglected in DI-FT-ICR-MS (except from 2D-FT-ICR-MS). The ion beam is then bundled in the ion transfer optic (6) and focused through lenses (7) to enter the area of highest vacuum. Once arrived in the ICR-cell (8), the ions get trapped by the potential of the trapping plates. Utilizing the high magnetic field of a superconducting magnet, the mass of the ions is analyzed by the induced cyclotron motion after excitation.

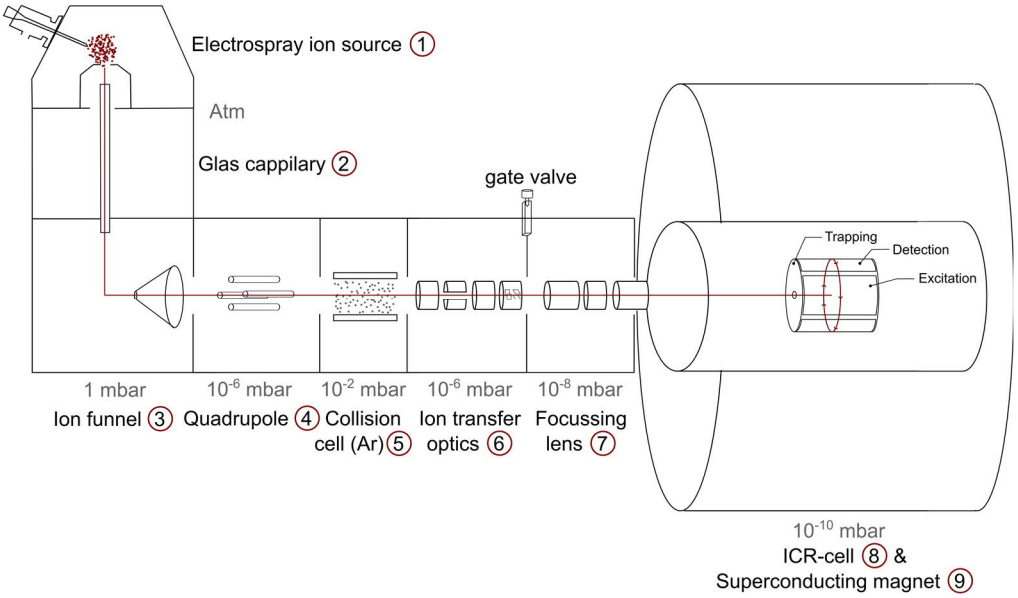

Figure 1.5 | Schematic structure of an ESI-DI-FT-ICR mass spectrometry system.

From moving charged particles in a magnetic field to mass values and chemical compositions. The physical phenomena that occur in the ICR cell and lead to the simultaneous recording of thousands of m/z-values are specified comprehensively by Easterling and Agar [229]. The main basic principles are described in the following. When applied to the homogenous high magnetic field (superconducting magnet) and triggered by the excitation plates, the charged particles of non-zero velocity experience a constant, inward force in the plane perpendicular to that magnetic field. This force is referred to as electromagnetic force or Lorentz force [230] (Eq. 1), where F is the Lorentz force, q the charge state of the ion, V the velocity and B the magnetic field.

$$F = qV\,B \qquad \text{(Eq. 1)}$$

The equilibrium of this inward force with the centrifugal force of the excited velocity motion results in a circular trajectory. The fundamental angular frequency for this type of motion (ω_c) is expressed in the following equation (Eq. 2). It is referred to as the cyclotron equation in reference to the cyclotron experiments by Lawrence in the early 1930s [231].

$$\omega_c = \frac{qB}{m} \qquad \text{(Eq. 2)}$$

This cyclotron motion is the most characteristic and analytically useful, as it is directly related only to the mass (m) and charge (q) of an ion (under the condition of a constant, homogeneous magnetic field). Unlike in other mass analyzers like time-of-flight instruments, there is no need to compensate for the initial kinetic energy of the ions [232]. However, the ions in the ICR cell do not describe an optimal circular path. To increase the residence time inside the cell, a DC-electrical field that limits ions' travel along the magnetic axis is required. Once the ions, due to their velocity in the magnetic axis, reach the trapping plates' potential of similar polarity, they get decelerated and finally reflected. This causes an alteration of the path on which the ions move towards the middle of the cell (trapping motion or trapping oscillation). As a by-product of the trapping potential, there is a radial electric field in the plane normal to the magnetic field axis. The radial electric field and the magnetic field result in the final characteristic ion motion, the magnetron motion [233]. It causes the origin of the cyclotron motion to move along the radial electric field in the same direction of the cyclotron motion. All forces together result in the modified cyclotron motion (Figure 1.6). As the equation of the magnetron motion (Eq. 3) lacks both the mass and the charge variable, it provides no m/z-information and rarely is measured. It depends on the geometric parameter of the cell α, the maximum trapping potential V, the magnetic field strength B and the distance between opposing excitation and detection plates α.

$$\omega_M = \frac{2\alpha V}{\alpha^2 B} \qquad \text{(Eq. 3)}$$

However, detailed characterization is necessary to determine the position of an ion package in the plane perpendicular to the magnetic field. Furthermore, the collision of ions with background neutrals causes the magnetron motion to destabilize and the ions to move towards the electrodes where they are neutralized. Hence, to avoid the loss of ions, a ultra-high vacuum is an important requirement (approx. 10^{-10} mbar). Besides that, the strength of the magnetic field linearly contributes to the cyclotron frequency and ultimately the resolution power of an FT-ICR-instrument, as given in Eq. 2, while also improving several other performance parameters [234].

Describing the (modified) cyclotron motion, the ions induce an altering current between the two detector plates. The induced current frequency is (with compensatory consideration of the magnetron motion) equivalent to the cyclotron frequency and its intensity proportional to the number of ions. Given that thousands of different m/z-packages simultaneously induce current frequencies, a complex frequency vs. time spectrum is observed, the free induction decay FID. By the Fourier transform, a mathematical operation to deconvolute signals into the different underlying frequencies, the (intensity vs.) frequency domain is received. The accurate masses can finally be obtained via the natural inverse relationship between the cyclotron frequency and the m/z-values (Eq. 2).

Mass values on their own, however, do not carry chemical information. The biggest advantage of FT-ICR-Mass spectrometry besides the unrivaled mass resolution is the mass accuracy coming with it. Accurate mass values with an error below 200 ppb (a fraction of the mass of an electron) allow to directly proceed to the compositional space of the measured sample. The combinatory of all plausible atoms making up an ion often results in one molecular formula candidate when the seven golden rules [235], small margins of mass error, and given compositional restrictions [126] are applied; the formula calculation approach. At higher masses and in biological systems that are enzyme-mediated, the molecular formulae that occur are not always unambiguous or within the range of the self-imposed restrictions (e.g. N-atom count > 4) that successfully are established for applications such as natural

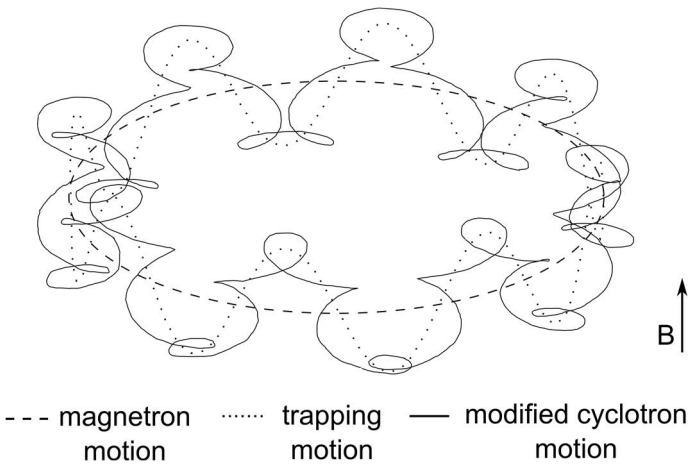

Figure 1.6 | Modified cyclotron motion as resulting from the unperturbed cyclotron motion, magnetron motion and trapping motion.

organic matter (NOM) [126] or extraterrestrial materials [236]. For such unsuitable applications and according to network strategies developed by Tziotis, et al. [237], a further approach was established. The network calculation approach is based on accurate masses of known composition that are validated by isotopologue pattern and function as starting points (Table A.2 in Supplementary Chapter 1, for beer analysis). Further, links to other m/z-signal are created by defined exact mass differences that reflect compositional changes coming with (bio-)chemical reactions (Table A.3 in Supplementary Chapter 1, for beer analysis). A whole network is set up that eventually assigns a molecular formula to each composition.

From unrivaled mass resolution to pictures of molecular complexity. As already stated, DI-FT-ICR-MS on its own does not meet the definitions of metabolomics introduced by Fiehn [4], as it lacks a strategy of compound identification. In the field of profiling and characterization of metabolomic information, it performs what is probably the most important requirement to be fulfilled: “The comprehensiveness in their scope”. DI-FT-ICR-MS enables to comprehensively resolve the entire small molecular complexity a sample contains with no major dependency on the physicochemical properties (polarities) of metabolites involved. Neither a selective sample preparation nor extraction or a discriminatory chromatographic separation is necessary. The differentiation of all accurate mass signals requires great mass resolving power. As well, corresponding mass accuracy of at least 0.1 mDa is needed to assign the elemental compositions within a sample, including isotopic fine structure (0.1 mDa for CHNOS chemical space with m/z up to ~500 Da [238]). According to today’s status, these conditions have only been met in a wide range of applications by Fourier transform mass analyzers such as FT-ICR-MS (Resolving power ~400,000 at m/z 400 for the used 12 Tesla instrument; defined as shown in Figure 1.7). Orbitrap instruments, also based on the Fourier transform of periodic motions (oscillation), are usually linked to liquid chromatography in the routine [239,240]. Individual research applications ventured to evaluate their applicability to fields typically occupied by FT-ICR-MS where highest mass resolution

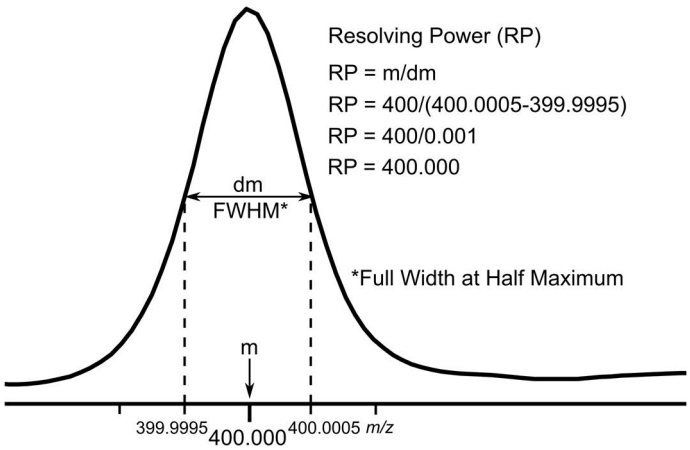

Figure 1.7 | The resolving power defined as Δm at FWHM divided by m.

is necessary [241]. An advantageous property of the orbitrap mass analyzer is that the mass resolving power only decreases to the square root as a function of m/z-values [242], as opposed to a linear negative proportional in FT-ICR-MS. Hence, the more distinctive field of application of orbitrap instruments [243,244] used to be the analysis of higher mass molecules like in proteomic approaches.

The early application field of FT-ICR was petroleomics [245-247], where the big picture of chemical complexity carries information about the interactions and reactivity of petroleum or crude oil constituents. Nowadays, FT-ICR-MS has long found its way into describing complex systems in life sciences as well. Schmitt-Kopplin, et al. [26] quote a colleague's view on chemical complexity as it occurs on a natural level as "complex is synergistic interactions of organic molecules and microbial transformations in natural systems". As vivid as this definition is concerning the analytics of higher organisms or whole ecosystems, it is also true about the production process and analytics of fermented beverages; where the rich chemical composition of organics extracted from raw materials interact during the production process and are subject to microbial fermentation. This applies to ancient, largely uninfluenced fermentation of bread or cereals as well as the highly industrialized and controlled brewing process towards optimized conditions. Maintaining a high-throughput scale, the unique feature of DI-FT-ICR-MS is to resolve this complexity, to provide visualization capabilities, to reveal metabolic patterns and, via accurate mass differences, to describe (bio-)chemical processes (as detailed in Chapters 2-5).

Challenges – adduct formation. In ESI, adducts are referred to as non-covalent complexes of cations (positive ionization) or anions (negative ionization) attached to neutral molecules, forming an ion that contains all involved constituents. The detected mass of this complex corresponds to the sum of all constituents. Therefore a different mass value is observed when compared to simple $[M+H]^+$ / $[M-H]^-$ ions of targeted molecules. In the case of direct-infusion, where all available molecules and inorganic ions are subjected to ESI without prior separation, adduct formation is abundant. Steric effects and intra-molecular geometry of electron clouds define the affinity of certain ions towards adduct formation. In a typical negative FT-ICR mass spectrum of a beer, at least three signals of numerous sugar species occur: The $[M-H]^-$, $[M+Cl]^-$ and $[M+H_2PO_4]^-$ -ions. The adduct ions in particular are very dominant in terms of signal intensity. The glycation pattern of oligosaccharides from C_6 to C_{36} sugars can be traced within a spectrum even on the large-scale view (Figure 1.8). Where little is known about the adduct formation with dihydrogen phosphate, the affinity of sugars with chloride ions is well described in several studies [248-250]. Boutegrabet, et al. [249] even suggest HCl as a hydrophilic dopant for the efficient detection of sugars or glycosylated metabolites to overcome high gas-phase deprotonation energies necessary to form $[M-H]^-$ -ions. In the studies summarized in this thesis, adducts were annotated and phosphate-containing ions were retained as such since it is not possible to differentiate between covalent and non-covalent species solely based on their mass. Assuming that only a few covalently

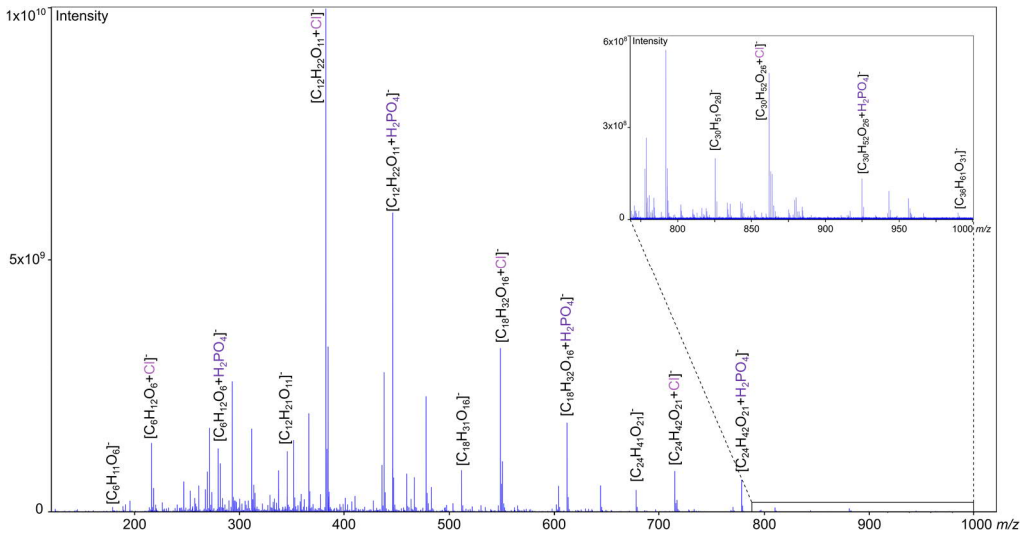

Figure 1.8 | The large-scale view of an FT-ICR mass spectrum featuring $[M-H]^-$, $[M+Cl]^-$ and $[M+H_2PO_4]^-$ ions of saccharides.

chlorinated compounds are to be expected in beer, chlorine-containing compositions were converted into their equivalent $[M-H]^-$-ion in silico, resulting in the overall CHNOSP-chemical space.

Adduct formation provides the opportunity for sensitivity increase and potential structural information about functional groups that correlate with the affinity to form adducts. In contrast, there is a very decisive disadvantage in the intensive formation of sugar (pseudo-)ions: Ion suppression and ICR cell overload. As the solvent evaporates in ESI, limited charges in a solvent cluster are available to ionize molecule species [251]. Due to their great abundance and high affinity for adduct formation, numerous charges are claimed by sugar ions and clusters. In addition, the efficiency of droplet formation and evaporation is influenced by salts, which in turn affects the ionization rates and ultimately the sensitivity of the remaining molecular diversity [252]. Polar analytes, which are intended to be reached through the direct-infusion approach, in particular, are more susceptible to suppression [253]. For this reason, and because an extensive sample preparation would lead to a loss of the claim to comprehensiveness, a suitable dilution had to be found to achieve the optimal state of lowest ion suppression at highest sensitivity. A representative beer sample aliquot was measured in different dilution ratios (in MeOH, triplicates). The quality parameters mass resolution, mass error, annotated monoisotopic formulae and sum of ion intensities (ICR cell load) showed that a 1:500 dilution is the best compromise between reproducible high spectral quality and sensitivity (Figure 1.9). Additionally, the ion accumulation time was lowered to 0.25 seconds to avoid overload of the ICR cell. Thereby, a phenomenon called the space-charge-effect (SCE) could be minimized.

Challenges – space charge effects. The accumulation of many ions of high intensity in the ICR cell has an adverse effect on the mass accuracy and resolution, the so-called space-charge-effect (compare Figure 1.9). The phenomenon often occurs when a mass or frequency range of the spectrum is dominated by large signals. It can be the case if samples are generally relatively poor in diversity (e.g. found for alcohol-free beers) and especially when at the same time a small number of ions (mostly adducts) are very dominant. In beer, these adducts are common for sugars, as shown in Figure 1.8. The space-charges are spatially distributed electric charges in a non-conductive medium caused by an excess of negative or positive charge carriers. Such space charges occur only in dielectric media (e.g. vacuum). Space charges are accompanied by unwanted electrical fields causing space-charge-effects.

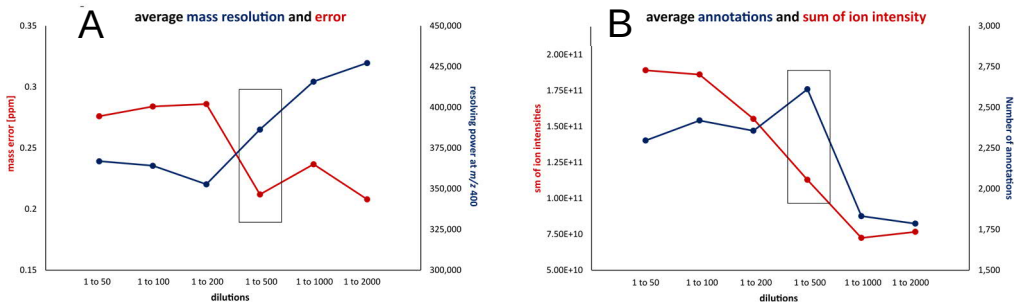

Figure 1.9 | Average mass resolutions and errors (A) and average number of annotations and the sum of ion intensities (B) found for triplicates of FT-ICR mass spectra of beers in different dilutions.

In the case of FT-ICR-MS, they arise from the influence of the electronic field of ions in the trapped analyzer ICR cell upon each other [254]. It results in a significant change in the observed cyclotron frequency. The actual observed frequency of motion of an ion in the homogeneous magnetic field was approximatively described as in Eq. 4 by Jefries, et al. [255] and Francl, et al. [256]. The first term $\frac{qB}{m}$ is the unperturbed cyclotron frequency. The second term $\frac{2\alpha V}{a^2 B}$ is equal to the magnetron frequency of the ions. The third term now describes the influence of the space-charge-effects. Besides a constant related to the geometry of the ion cloud (G_i) and the permittivity of free space (ε_0), it mostly depends on the ion density (ρ). The influence of the charge state (q) is under debate [254]. The SCE is shown to usually happen in MALDI due to inconsistent ion yield [257]. In ESI, big ion densities occur when either the sample is too concentrated or ion clusters or adduct formation drastically increase the number of charged particles. The described SCE is referred to as the 'global' SCE. It is worth noting that the strength of the magnetic field (B) is inversely proportional to the 'global' SCE.

$$\omega_{obs} = \frac{qB}{m} - \frac{2\alpha V}{a^2 B} - \frac{q\rho G_i}{\varepsilon_0 B} \quad \text{(Eq. 4)}$$

It is not only the overall sum of ions in the cell that defines the effect of space-charge. The phenomenon also occurs as 'local' SCE as described in approximation by Masselon, et al. [258] with Eq. (5).

$$(m/z)_i = \frac{A}{f} + \frac{B}{f^2} + \frac{CI_i}{f^2} \quad \text{(Eq. 5)}$$

The three coefficients A, B and C are explained in-depth by the later authors and account for important factors in FT-ICR mass measurements, including the 'global' space-charge-effect. The third term describes the 'local' SCE and indicates that it is dependent on the signal intensities I_i. A signal of high intensity will influence the cyclotron motion by a more intense specific electric field. The effect of big ion clouds of molecules (and their electric field) is of greater importance to ions of similar frequencies (masses) as their interaction prolongs continuously during the entire measurement. The relative concentration of the ion species, especially of those with similar frequencies and parallel circular motion, determines the 'local' SCE. Thus, deviations from the theoretical cyclotron motion can be seen for certain frequencies and ultimately m/z-areas in the FT-ICR mass spectrum even in case the overall ion density is balanced by sample concentration and ionization/ion transfer parameters.

One approach to counter the SCE phenomenon is a dynamic calibration. This type of calibration is not dependent on linear or quadratic calibration functions. The method developed is described in Smirnov, et al. [259] and can be summarized as follows. The method is based on the estimation of the density of data points on mass difference maps (MDiM) using Gaussian kernels followed by a curve fitting with an adapted version of the particle swarm optimization (PSO) algorithm. The MDiM is defined by the m/z-differences of respective experimental data points to an extensive calibration list in the ppm scale. For the kernel density estimation, Gaussian kernels are used to evaluate the closeness of the data points. The calibration curve is created by an adapted particle swarm optimization algorithm going through the maximum density path. The PSO is a gradient-free form of an algorithm, meaning that it is applicable for optimization problems where derivative functions are difficult or not possible to calculate. Thus, it is flexible; it does not depend on linear or quadratic relations and can be used for optimization problems of discrete, discontinuous or noisy data.

The practical integration was realized in an in-house developed calibration tool based on error densities. By that, it is possible to cut the spectra into different sections and recalibrate them based on error distributions without a limitation to linear or quadratic functions (Figure 1.10 A, B). The best results were achieved when different error profiles in the samples were cut and viewed individually. To find a systematic, distinct error distribution, a comprehensive calibration list is necessary. In the presents studies, about 2,400 mass values of chemical compositions occurring

in the majority (at least 33 %) of 200 measured samples were used. A trustworthy exhaustive calibration list is mandatory and was achieved by the annotation of a matrix including all measurements with different annotation techniques (formula and network calculation) and error margins (0.3 ppm to 0.1 ppm). Only consistent annotations were kept and the list was validated by the respective ^{13}C-isotopologues.

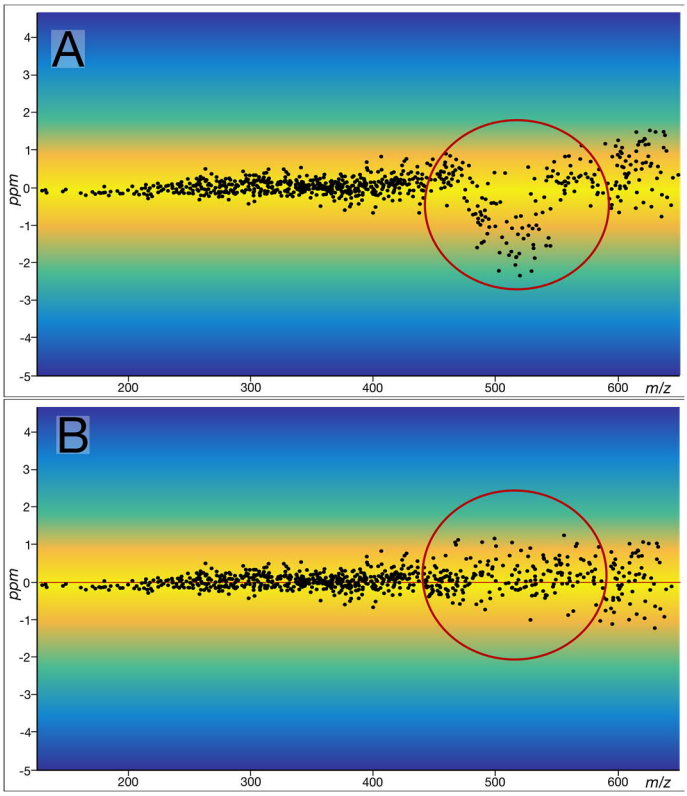

Figure 1.10 | Density of mass errors found in FT-ICR mass spectra of beer before (A) and after (B) density-based spectral calibration.

1.3.3 Liquid-chromatography-coupled mass spectrometry (LC-ToF-MS)

Schematic structure and components. The high-resolution mass spectra were acquired on a time of flight maXis mass spectrometer (Bruker Daltonics, Bremen, Germany), coupled to a UHPLC system (Acquity, Waters, Eschborn, Germany) (Chapter 2) and a Shimadzu LCMS-9030 Q-ToF-System (Shimadzu Deutschland GmbH, Duisburg, Germany) (Chapter 3-5). Featuring the same main components, the schematic structure of the latter mass analyzer is described below (Figure 1.11).

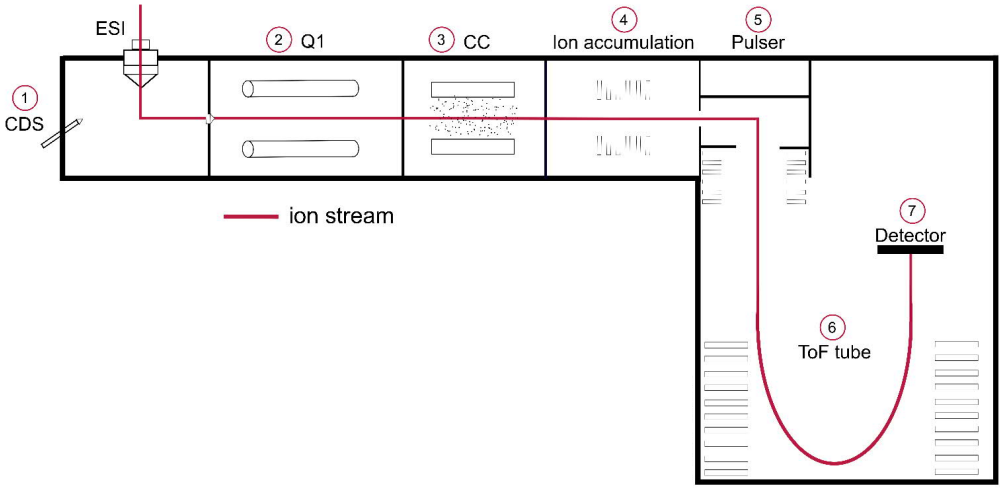

Figure 1.11 | Schematic structure of an ESI-Q-ToF mass spectrometry system.

As described for FT-ICR-MS, an electrospray ion source is used. Additionally to the analyte eluent spray, a second ESI-source is integrated into the ion chamber. It is connected to the calibrant delivery system (CDS) (1) that enables the addition of known calibrant ions to the ion stream. By this, it is possible to recalibrate either every sample run or even every measurement scan to obtain high mass accuracy (~ 0.5-2 ppm). In the quadrupole (2), ions of a specific mass range (m/z 50-1500) or a specific mass value (1 Da window) are filtered for MS^1 or MS/MS data acquisition respectively. Inside the collision cell (3), all selected MS^1 ions can be fragmented through collision with neutral gas molecules to obtain molecular structure information. In the ion accumulation unit (4), the ions are accumulated through a damming electric field. Once the ions get released, they reach the pulser (5), where the ion package is pushed orthogonally into the ToF (time of flight) tube. Inside the ToF tube (6), a focusing non-linear potential is located at the reflecting point to compensate for several phenomena causing different kinetic energies and starting points for masses

of different m/z-values. After the ions reach the detector (7), the mass values can be calculated through their time of flight (from pulse trigger to detection). The ToF for the charged molecules is quadratically proportional to their m/z-value leading to higher mass resolution for higher masses.

Additional analytical dimensions. The mass resolution of ToF-instruments, although it is constantly being improved, does not reach the level of magnetic resonance mass spectrometry by (at least) one order of magnitude. This comes with the disadvantage of required pre-separation of the analyzed mixture as m/z-signals would overlap otherwise. The mass accuracy (molecular formula) and isotopologue pattern of separated compounds might often be ambiguous. However, the crucial benefit of ToF-mass analyzers is that they can be operated at a high scan frequency (~ 25 Hz) when compared to the DI-FT-ICR-MS approach described (~ 2 Hz). The high scan rate enables the detection of mass signals with numerous data points per chromatographic peak at sufficient sensitivity when coupled to liquid chromatography. Furthermore, ion fragmentation in the collision cell can be performed.

Liquid chromatography does not only separate the highly complex analyte mixture in different segments on a time scale. It also carries information about the physicochemical properties of respective compounds as expressed in retention times at certain conditions. Accurate m/z-values on their own, as in DI-FT-ICR-MS, only provide information about the compositional nature of a molecule. Combined with specific retention behavior, isomeric molecules can be separated and defined as different compound signals. In the range of metabolite analysis, large public databases show values between 1 and 1000 for the multiplicity of exact masses (number of isomers for that specific formula). Theoretical calculations of potential yet-unkowns demonstrate that the chemical richness might exceed these values in many orders of magnitude [26]. Hence, the separation of potential isomeric compounds adds a significant dimension to the characterization of complex biochemical systems. Mass features can be detected as separated molecular compounds. A disadvantage is that a large number of more polar metabolites unavoidably will be lost due to insufficient retention behavior (when one-dimensional non-tandem LC is used).

The comparatively high scan speed enables to interrupt the measurement of all ions by specific ion fragmentation experiments. In the data-dependent analysis (DDA) one full-range MS^1 event (50-1500 m/z) serves as survey scan. Based on that, subsequent MS/MS-fragmentation events are executed with precursor ions initially detected in the corresponding MS^1-data point. Depending on the scan rate of the instrument and the necessary mass resolution and sensitivity, the two to ten ions with the highest intensity are fragmented before the cycle starts again with a full scan.

The Metabolomic Standards Initiative categorizes metabolite identification as complete identification of the structure, including molecular connections and stereochemical assignments [10,134]. As far as mass spectrometric analytics is concerned on its own, this goal can only be achieved by narrowing down possible structures and synthesizing reference standards for confirmation. A second route, no

less time-consuming and uneconomical, would be to laboriously isolate unidentified compounds by chromatographic techniques and subject the pure substances to NMR-analysis. The gold standard cannot realistically be achieved for all hundreds to thousands of compounds in a complex mixture. Nevertheless, certain fragment ions and neutral losses are significant indications of the molecular identity of analyzed compounds, as best shown for lipidomic approaches differentiating lipid classes [260]. MS/MS-fragmentation patterns are still not able to offer a comprehensive identification, but it is possible to narrow down molecular identities to certain substructures. Together with physicochemical information from chromatographic behavior, marker compounds can be classified (level 3 identification [10]). A way to further improve identifications is literature and library research as already discussed in chapter 1.1.4. Despite the undoubtedly limited availability of standard spectra, the compound libraries are a rich source of numerous chemical structures that can be used as a proxy for computed fragmentation spectra. In-silico prediction tools like MetFrag [261,262] compute likely fragments of database known compounds by bond dissociation approaches and neutral loss rules to score a potential match with experimental data. MS-Finder [263], also bond dissociation driven, adds the dimension of mass accuracy and isotope ratios. Competitive fragmentation modeling [264] is an alternative approach utilizing a machine learning-based probabilistic generative model for MS/MS fragmentation processes. Blazenovic, et al. [265] showed during the 2016s CASMI-contest (critical assessment of small molecule identification) that the combination of different approaches leads to the best coverage and accuracy for identifying natural products. For de-novo identification strategies, fragmentation trees and mass spectral trees can be utilized [266].

Based on experimental data and potential decisive compounds for differentiating sample characteristics, MS/MS similarity networks as computed by Cytoscape [267] mirror molecular similarities. Compounds that share similar fragmentation patterns correlate with strong chemical similarities. In-silico fragmentation comparison, as described above, can then offer tentative structural information by the assignment of structures and alignment of known compounds to still-unkowns. Matching retention behavior and fragment signals indicate similar compound classes, create links between chromatographic features, and enable level 2 to level 3 identifications for compounds of interest (the necessity of experimental fragmentation data for comparison for level 2 identification is under debate and depending on the case). In case a specific compound is of highest interest and a level 1 identification is necessary, the information provided by LC-ToF-MS can pave the way for deeper investigations (compare Chapter 4).

1.3.4 Positioning in the field of metabolome analysis

To fit the original definition of metabolomics [4], an analytical approach targeting metabolites needs to be (1) comprehensive and avoid the exclusion of metabolites, (2) high-resolving and sensitive, (3) universally applicable to different matrices, (4) include a concept for metabolite identification and (5) quantification. The combined approach that is applied in this thesis arguably meets most or even all of these requirements.

By minimal sample preparation (dilution in methanol), it is possible to address the vast majority of the metabolic diversity, including compounds of very different polarities. Coupling to soft electrospray ionization enables the detection of molecules of a wide range of physicochemical properties. Nuclear magnetic resonance spectroscopy, complementing the analytical approach in Chapter 5, does not show any discrimination (with limitations regarding sensitivity). The unrivaled mass resolution of DI-FT-ICR, chromatographic resolution of LC-ToF-MS and the superior sensitivity of mass spectrometry when compared to other analytical techniques surely fulfill the second requirement. Even if the approach should be adapted for each matrix to achieve best sensitivities, it can be used universally. Less concentrated solutions (NOM/DOM) should be extracted and concentrated beforehand [126]. For very volatile mixtures, SICRIT (soft ionization by chemical reaction in transfer) [268] is a suitable alternative ionization method (data not part of the thesis). The concept of identification is realized in ion fragmentation experiments and library or literature search leading to identification levels of 1-3. The quantification requirement of the compounds alone is not fully met solely by the mass spectrometric approaches. Under the common premise that quantification refers to concentration determination in SI units and not a semi-quantitative evaluation of the concentration in detector units, this aspect of true metabolomics might not be accomplished to its fullest without the use of qNMR (Chapter 5). Therefore, it remains to be discussed whether the DI-FT-ICR-MS/LC-ToF-MS analytical approach should be called true metabolomics. The more colloquial definition of metabolomics as given by the Metabolomics Society [13] certainly fits. It represents an analytical method well-suitable to elucidate the molecular diversity and chemical complexity of beer and the brewing process. In-depth compositional and molecular knowledge, extracted from a comprehensive metabolite picture, can be revealed.

Chapter 2 |
Decomposing the Molecular Complexity of Brewing

The compositional space of a set of 120 diverse beer samples was pro*fi*led by rapid direct-infusion (DI) Fourier transform ion cyclotron mass spectrometry (FT-ICR-MS). By the unrivaled mass resolution, it was possible to uncover and assign compositional information to thousands of yet unknown metabolites in the beer matrix. The application of several statistical models enabled the assignment of different molecular patterns to certain beer attributes such as the beer type, the way of adding hops and the grain used. The dedicated van Krevelen diagrams and mass difference networks displayed the structural connectivity of the annotated molecular formulae. Thereby it was possible to provide a base of knowledge of the beer metabolome far above database-dependent annotations. Typical metabolic signatures for beer types, which re*fl*ect differences in ingredients and ways of brewing, could be extracted. Besides, the complexity of isomeric compounds, initially pro*fi*led as single mass values in fast DI-FT-ICR-MS, was resolved by selective UHPLC-ToF-MS/MS analysis. Thereby structural hypotheses based on FT-ICR's molecular formulae could be con*fi*rmed. Benzoxazinoid hexosides deriving from the wheat's secondary metabolism were uncovered as suitable marker substances for the use of whole wheat grains, in contrast to merely wheat starch or barley. Furthermore, it was possible to describe Hydroxymethoxybenzoxazinone(HMBOA)-hexosesulfate as a hitherto unknown phytoanticipin derivative in wheat containing beers. These *fi*ndings raise the potential of ultra-high-resolution mass spectrometry for rapid quality control and inspection purposes as well as deep metabolic pro*fi*ling, profound search for distinct hidden metabolites and classi*fi*cation of archeological beer samples.

This chapter has been published as Pieczonka, S. A., Lucio, M., Rychlik, M. & Schmitt-Kopplin, P. Decomposing the molecular complexity of brewing. Nature Partner Journal Science of Food 4 (11), 1-10, (2020). The term FIA-FT-ICR-MS was exchanged due to uniform naming of the approach, with explicit permission.

Candidate's contributions: S.A.P. designed the experiments, analyzed and interpreted the data. S.A.P wrote, revised and approved the final paper. S.A.P. performed the instrumental experiments. S.A.P. performed the statistical treatment, data mining, interpretation and visualization.

2.1 Introduction

The yearly worldwide consumption of beer adds up to 1.96 billion hectoliters (as of 2016). Thus, beer is, besides wine, the most consumed fermented alcoholic beverage. Brewing handicraft evolved in more than 5000 years from ancient brewers over the German purity law from 1516 to high scaled, modern industrial brewing [269]. The most recent developments, namely the 'craft beer revolution', refuse the trend of 'macrobreweries' and emerge a multitude of smaller, more diverse brewhouses. Hops (Humulus lupulus L.), which are the main focus of experimentation, are one of the defining ingredients of beer. Besides that, (barley) malt, water and yeast contribute to the complex aqueous mixture of volatile and non-volatile molecules known as beer. The small molecules (<1000 Da) are referred to as the beer metabolome and play an important role in beer characteristics such as taste, aroma, yeast fermentation, foam stability, or beer aging. The measurement of a group of chemically characterized and biochemically annotated metabolites is known as targeted metabolomics. Using different analytical methods such as GC- and LC-(ToF)-MS/MS allowed to characterize the phenols and polyphenols [270], hop bitter acids [271], the carbohydrates and their degradation during storage [272], or their reactions with amino acids and proteins analyzing Maillard reaction markers [273]. Profiling specific volatile compounds in beer enable to show a difference between top and bottom-fermenting yeasts [274]. In contrast, non-targeted metabolomics means a comprehensive analysis of all measurable analytes, including chemical unknowns [7] achieving an optimal metabolome coverage [275]. It provides extensive datasets, which are used to explore novel features or characterize differences between samples using biostatistics, biochemistry, and informatics for data mining and interpretation [6,276]. By non-targeted metabolic profiling it is possible to differentiate beer types [112,277], age groups [204], origins [113], different storing conditions [203], color characteristics [193], or hop varieties [175,176] using high-resolution analytical methods. Profiling of volatile fingerprints of hops and barley [181], yeast strains [174], or different beer types [278] was carried out by means of either headspace or bubbling burst (GC)-MS analysis. Besides mass spectrometry, nuclear magnetic resonance (NMR) spectroscopy was applied to beer analysis to differentiate beer types [197], brewing sites [196], raw materials, or influences on yeast fermentation [188]. The range of analyzed molecules, which characterize the differences of the samples, reaches from carbohydrates, amino acids, small organic acids over bitter acids, (poly-)phenols and purines to more volatile terpenes, esters, alcohols, aldehydes, and ketones. One major drawback of non-targeted metabolomics is the dependence on and limitation to database annotations. The outnumbering unknown signals often referred to as "molecule features" are not characterized.

Non-targeted metabolic profiling can exceedingly benefit from a promising mass spectrometric method in beer analysis, the Fourier transform ion cyclotron resonance (FT-ICR) mass spectrometry. Gougeon et al. [111,279] already described the chemical space of wine by a direct-infusion ESI-method coupled to the FT-ICR instrument. It was shown that this approach has the power of resolving not hundreds,

but thousands of molecules in a short time. Indeed, Fourier transform mass spectrometry techniques are the most advanced mass analyzers concerning mass accuracy and resolving power. The unrivaled mass resolution enables a direct-infusion approach, which gives access to compounds of a wide polarity range. Due to ultra-high-resolution (~500,000 res. power at m/z 400) and accurate mass measurement (~0.1 ppm), FT-ICR-MS can separate and assign a molecular formula to each signal, providing information about the (bio-)chemical class of these often yet unknown analytes. As thousands of features can be characterized it provides universal information about the analyzed samples that remain hidden otherwise. Furthermore, by connecting marker substances by mass difference networks [237] and displaying patterns of chemical compositions in van Krevelen diagrams [126], it is possible to infer the markers' compositional nature. These visualization methods allow us to make well-sustained assumptions of molecule groups, which differentiate diverse samples. As a result, the disclosed metabolic signature of unknown samples can be recognized and assigned. Specific compositions, which are essential for characterizing certain metabolic profiles, can be perceived by statistical evaluation of rapid and holistic FT-ICR measurements. However, DI-FT-ICR-MS lacks information about isomers and concrete molecular structures, which requires a second analytical technique. Tandem UHPLC-ToF-MS is able to resolve isomeric compounds and provide deeper structural information. Based on the exact m/z-values found in FT-ICR, the fragmentation of dedicated compounds and isomers enables identification of the most significant molecules on a structural level. The presented approach closes a gap between the availability of a huge multitude of analyzed features, their compositional annotation and deep structural information. It opens the application for the recognition of the metabolic signatures and the profound search for distinct hidden metabolites.

2.2 Results

2.2.1 Visualization of the molecular complexity

A diverse set of 85 bottled beers from different countries and of different types was profiled as the first batch. To explore the compositional diversity and molecular complexity of each individual beer the samples were analyzed by direct-infusion ESI (–) FT-ICR-MS. The chemical space of beer is as diverse as the variety of different raw materials and their treatment during the brewing process including malting, roasting, boiling, fermentation, and filtration. As an example, Figure 2.1 shows the spectrum of a Pilsner beer. The macroscopic general view (Figure 2.1A) shows the abundance of (oligo-)saccharide patterns. However, the detailed view of a single nominal mass (Figure 2.1B) revealed up to 27 m/z-values within the mass of 391, which could be assigned to molecular formulae with a mean error of <0.1 ppm (<1/10 of an electron mass, respectively). The molecular variety of the

beer samples, which ranges from peptides [$C_{19}H_{28}N_4O_5$], carbohydrates [$C_{13}H_{24}O_{11}$], fatty acids [$C_{21}H_{40}O_4$] through their sulfates [$C_{18}H_{31}O_7S$] to isotopologues of potential Maillard reaction products like desoxyfructosyl(iso-)leucine [$^{13}C_1C_{11}H_{23}NO_7$], could be displayed in one single nominal mass by highly resolved FT-ICR measurements. In total, an average of 2800 compositions could be found in each beer spectra. Bearing in mind that distinct isomers exist for a given formula, the 27 molecular formulae in the spectrum excerpt represent 68 hits reaching from 0 to 11 isomers in common databases. Therefore, the DI-FT-ICR-MS spectrum of a single beer can be considered as an instantaneous overview of several thousands of compounds present in various concentrations.

All m/z-values assigned to a molecular formula and present in at least 5 % of all beer samples are depicted in a two-dimensional van Krevelen diagram (Figure 2.2). Thereby the masses can be associated to chemical families like carbohydrates, peptides, organic acids, phenolics, lipids, nucleotides or even hop bitter acids and their corresponding derivatives [26]. Plotting in the van Krevelen diagram the 350 formulae, which were present in over 95 % of the beers spectra, we can recognize that the beer matrix seems, in general, to be defined by carbohydrates and derivatives, peptides, but also the hop bitter acids. In contrast to this, lipids and phenolic compounds were more specific for the single beers or group of beers (Figure B.1 in Supplementary Chapter 2).

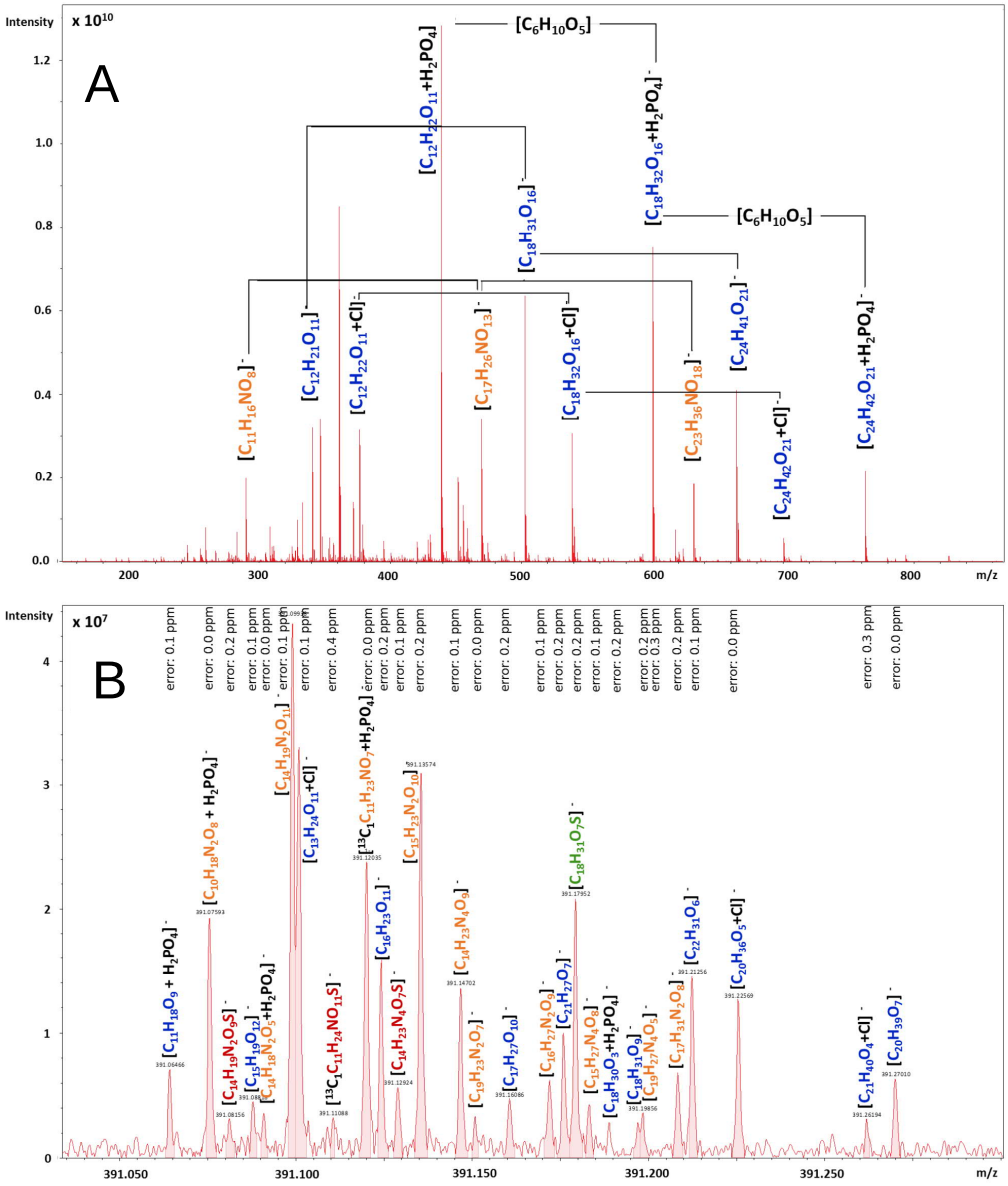

Figure 2.1 | FT-ICR-MS spectra of a Pilsner beer. The full-scale view (A) shows hexose condensation patterns and an excerpt of the nominal mass m/z 391 (B) illustrates the resolved chemodiversity of the beer inside one single nominal mass. Annotated molecular formulae and mass errors are given above the mass peaks. Color code of the molecular formulae: CHO blue; CHNO orange; CHOS green; CHNOS red. Adduct formation is expressed by $+H_2PO_4$ for dihydrogen phosphate and +Cl for chloride

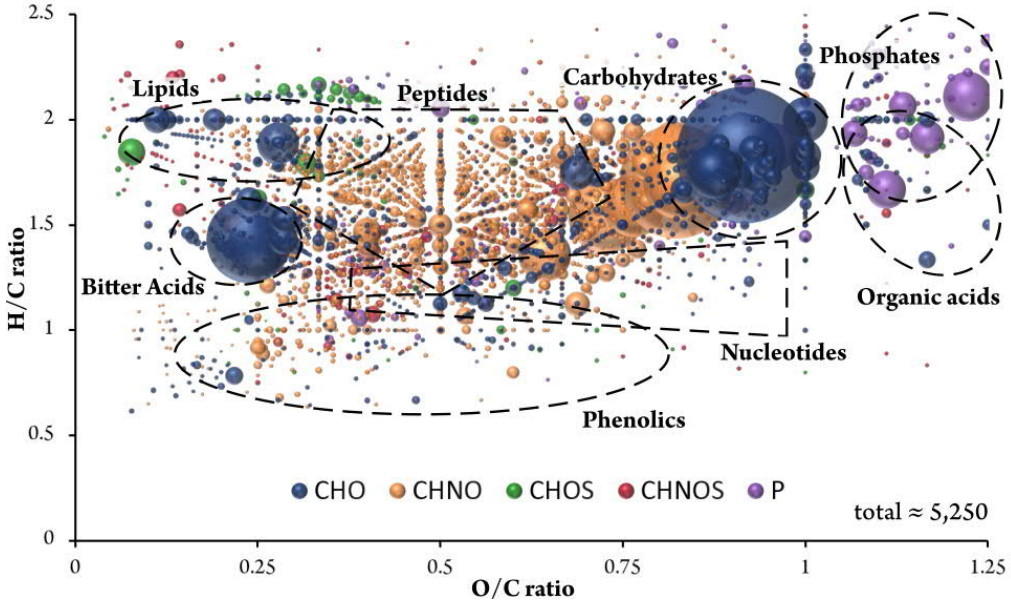

Figure 2.2 | Van Krevelen diagram (H/C vs. O/C) of the annotated molecular formulae appearing in more than 5 % of all beer samples. Areas specific for certain compound classes are marked with dotted lines. Color code: CHNO blue; CHNO orange; CHOS green; CHNOS red; P violet; Cl light violet. The bubble size indicates the mean relative intensities.

By displaying assigned elemental formulae in a mass difference network [237] one can exploit the exact mass information provided by FT-ICR-MS and set the CHO, CHNO, CHNOS, CHOS, and P chemical spaces into relation. Figure 2.3A shows that the sulfur-containing spaces were separated from a highly connected CHO/CHNO sphere. The same holds true for phosphate-containing molecules, which were mostly connected to the other spaces by glycerolphosphate, phosphoethanolamine, hexosephosphate, and phosphorylation itself. Mass differences indicating mainly reactions with amino acids were the most dominant inside the CHNO chemical space and between CHO and CHNO spaces (~50 %). Condensation of hexose and pentose species are the most abundant sugar-related reactions connecting (oligo-)saccharides with their dedicated aglyca. Reactions regarding more specific metabolic pathways like prenylation (terpenoids) could be found besides the

A

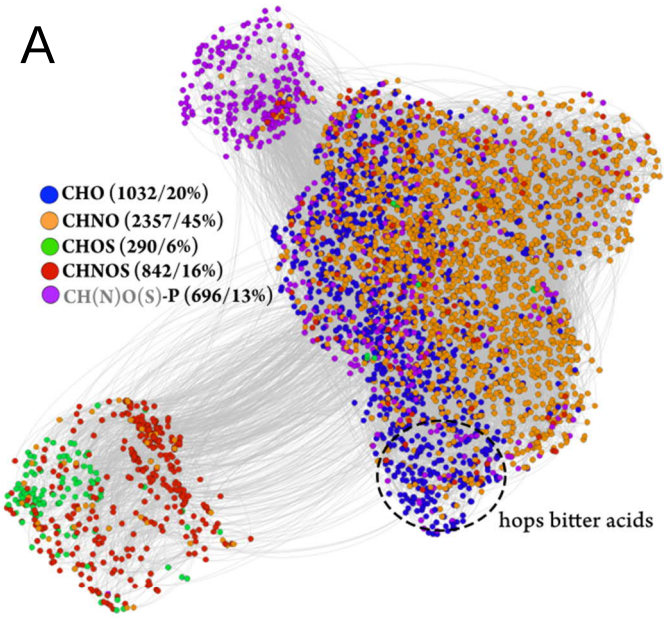

B

reactions	difference		frequency
	Mass [u]	sum formula	
glycerol condensation	74.03678	C_3H_4O	1572
glycine condensation	57.02146	C_2H_3NO	1539
alanine condensation	71.03711	C_3H_5NO	1527
serine condensation	87.03203	$C_3H_5NO_2$	1323
…			
deoxy-pentose condensation	116.04735	$C_5H_8O_3$	1157
pentose condensation	132.04226	$C_5H_8O_4$	1149
hexose condensation	162.05283	$C_6H_{10}O_5$	1112
…			
prenylation	68.06260	C_5H_8	807
hexanoic acid condensation	98.07317	$C_6H_{10}O_1$	685
shikimic acid condensation	156.04226	$C_7H_8O_4$	672
…			
uracil condensation	94.01671	$C_4H_2N_2O$	615
thymine condensation	108.03236	$C_5H_4N_2O$	603
ribose-5-phosphate condensation	212.00859	$C_5H_9O_7P$	139
…			
palmitoleic acid condensation	236.21402	$C_{16}H_{28}O_1$	51
stearidonic acid condensation	258.19837	$C_{18}H_{26}O_1$	30
eicosenoic acid condensation	292.27662	$C_{20}H_{36}O_1$	5

Figure 2.3 | Mass difference network of the beer samples (A) and frequencies of (bio-)chemical reactions therein (B). Chloride adducts were converted into their dedicated [M-H]-ions in silico. Color code compare Figure 2.2. The area of hops bitter acid derivatives inside the mass difference network is marked. An excerpt of (bio-)chemical reactions with their dedicated mass and molecular formula differences and the frequencies they occur in the network is given below.

condensation of nucleic bases and glycerol. Overall, raw chemical-related reactions (roasting / malting / boiling) were represented on a par with biochemically driven reactions (raw material/fermentation). An extract of the frequencies of individual modifications can be found in Figure 2.3B.

2.2.2 Multivariate analysis

The hierarchical clustering analysis (HCA) showed a general overview of the similarities across the different samples revealed a cluster of typical lager beers samples (Figure 2.4). The quality control samples, namely aliquots of one same lager beer, were correctly located in exactly this group and built their own sub-cluster, which showed that the fingerprint of this beer is conserved through the different batches. Beers with special grains like roasted malt, oat, or gluten-free grain were grouped as well as wheat beers and alcohol-free beers. Besides these clusters, there was a group mainly but not exclusively consisting of craft beers and special Belgian beers. Some more conventional beers were also allocated inside this group, probably due to the overlap of specific molecular patterns. A detailed inspection of the dendrogram plot revealed two pairs of beer from one brewery (denominated "brewery A" in the following)—namely the brewery A's lager and wheat beer with their corresponding alcohol-free versions. These pairings reflect the fact that the dealcoholization process in this brewery consists mainly of downdraft evaporation of the original alcohol-containing beer. The brewing process itself stays the same, which makes these beers very similar.

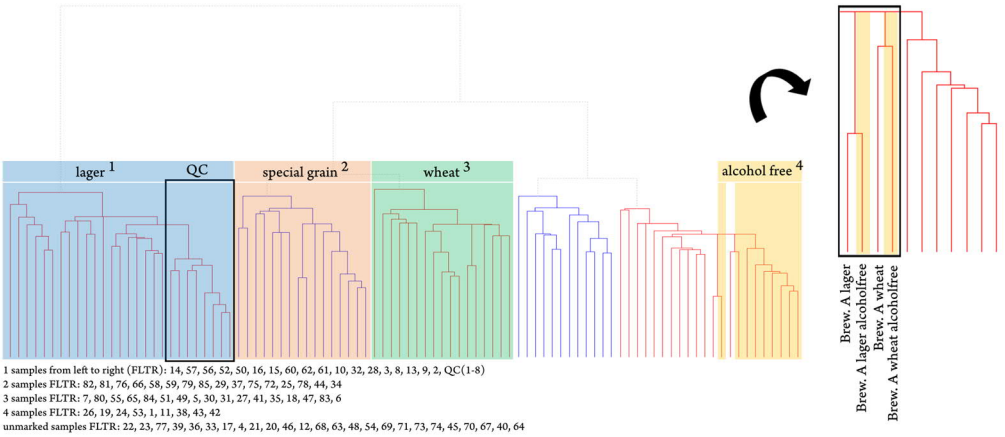

Figure 2.4 | Hierarchical clustering of the beer samples' FT-ICR mass spectra. Color code of the observed clusters: lager beer blue; beer brewed with special grain red; wheat beer green; alcohol-free beer yellow. The cluster of QC lager beer samples is framed. The enlarged excerpt shows the cluster of one brewing site's alcohol-containing and alcohol-free beers. The samples' order is stated below.

2.2.3 OPLS-DA model 1: beer type

The first OPLS-DA model distinguishes between the different beer types (Figure 2.5). Wheat beers were separated from the other beer types in the first component (x-axis). In the orthogonal second component (y-axis) it was possible to differentiate between classical lager beers and craft beers. The fourth class, the traditional Belgian abbey beers, were located in the middle of the score plot, whereas the spontaneous inoculated geuze beers were excluded from the model as outliers. The detailed statistical (Table B.1 in Supplementary Chapter 2), loading plots (Figure B.2 in Supplementary Chapter 2), and score plot coordinates (Table B.2 in Supplementary Chapter 2) for each model are given in Supplementary Chapter 2.

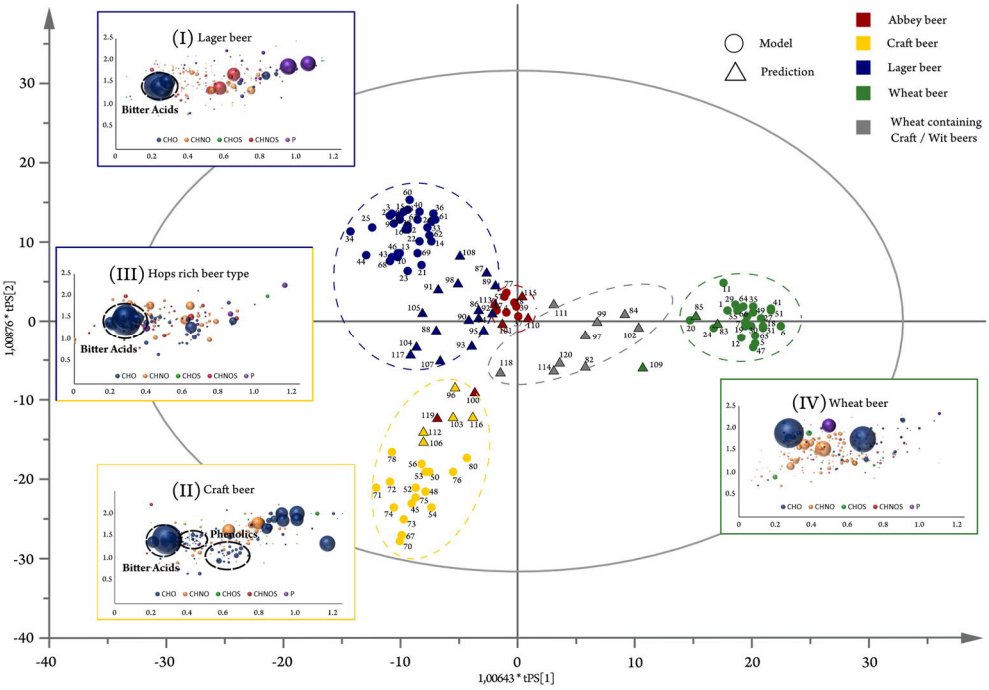

Figure 2.5 | OPLS-DA model's score plot for the beer type observation. The score plot is surrounded by the different observations' van Krevelen diagrams (lager beers (I); craft beers (II); hops-rich beer types (III); wheat beers (IV). Color code and bubble size compare Figure 2.1. Samples included in the model calculation are depicted as circles, whereas predicted samples are represented as triangles. Craft and lager beers are summarized as hops-rich beer types to reflect the separation of metabolites in the first component.

The first component revealed the most significant molecular pattern separating wheat beers from the lager and craft beers. Both the latter beer types feature a great amount of hops compared with wheat beers and thus can be denominated “hops-rich beer types”. The masses with the most negative loadings reflected this characteristic of a strong hop profile. The Van Krevelen diagram of their formulae showed a specific cluster of CHO-molecules in the region of 0.2 < O/C < 0.4 and 1.2 < H/C < 1.6, respectively (Figure 2.5-I). As mentioned before, this area of the diagram is typical for terpenoids and more accurately hop bitter acids (terpeno-phenolics) in the beer matrix. This pattern was also observed in the mass difference network, showing an area (Figure 2.3A). The annotation of the given masses in databases offered exactly those hop bitter acids. Therefore, it is possible to uncover the area of the mass difference network, where the chemistry of the hop bitter acids is located. A number of 58 marker substances for rich hopped beers could be determined as derivatives by their molecular formula, whereas only 20 of them (35 %) were found to have equivalent structures in the databases and pertinent literature (Table B.3 in Supplementary Chapter 2). As FT-ICR-MS is not capable of distinguishing isomers, the [$C_{21}H_{30}O_5$] marker can represent humulone, adhumulone or iso-humulone, but most likely a mixture. Further already known precursor molecules like prenylphlorisobutyrophenone [$C_{15}H_{20}O_4$] and prenylphlor-isovalerophenone [$C_{16}H_{22}O_4$], as well as bitter acid derivatives like cohumulone [$C_{20}H_{28}O_5$], deoxycohumulone [$C_{20}H_{28}O_4$], dihydrohumulone [$C_{21}H_{32}O_5$], or humulinone [$C_{19}H_{26}O_5$], are surrounded by molecular formulae without suitable hits (Figure 2.6A). A demethylation reaction of the potential cohumulinone [$C_{20}H_{28}O_6$] leads to the molecule [$C_{19}H_{26}O_6$], whereas a decarboxylation of [$C_{20}H_{30}O_7$] leads to humulone [$C_{21}H_{30}O_5$]. Overall, finding literature equivalents of oxygenated structures like [$C_{19}H_{26}O_6$], which might indicate hydroxyl-, epoxy-, carboxy-, or peroxyderivatives, turned out considerably difficult. Furthermore, reduction/hydration and addition/elimination of water seem to be important reactions inside this excerpt network of marker substances. Pairs of marker molecules within the same nominal mass (e.g., $C_{20}H_{28}O_6$/$C_{21}H_{32}O_5$; $C_{19}H_{26}O_6$/$C_{20}H_{30}O_5$; $C_{20}H_{26}O_6$/ $C_{21}H_{30}O_5$) underlined the necessity of high resolving analytical acid species, as well as phenolic and polyphenolic compounds and their dedicated glycosides, seem to be characteristic for craft beers due to the typical dry-hopping process (Figure 2.5-II).

It was possible to confirm the calculated profiles of the beer types by the vicinity of the different types between the model and prediction sample sets (Figure 2.5). Only the position of two samples in the score plot defies the cluster. Sample numbers 100 and 119, both brewed in a certified abbey and, therefore, characterized as abbey beer, were located inside the craft beer region. Besides this origin, the actual brewing technique of these beers is described as amber ale and triple ale, both in agreement with craft beer styles including dry hopping. Therefore, not the brewing location itself, but the molecular signature of the brewing process stands in the foreground. A second group of beers, that could not be assigned precisely, were craft beers brewed with wheat and Belgian wit beers made with raw wheat. These beers share the signature of craft beers (ale yeast; preferably strongly hopped) and the signature of wheat beers (wheat grain as an ingredient), for which reason they were located between those beer types. The organic wheat

beer (sample 109) differed slightly as well. These findings suggested that the compounds with the most positive loadings define the molecular pattern of wheat. For the investigation of specifically the wheat signature, a second model was created.

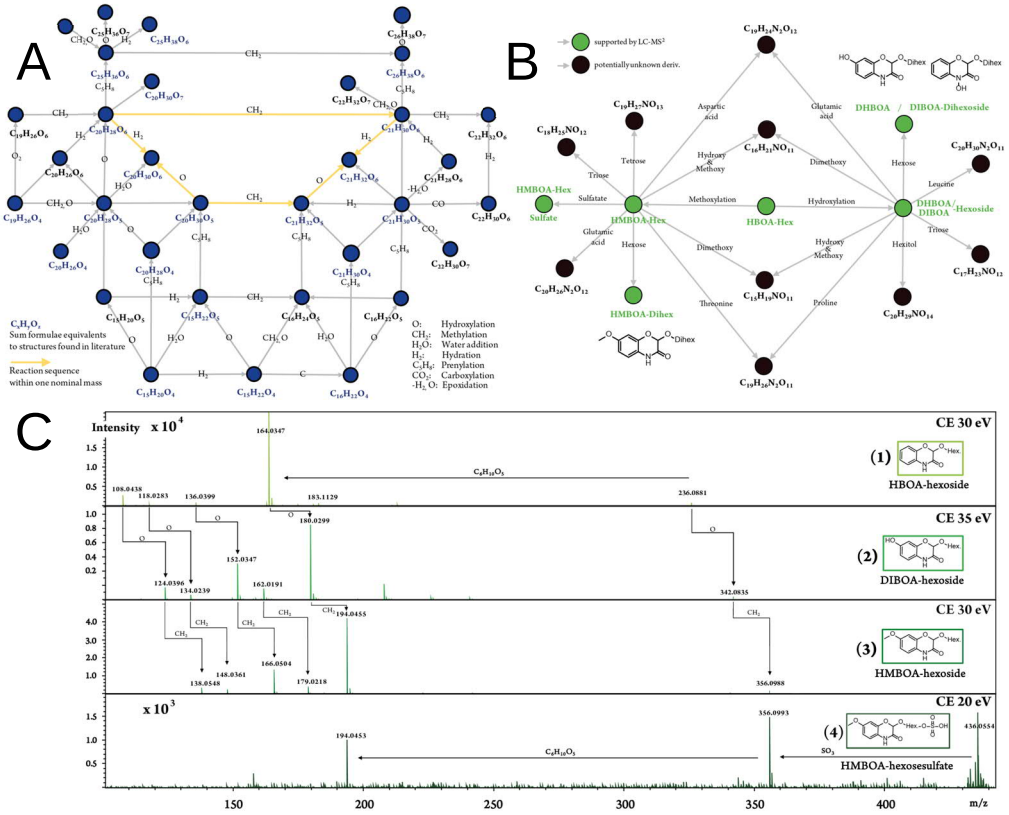

Figure 2.6 | Detailed excerpts for selected hops-rich beer type markers (A) and wheat grain markers (B). The nodes represent the annotated ions with given molecular formulae or molecule names and are connected by edges representing the molecular formula differences or the biochemical reaction respectively. All nodes depicted are considered marker substances. Wheat grain markers are additionally characterized by UPLC-MS/MS of sample 41 with literature matching retention time order and MS/MS-spectra showing respective fragmentation and mass difference pattern (C) [280,281].

2.2.4 OPLS-DA model 2: grain

The second OPLS-model was created to extract the influence of the ingredient wheat on the beer's metabolome (Figure B.3 in Supplementary Chapter 2). All beers brewed with some amount of wheat were defined as wheat-containing beers, regardless of their beer type and other brewing parameters. These stood against beers brewed exclusively with barley. Notwithstanding, that the model sample set consisted of beers with a plurality of various characteristics, it was possible to perform the separation based on the grain used without any ambiguous assignments. In addition to the intended separation, it could be remarked that the wheat-containing craft beers (samples 53, 54, 73), which were brewed with ale yeasts and dry-hopped, were separated by the orthogonal information by the second component (y-axis). In the loading plot, several highly significant wheat grain markers, such as [$C_{14}H_{17}NO_8$], [$C_{14}H_{17}NO_9$], and [$C_{15}H_{19}NO_9$], are separated by simple biochemical reactions (e.g., hydroxylation; methylation) and most likely belong to the family of benzoxazinoid hexosides. The intensity distribution of the mentioned markers is given in Supplementary Chapter 2 (Figure B.4 in Supplementary Chapter 2). These compounds are described to be specific phytoanticipines for wheat [282] compared with barley and partially described in wheat beer [283]. Again, an excerpt of the mass difference network of the wheat marker substances revealed six masses corresponding to benzoxazines, which were already characterized by de Bruijn, et al. [281], and a plurality of potential derivatives (Figure 2.6C). Against this background, the sulfation reaction of the HMBOA-hexoside to the respective sulfate appeared especially promising. These secondary metabolites and their dedicated derivatives seemed to be a crucial part of the metabolic signature of wheat-containing beers.

The prediction model (Figure B.3 in Supplementary Chapter 2) showed that the typical German wheat beers containing malted wheat were as well recognized as the Belgian wit beers, which contain unmalted wheat. In contrast, the metabolic pattern of the wheat grain in wheat-containing craft beers (sample numbers 100, 114, 118) was recognized less strongly. The comparatively low amount of wheat was opposed by the contrary heavy hop signature. For beers brewed with merely wheat starch, no wheat signature could be observed. These findings confirmed the applicability of the calculated pattern and advice to identify certain specific marker substances to detect even low amounts of wheat metabolites.

2.2.5 UHPLC-ToF-MS: marker identification

To support the interpretation of the FT-ICR-MS data and verify the predicted structures, we performed UHPLC-ToF-MS/MS measurements on selected samples. The marker substances for a rich hop profile and the wheat metabolome were investigated in depth. The marker substances of beers with a rich hop profile in the

van Krevelen region of 0.2 < O/C < 0.4 and 1.2 < H/C < 1.6, respectively (Figure 2.5-I), were proposed as hop bitter acid derivatives. The UHPLC-MS measurements of a hops-rich beer revealed mass traces fitting to 46 of the 58 molecular formulae (80 %) of the mentioned markers (Figure B.5 in Supplementary Chapter 2). This is a notably high rate because only 35 % of the markers were found to have structural equivalents in mentioned databases or cited pertinent literature (Table B.3 in Supplementary Chapter 2). Moreover, the LC-dimension gave a better idea of how complex the structures behind these masses are, as up to 21 peaks could be found for one single formula, all being eluted in the chromatogram region, where hop bitter acid derivatives were found (3.5-7.0 min). The 22 detected isomeric compounds for humulinone [$C_{21}H_{30}O_6$] stood in contrast to other formulae like [$C_{19}H_{26}O_4$] (cohulupone), which were represented by only one chromatographic peak (Figure B.5 in Supplementary Chapter 2). By tandem mass spectrometry we were able to identify twelve hop bitter acid derivatives like cohumulinic acid [$C_{14}H_{20}O_4$], hulupinic acid [$C_{15}H_{20}O_4$], cohulupone [$C_{19}H_{26}O_4$], (ad-)humulone [$C_{21}H_{30}O_5$], tricyclocohumol [$C_{20}H_{30}O_6$], or tetracyclohumol [$C_{20}H_{30}O_6$] on level two [10] by comparison of fragmentation patterns and intensities with literature data (Table B.4 in Supplementary Chapter 2). Opposing a wheat beer, which does not feature a rich hop profile, shows, that the corresponding mass traces are decisively higher in hops-richer craft and lager beers verifying their discriminating character (Figure B.5 in Supplementary Chapter 2). It is worth noting that more than 100 MS/MS spectra did not lead to hits in databases or literature, and therefore are considered level 3 identifications (Table B.5 in Supplementary Chapter 2).

Benzoxazinoidic phytoanticipines of the wheat plant were proposed as specific wheat grain markers in the beer matrix (Figure 2.6C). Again, the marker formulae of the FT-ICR-MS models were transferred into a preference list to selectively acquire tandem mass spectrometric spectra. By comparison with literature known MS/MS-fragmentation, eight HBOA-derivatives could be identified in wheat beer (level 2) (Table B.6 in Supplementary Chapter 2). The retention time sequence of the HBOA-, DHBOA-, DIBOA-, and HMBOA-hexoside coincides with the one described by de Bruijn, et al. [281], whereas the predicted HMBOA-hexosesulfate was eluted earlier than the corresponding hexoside due to the polar sulfate group. The MS/MS-spectra of the monohexosides are compared in Figure 2.6C. The cleavage of the hexose group from the HBOA-hexoside (1) $[M–H]^-$-ion [$C_{14}H_{16}NO_8$] results in an m/z-value of 164.0348 [$C_8H_6NO_3$]. The additional hydroxyl group of the DIBOA-hexoside (2) leads to the 180.0299 m/z ion [$C_8H_6NO_4$]. Replacing the hydroxyl group by a methoxy group, the m/z-value of 194.0455 [$C_9H_8NO_4$] can be found for the HMBOA-hexoside (3). The same pattern holds true for the 136.0399 [$C_7H_6NO_2$], 118.0283 [C_7H_4NO], and 108.0438 [C_6H_6NO] fragment ions of the HBOA-hexoside. It was not possible to extract complex fragmentation pattern of the HMBOA-hexosesulfate (4) as it was a minor component with a peak intensity about 30 times lower than the respective hexoside. However, the loss of the sulfate group from the quasi-molecular ion 436.0554 [$C_{15}H_{18}NO_{12}S$] to the dedicated HMBOA-hexoside (3) $[M–H]^-$-ion 356.0993 [$C_{15}H_{18}NO_9$] could be observed. Hereupon both compounds share the loss of the hexose sugar. The dihexoside DHBOA-, DIBOA-, and HMBOA-equivalents showed several closely eluting isomeric peaks and

were detected with lower retention times as they are more polar. All the substantiated compounds were only observed in wheat beer and none of them is present in beer exclusively brewed with barley, which confirms the assumption that benzoxazinoidic phytoanticipines are suitable specific compounds for the use of wheat grain. To our knowledge, the existence of a HMBOA-hexosesulfate has not been described before. However, for definite identification, the synthesis of a corresponding standard would be needed.

2.3 Discussion

Many studies have been published in the literature about beer metabolome analysis employing LC- and GC-MS either with time-of-flight or orbitrap instruments. The use of high-field Fourier transform ion cyclotron mass spectrometry is shown here for the non-targeted metabolic profiling of a diverse set of beer samples and enables a direct-infusion analysis due to the ultra-high-resolution provided. We were able to demonstrate the benefits of superior mass accuracy paired with the annotation in compositional networks. Constructing compositional mass difference networks exploits the exact mass information provided by FT-ICR-MS and enabled coverage of complex formulae and the whole compositional space. Thereby it was possible to assign molecular formulae like [$C_{29}H_{35}N_5O_{10}S$] to an exact mass likely corresponding to an Asp-Asp-Phe-Phe-Cys peptide or [$C_{10}H_{14}N_5O_8P$] to guanosine-monophosphate (GMP). Even at low masses (m/z 362.05072 for GMP) over 10 formulae are valid inside a 3 ppm window (Figure B.6 in Supplementary Chapter 2). By the provided mass error window of 0.1 ppm (0.002 ppm for GMP) and the possibility to resolve isotopic fine structure, we could ensure correct annotations with our DI-FT-ICR-MS approach. It allows us to directly proceed from m/z-values to the compositional space, depict thousands of yet unknown structures and assign their structural family concerning their position in the van Krevelen diagram and connectivity inside the mass difference network. Respective patterns were found for hop bitter acids and biochemical connectivity of blepharine derivatives.

By supervised OPLS-DA modeling, we were able to extract the profound metabolic signature underlying different beer types within the brewing process. The classification power of the models was highly significant. The p-values (calculated after the CV-ANOVA) were lower than 2E−19; such values bring us to exclude possible overfitting. Both models exceed Q^2-values of 0.6, for the quality of prevision, and R2Y-values of 0.95, for the goodness of the fit, proving their statistical relevance [215]. The molecular signatures for both lager and craft beers were dominated by the quantity of hops used. However, lager beer is predominantly brewed with hop varieties, which are rich in bitter acid compounds. Confirmatory, humulone and cohumulone isomers and derivatives appeared as marker masses for these types of beers. By the analysis of the mass differences of masses dedicated to precursors and intermediates, even the whole biosynthesis of these typical hop metabolites could be traced inside the beer matrix. The position of discriminating compositions in the Van Krevelen diagram showed, that more oxygenates bitter acid species, as well as phenols, polyphenols, and dedicated glycosides, are characteristic for craft beers.

Dry-hopping of aroma hops after the boiling or fermentation process, which is typical for this type of beer, adds a multitude of mentioned compounds to their dedicated metabolic profile due to ethanolic extraction of the hops [284]. Moreover, adding hop umbels to the wort or young beer represents a heavy input of oxygen, which advances oxidation processes. Hydrolysis, (de-)hydration, epoxidation, peroxidation, and cyclization mechanisms of hop compounds, which also lead to an altered bitterness perception, are known and described in literature as well as the presence of phenolic acids, coumarins, flavonoid polyphenols, and their glycosides [167]. However, the immense compositional complexity, which evolves from these reactions and is addressed in this work, still needs to be discovered. Duarte, et al. [198] already suggested using ^{1}H-NMR that the main difference between lager and craft beers in terms of the metabolome can be traced back to aromatic compounds. The prevision of a sub-sample set confirmed the universal applicability of our model and strengthen the fact that we were able to differentiate the type and parameters of brewing. Both beer types are commonly brewed without wheat. Therefore, the wheat metabolome was assumed to be an important discriminating and defining factor for wheat beers. ^{1}H-NMR analyses [195,197] again held aromatic compounds responsible for the differentiation of grains. A statistical model opposing the grains used was established to tackle the challenge of a comprehensive description of the wheat metabolome and eventually gain access to structural information. The fact that some beers share the molecular signature of hops and wheat (see prevision of the first OPLS-DA model) and the circumstance that wheat beers are to different extents brewed with barley malt as well, made this step of a second model essential.

The occurrence of blepharine derivatives as secondary metabolites derived by the wheat grain as marker substances in beer emphasizes the holistic and deep nature of our profiling approach. Hydroxybenzoxazinone (HBOA) and its derivatives are known to be phytoanticipines with antifungal, antimicrobial and insecticide properties in the wheat plant [282]. Blepharines are stored in the vacuole and activated following cell damage through β-glucosidase activity [282]. It may be anticipated that the described sulfate plays a role in either storage or transportation of the phytoanticipines. It was previously shown that the phytoanticipines are modified during food processing and fermentation [280,285]. Thus, chemical reactions during malting and boiling may also contribute to the multitude of possible derivatives yet unknown in the wheat and beer matrix. Compositional networks provided access to new metabolites even in the beer matrix, which makes an especially promising. Worth mentioning is the fact that no signature of wheat metabolites could be found in FT-ICR- and LC-ToF-MS measurements with regard to beers merely brewed with wheat starch. These beers lack the secondary metabolome of the wheat grain. The combination of analytical and statistical techniques presented here raises the potential of substantial advances in yet open questions regarding both brewing science and industry. In total, the metabolic profile of beer type and grains provided by DI-FT-ICR-MS could be verified by the identification of 18 (level 2) and 118 (level 3) compounds, respectively, for the signature of rich hopping and the use of wheat. As an outlook, the potential of ultra-high-resolution for food inspection or quality control applications is shown by the differentiation between beers brewed with wheat and merely wheat starch. Ongoing work focuses on expanding the approach toward other

descriptive parameters and archeochemical application of the presented metabolic signatures. Archeochemical investigations on wines and beers are generally executed by GC-MS-[286] and IR-based [159] measurements or are restricted to targeted approaches [287]. The presented metabolic profiles in future will be beneficial in deep profiling of ancient beer-like beverages and beers of the earlier modern era.

2.4 Materials and methods

2.4.1 Beer samples

A total of 85 samples of bottled beers produced in different countries were analyzed. They range from common lager or wheat over craft and abbey to lacto-fermented geuze beers. Light and dark, top and bottom-fermented, filtrated and non-filtrated, organic and gluten-free samples with alcohol contents of 0-12 % are covering the whole variety of purchasable beers in close to any possible combination. Thereby the most comprehensive mapping of beers' metabolome and prevention of covarying metadata was achieved. The samples were purchased at local grocery stores in December 2017 and stored at −20 °C prior to preparation for analyses. A second independent sample batch, which includes 35 beers, was purchased in 2019 and used as a prediction and validation set. The beer specifications are summarized in Supplementary Chapter 2 (Table B.2 in Supplementary Chapter 2).

2.4.2 DI-FT-ICR-MS measurements

High-resolution mass spectra were acquired on a Bruker solariX Ion Cyclotron Resonance Fourier Transform Mass Spectrometer (Bruker Daltonics GmbH, Bremen, Germany) equipped with a 12 Tesla superconducting magnet (Magnex Scientific Inc., Yarton, GB) and a APOLO II ESI source (Bruker Daltonics GmbH, Bremen, Germany) operated in negative ionization mode. The negative ion mode was preferred based on greater variety in the composition, abundance of compounds and a smaller number of suppressing adducts with respect to heavy potassium adduct formation in the positive ionization mode. The beer samples were injected once into the micro-electrospray source diluted 1:500 in methanol and the total analysis time of a sample was 10 min. The used reagents, sample preparation, and instrumental parameters are given in Table B.7 in Supplementary Chapter 2. Possible space charge effects were recalibrated by mass difference mapping [259]. The samples were measured over a period of 18 months in randomized order using a representative

lager beer as quality control. Mass accuracies reached values lower than 0.1 ppm between and within measurement days. Furthermore, the conservation of the ion intensities and the molecular fingerprint could be observed by this approach (see data-mining HCA).

2.4.3 FT-ICR-MS data processing and visualization

The FT-ICR spectra were exported to peak lists with a cut-off of signal-to-noise ratio (S/N) of 6 using the DataAnalysis 4.2 software. Only singly charged ions were included. Processing and filtration of the peak lists (FT-side loops and isotopologue filtering) were performed by an in-house R-based software tool on basis of single spectra. Peak alignment was performed within a threshold of 1 ppm. Thereby an overall matrix of 13,800 masses was created. To obtain molecular formulae, the exact masses were subjected to mass difference network (MDN) analysis using the NetCalc software tool [237]. The network calculation was repeated ten times and coinciding formula assignments were kept, which led to approximately 10,500 unambiguous molecular formulae in the C, H, N, S, O, P, Cl space. The developed mass difference network, in which nodes represent molecular formulae and edges represent chemical reactions, was visualized by the open accessible Gephie Viz Platform [288] using the open order algorithm. The masses with a frequency below 5 % through all the samples were not considered during further data mining. Small mass transitions like oxidation, methylation, hydrogenation, or amination were withheld for visualization due to computing power. Van Krevelen diagrams were chosen to associate annotated m/z-values to chemical families based on the procedure illustrated by Schmitt-Kopplin, et al. [26]. Library searches were executed using an R script based on the MassTRIX approach [289] including the Human Metabolome Database (HMDB) [290], the Chemical Entities of Biological Interest (ChEBi) [291], Metacyc [292], Lipid maps [293], the Yeast Metabolome Database (YMDB) [294], and an in-house peptide database consisting of all in silico peptides.

2.4.4 UHPLC-ToF-MS measurements and structural identification

The beer sample 52 (hops-rich craft beer) and sample 41 (wheat beer) were analyzed in a fivefold concentration on a time-of-flight mass spectrometer (maXis, Bruker Daltonics, Bremen, Germany), coupled to a UHPLC system (Acquity, Waters, Eschborn, Germany). The preference list for fragmentation was compiled based on the substances' masses, which occurred as a marker for the hops-rich beer types (sample 52) and wheat grain (sample 41) observations (Table B.4-B.7 in Supplementary Chapter 2). Further instrumental parameters are given in Table B.7 in Supplementary Chapter 2. The search for comparable tandem mass spectrometric

data was executed using the MassBank of North America [295] and in silico fragmentation by MetFrag [262] based on the KEGG [24], HMDB [290], and YMDB [294] databases. Spectra were checked in mentioned literature source. The level of identification was assigned based on the criteria given by Sumner, et al. [10].

2.4.5 Statistical analyses

The dataset, divided into a first batch defining the model and a second batch used for prevision and validation, was analyzed with different multivariate techniques. First, we used an unsupervised technique to cluster the different beer samples. The intensities were normalized (z-scores) and the clustering was calculated by using the average group linkage and the Pearson correlation coefficient for the distance measure (Hierarchical Clustering Explorer tool; HCE, 3.0). Afterward, the dataset was analyzed by different classification models applying supervised orthogonal partial least-square discriminant analysis (OPLS-DA). The Hotelling's T2 test (95 %) was applied to prohibit the influence of strong outliers on the models. For both the beer type and grain model it was possible to extrapolate the most discriminant features (m/z-values). The lists of the most important masses were defined choosing the highest loadings values. The top characteristic masses were selected within the 95th percentile (264 masses for each class). The goodness of the fit and of the prediction were evaluated with the R2- and Q^2-values. To exclude overfitting, we provide the p-value of the cross-validation analysis of variance (CV-ANOVA). In addition, based on the robustness of the classification models we could use them to make a prevision of a second sample set. The recognition of molecular patterns for the independent samples and thus the localization of those in the score plot could verify the universal applicability of the models. Those elaborations were done in SIMCA 13.0.3.0 (Umetrics, Umeå, Sweden). The marker formulae were depicted in van Krevelen diagrams for each class. By plotting H/C- versus O/C-atomic ratios it is possible to depict common compositional patterns within observations' markers [111,126].

Chapter 3 |
Hidden in its Color: A Molecular-level Analysis of the Beer's Maillard Reaction Network

We here report a comprehensive non-targeted analytical approach to describe the Maillard reaction in beer. By Fourier transform ion cyclotron mass spectrometry (FT-ICR-MS), we were able to assign thousands of unambiguous molecular formulae to the mass signals and thus directly proceed to the compositional space of 250 analyzed beer samples. Statistical data analyses of the annotated compositions showed that the Maillard reaction is one of the driving forces of beer's molecular diversity leading to key compositional changes in the beer metabolome. Different visualization methods allowed us to map the systematic nature of Maillard reaction-derived compounds. The typical molecular pattern, validated by an experimental Maillard reaction model system, pervades over 2,800 (40 %) of the resolved small molecules. The major compositional changes were investigated by mass difference network analysis. We were able to reveal general reaction sequences that could be assigned to successive Maillard intermediate phase reactions by shortest path analysis.

This chapter has been published as Pieczonka, S. A., Hemmler, D., Moritz, F., Lucio, M., Zarnkow, M., Jacob, F., Rychlik, M. & Schmitt-Kopplin, P. Hidden in its color: A molecular-level analysis of the beer's Maillard reaction network. Food Chemistry 361(130112), 1-9, Copyright Elsevier (2021). It is reproduced with explicit permission.

Candidate's contributions: S.A.P. designed the experiments, analyzed and interpreted the data. S.A.P wrote, revised and approved the final paper. S.A.P. performed the instrumental experiments. S.A.P. performed the statistical treatment, data mining, interpretation and visualization.

3.1 Introduction

Beer belongs to the oldest fermented beverage in the world [159]. Thousands of years ago, humankind already commenced to purposefully produce durable and nutrient-rich beverages timely concordant with the domestication of cereals [296]. While the shelf life of beer is notably due to hop constituents, the alcohol content and the stable pH-value, the raw material's durability is maintained by reducing the water content. The underlying process of malting was widespread in ancient Egypt, where the good taste of heat-treated cereals already was valued [160]. It still represents one of the manifold-guided processes that make up modern beer brewing, the complexity of which is mirrored in the diverse molecular composition of beer. Beer can be considered as an exceedingly complex organic mixture in an aqueous solution, to which the brewing process contributes as considerably as the ingredients themselves. The heat treatment of the carbohydrate source is a unique step that notably lifts the molecular complexity of beer from that of other beverages. Malting the grain (steeping, germination, kilning/roasting) leads to a series of chemical reactions that are reflected in the "beer's metabolome".

Brewing science and beer analysis has been integrating empirical knowledge about its chemical composition over centuries [227]. Using numerous analytical approaches including UHPLC-MS, GC-MS and NMR spectroscopy, both targeted and non-targeted strategies described the beer composition with regard to metabolic profiles characteristic for beer types [198], brewing sites [196], beer quality [195], aging [297] or the evolution of hops-derived compounds [186]. Recently, our group was able to demonstrate the power of the ultra-high-resolution mass spectrometric approach of direct-infusion Fourier transform ion cyclotron mass spectrometry (DI-FT-ICR-MS) providing a comprehensive picture of the beer's metabolome [225]. Out of the resolved molecular diversity, molecular networks of plant secondary metabolites that differentiate beer types and raw materials used could be made visible and characterized. Research on the driving force of chemical changes during the roasting process, the Maillard reaction (MR), is more so dominated by targeted approaches. Brewing research focused on understanding the series of complex reactions by studying reaction mechanisms of certain marker molecules and aroma compounds. For example, 5-hydroxymethyl-2-furfuralaldehyde (HMF) is generated by multiple pathways including caramelization and the MR starting from numerous possible precursors [298]. By comparison, the formation of maltol, characteristic for eponymous dark malt and beer, only occurs in disaccharide systems favored by stereochemistry and hindered dehydration of respective monosaccharide precursors [299]. Many studies followed this approach and studied new non-volatile or aroma-active compounds including their formation pathways [273,300,301]. However, a comprehensive and holistic approach remains inadequately pursued. Comprehensive and molecular-level detection of Maillard-derived compounds in beer forms the basis to describe general reaction sequences, driving forces and key intermediates. It carries the potential to guide the MR-related brewing processes towards desired attributes of the beer, as Maillard reaction products (MRPs) play a major role in its organoleptic,

physical and chemical properties. Melanoidins as MR end products determine the color of beer [302], they contribute to the stabilization of aroma compounds [303], have foam stabilizing properties [304] and show antioxidative properties [305]. The shelf life of beer is further increased due to the inhibition of bacterial growth [306]. Overall, beer quality could benefit from optimizing the MR not only towards the formation of a few targeted molecules but addressing and eventually controlling the entire compositional space, including the many still unknowns.

We have recently developed an analytical pipeline based on high-resolution mass spectrometry and data visualization that allows the comprehensive study of the early Maillard reaction network on a molecular level in sugar-amino acid model systems [168,307]. Studying exact mass differences as a proxy for the reactome was shown to be a valuable tool to monitor the formation of MRPs and to better understand their chemical interplay. In this study, we apply this analytical strategy to better understand non-enzymatic browning reactions in beer. We aim to capture the huge diversity of the beer metabolome, assess the contribution of MR products and extract related accurate masses. Visualization and integration of molecular compositions into molecular networks will enable us to capture a comprehensive picture of the Maillard reaction as it may occur in the (bio-)chemically complex beer system.

3.2 Materials and methods

3.2.1 Beer samples and Maillard model system

A total of 250 samples of bottled beers from over 40 different countries were analyzed. They represent the variety of different beer styles, fermentation types (lager, wheat, craft, geuze, abbey) and raw materials available. The samples were purchased at local grocery stores between 2018 and 2020 and stored at –20 °C prior to preparation for analyses. For the model system, the concentration of 19 amino acids, accessible for derivatization with o-phthaldialdehyde, and 5 saccharides were analyzed in a biological triplicate and technical duplicate of green malt as described in Table C.1 in Supplementary Chapter 3. The concentrations of the amino acids and sugars, as described in Table C.2 in Supplementary Chapter 3, were recreated in Milli-Q purified water (Merck Millipore, Darmstadt, Germany) immediately prior to thermal treatment. The concentration of all amino acids added up to 0.12 M and the sum of saccharides' concentration was 0.26 M. The sample was heated in a closed glass vial until the increase in mass features flattened out and the final phase of the MR was reached (20 h at 100 °C). The model system was created and measured in triplicates.

3.2.2 UV–Vis measurements

The beer samples and Maillard model system were diluted 1:40 in Milli-Q purified water and centrifuged (14.000 rpm, 4 min.). An aliquot of 100 µL of the supernatant was used for UV/Vis analysis in Nunc UV-transparent 96-well microtiter plates (Thermo Fisher Scientific, Waltham, MA). The absorption values at 294 nm and 420 nm were measured on a Multiskan Sky UV-Vis reader (Thermo Fisher Scientific) with temperature control (23 °C).

3.2.3 DI-FT-ICR-MS measurements

High-resolution mass spectra were acquired on a Bruker solariX ion cyclotron resonance Fourier transform mass spectrometer (Bruker Daltonik GmbH, Bremen, Germany) equipped with a 12 T superconducting magnet (Magnex Scientific Inc., Yarnton, UK) and an APOLLO II ESI source (Bruker Daltonik GmbH) operated in negative ionization mode. To minimize ion suppression while allowing detection of a maximum number of monoisotopic signals, we carefully optimized sample dilution. The best compromise could be achieved when beer samples and model systems were diluted 1:500 in methanol prior to injection into the micro electrospray source. The samples were measured over a period of 24 months in randomized order using a representative lager beer as quality control. 80 % of all detected monoisotopic signals could be assigned to a molecular formula within an error range of ± 0.2 ppm and the mass resolution was stable at 400,000 at m/z 400 between and within measurement days. The used reagents, sample preparation and instrumental parameters are given in Table C.3 in Supplementary Chapter 3.

3.2.4 FT-ICR-MS data processing

The FT-ICR spectra were exported to peak lists with a cut-off signal-to-noise ratio (S/N) of 6 using Data Analysis 4.2 software. Only singly charged ions were included. Spectra were first externally calibrated by ion clusters of arginine prior to internal calibration by a calibration list of 2000 compositions commonly found in beer. Possible space charge effects were recalibrated by mass difference mapping [259]. Processing and filtration of the peak lists (FT-side loops and isotopologue filtering) were performed by an in-house R-based software tool on the basis of single spectra. Peak alignment was performed within a threshold of 0.5 ppm as described Lucio, et al. [308]. Thereby an overall matrix of 11,500 masses was created. To obtain molecular formulae, the accurate masses were subjected to mass difference network (MDiN) analysis using the in-house NetCalc software tool [237]. The network calculation was

repeated five times and coinciding formula assignments were kept, which led to approximately 9,500 unambiguous molecular formulae in the CHNOSPCl space. $[M+Cl]^-$ adducts were converted into the respective $[M-H]^-$-ion. Of those, all annotations that are featured in at least three beers were kept for statistical analysis (6,750). A full mass difference statistic was computed on the theoretical neutral masses of each sample. The set of unique mass differences existing within all full mass difference graphs was computed and the relative abundances of each mass difference were obtained. Mass differences that occurred at least 100 times in a single beer sample (15,500) were used for further statistical analysis (PCA, OPLS) on the relative abundances of each mass difference within the different samples.

3.2.5 Statistical analyses

Firstly, we used an unsupervised principal component analysis to separate the beer samples based on the molecular signatures that determine the biggest variance. In the second step, an OPLS-DA was performed to extract the molecular pattern which correlates with the absorption at 294 nm. The Hotelling's T2 test (95 %) was applied to prohibit the influence of strong outliers on the models. The lists of the highest loadings values. The top characteristic masses were selected within the 90^{th} percentile (674 masses for each dark and pale beer) and referred to as dark and pale markers in the following, respectively. The goodness of the fit and of the prediction were evaluated with the R2Y and Q^2-values. To exclude overfitting, we computed the p-value of the cross-validation analysis of variance (CV-ANOVA). The same approach was carried out with the relative abundances of mass differences occurring in the beer samples. Additionally, based on the robustness of the models, we performed a prevision on the Maillard model system. The recognition of compositional patterns could verify the MR origin of the found patterns and set both models in relation. Those elaborations were done in SIMCA 13.0.3.0 (Umetrics, Umeå, Sweden). The statistical parameters of the beer samples and Maillard model system (Table C.4 in Supplementary Chapter 3) and PCA and OPLS models (Table C.5 in Supplementary Chapter 3) can be found in Supplementary Chapter 3.

3.2.6 Mass difference network analysis

Besides the mass difference network that was used for the annotation of the FT-ICR-MS data (FT-ICR-MS data processing), a second MDiN was created, which includes all compositions found in both the beer samples and the model system. These nodes were connected by edges representing transformations from the Hodge's scheme [309] and expanded by reactions including MR fission products (Table C.6 in Supplementary Chapter 3). They are referred to as small Maillard intermediate phase reactions and mass differences in the following. In total, ~ 65,000 connections were received. Based on this second network, the nine most significant compositional changes elucidated by OPLS statistical treatment of the first full MDiN were broken down into smaller individual reaction sequences. More precisely, we computed the shortest paths connecting any source-target pair of the statistically significant, composite mass differences using the unweighted Dijkstra algorithm in the Python 3.7 programming environment on a compatible network library [310]. For each statistically significant mass difference, a dominant combination of small reactions of the modified Hodge's scheme was determined. The chronological orders of the individual reactions were compared, giving us a dominant reaction sequence. By this approach, we received a chronological reaction sequence that built up the ten statistically most significant compositional changes during the MR.

3.2.7 Data visualization

The marker formulae were depicted in van Krevelen. By plotting H/C-versus O/C-atomic ratios it is possible to depict common compositional patterns within observations' markers [126]. The degree of unsaturation of the compositions was calculated as double-bond equivalents (DBE, sum of rings and double bonds in a molecule) and plotted against the number of carbons. A modified Kendrick mass defect analysis [311] was applied to visualize the role of dehydration reaction cascades in both marker subsets. The DBEs, modified KMDs and length of homologous series were calculated as described recently [168,312]. The assignment of corresponding chemical spaces to markers' compositions, their number of nitrogen and their number of oxygen atoms were plotted according to the respective frequency. The developed mass difference network was visualized by the open-access Gephi Viz Platform [288] using the Force Atlas algorithm.

3.3 Results

3.3.1 Contribution of the MR to the beer's molecular complexity

In our study, we investigated the chemical diversity of a total of 250 bottled beer samples that cover the many facets of beer brewing by DI-FT-ICR-MS. As shown in a previous study [225] our non-targeted analytical approach can resolve the entire molecular complexity of beer in a single measurement. Covered compounds include carbohydrates, peptides, lipids, polyphenols, hop bitter acids, sulfates and phosphates as well as mostly yet inadequately characterized Maillard reaction products (MRP). The richness and diversity of the selected beer samples capture the great chemical space of the beer metabolome and provide a well-suitable basis to study the contribution of the MR. We were able to assign 7,000 unambiguous molecular compositions to the accurate monoisotopic masses (Figure 3.1A) within the sample set reaching from very dark (Figure 3.1) to very pale (Figure 3.1C) beers (EBC color values reaching from 5 to 150, Table C.1 in Supplementary Chapter 3). The m/z-values reached from 100 to 1000. The molecular formulae were annotated in the CHNOSP chemical space and subjected to further statistical analyses.

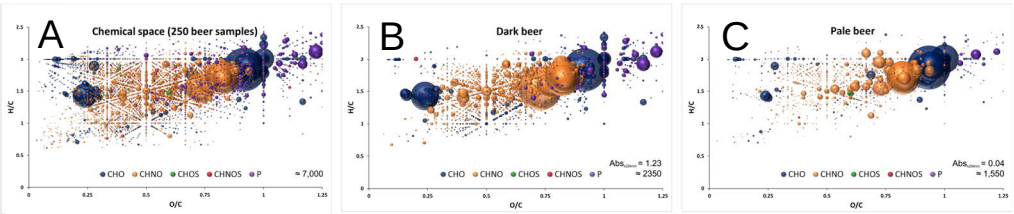

Figure 3.1 | Van Krevelen diagram of molecular formula annotations found in 250 beer samples (A), the darkest (B) and palest (C) beer sample. Color code: CHO blue; CHNO orange; CHOS green; CHNOS red; P purple. Neutral molecular formulae are plotted. The bubble size indicates the mean relative intensities of corresponding peaks in the spectra.

We used principal component analysis (PCA) to assess the impact of MRPs on the molecular beer composition (Figure 3.2A). The unsupervised statistical treatment reveals the greatest molecular differences between the beer samples as well as their underlying brewing principles and techniques. The PCA score plot was colored according to each beer's absorption at 294 nm, measured by UV-Vis spectroscopy and reported characteristics to follow the evolution of MR [313]. The plot reflects the samples' degree of browning with the tendency to lower left positions. Therefore, non-enzymatic browning can be considered to be of major importance for the chemodiversity in beer. It leads to key compositional changes already visible in unsupervised statistics.

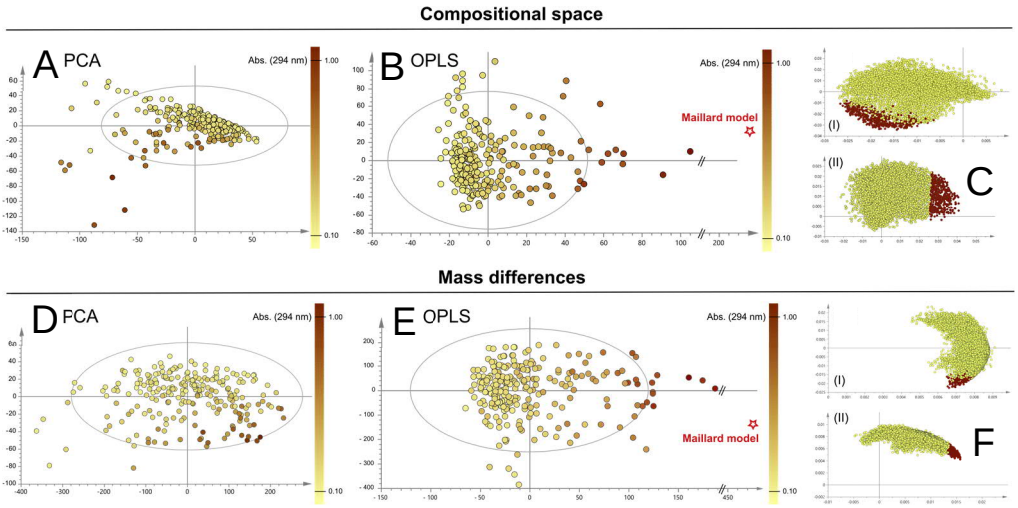

Figure 3.2 | Score plot of the PCA (A) and OPLS (B) analysis of the compositional space of 250 beer samples and the corresponding loading plots (C-I, PCA) (C-II, OPLS). Score plot of the PCA (D) and OPLS (E) analysis of the computed mass differences in 250 beer samples and the corresponding loading plots (F-I, PCA) (F-II, OPLS). The position of the beer samples is marked by dots colored according to their absorption at 294 nm. The prediction of the Maillard model system in the OPLS models (B and E) is highlighted as a red star. Masses in the PCA-loading plot (C-I and F-I) that match the most significant masses for dark beers in the OPLS-loading plot (C-II and F-II) are colored brown.

We applied a second statistical analysis, a supervised OPLS-DA, to generate in-depth knowledge of compositions driving the differentiation of dark beers (Figure 3.1B) and pale beers (Figure 3.1C). Compared to PCA, OPLS-DA allowed the extraction of accurate masses without an influence of orthogonal metabolic information, which does not contribute to the compositional changes affected by the MR. The received R2Y-, Q^2- and ANOVA p-value indicate a highly significant multivariate model [214-216] (Table C.5 in Supplementary Chapter 3). The gradient of absorption values, already visible in the PCA and established as driving the Y-variable, is reflected in the first component of the OPLS score plot (Figure 3.2B). The comparison of both statistical models' loading plots shows that the OPLS can extract the same features that drive the MR-related separation of the beer samples in the PCA (Figure 3.2C). We further analyzed an experimental Maillard reaction model system and integrated the results into the OPLS-DA. According to the amino acid and carbohydrate profiles and concentrations of analyzed green malt (Table C.2 in Supplementary Chapter 3), we designed the MR model system, which we heated to 100 °C in order to simulate the processes during malting and brewing. To a certain extent, this model represents Maillard reactions between multiple sugars and amino acids in beer. The experimental model system allowed us to validate the assumption that monitoring the absorption at 294 nm can be used to study the MR in beer. The

prediction of the model system's position in the OPLS score plot locates it to the far right validating that our OPLS model is capable to recognize the intrinsic nature of Maillard-derived complex systems (Figure 3.2B). The MR molecular pattern in beers, which is extracted by the statistical treatment and classified with regard to the compounds' significance, matches the chemical space of the MR model system (Figure C.1 in Supplementary Chapter 3). We could reproduce 80 % of the most significant compositions found in beer (90^{th} percentile of most positive loadings) in the saccharide and amino acid experimental model system (Figure C.2 in Supplementary Chapter 3). The overlap between the masses found in beer and those of the model system decreased with decreasing loading values of the respective masses. In comparison, compositions characteristic for pale beers (90^{th} percentile of most negative loadings) showed an overlap of less than ten percent.

3.3.2 The compositional nature of the MR in beer

The OPLS loadings plot allowed the extraction of compositions related to the MR from the rich diversity of beer metabolites and rank them according to their significance. To study the molecular pattern of MRPs, we focused on the top ten percent (90^{th} percentile) of the most significant marker compositions for both the dark and pale beer characteristics. Yet, the typical compositional pattern of the Maillard reaction, reported by Hemmler, et al. [168] and reflected in the MR model system, pervades at least 40 % (2.800) of all annotations (Figure C.1 in Supplementary Chapter 3).

Several plots and visualizing tools can be used to depict and describe the compositional nature of complex (bio)chemical systems [126,307,311]. The annotations of the dark beer markers are almost exclusively limited to the CHO (52%) and CHNO (48%) space (Figure 3.3A-I). The number of molecular formulae that contain nitrogen atoms decreased linearly with the number of nitrogen atoms, which implies a compositional space built up by chemical kinetics (Figure 3.3B-I). The frequency of molecular formulae is Gaussian-like distributed against the number of oxygen atoms contained but lacks compositions with less than four oxygen atoms (Figure 3.3C-I). Compounds with very low oxygen numbers that can be detected by FT-ICR-MS in negative electrospray mode are most commonly annotated as fatty acids or lipids [26,225]. Such compositions can be found in the marker masses of pale beers (Figure 3.3C-II). Overall, in contrast to the dark beer markers, the plots of beer metabolites that are characteristic for pale beers and do not come from the MR do not share a distinct compositional space, as comparatively described in other fermented beverages missing heat load [57,111] (Figure 3.3A-C-II).

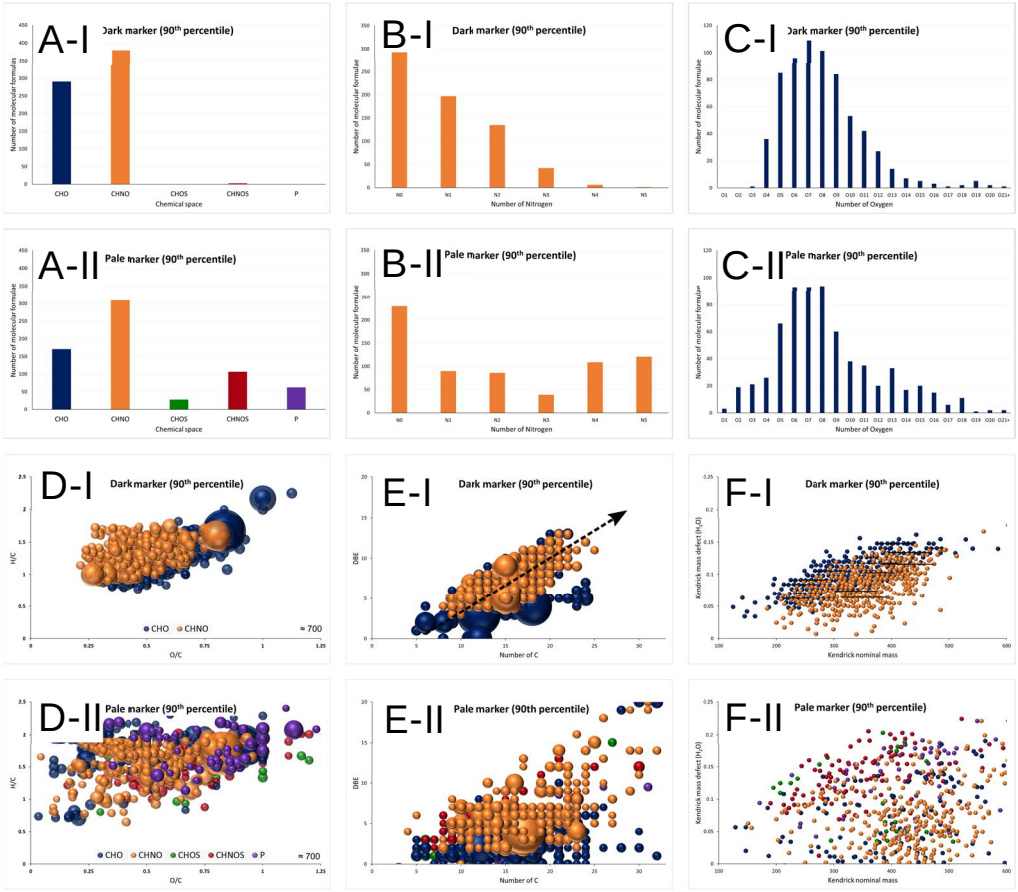

Figure 3.3 | Comparison of dark (I) and pale (II) beer marker molecular formulae by different visualizing plots (A-F). Number of annotations in the chemical spaces (A), number of nitrogen atoms (B), number of oxygen atoms (C), Van Krevelen diagram (D), Double bond equivalents against Number of Carbon atoms (E) and Kendrick mass defect plot with H_2O homologous series (F). Color code: CHO blue; CHNO orange; CHOS green; CHNOS red; P purple. Neutral molecular formulae are plotted. The bubble size indicates the mean relative intensities of corresponding peaks in the spectra (D, E). Rising DBE with higher masses for dark markers is indicated in (E-I). Homologous series of H_2O-reactions are marked exemplary in the KMD plot (F-I). The intrinsic systematic pattern of dark beer markers is opposed to non-systematic annotations of the pale marker masses.

Furthermore, the comparison of marker masses of pale and dark beer markers in the van Krevelen diagram shows substantial differences (Figure 3.3D). The Maillard reaction leads to a highly organized compositional pattern of compounds which is mainly formed through consecutive dehydration, carbonyl cleavage and redox reactions [312]. Interestingly, the extracted molecular formulae of the dark beer marker masses indicate the same compositional pattern. Compositions corresponding to well-known MRPs like 5-hydroxymethylfurfural (HMF, $C_6H_6O_3$),

pronyl-lysine ($C_{15}H_{24}N_2O_6$) or maltosine ($C_{12}H_{18}N_2O_4$) as well as early intermediates like desoxyosones (e.g., $C_6H_{10}O_5$) and Amadori rearrangement products (deoxyhexosylglycine, $C_8H_{15}NO_7$) can be found in both the model system and the dark beer markers. This systematics is contrasted with the van Krevelen diagram of pale beer compounds (Figure 3.3D-II). The generally more saturated molecular formulae do not cluster in a discrete area. Merely, the areas in the van Krevelen diagram indicate thermolabile lipids and peptides [225] which may function as MR precursors. The degree of unsaturation of MR-derived compounds, expressed as double-bond equivalents (DBE), follows a highly systematic structure compared to markers for pale beers (Figure 3.3E). Only a group of early MR intermediates of higher-chain saccharides (e.g., $C_{24}H_{40}O_{20}$, $C_{24}H_{38}O_{19}$, $C_{24}H_{36}O_{18}$ at $C > 20$ and $DBE < 8$) resist the clear, almost linear trend of higher DBEs for higher masses (Figure 3.3E-I). The biggest differences between the highly structured MR compositions, which are based on defined chemical reaction cascades, and other beer metabolites are shown in the modified Kendrick mass defect (KMD) plot (Figure 3.3F). Elimination reactions can be observed in both the CHO and CHNO chemical space homologous series of water. The maximum length of water elimination cascades equals seven with an average of 3.9. This is in agreement with values for MR models reported in the literature (7 and 3.9) [168] and values computed for our model system (8 and 4.0). In contrast, the pale beer markers do not exceed a homologous series of more than three consecutive dehydration events.

By these visualization methods, we could confirm the MR origin of hundreds to thousands of compositions in beer attributed significantly for darker beers in the statistical data evaluation and describe their intrinsic compositional structure. The modified KMD plot furthermore implies that the reaction cascade of the MR is captured in the marker compositions.

3.3.3 The Maillard reaction molecular network in beer

To get deeper insights into the Maillard reaction cascade that leads to the deciphered molecular complexity, we applied a mass difference network (MDiN) analysis. Based on the relative abundances of mass differences that connect the elementary compositions of each sample and represent chemical reactions or reaction sequences, both PCA (Figure 3.2D) and OPLS (Figure 3.2E) statistical analyses were used. Similar to the statistics on the compositions above, the PCA plot shows a gradient of darkening colors with the tendency to lower positions of the beers in the score plot (negative PC2-values). Using the absorption values of beers at 294 nm as Y-variable in an OPLS-DA, we were able to extract the most significant mass transformations for dark beer samples. This is in agreement with the mass differences (MDs) driving the separation in the PCA (Figure 3.2F). Again, the MDs match the dominant ones of the Maillard model system (Figure 3.2E).

These exact mass differences can be equated with changes in the molecular formulae and therefore compositional changes. They describe the compositional change a source compound undergoes to build a target composition. The ten most significant compositional changes are almost exclusively limited to the CHO chemical space and reach from 68 Da to 154 Da. Based on the shifts in the respective molecular formula, there are no single reaction equivalents that describe these changes. Consequently, they rather represent (reaction) sequences of individual smaller compositional changes and are referred to as composite mass differences in the following.

The van Krevelen diagram of the reaction pairs shows that higher weight reactants appear in the area of early MR products (Figure 3.4A). The associated compounds with lower m/z-values can be assigned to the area of unsaturated advanced MRPs (Figure 3.4B). Accordingly, source compounds of the composite reactions have higher masses than the target compounds. The most significant

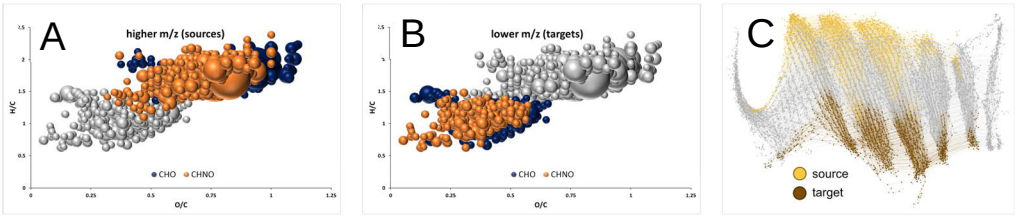

Figure 3.4 | Van Krevelen diagrams of compositions connected by the ten most significant mass differences for dark beers (A and B) and their breakdown into small reaction series by a mass difference network (C). Higher mass values (A) and lower mass values (B) of the mass pairs. The entirety of compositions is depicted in the background in gray. The lower left position of low m/z values indicates degradation reaction sequences. Nodes in the mass difference network (C) represent all annotated compositions connected by edges representing small Maillard intermediate phase reactions (Table C.6 in Appendix Chapter 3). Sources and targets of the statistically most significant big composite mass differences are colored.

reactions could be defined as degradation processes.

To decipher the individual reactions, a MDiN analysis was applied on all annotated compositions (N = 7000). The nodes in the network shown in Figure 3.4C represent compositions annotated in both beer samples and the model system. The compositions are connected by edges representing the mass differences typical for the MR intermediate phase. This includes transformations, such as dehydration, decarboxylation, and carbonyl cleavage reactions (for a full list of 11 transformations see Table C.6 in Supplementary Chapter 3). Due to the lack of a universally applicable nitrogen-containing mass transition, the tenth MD was omitted. We were able to

connect the majority (>95 %) of source-target pairs of the statistically significant composite mass differences by individual small reactions and define the shortest paths by the unweighted Dijkstra algorithm. For each big compositional change, a certain combination of intermediate phase reactions was dominant (Table 3.1). The chronological order of the respective individual Maillard intermediate phase reactions was compared (Figure C.3 in Supplementary Chapter 3). The order can be assumed to represent the evolution of the composite MR compositional changes. With up to 175 different chronological orders, for each composite mass difference one reaction sequence was very dominant. An overview of the ten most significant compositional changes and their breakdown into chronological reaction sequences is given in Figure 3.5. They share a similar structure: all feature a dehydration cascade, whereas most of them end with a decarboxylation reaction. Fission products of early MR intermediates such as glyoxal, methylglyoxal and diacetyl mark the beginning of the reaction sequence in many cases.

Table 3.1 | The ten most significant compositional changes during the MR in beer and their break down into small reactions.

Loading	**Δ** m/z	Formula	Fre-quency	Decomposition into individual MDs	% of shortest
0.01581	-128.053	$C_1H_{-12}O_{-8}$	543	Dehydration (8), Glyoxal, Decarboxylation	64
0.01576	-140.053	$H_{-12}O_{-8}$	714	Dehydration (8), Hydrogenation (2)	65
0.01576	-142.069	$H_{-14}O_{-8}$	576	Dehydration (8), Hydrogenation	82
0.01571	-98.0427	$C_2H_{-10}O_{-7}$	685	Dehydration (7), Methylglyoxal	75
0.01566	-110.043	$C_1H_{-10}O_{-7}$	879	Dehydration (7), Acetaldehyde, Decarboxylation	65
0.01565	-112.058	$C_1H_{-12}O_{-7}$	722	Dehydration (7), Glyoxal, Decarboxylation	66
0.01551	-82.0477	$C_2H_{-10}O_{-6}$	890	Dehydration (6), Methylglyoxal, Dehydrogenation, Decarboxylation	83
0.01549	-68.0321	$C_3H_{-8}O_{-6}$	830	Dehydration (6), Diacetyl, Dehydrogenation, Decarboxylation	94
0.01549	-154.069	$C_{-1}H_{-14}O_{-8}$	746	Dehydration (6), Dehydrogenation, Decarboxylation	90
0.01543	-93.0637	$C_1H_{-11}N_1O_{-5}$	861	-	-

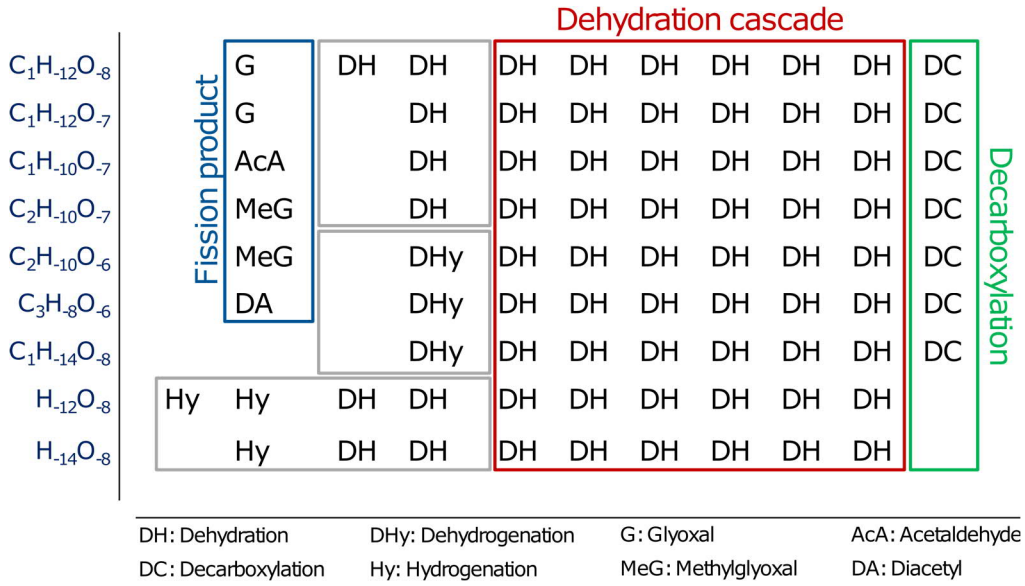

Figure 3.5 | Reaction sequences of the ten most significant compositional changes during the MR in beer. All reaction sequences feature a dehydration cascade. In many cases, MR fission products start the reaction sequence, which ends with a decarboxylation reaction.

3.4 Discussion

The progress of the early MR was followed by the absorption at 294 nm. The UV absorbance at 294 nm is commonly used to indicate Maillard reaction products of the intermediate phase [313]. Absorption values of the beer samples measured at 294 nm (MR intermediates) and 420 nm (advanced MR products) showed a very strong correlation (Pearson correlation coefficient: 0.98). Consequently, our identified marker candidates include MRPs from the entire reaction network (initial, intermediate and final MRPs). The MR-correlating compositions lead to a differentiation of the beers already in the first principal components of the unsupervised statistical analysis. It shows that the reaction of sugars and amines defines a large part of the beer metabolites. Besides the OPLS statistical parameters ($R2 > 0.92$, $Q^2 > 0.79$ and ANOVA p-value $\ll 0.05$), the decreasing coverage of the marker's chemical space by the MR model system with decreasing loading values confirm the power of our approach. The typical Maillard reaction signature [168] is dominant and shows up to at least 40 % of the whole chemical diversity resolved by FT-ICR-MS.

Different plots and visualization techniques confirm that the markers we found represent a highly systematic and distinct chemical space within the big variety of beer metabolites. Consistent with literature findings, the CHNOS chemical space did not significantly contribute to the universal signature of the MR in beer. This agrees with low cysteine and cystine concentrations reported in malt, wort and beer [314]. As confirmation, an inhibiting effect on the progression of the MR and the formation of final MRPs is described for sulfur-containing amino acids [315]. The difference in the chemical signature of compositions specific to dark and pale beers could be attributed to their different origins. MRPs arise from chemical reactions, which follow kinetic and thermodynamic laws, and are not influenced by enzymatic catalysis. As already described in model systems [312], Maillard-derived CHNO compositions can carry multiple nitrogen atoms based on multiple condensation reactions of amino compounds to a sugar backbone. These reactions depend on the reactivity of amino acids involved and the MR intermediate's tendency towards carbonyl cleavage, resulting in new reducing ends of the sugar backbone. The formation of such nitrogen-rich compositions is described to accumulate with the progress of the MR [168]. In the complex beer system, involving numerous and interacting amino compounds, we detected compositions with up to four nitrogen atoms (CHN_1O to CHN_4O). Interestingly, we could observe a linear decrease in the composition frequencies with increasing nitrogen number. This agrees with the formation of nitrogen-rich compositions in the later stage of the MR and might confirm the kinetic nature of the dark beer markers. The number of oxygen atoms, not in the focus of previous studies, was also found to be highly systematic. With oxygen numbers exceeding 20 oxygen atoms and mass values over m/z 650, both oligo-saccharide precursors and condensation reactions can be regarded as important factors in the formation of MRPs in beer. These high-mass compounds also could be classified in the MR scheme. The evolution of the MR is characterized by dehydration reactions, which are reflected in the van Krevelen diagram where early MRP ($1.5 < H/C < 2$; $0.75 < O/C < 1$) evolve to highly unsaturated and aromatic compositions ($H/C < 1.5$; $O/C < 0.5$). The dehydration reactions inevitably come with introducing a DBE to the respective target formula. Both the increasing number of DBEs with higher mass and dehydration cascades for com-positions with Kendrick nominal mass > 400 reinforce the meaning of higher mass, non-volatile MRPs in the complex food system.

Studying exact mass differences, which represent certain compositional changes, we were able to reveal general and conceptual reaction sequences that can describe a part of the Maillard reaction in beer. Condensation reactions lead to compounds with higher mass and lead to a change in the composition, which always depends on both the carbonyl and amino compounds. Although the condensation of glycine ($C_2H_5NO_2$) and isoleucine ($C_6H_{13}NO_2$) with a carbonyl moiety are very similar in their underlying reaction mechanism, they lead to different compositional changes (C_2H_3NO and $C_6H_{10}NO$, respectively). The same is true for the condensation and interaction of MR intermediates. Other reactions like simple dehydration or glycation are characteristic of the MR but not specific as a multitude of biochemical transformations includes a loss of water or glycation as well. Accordingly,

compositional changes that neither depend on amino acids nor correspond to the condensation of complex intermediates or very simple reactions were to be expected.

Therefore, the ten most significant compositional changes are changes including CHO-transformations coming with a loss of mass. Consequently, at this point, our data cannot provide conclusions about the role of single amino compounds but describe the complex system holistically. What was found to be statistically significant can refer to very general chemical changes that early MRPs or intermediates of diverse origins undergo to build a Maillard reaction end product. By our network and shortest path approach, we furthermore were able to decipher the combination and chronological order of Maillard intermediate phase reactions that match these compositional changes. All intermediates were found in either beer or the Maillard model system and despite hundreds of possible combinations, the chronological order was consistent within the source and target pairs. This leads us to regard the results of the network approach as reaction sequences.

These sequences share a common inherent structure: Starting with the condensation of a small MR fission product, a dehydration cascade and finally a decarboxylation reaction occurs. These fission products like glyoxal, methylglyoxal or diacetyl arise from retro–aldolization of sugar molecules or cleavage of respective dicarbonyls [316]. Dehydration cascades are well described to play a major role in the formation of MRPs. In several ribose–amino acid model systems we were able to highlight the role of early diketosamine formation and its subsequent degradation in the MR [312]. Molecular formulae equivalent to six consecutive dehydration products could be described. Our presented results indicate that such a degradation process might also be caused by the condensation of a fission product when describing a complex system in general. In the context of the MR, loss of CO_2 likely occurs due to an α-dicarbonyl-assisted oxidative decarboxylation (e.g., Strecker degradation) [317]. In this case, the resulting imine is hydrolyzed to give the so-called Strecker aldehyde. The hydrolysis reaction leads to the loss of the specific amino acid residue at the initial dicarbonyl unit. These reactions would be no longer tangible for our general approach. Purely thermally induced decarboxylation reactions, on the other hand, could occur during the roasting process. They require very high temperatures (>200 °C) [318] and thus naturally happen at the end of the heating process and reaction sequences. It is worth noting that the presented pathways and their interpretation are restricted to compositional information obtained by accurate mass measurements. They describe very general and conceptual patterns within a complex food system. Mechanistic studies including various model systems, resolved in time, should be performed to fully understand the reaction sequences we proposed to describe the MR in beer.

In industrial practice, the extensive chemical changes that are associated with the heat load are usually monitored by the unspecific reaction of 2-thiobarbituric acid (TBA) [319]. It is based on the photometric tracking of the reaction of TBA with dicarbonyl functions. However, the origin of the dicarbonyls (e.g., MR or lipid oxidation) and their follow-up reactions cannot be differentiated. By comparison, we recorded over 2,500 compositions that describe the MR in beer comprehensively

alongside the reaction network leading to such a multitude of MRPs. Our analytical approach may offer a unique method to guide MR-related brewing processes, such as malting and boiling, towards desired attributes of the final beer end product. Having the opportunity to resolve the Maillard reaction cascades and resulting molecular complexity, effects of changed kilning or roasting parameters can be monitored as well as the progress of the MR throughout the whole brewing process.

3.5 Conclusion

Overall, this study reports a comprehensive analytical approach addressing the great variety of MR-derived products in a complex food system, the description of their compositional nature and the general reaction cascades that lead to the diversity observed. It contributes to a better understanding of the complex molecular processes involved in the MR and might be a starting point for potential process development and quality control in both the malting and brewing industries.

Chapter 4 |
On the Trail of the German Purity Law: Distinguishing the Metabolic Signature of Wheat, Corn and Rice in Beer

Here, we report a non-targeted analytical approach to investigate the influence of different starch sources on the metabolic signature in the final beer product. An extensive sample set of commercial beers brewed with barley, wheat, corn and/or rice were analyzed by both direct-infusion Fourier transform ion cyclotron mass spectrometry (DI-FT-ICR-MS, 400 samples) and UPLC-ToF-MS (100 samples). By its unrivaled mass resolution and accuracy, DI-FT-ICR-MS was able to uncover the compositional space of both polar and non-polar metabolites that can be traced back to the use of different starch sources. Reversed-phase UPLC-ToF-MS was used to access information about molecular structures (MS^2-fragmentation spectra) and isomeric separation, with a focus on less polar compounds. Both analytical approaches were able to achieve a clear statistical differentiation (OPLS-DA) of beer samples and reveal metabolic profiles according to the starch source. A mass difference network analysis, applied to the exact marker masses resolved by FT-ICR, showed a network of potential secondary metabolites specific to wheat, corn and rice. By MS^2-similarity networks, database and literature search, we were able to identify metabolites and compound classes significant for the use of the different starch sources. Those were also found in the corresponding brewing raw materials, confirming the potential of our approach for quality control and monitoring. Our results also include the identification of the aspartic acid-conjugate of N-β-D-glucopyranosyl-indole-3-acetic acid as a potential marker for the use of rice in the brewing industry regarding quality control and food inspection purposes.

This chapter has been published as Pieczonka, S. A., Paravicini, S., Rychlik, M. & Schmitt-Kopplin, P. On the trail of the German Purity Law: distinguishing the metabolic signatures of wheat, corn and rice in beer. Frontiers in Chemistry: Analytical Chemistry, 9 (715372), 1-12 (2021).

Candidate's contributions: S.A.P. designed the experiments, analyzed and interpreted the data. S.A.P wrote, revised and approved the final paper. S.A.P. performed the instrumental experiments. S.A.P. performed the statistical treatment, data mining, interpretation and visualization.

4.1 Introduction

Beer is defined as a fermented, but not distilled, beverage that is made from starch sources. Seen as one of the first food laws, the Bavarian Purity Law [161] stipulates only the ingredients barley, hops and water to ensure the quality standard of beers, its shelf-life, preservation and safety. Nowadays, beverages that are sold as beer are open to a large number of brewing types and raw materials [320]. As an example, the German feudal purity law of 1516 does not allow wheat as an ingredient of beer, because valuable wheat and rye grain should be exclusively used for baking. This contrasts with today's Bavarian wheat beer, which according to current law (German Beer Purity Law, Vorläufiges Biergesetz) must be brewed from at least 50 % of wheat malt and top-fermented. With Belgian wit beers as a second classic wheat-based beer and especially the rising market of alcohol-free beers, the role of wheat and wheat malt significantly changed during the last centuries [321].

Other malted grains that are not mentioned in the purity law of 1516 and traditionally used for beer brewing on the international landscape are corn and rice. Rice beers, locally referred to as zutho, are found in the Indian cultural area [322]. In the production of gluten-free beer, rice plays a special role as a naturally safe source of starch. Ceccaroni, et al. [323] optimized the malting process of rice for a top-fermented gluten-free beer available to individuals affected by celiac disease. By adding caramelized specialty rice malt, a malted and rich aroma profile and amber color of the rice-only beer were achieved, as the authors report [324]. Mayer, et al. [325] claimed to overcome the problems when beer is brewed with rice malt only and reported a bottom-fermenting brewing process based on rice-endogenous enzyme activities. Bailly, et al. [326] report brewing with malted corn on a laboratory scale, significantly rising the enzyme activity compared to unmalted corn [327].

Brewing with corn and rice is therefore diverse but comes with well-described disadvantages compared to barley malt [328-332]. It also has a significant impact on the beer's sensory profile [333]. For these reasons, brewing with a certain proportion of raw grain adjuncts of rice and corn is much more common. In the contemporary brewing industry, barley malt is often partially replaced with adjuncts like corn, rice, starch or sugar. Especially the competitive price [334], but also shortened mashing times and lower mashing temperatures make them valuable in modern industrial brewing. The associated changes in enzyme activities, free amino nitrogen and protein content can be balanced out with exogenous enzymes and extracts [335,336]. The use of raw grain and other adjuncts as an inexpensive alternative to barley or wheat malt is forbidden in Germany.

As early as the 1960s, the analytical determination of the use of raw grain adjuncts was in the focus of brewing research in Germany [337]. Where at that time the original wort difference, mineral content, total and coagulable nitrogen turned out to be characteristics, the carbon isotope determination of the C4-plant corn was subsequently added [338]. Analysis methods based on immunological concepts often showed weak points due to the big expense necessary, cross-reactions or major

changes in the beer ingredients during the brewing process [339,340]. Iimure and Sato [341] investigated the proteome of beers brewed with barley, rice and corn by 2-D gel electrophoresis combined with MS. Following the proteomics approach, two proteins were determined as corn-specific but not relevant for the beer quality and thus not further characterized. Fenz [342] reported the detection of corn adjuncts in beer by HPLC-UV analysis of the corn-specific oxindole derivative 7-hydroxy-2-oxindole-3-acetic acid and glycerol esters of polyphenols [343] after previous extraction and adsorption chromatography. The method described has been further simplified [344] and can be used on corn, but not on rice.

The technical advances in separation methods, detector units and mass analyzers, as well as the further development of data collection and analysis, are showing new perspectives for modern beer analysis [227]. The entire molecular diversity of beer can be shown and the influence of different raw materials such as hops and wheat on its metabolome can be captured [225]. Complex reaction networks during the brewing process can be described [226]. In our study, we report a comprehensive non-targeted analytical approach involving direct-infusion Fourier transform ion cyclotron mass spectrometry (DI-FT-ICR-MS) and UPLC-ToF-MS combined with statistical and network analyses to investigate simultaneously the influences of wheat, corn and rice on the beer's metabolic signature. The findings could be of great interest with regard to quality control in the brewing industry and foodstuff inspection in the context of the Purity Law.

4.2 Materials and Methods

4.2.1 DI-FT-ICR-MS measurements and data processing

A total of 400 samples of commercially available beers from over 40 different countries were analyzed. The sample set is a cross-section representing all possible combinations of beer styles, fermentation types, raw materials, color impressions and alcohol contents available. Thus, metadata co-varying with the characteristic in focus could be excluded. The samples were purchased at local grocery stores between 2018 and 2020 and stored at -20 °C prior to preparation for analyses. High-resolution mass spectra were acquired on a Bruker solariX Ion Cyclotron Resonance Fourier Transform Mass Spectrometer (Bruker Daltonics GmbH, Bremen, Germany) equipped with a 12 Tesla superconducting magnet (Magnex Scientific Inc., Yarton, GB) and a APOLO II ESI source (BrukerDaltonics GmbH, Bremen, Germany) operated in negative ionization mode. The sample preparation, measurement and data processing parameters were chosen as reported recently [225,226]. An average mass error of < ±0.15 ppm was reached within and between measurement batches. The resulting 7,700 unambiguous molecular formulae in the CHNOSPCl chemical space that occur in at least five samples were kept for further statistical analysis. An

overview of the sample set is given in the Supplementary (Table D.1 in Supplementary Chapter 4).

4.2.2 UPLC-ToF measurements and data processing

Solid-phase extraction (SPE) was applied to a sub-sample set including 100 beers. The SPE parameters are given in Table D.2 in Supplementary Chapter 4. The eluate was evaporated to dryness (25 °C, 1 mbar, 3 h, Christ Martin™ RVC 2-25 CD vacuum concentrator) dissolved in the starting conditions of the UPLC-gradient, vortexed and centrifuged (4 min at 14000 rmp). The supernatant, five times concentrated compared to the initial beer sample, was used for UPLC-ToF-MS ESI-negative analysis on a Shimadzu LCMS-9030 Q-ToF-System (Shimadzu Deutschland GmbH, Duisburg, Germany) in randomized order. The parameters of the chromatography and ToF-measurements are given in Table D.3 in Supplementary Chapter 4. A pooled QC consisting of all measured samples was used for system conditioning and measured after every 10th injection. On this basis, the batch was normalized (compensation for intensity fluctuations) by the LOWESS algorithm. A class QC, including all samples with the same carbohydrate source, was used for each of the barley, wheat, rice and corn classes. Features that occur in at least 33 % of all samples belonging to the respective class were kept as potential maker features for statistical analysis. The data processing and extraction of chromatographic features was carried out with the open-source MS-DIAL software [345] after the export of the raw data to the centroided mzML-format within the LabSolutions™ 5.99 SP2 software (Shimadzu Corp., Kyoto, Japan). The data treatment parameters were optimized and are given in Table D.4 in Supplementary Chapter 4.

To validate the origin of the statistically most significant features, 10 g of respective foodstuff (corn grits, corn flour, corn starch, corn oil, wheat grits, wheat flour, whole-wheat flour, wheat starch, rice grits, rice flour, rice starch), including typical grain adjuncts in the brewing industry was extracted with 40 mL MeOH for 1 h on the shaker (250 min^{-1}). The suspensions were centrifuged (5 min, 14.000 rmp) and the supernatant was evaporated to dryness (25 °C, 1 mbar, 8 h). The residue was resolved in 2 mL starting conditions by vortexing and supersonification and syringe filtrated (0.2 µm) before UPLC-ToF-MS analysis. Furthermore, potential marker substances were measured in positive ESI mode to obtain another complementary fragmentation spectrum.

The aspartic acid conjugate of (6,6-d_2) N-β-D-glucopyranosyl-indole-3-acetic acid was synthesized as described by Kai, et al. [346] and kindly provided by the latter authors. The standard was resolved in methanol (6 µg.mL^{-1}) and added to a worked-up beer sample (sample 325) in equal volumes for co-chromatography.

4.2.3 Data treatment and visualization

We performed a supervised OPLS-DA analysis on both the FT-ICR and UPLC-ToF dataset matrices consisting of metabolite features and intensities. Data pretreatment included zero-filling, data normalization, scaling and transformation (Table D.4 in Supplementary Chapter 4). The Hotelling's T2 test (95 %) was applied to prohibit the influence of strong outliers on the models. The lists of the most important masses were defined choosing the highest loadings values. The top characteristic masses were selected within the 95th percentile (385 masses for each carbohydrate source for FT-ICR and 89 for UPLC-ToF respectively). Potential markers for the use of barley were neglected due to co-varying metadata (Figure D.1 in Supplementary Chapter 4). The goodness of the fit and of the prediction were evaluated with the R2 and Q^2 values. To exclude overfitting, we provide the p-value of the Cross-Validation Analysis of Variance (CV-ANOVA). With high values for the quality of prediction (Q^2) that do not exceed those of the goodness of the fit (R2Y) and CV-ANOVA p-values far lower than 0.05 for the comparison of between-class against within-class variance, the significance of the models could be confirmed and overfitting excluded [214,215]. Those elaborations were done in SIMCA 13.0.3.0 (Umetrics, Umeå, Sweden). The statistical parameters of the beer samples (Table D.1 in Supplementary Chapter 4) and OPLS models (Table D.5 in Supplementary Chapter 4) can be found in the Supplementary section. Eight samples with inadequate measurement quality were not integrated into the FT-ICR-MS statistical model. Three samples were excluded from the models because of information on the ingredient list contrary to their positions in the score plots (FT-ICR and UPLC-MS). Predicted score values were calculated.

The FT-ICR-MS marker formulae were depicted in van Krevelen diagrams for each starch source. By plotting H/C- versus O/C-atomic ratios it is possible to depict common compositional patterns within observations' markers [26,111,126]. A mass difference network (MDiN) was applied utilizing the NetCalc approach [237]. The nodes, representing the annotated molecular formulae, were connected by edges that represent compositional changes corresponding to 250 different (bio)chemical reactions.

The UPLC-ToF marker features were subjected to the open-source Cytoscape software environment [267] to visualize an MS^2-similarity-network based on similar fragments and neutral losses. The similarity cutoff was set to 0.65. Database search for matching fragmentation spectra was performed using the MS-FINDER [347] and MetFrag [262] software tools. The entries in the HMDB, FooDB, ChEBI, LipidBlast, LipidMaps, KNApSAcK and PubChem databases were used to carry out a comparison of respective in silico fragmentation with our experimental data. The best five hits were examined for their plausibility. When possible, the hits were confirmed through experimental spectra of primary literature. The levels of identification were assigned as suggested by the Metabolomics Standards Initiative [10].

The FT-ICR-MS and UPLC-ToF-MS data were compared with a mass tolerance of ±5 ppm. Isomeric compounds were merged with the same error tolerance for the UPLC-ToF-MS features. The overlaps were illustrated using pie charts.

4.3 Results

4.3.1 Direct-infusion Fourier transform ion cyclotron mass spectrometry

In the first analytical step, we investigated the metabolome profile of a total of 400 bottled beer samples by direct-infusion Fourier transform ion cyclotron mass spectrometry (DI-FT-ICR-MS) using electrospray (-) ionization. The commercial beer samples covered the numerous facets of beer brewing and included beers manufactured in over 40 countries around the world. By that, we could exclude most co-variating metadata. Despite the abundance of different and combined brewing styles, the craft beer style including the step of dry hopping was found to co-variate with beers brewed with barley only (Figure D.1 in Supplementary Chapter 4).

The non-targeted and holistic approach, renouncing discriminatory sample processing and chromatography, is capable to resolve the entire molecular complexity of beer within a quick (10 minutes) measurement. About 7.700 unambiguous molecular compositions could be assigned to exact monoisotopic masses spanning the mass range of m/z 100 to 1000 (Figure 4.1A) within the sample batch. They reach from polar sugars, phosphates and sulfates over diverse secondary metabolites and peptides to non-polar lipids, hop bitter acids and highly unsaturated polyphenols and Maillard reaction end products [225,226]. We were able to resolve up to 40 monoisotopic mass features within one single nominal mass including several significant compositions regarding carbohydrate sources, as will be seen later (Table D.6 in Supplementary Chapter 4). The molecular formulae were annotated in the CHNOSP chemical space and subjected to further statistical analysis.

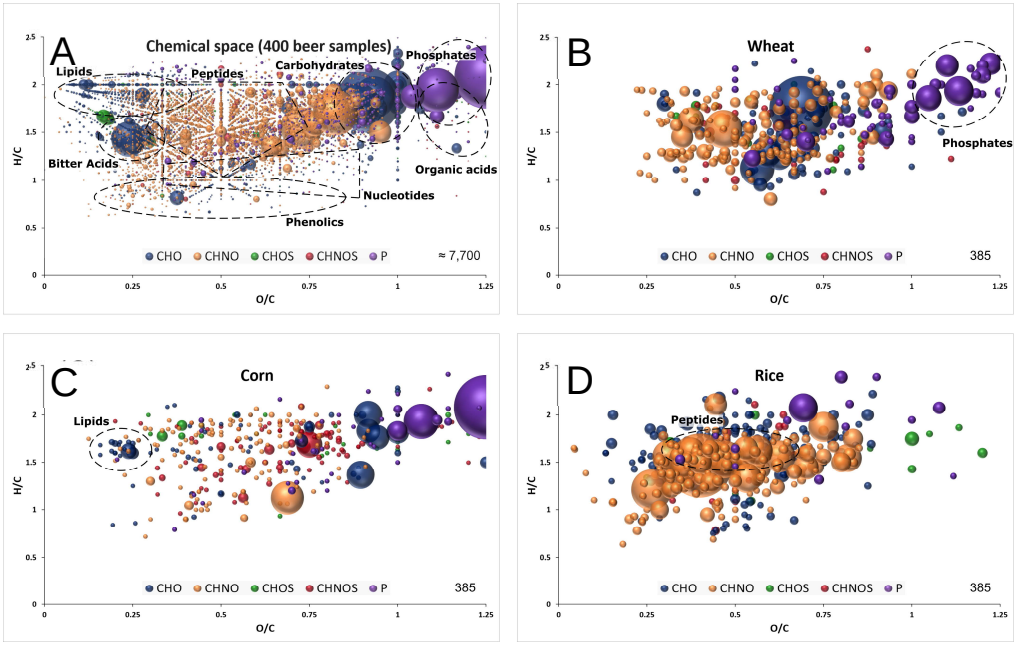

Figure 4.1 | Van Krevelen diagram of molecular formula annotations found in 400 beer samples (A) and significant for wheat (B), corn (C) and rice (D) by DI-FT-ICR-MS as extracted after OPLS-DA modeling presented in Figure 4.2. Regions specific to certain compound classes are highlighted. Color code: CHO blue; CHNO orange; CHOS green; CHNOS red; P purple. Neutral molecular formulae are plotted. The bubble size indicates the mean relative intensities of corresponding peaks in the spectra.

We applied supervised orthogonal partial least-squares discriminant analysis (OPLS-DA) to the metabolite data resolved by DI-FT-ICR-MS, using the carbohydrate source as Y-variable. The classification power of the model was highly significant (Table D.5 in Supplementary Chapter 4). The Q^2 value for the quality of prevision (>0.6) and the R2Y value for the goodness of the fit (>0.85) prove the statistical relevance whereas overfitting was excluded by the p-value calculated after the CV-ANOVA (<<0.05) [214,215]. The associated score plot (Figure 4.2A) showed a clear differentiation of barley, wheat, corn and rice beers. In the first principal component, beers brewed with barley only are separated from beers with an additional carbohydrate source. The second component separates beers brewed with wheat from those brewed with corn or rice (Figure 4.2A-I). Ultimately, the third component differentiates rice and corn beers (Figure 4.2A-II). Accordingly, a statistical model was achieved that uncovered the influence of all considered carbohydrate sources on the metabolic signature of beer. Metabolite features that drive the separation were extracted from the respective loadings plot (Figure D.2 in Supplementary Chapter 4). Compositions causing the agglomeration of corn and rice

beers in the first and second component are referred to as “corn and rice” features in the following.

The marker metabolites for corn described by Fenz [342] could be confirmed with significant mass values equal to p-coumaroyl glycerol [$C_{12}H_{14}O_5$], caffeoyl glycerol [$C_{12}H_{14}O_6$] and hydroxyoxindoleacetic acid [$C_{10}H_9NO_4$]. In addition to individual masses, the van Krevelen diagram of the respective compositions revealed characteristic patterns for the carbohydrates sources. Beers brewed with wheat featured a multitude of very polar phosphates (Figure 4.1B) and beers brewed with corn showed a specific pattern of lipids (Figure 4.1C). Many compositions characteristic for rice beers are located in the area where peptides are expected

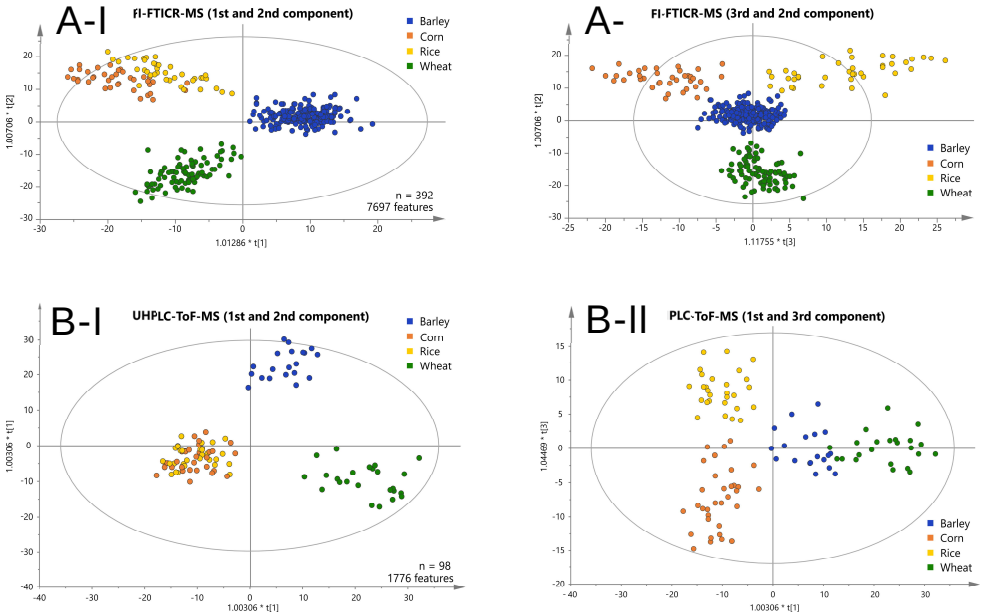

Figure 4.2 | Score plots of the OPLS-DA of the DI-FT-ICR-MS (A) and UPLC-ToF-MS (B) data differentiating the carbohydrate sources used. The position of the beer samples is marked by dots colored according to their carbohydrate source. The first and second components are shown in (A-I) and (B-I). The third against the second and the first against the third component are shown in (A-II) and (B-II) respectively.

(Figure 4.1D).

Additionally, compositional mass difference networks (MDiN) have proven to be powerful tools to set significant compositions in relation. It can utilize the exact mass information FT-ICR-MS provides, where compositions are represented as nodes that are connected by edges representing distinct mass differences that

describe (bio)chemical relations. Such a MDiN sets in relation the lipid pattern found specific to corn by (de)hydrogenation, hydroxylation, water or glycerol addition and chain elongation reactions (Figure D.3 in Supplementary Chapter 4). Several derivatives of the lipid with the mass m/z 335.22278 [$C_{20}H_{32}O_4$] could be explained by e.g. hydrogenation [$C_{20}H_{34}O_4$] and hydroxylation [$C_{20}H_{32}O_5$] reactions. Accordingly, the characteristic composition [$C_{21}H_{34}O_4$] is connected to [$C_{21}H_{36}O_4$] and [$C_{21}H_{34}O_5$] by hydrogenation and hydroxylation respectively.

A second MDiN excerpt that sets wheat, corn and rice markers in biochemical relation was investigated in more detail (Figure 4.3). As reported before [225], the metabolome wheat adds to the beer's complexity specifically is characterized by compositions corresponding to benzoxazinone derivatives. The mass corresponding to possible blepharin [$C_{14}H_{17}NO_8$], a plant phytoanticipine, is connected to the related HMBOA-glucoside [$C_{15}H_{19}NO_9$] by methoxylation. A subsequent sulfation gives [$C_{15}H_{21}NO_{12}S$]. An equivalent pattern links the hydroxylated DHBOA-glc [$C_{14}H_{17}NO_9$], the DIMBOA-glc [$C_{15}H_{19}NO_{10}$] and the respective sulfate [$C_{15}H_{21}NO_{13}S$]. Besides methoxylation, hydroxylation, sulfation and water addition, several glycation reactions of described molecular formulae lead to a complex network of known and unknown compounds specific for wheat. Those reach from rather unsaturated compositions [e.g. $C_{10}H_9NO_3$ and $C_{11}H_{11}NO_3$] to very polar glucosides of the potential aglyca [e.g. $C_{23}H_{31}NO_{13}$, $C_{26}H_{39}NO_{20}$ and $C_{26}H_{37}NO_{19}$]. A similar, but smaller, network is being built up for corn-based on compounds likely arising from the indoleacetic acid (IAA) biosynthetic pathway. Chloride adduct formation of the respective aglycon hydroxyoxindoleacetic acid [$C_{10}H_9NO_4$] reinforces the presence of a carboxylic acid group of these compounds on the molecular structure level. Based on this annotation, known to be specific for the use of corn (Fenz, 1991), two glycation reactions lead to the respective derivatives [$C_{16}H_{19}NO_9$] and [$C_{22}H_{29}NO_{14}$]. Again, several compositional changes equivalent to hydroxylation, hydrogenation, methoxylation or water addition form a network of masses specific to corn. In parallel, there is a similarly structured network starting from [$C_{10}H_9NO_5$] for rice. The composition could potentially be annotated to hydroxydioxindoleacetic acid, found in rice bran by [348]. The described biochemical relations again lead to compositions specific for rice [e.g. $C_{16}H_{21}NO_{11}$, $C_{22}H_{31}NO_{16}$, $C_{16}H_{23}NO_{11}$, $C_{22}H_{33}NO_{16}$], but also includes compositions characteristic for corn and rice [e.g. $C_{10}H_{13}NO_7$ and $C_{16}H_{19}NO_{10}$]. Overall, secondary metabolites deriving from tryptophan-dependent pathways drive the differentiation of the carbohydrate sources wheat, corn and rice for brewing. The metabolites cover a wide range of polarity, all accessible from direct-infusion with FT-ICR-mass spectrometry. However, metabolites could only be annotated by exact masses and their biochemical relations (expressed as mass differences) in combination with database and literature data. For definite structural confirmation, a chromatography-coupled mass spectrometric approach including ion fragmentation is necessary (UPLC-ToF-MS).

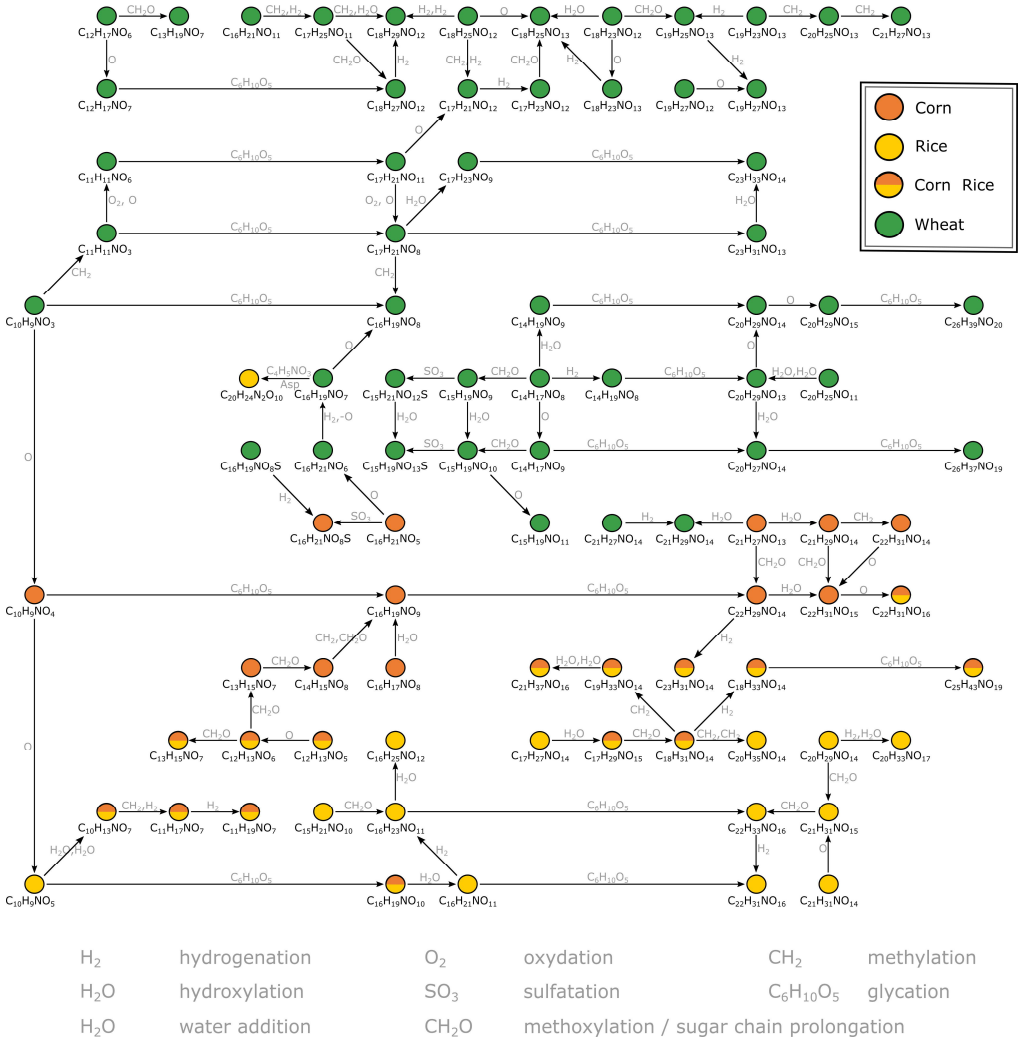

Figure 4.3 | Mass difference network excerpt of compositions characteristic for wheat, corn and rice. The nodes representing annotations are connected by edges representing potential biochemical reactions. Some connections are neglected for reasons of clarity. The annotations likely correspond to secondary metabolites deriving from the indoleacetic acid and benzoxazinone biosynthetic pathways respectively.

4.3.2 UPLC-Time of flight mass spectrometry

A representative sub-sample set (100 samples) was treated by solid-phase extraction (SPE) and subjected to reversed-phase UPLC-ToF-MS. An average of 680 chromatographic features per sample was obtained after applying filter criteria. The peaks shared by at least one-third of all beer samples within a carbohydrate source class (1750 peaks) were used for statistical analysis (OPLS-DA). The classification power of the model was highly significant (Table D.5 in Supplementary Chapter 4). The Q^2 value for the quality of prevision (>0.6) and the R2Y value for the goodness of the fit (>0.85) prove the statistical relevance whereas overfitting was excluded by CV-ANOVA (p-value <<0.05) [214,215]. As for the FT-ICR-MS data, the associated score plot (Figure 4.2B) showed a clear differentiation of barley, wheat, corn and rice beers. In the first two principal components, beers brewed with barley only are separated from wheat beers. Again, beers brewed with corn or rice are agglomerated against the two others (Figure 4.2B-I).

The third component enables the differentiation of corn and rice beers (Figure 4.2B-II). Ultimately, a statistical model distinguishing all carbohydrate sources could also be achieved by the isomeric resolved UPLC-ToF-MS data of the pretreated sub-sample set. The metabolite features that drive the separation were extracted from the respective loadings plot accordingly (Figure D.2 in Supplementary Chapter 4).

The available MS^2-spectra of the potential marker compounds were utilized in a mass spectral similarity network (Figure 4.4). The fragmentation spectra of compounds that were examined in more detail can be found in the Supplementary (Table D.7 in Supplementary Chapter 4). Two clusters with similar fragmentation patterns could be observed for the wheat-specific compounds. The first cluster (Figure 4.4I) could be identified as an agglomeration of benzoxazinone derivatives, known to be phytoanticipines in the wheat plant and validating the findings with DI-FT-ICR-MS data. By database and literature research [225,281,349] four compounds could be identified as MOBA, HBOA-glucoside, DIBOA-glucoside and HMBOA-glucoside (identification level 2 [10]). For the second cluster (Figure 4.4II), only in silico fragmentation spectra of database entries were available. All matching spectra found for the five peaks indicate the potential compound class of N-acyl-glutamines (identification level 3). Their almost identical retention behavior (4.32 to 4.62 min) and proposed molecular formulae ($[C_{23}H_{38}N_2O_5]$, $[C_{23}H_{40}N_2O_5]$, $[C_{25}H_{40}N_2O_4]$, $[C_{23}H_{38}N_2O_6]$ and $[C_{23}H_{40}N_2O_6]$) support their close chemical relation.

For corn markers, two clusters of compounds with related fragmentation spectra and thus similar structure and origin could be observed. The cluster with the greater significance (Figure 4.4III) was studied in more detail. The nine compounds examined were found to be isomeric pairs of m/z-values matching the molecular formulae [$C_{20}H_{34}O_4$], [$C_{20}H_{32}O_5$], [$C_{21}H_{36}O_4$] and [$C_{21}H_{34}O_5$]. The close retention time window between 6.0 and 7.1 minutes supports their close chemical relation. Together

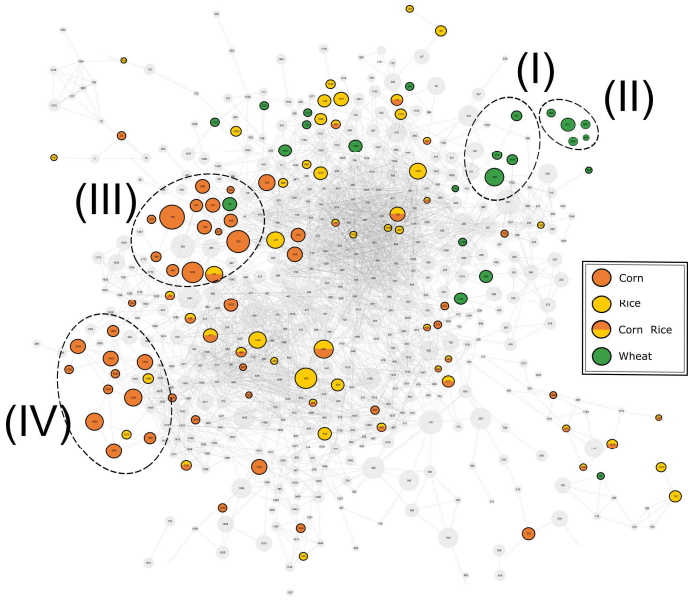

Figure 4.4 | Mass spectral similarity network of the fragmentation spectra of compounds detected by UPLC-ToF-MS. The nodes representing the respective compounds are connected by edges representing their spectral similarity. Compounds found to be specific for a carbohydrate source are colored accordingly. Two clusters of potential markers are highlighted for wheat (I & II) and corn (III & IV).

with the similar molecular composition and fragmentation spectra, it brings us to suggest a shared compound class of a non-polar character. The best hits with regard to in silico fragmentation spectra all agree on lipid-type structures for the mentioned compounds. Besides, the fragmentation pattern of [$C_{20}H_{34}O_4$] and [$C_{20}H_{32}O_5$] compounds show a great similarity to DiHEtrE and TriHETE fragmentations spectra respectively, when compared to literature data [350,351]. However, based on our data, the exact molecular structure and in particular the position of possible hydroxylation cannot be determined. Accordingly, the identification level of this group of corn-specific compounds was indicated to level 3, as suggested by Sumner, et al. [10]. In addition to this not yet described cluster of lipid-type molecules, we were able to confirm the hydroxyoxindoleacetic acid as a marker substance for the use of corn by comparison of both in silico and literature fragmentation data [342] (identification level 2).

The rice-specific compounds, few of which were found highly significant in the loadings plot already, did not cluster with regard to their fragmentation pattern. Two of those could be characterized by their molecular formula [$C_{24}H_{40}N_6O_8$] and [$C_{22}H_{35}N_5O_{11}$] as being in accordance with mass values found to be specific in FT-ICR-MS. A second pair of highly significant peaks could be described as potential Glu-Trp-Leu/Ile-Pro [$C_{27}H_{37}N_5O_7$] and a cyclic Asp-Ser-Val-Leu-Trp peptide [$C_{29}H_{40}N_6O_8$], respectively, by comparison of in silico fragmentation data (identification level 3). The fifth potential marker of highest interest could be assigned based on both matching fragmentation patterns and co-chromatography (identification level 1). Kai, et al. [346] reported an aspartic acid-conjugate of N-β-D-glucopyranosyl-indole-3-acetic acid to be found in rice with a matching fragmentation pattern. The respective d_2-standard, synthesized and provided by the mentioned authors, was used for co-chromatography. The rice secondary metabolite was identified by matching retention time and fragmentation pattern (Figure 4.5). We were able to detect the corresponding peak in the vast majority of rice beers and two beers brewed with corn. To confirm our findings and the origin of the potential marker compounds, we analyzed methanol extracts of food made from the appropriate grain raw materials. Grits, starch and flour of wheat, corn and rice and corn oil were screened for the presence of the specific respective compounds (Table D.8 in Supplementary Chapter 4). Wheat benzoxazinones and potential acyl-glutamines were present in the wheat products. The exception is pure wheat starch, in which none of the compounds were found, as in beers brewed with merely wheat starch [225]. We were able to confirm the hydroxyoxindoleacetic acid in all corn products except for the oil. The isomeric pairs of lipid class compounds [$C_{20}H_{34}O_4$] and [$C_{21}H_{36}O_4$] were found in the corn oil, whereas the other specific oxygenated lipids might be formed during the brewing process. The same is suspected for the [$C_{29}H_{40}N_6O_8$] cyclic peptide in rice. The other rice metabolites,

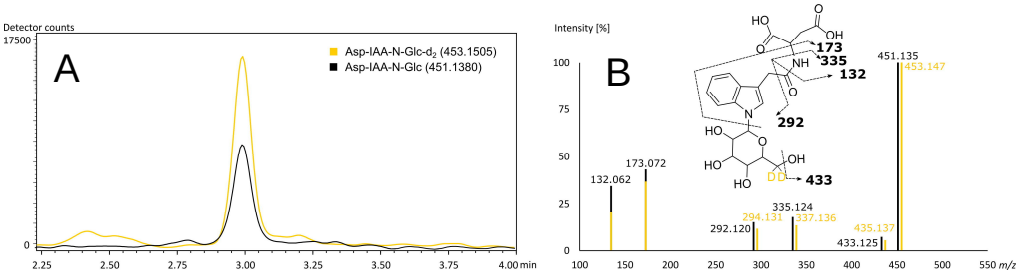

Figure 4.5 | Co-chromatography of the (6,6-d2)-N-β-D-glucopyranosyl-indole-3-acetic standard and its isotopologue naturally occurring in beer (A) with matching MS2-fragmentation spectra in ESI-negative (B). Extracted ion chromatograms of the corresponding m/z-values of Asp-IAA-N-Glc-d2 (yellow) and of Asp-IAA-N-Glc (black) (A). Mass fragmentation spectra of Asp-IAA-N-Glc-d2 (yellow) and of Asp-IAA-N-Glc (black) with corresponding suggested fragments of the mono-isotopologue (B).

including the aspartic acid-conjugate of N-β-D-glucopyranosyl-indole-3-acetic acid, were confirmed by the analysis of rice products. An overlap of the potential markers between the carbohydrate groups was not observed. Interestingly, the coumaryl and caffeoyl glycerols described by Fenz, et al. [343] and confirmed by FT-ICR-MS were found and identified in the methanol extract of corn grits but not the beers. We assume that they were lost through the SPE sample processing of the beers.

4.3.3 Comparison and conclusion

The investigation of the influence of different carbohydrate sources on the metabolome of the beer end product was carried out using two different, complementary mass spectrometric methods. Even with different sample numbers (400 for DI-FT-ICR-MS and 100 for UPLC-ToF-MS), fundamental differences and commonalities between the analytical approaches could be observed. Based on the direct-infusion approach without extensive prior sample preparation, compounds of all polarities (ionizable by ESI) are accessible with FT-ICR-MS. This is reflected in the MDiN of the secondary metabolites, which maps numerous glycosylation steps up to highly oxygenated compositions. This wide polarity range was not tangible by RP-HPLC-ToF-MS. The corn marker hydroxyoxindoleacetic acid was found with an early retention time (3.02 min), whereas glycosylated derivatives of the aglycone were lost by sample preparation and chromatography. The phosphate-structures found in FT-ICR-MS could not be found either and thus not be further characterized by fragmentation spectra. The average mass values also differ between FT-ICR-MS (m/z 409) compared to ToF-features (m/z 341.553), which could be attributed to different accessible mass ranges (100-1,000 Da for FT-ICR-MS, 50-1,500 Da for ToF-MS). The mass features showed a moderate overlap within a ±5 ppm range, in accordance with the different and complementary chemical spaces analyzed (Figure D.4 in Supplementary Chapter 4). About 35 % of the chromatographic features showed had a corresponding m/z-value in FT-ICR-MS, whereas less than 10 % of FT-ICR-MS-masses were found with an equivalent peak in LC-MS. Here, the different numbers of samples should be emphasized again. The majority of the chromatographic peaks showed at least one isomeric compound (up to 16), which confirms the complementarity of the information obtained by coupling chromatography to mass spectrometry. We observed a similarly low m/z-overlap with regard to the potential marker features. In particular, it is the statistically most significant compounds, which were detected in large parts in both DI-FT-ICR-MS and UPLC-ToF-MS. This enabled a deeper characterization through exact mass values and fragmentation mass spectra. Only the group of potential acyl-glutamines and some rice peptide-like structures are not present in the FT-ICR-MS-data.

Overall, with two complementary mass spectrometric approaches, we have uncovered deep metabolic signatures that the use of wheat, corn and rice in brewing entails. The majority of the decisive compounds can already be found in the

corresponding raw materials and survive the entire brewing process. We were able to set the compositions in relation by mass difference network analysis and uncovered a whole network of secondary metabolites specific to the respective grains. By mass fragmentation, the compounds could be characterized in detail and known reported marker substances could be confirmed. Finally, we want to highlight that in the aspartic acid conjugate of N-β-D-glucopyranosyl-indol-3-acetic acid we report a potential marker for the use of rice in beer.

4.4 Discussion

Both DI-FT-ICR-MS and UPLC-ToF-MS showed the power of mass spectrometric analysis with regard to food and beverage authenticity. As already shown for wine [352], the two approaches describe two different and complementary chemical spaces. However, we were able to differentiate simultaneously beers brewed with wheat, corn and rice against those with barley only in both DI-FT-ICR-MS and UPLC-ToF-MS. The metabolic signatures of the carbohydrate sources commonly used in brewing could be characterized by networks of secondary metabolites, resolved with regard to isomeric distribution and identified by MS^2-fragmentation information on different levels. Such comprehensive analysis of grain-specific metabolites was not carried out with regard to barley as all measured beers contained it to various extents and co-varying metadata was observed (Figure D.1 in Supplementary Chapter 4). In addition, beer samples that were brewed with merely wheat starch could not be identified as they lack the grain's metabolite signature. In the other grain-based foodstuffs, including typical grain adjuncts used in the brewing industry, we were able to detect the potential marker substances to various extents. All compounds could be found at least once, except for two annotated (cyclic) peptides and corn lipids, which indicates formation or alteration during the brewing process or insufficiently optimized extraction. Two barley beers of the same non-German brewery were neglected because they showed a clear signature of corn metabolites in spite of the contradicting information in the ingredient list. Although this is an exception, it brings us to the conclusion that, particularly with regard to the use of corn and rice, the metadata of commercial beers must be questioned. Authenticity control of the beer should be considered.

The statistical analysis shows that in both analytical approaches the metabolite profiles of beers brewed with corn and rice are very similar. Only in the third principal component, we could tell the respective clusters apart. A possible reason for this could be the closely related genetic evolution [353] and botanical relationship [354] of the plants and thus the similarity of their metabolic signatures even when analyzed in beer. Bearing in mind that barley, wheat, corn and rice all belong to the family of Poaceae and show collinearity [355], the reason for the observed similarity may also be found in the similar way of brewing when corn or rice adjuncts are used. Moreover, benzoxazinones found to be specific for wheat beers are not exclusively produced by Triticum aestivum, but analogous genetic information is also present in corn [356]. This indicates that both the concentrations and the distribution of the

secondary metabolites in the plant and thus the parts of the plant that are used for brewing play a decisive role [357]. The more pronounced diversity of benzoxazinone secondary metabolites induced by germination [357,358] could also be of importance and a starting point for further authenticity determinations with regard to the use of wheat raw grain adjunct. With this in mind, we hesitate to refer to the grain-specific compounds identified as biomarker molecules. Rather, the aim should be to quantify the metabolites with most sensitive instrumental analytics (e.g. triple quadrupole instruments) in numerous commercial and experimental beers in order to confirm the biomarker nature or define a concentration limit of confidence. Nevertheless, the metabolic signatures found in our study are unambiguous as a whole.

Such compounds that show strong evidence for the use of wheat [225,283] and corn [342,343] in brewing have been adequately described and have been confirmed in our study. In addition, numerous derivatives of these compounds could be characterized. Of particular note are the sulfate derivatives, some of which we already reported [225]. Little is known about the biological function of these compounds, but their function as polar regulation or storage conjugates can be assumed. Tang, et al. [359] also described these sulfates in human urine samples after wheat intake.

We were able to describe another conjugate of a secondary metabolite as a potential marker substance for the use of rice. To the best of our knowledge, literature has not yet reported a rice-specific compound for authenticity control. The aspartic acid conjugate of N-glucosyl-indoleacetic acid was described by Kai, et al. [346] in rice extracts for the first time, as the authors report. In general, IAA is known to regulate many aspects of growth and development in plants. For instance, it is reported to specifically induce a big grain1 gene, which expresses an auxin transport protein and ultimately results in a bigger rice grain size [360]. In that regard, the concentration of free IAA concentrations is well-balanced by biosynthesis, catabolism and transport mechanisms [361]. The conjugation of the auxin to glucose or amino acids is one part of the so-called IAA homeostasis. The aspartic acid and glutamic acid (to a lesser extend) conjugates are found to be the major storage or transport forms of the respective N-glucosyl-indoleacetic acid in rice [346]. Given that the N-glucoside likely is biosynthesized from the amide conjugates, this relationship could also apply to the reverse. However, the rice characteristic metabolite we found in beer appears to be an inactivated form of the auxin. Kai, et al. [346] described that the free N-glycosyl-indol-3-acetic acid is as well found in corn seedlings and alkaline hydrolysis releases additional amounts (0.45 nmol g^{-1} total amount). However, the conjugated form was not specified and corn grains were not investigated. Accordingly, incorrect information about the ingredients on the beer label of the two potential “corn and barley only” beers cannot be ruled out as all beers were purchased as presented to the consumer. As little is known about the distribution of the auxin derivatives in the plant tissues and thus about the tendency to be extracted during the brewing process, the biomarker character of Asp-IAA-N-Glc needs to be further investigated. With the huge majority of rice beers showing an Asp-IAA-N-Glc signal, a more specific extraction method or more sensitive mass spectrometric approach (e.g. MRM in triple quadrupole) could verify its presence in all beers brewed with rice. We also found the derivative in two corn beers, which might indicate the

rare presence of Asp-IAA-N-Glc in corn beers as well. Further investigations must clarify these findings and exclude potential incorrect information on the ingredient list. In any case, the presented potential rice-characteristic compound is, to our knowledge, not found nor reported in either barley or wheat beers or the respective plants.

Chapter 5 |
Archeochemistry Reveals the First Steps into Modern Industrial Brewing

A historical beer, dated to the German Empire era, was recently found in northern Germany. Its chemical composition represents a unique source of brewing culture at the end of the 19th century when pioneer innovations laid the foundations for industrial brewing. Complementary analytics including metabolomics, microbiological, sensory, and beer attribute analysis revealed its molecular profile and certify the unprecedented good storage condition even after 130 years in the bottle. Comparing its chemical signature to that of four hundred modern brews allowed to describe molecular fingerprints teaching us about technological aspects of historical beer brewing. Several critical production steps such as malting and germ treatment, wort preparation and fermentation, filtration and storage, and compliance with the Bavarian Purity Law left detectable molecular imprints. In addition, the aging process of the drinkable brew could be analyzed on a chemical level and result in an unseen diversity of hops- and Maillard-derived compounds. Using this archeochemical forensic approach, the historical production process of a culturally significant beverage could be traced and the ravages of time made visible.

This chapter has been published as Pieczonka, S. A., Zarnkow, M., Diederich, P., Hutzler, M., Weber, N., Jacob, F., Rychlik, M. & Schmitt-Kopplin, P. Archeochemistry reveals the first steps into modern industrial brewing. Nature Scientific Reports, 12 (9251), 1-15 (2022).

Candidate's contributions: S.A.P. designed the experiments, analyzed and interpreted the data. S.A.P wrote, revised and approved the final paper. S.A.P. performed the mass spectrometric instrumental experiments. S.A.P. performed the statistical treatment, data mining, interpretation and visualization.

5.1 Introduction

The birth and social evolution of humans and civilizations are closely related to the cultural heritage of beer production [158,362]. The reason for settling down may have been feasting, as suggested in the 11,000 thousand-year-old excavation site of Göbekli Tepe [296]. The latest excavations from Abydos, which reveal the oldest known mass-production brewery (over 20,000 liters a batch) dated at around 3,000 BC, again highlighted the importance of beer as food and ritual addition in early civilizations [363]. Domesticated grain cultivation was not only aimed at baking bread but goes hand in hand with brewing. In addition to the history of its ancient origins, the durable fermented beverage hides many other questions. Such as the development of its historical method of production, whose nowadays characteristic was shaped by one of the most famous historical food legislations, the Bavarian Purity Law of 1516 [161]. The fascination of fermentation processes, which was puzzling until the early modern era, fostered and was a driving force for innovation and science. The discovery of aerobic and anaerobic metabolic pathways [364] and the principle of pasteurization [162], thus the concept of modern food hygiene are closely linked to beer and yeast research. The isolation of individual yeast cells and cultured yeasts [163], as well as the first “refrigeration apparatus” by Linde [164] for brewing bottom-fermented beer, are significant achievements for today’s advancing civilization.

Rising from such pioneer works, the field of analytical chemistry nowadays is implemented to characterize the organic and inorganic residues of ancient and historical finds. In the recent past, archeochemistry evolved from the analysis of single marker compounds like tartaric acid (indication of winemaking) [365 ,366], oxalic acid (indication of brewing) [159] or acetic acid / lactic acid (indication of spoilage after fermentation) [367] to a more holistic approach integrating multiple analytical fields and metabolomics. Walther, et al. [368] sequenced the genome of the oldest pure culture yeast strain Saccharomyces carlsbergensis (1883), thereby specified their ploidy and genetic evolution, and detected it in beer samples presumably from the 1880s to 1900s [369]. Beer bottles found in a shipwreck in the Baltic Sea dated to the 1840s [287] were analyzed by means of reversed-phase and ion exchange LC and GC targeted approaches revealing insights in their hops and aroma compounds, despite contamination. Comprehensive non-targeted approaches utilizing the mass resolution and accuracy of high-field Fourier transform ion cyclotron mass spectrometry (FT-ICR MS) and Nuclear Magnetic resonance spectroscopy (NMR) were carried out investigating a bottle of champagne dated to the 1840s [370] and an unidentified wine sample from the late 18th to 19th century [371]. Based on the resolved molecular composition, the story of historical winemaking and champagne production could be traced step by step [370] in comparing modern and historical references. In addition to beer attributes, sensory and microbiological investigations, we adapted here such a comprehensive concept for the FT-ICR-MS and NMR-based characterization of a historical beer sample estimated from 1885. The resolved metabolic profile, including thousands of yet-unknown structures (“dark metabolome”), provides a chemical insight into the beer composition and conclusions with regard to the industrial brewing revolution at that time.

5.2 Results and Discussion

5.2.1 Discovery, beer attributes and sensory characterization

A newspaper article from June 19th, 1978 refers to an extraordinary find: Corked, wired and sealed, a bottle was found during the clearing up of a commercial building, the content of which is presumed to be beer from the German Empire era. Reconstructions of the label refer to the traditional Barre brewery in Lübbecke in northern Germany, which supplied New York and the whole world with beer in 1885. In a contractually agreed collaboration with the Lloyd shipping company, every year over 300,000 beers sealed with wax left Germany, but the found one did not.

The green bottle (Figure 1B-III) has a volume of about 0.75 liters and was sealed with a cork, fuse wire and wax. The bottle was still a good four-fifths full. The beer had very little sediment. The supernatant was clear and had an amber color. The tasting among four certified tasters resulted in a coherent and well-balanced beer. The smell and taste had sherry and port notes [372]. Likewise, it smelled of prunes. The beer had a slightly weaker palate fullness and somewhat low sparkling. But it was very harmonious in the overall impression and the bitterness.

The classic beer attributes are listed in Table E.1 in Supplementary Chapter 5, compared to other known bottom-fermented beers analyzed in that period and a current Barre beer from 2019 (B2019). The Vienna, Bohemian and Bavarian bottom-fermented beer types popular in the late 19th century showed an analytical range of original gravity, alcohol content, real extract and attenuation limit in which the historical beer fit well [373]. The comprehensible and coinciding attributes do not suggest that alcohol has escaped from the bottle in relevant quantities.

With all the characteristics that point to the great preservation of the beer, there were also references to the aging process that the beer has undergone. The color is expected to have been lighter originally. Alteration of hop components over the 130 years led to altered bitter units. However, at over 18 EBC, it still turned out surprisingly high. Yet, not enough to be allowed to call it Pilsner from today's legal point of view. Despite the light-protected surroundings of the finding and the bottling of the beer in a sealed brown glass, oxidation-sensitive vitamin B9 folates [374] were almost entirely degraded when compared to fresh beer samples [375] (Table E.1 in Supplementary Chapter 5). The nearly optimal conditions, apart from oxygen left in the headspace and the temperature fluctuations, were therefore not sufficient to protect these compounds from aging over many years.

5.2.2 Microscopy, microbiological cultivation, DNA-Screening for wort and beer-related microbes

No yeast and bacteria could be detected via microscopic analysis of the 1885 beer, neither could be cultivated via applied cultivation methods nor could any DNA of specific target DNA-sequences be amplified. Hence, living beer-associated microbes and non-fragmented target DNA could not be detected in the analyzed sample volume. Microscopic analysis revealed no yeast cells-like, rod-like and cocci-like structures and other microbe-like structures. Therefore, we suppose that the 1885 beer was filtered. In unfiltered old beer samples, microbe-like structures like yeast cells are reported to still be visible [287,376,377]. We also suppose that no post-filtration / bottling-derived / cork-derived contamination with beer spoiling microbes took place because no traces for wild yeast, super-attenuating yeast, lactic acid bacteria, acetic acid bacteria, and brewing background bacteria could be detected using the applied methods. Despite analyses of various genomic markers for bottom-fermenting lager yeast S. pastorianus and top-fermenting Ale yeast S. cerevisiae and a very low detection limit of those qPCR-based systems, there was no evidence for brewing yeast in quantities above the detection limit. We suppose a rather efficient sedimentation and filtration process, a few years after the first filtration apparatus was invented by Enzinger [378]. After filtration, during storage, a complete DNA-fragmentation of residual yeast cells took place. Single amorphous cloudy particle structures could be observed via phase-contrast microscopy (magnification 1000-fold) with a size between approx. 5 and 180 µm (Figure E.1 in Supplementary Chapter 5). The structure of the amorphous particles is typical for polyphenol-protein complexes that cause opalescence to turbidity when their concentration increases during beer aging. The amorphous particles were partially dissolvable in 10% KOH and completely dissolvable in concentrated sulphuric acid which indicates the protein fraction of the particles and their organic nature.

5.2.3 Persistent metabolome and ravages of time revealed by ^{1}H-NMR

The 1D ^{1}H-NMR spectra of the 19th century beer (Figure 1B-I) and its modern equivalent (Figure 1A-I) are shown in Figure 1. The overall signature indicates two beer samples that are characterized by a large similarity of metabolite signals, compiled in Table E.2 in Supplementary Chapter 5. The aliphatic region of the spectra (0 3 ppm) showed signals originating from alcohols (ethanol, iso butanol, iso pentanol), amino acids (alanine, proline, γ aminobutyric acid, valine), small organic acids (acetate, lactate, succinate, pyruvate, maleic acid, citric acid) and fatty acids. The midfield region (3 6 ppm) was mostly characterized by carbohydrate signals such as fermentable sugars (glucose, maltose), sugar derivatives (kojibiose) and differently branched dextrins. The aromatic region (6 9 ppm) showed signals of aromatic amino acids (phenylalanine, tryptophan, tyrosine), heterocyclic aromatic compounds

(nucleosides, niacin) and polyphenolic compounds that caused the underlying background from which the defined signals rise (6.8 7.5 ppm) [194]. One of the more conspicuous regions was that of aldehydes (>9 ppm) featuring signals of Maillard- and caramelization-derived 5-hydroxymethyl-2-furaldehyde (HMF) and 4-Hydroxy-2,5-dimethyl-3(2H)-furanone (furaneol). Overall, the qualitative metabolome signature resolved by ^{1}H-NMR showed a plurality of matching signals between both samples, underlining their great similarity even after more than 130 years. Differences associated with years of storage and the historical brewing method were, with the exception of few specific signals, primarily determined by the quantitative variance in the signal intensities (Table 1).

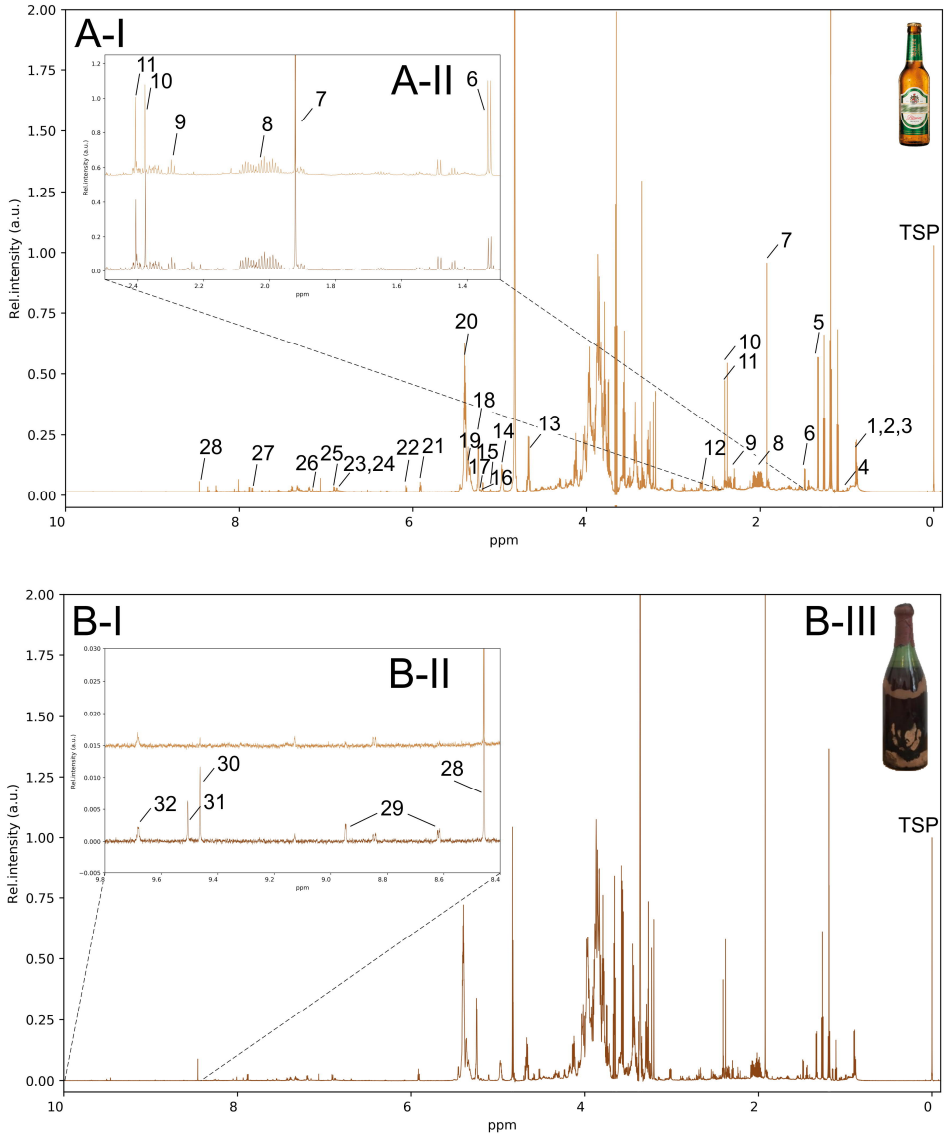

Figure 5.1 | 800 MHz 1D ^{1}H–NMR spectra of the modern lager beer (A-I, light brown) and the historical beer (B-I, dark brown). A-II highlights and compares the regions from 1.3-2.5 ppm containing the signals of small organic acids. B-II highlights and compares the aldehyde region of both beers (modern light brown, top; historical dark brown, bottom). B-III shows the waxed beer bottle from 1885 as it was found. Peak assignments: see table 1. Peak intensities are normalized to TSP.

Table 5.1 | Quantitative determination and change (B1885/B2019) of compounds identified in B1885 and B2019 with ^{1}H-Shifts of respective characteristic signals. [a] s singlet, d doublet, t triplet, q quartet, dd doublet of doublets, m multiplet. [b] +++ strong increase in B1885, ++ increase, + moderate increase, 0 no change, – moderate decrease, –– decrease, ––– strong decrease. [c] Carbohydrate. [d] n.d. not detected, trace found above the limit of detection, but below the limit of quantification, empty cells could not be quantified due to overlapping signals. [e] Identified through spiking of respective standard.

Compound (No.)	^{1}H-Shift (ppm)[a]	Change[b]	Concentration [mM][d]		Quanti-fication	Ref.
			B1885	B2019		
Acetic acid (7)	1.92 (s)	+++	3.38	1.38	integral TSP	[194,197,297]
Furfural (31)	9.50 (s)	+++	0.09	n.d.	integral TSP	Std.[e]
HMF (30)	9.46 (s)	+++	0.10	trace	integral TSP	[297]
Niacin (29)	8.9 (dd) 8.6 (dd)	+++	0.05	n.d.	integral TSP	Std.[e]
Unknown N-Heterocycle	8.23 (s)	+++				[379]
Unknown N-Heterocycle	8.21 (s)	+++				[379]
Unknown N-Heterocycle	7.94 (s)	+++				[379]
Acetaldehyde (32)	9.68 (q)	++	0.08	trace	integral TSP	[194,197,297]
Formic acid (28)	8.45 (s)	++	0.47	0.21	integral TSP	[194,197,297]
Kojibiose (15)	5.11 (d)	++				[379]
α-(1-4)-branched CH[c] (20)	5.35-5.45 (m)	+				[379]
CH[c] reducing end (18)	5.23-5.27 (m)	+				[379]
Glucose (17)	5.19 (d)	+				[379]
Uridine (21)	5.92 (d)	+	0.38	0.30	line fitting	[194,197,297]
Valine (4)	0.99 (d)	+				[197,297]
2-Methyl-1-propanol (1)	0.88 (d)	0				[194,197,297]
3-Methyl-1-butanol (2)	0.89 (d)	0				[194,197,297]
α(1-6)-branched CH[c] (14)	4.95-5.00 (m)	0				[379]
Alanine (6)	1.48 (d)	0				[194,197,297]
β-branched CH[c] (13)	4.40-4.85 (m)	0				
Citrate (12)	2.53 (d), 2.66 (d)	0				[194,197,297]
GABA (9)	2.30 (t)	0	0.55	0.59	integral TSP	[194,197,297]
Histidine (26)	7.15 (s)	0	0.10	0.13	integral TSP	Std.[e]
Malto-oligo-CH[c] (19)	5.25-5.38 (m)	0				[379]
Phenylalanine (25)	7.34 (m) 7.43 (m)	0				[197,297]
Proline (8)	1.95-2.1 (m)	0				[194,197,297]
Propanol (3)	0.89 (t)	0				[194,197,297]
Pyruvate (10)	2.37 (s)	0	0.90	0.75	line fitting	[194,197,297]
Succinic acid (11)	2.40 (s)	0	0.50	0.50	line fitting	[194,197,297]
Tyrosol (23)	6.87 (m) 7.19 (m)	0				[197,297]
Tyrosine (24)	6.91 (m) 7.20 (m)	0				[194,197,297]
Xylose (16)	5.21 (d)	0				
Adenosin/ Inosine (22)	6.07 (d)	- -	trace	0.16	line fitting	[194,197,297]
Lactic acid (5)	1.33 (d)	- -	0.65	2.09	line fitting	[194,197,297]
Polyphenols	6.80-7.45 (m)	- -				[194]
Cytidine (27)	6.07 (d) 7.85 (d)	- - -	trace	0.23	integral TSP	[194,197,297]

With a slightly higher valine content in the historical beer, similar profiles of free amino acids were found. The role of nucleosides in beer aging has been described as conspicuous in several studies [203,204,206], pointing at 5 methylthioadenosine as a potential compound for oxidative staling. The occurrence of this metabolite from the methionine salvage pathway [380] could not be reproduced by Yao, et al. [205] in a forced-aging study and was not detected by ^{1}H-NMR in this work. A higher uridine concentration was found in historical beer with a lower level of adenosine/inosine. Furthermore, three unidentified signals corresponding to N heterocycles showed high intensities (7.94 (s), 8.21 (s) and 8.23 (s)).

Another compound featuring an N-heterocycle, niacin, was found in high concentration in the historical beer. Norris [381] reported the niacin content to be decreasing over the advancing industrialization of the brewing process. While the found content of 6.2 mg/L niacin in the historical beer is plausible for a lager beer of the time (compare 10.3 mg/L in a strong beer of 1872 [382]), no niacin signal above the detection limit could be found in the modern equivalent (Figure 1B-II). Niacin is stable throughout the brewing process and storage [383], directly correlates with the gravity of the beer and is not produced during fermentation in considerable amounts [381,384]. Its low content in nowadays beers [385] cannot be attributed to higher concentrations in historical barley cultivars with levels being consistent between 80 and 120 µg/g[381,382,386,387]. The accumulation of niacin in the germ layers of the barley grain [388] indicates that the germ was not or insufficiently removed in the historical brewing process.

With a similar overall carbohydrate profile, more α-(1-4)-branchings of dextrins were found, which could be attributed to the differences in the brewing barley or enzyme activities in the historical beer. An increased ratio of reducing α-ends can be attributed to long-term storage, comparable with the finding of oligosaccharide breakdown by Walther, et al. [369]. The higher amount of monomeric glucose, as also found for other historical beers [287,369], could be explained by the same reason or incomplete fermentation with the specific yeast used at the time. The caramelization or Maillard reaction derivatives of such reactive sugars, like kojibiose, consequently showed higher signal intensities after long-term storage.

The observation of decreasing signatures of polyphenols during non-optimal storage of beers has already been described in several studies [194,389] and was attributed to the reaction of polyphenols with free radicals, reactive oxygen species and acid-catalyzed polymerization [390]. Resulting polymers interact with proteins and form insoluble complexes and hazes, following the non-biotic sediment and microscoped particles settled in the beer bottle. One compound found to promote this process is acetaldehyde. Formed by yeast fermentation or ethanol oxidation, acetaldehyde induces ethyl bridges between the flavanols [391]. Forced aging studies did not show great alterations in the acetaldehyde concentration with a tendency to decrease due to its reactivity [392]. The higher content of this compound in the historical beer, therefore, should be attributed to the control of the fermentation process and

the yeast used at the time. Formic acid as another fermentation by-product, as well, is significantly accumulated.

A large increase was found for the acetic acid signal (Figure 1A-II). At around 155 mg/L, the acetic acid content is slightly above the range that can be expected in today's beer samples [393] and significantly increased compared to the modern lager with 63 mg/L. Again, the control of the fermentation and the type of yeast used define the acetic acid concentration. Hereby, the amount of yeast, higher fermentation temperature and aeration are beneficial to the acetate content. With a lack of studies on beer, resorting to wine studies [394], it is reported that the acetic acid concentration remains unchanged during forced aging. The significantly lower lactic acid concentration in the historical beer declines microbial spoilage and thus the origin of acetic acid due to Acetobacter.

In nowadays brewing practice, the mash or wort is intendedly acidified by so-called sour wort containing lactic acid to reach pH values around 5.5 (mash) and 5.2 (wort), respectively. Thereby, optimal enzyme activities, higher degrees of fermentation, protein breakdown, microbiological stability and a lighter color development can be achieved. The low lactic acid concentration indicates that such optimized acidification of the beer has not yet been carried out during historical brewing at the end of the 19th century.

The clearest indication of the decades of storage could be found in the area of aldehyde signals (Figure 1B-II). HMF, generated by multiple pathways during the Maillard reaction and caramelization [298], was detected in trace amounts in the modern lager beer. The amount of 12.6 mg/L quantified in historical beer exceeds the range of 2 mg/L (pale beer) to 8 mg/L (dark beer) expected for fresh beer of any kind [395]. Numerous forced-aging studies showed that the amount of HMF is independent of the oxygen load and increases significantly with the length of storage[272,390,396]. Another noticeable aldehyde signal could be assigned to furfural. As for HMF, the behavior of the furfural concentration during beer storage was described as increasing at an approximately linear rate with the storage time and exponentially with increasing temperature [396]. Malfliet, et al. [397] reported furfural concentrations between 15 and 35 µg/L in fresh beer. Although force-aged beers, with a maximum observed concentration value around 500 µg/L, never met the taste threshold of furfural (150 mg/L [398]), a clear correlation was found with a staling flavor [399]. The amount of furfural as an indicator compound for beer staling could be quantified to 8.35 mg/L in the historical beer with concentrations below the limit of detection in the modern equivalent. Londesborough, et al. [287] found a level of 664 µg/L furfural in the shipwreck beer from the 1840s that, underwater, was exposed to significantly lower temperatures. The furfural concentration found in the historical beer far exceeds what is described for beer in literature.

5.2.4 Chemical space of the historical brew resolved by FT-ICR-MS

The differences in the chemical space and metabolic range between the historical beer and its modern equivalent were investigated by long-time (2000 scans, 1 hour) DI-FT-ICR-MS analysis. The analytical approach offers the unique comprehensive compositional dimension when chemically characterizing beer samples. After data filtering and annotation through mass difference networks (MDiN), 5,200 compositions could be observed for the historical beer (B1885) and 4,250 for the modern equivalent (B2019), respectively. More than 40 molecular formulae could be detected in one nominal mass with great matches between the historical and modern sample (Figure E.2 in Supplementary Chapter 5). The molecular compositions were plotted in van Krevelen diagrams, which have proven to reveal compositional patterns within the metabolite profile of both wine [57,111,400] and beer samples [225,226,228].

Comparing the van Krevelen diagrams of both beer samples, it becomes apparent that the compositional space of the 1885s beer (Figure 2A) shows great overlap with the molecular formulae found in modern beers (Figure 2B). The dominant carbohydrate cluster (H/C ≈ 2, O/C ≈ 1) is accompanied by respective sugar-phosphates and small organic acids. The degradation of the sugar compounds, usually associated with the loss of H_2O, was more pronounced in the historical beer. These degradation processes, usually, are driven by the Maillard reaction and take place during malting and roasting of the grain itself and are intensified during the brewing process. Taking into account that the beer analyzed has been exposed to moderate temperature fluctuations for around 130 years, the additional breakdown presumably originates in the chemical changes during the storage. At natural room temperature, following unusual reaction conditions for the Maillard reaction in foods and beverages, disproportionately many of the sugar degradation products belonged to the CHO chemical space. In previous studies [226], analyzing 250 beer samples, one-third of the compositions resulting from the Maillard reaction could be assigned to the CHO- and two-thirds to CHNO-chemical space. In contrast, the chemical spaces are evenly distributed for the sugar degradation compositions only found in the 1885s beer.

Scientific brewing paved its way in those years with the work of Pasteur and Hansen. Without any clear indications for beer pasteurization, Walther, et al. [369] describe great stability to enzymatic and microbial degradation for beers at that time. The claim for chemical stability is contradicted by the non-enzymatic changes, namely the Maillard compositions described, at least to some extent. This indication of a change in the chemical signature of the beer due to exceedingly long-term storage is mirrored in further compound classes as well. The region of lipids was characterized by more oxygenated species due to oxidation processes (Figure 2C). Concerning the oxidative alteration of lipids, the formation of (E)-2-nonenal, which is linked to a cardboard-like off-flavor [401], from linoleic acid is a decisive criterion for the effect of lower oxidation stability in brewing practice [390]. Brewing research largely agrees that the so-called “(E)-2-nonenal potential” [402] is already generated during the wort production by enzymatic (lipases and lipoxygenases) and non-enzymatic

(autoxidation) processes [403]. Further oxidation of the lipids after bottling is considered negligible under normal storage conditions [404,405]. Saturated and comparatively more oxygenated molecular formulae like $C_{12}H_{22}O_5$, $C_{12}H_{24}O_5$ or $C_{16}H_{30}O_8$ as characteristic products in the 1885s beer gave insights into processes that occur during extreme storage times, apart from specific known marker compounds. By hydroxylation (O), chain prolongation (CH_2), (de)hydrogenation (H_2) and epoxidation ($-H_2/+O$) (bio-)chemical reactions and their combinations, the 150 compositions involved in the oxidation system could be set into relation, leading to a comprehensive mass difference network (Figure E.3 in Supplementary Chapter 5).

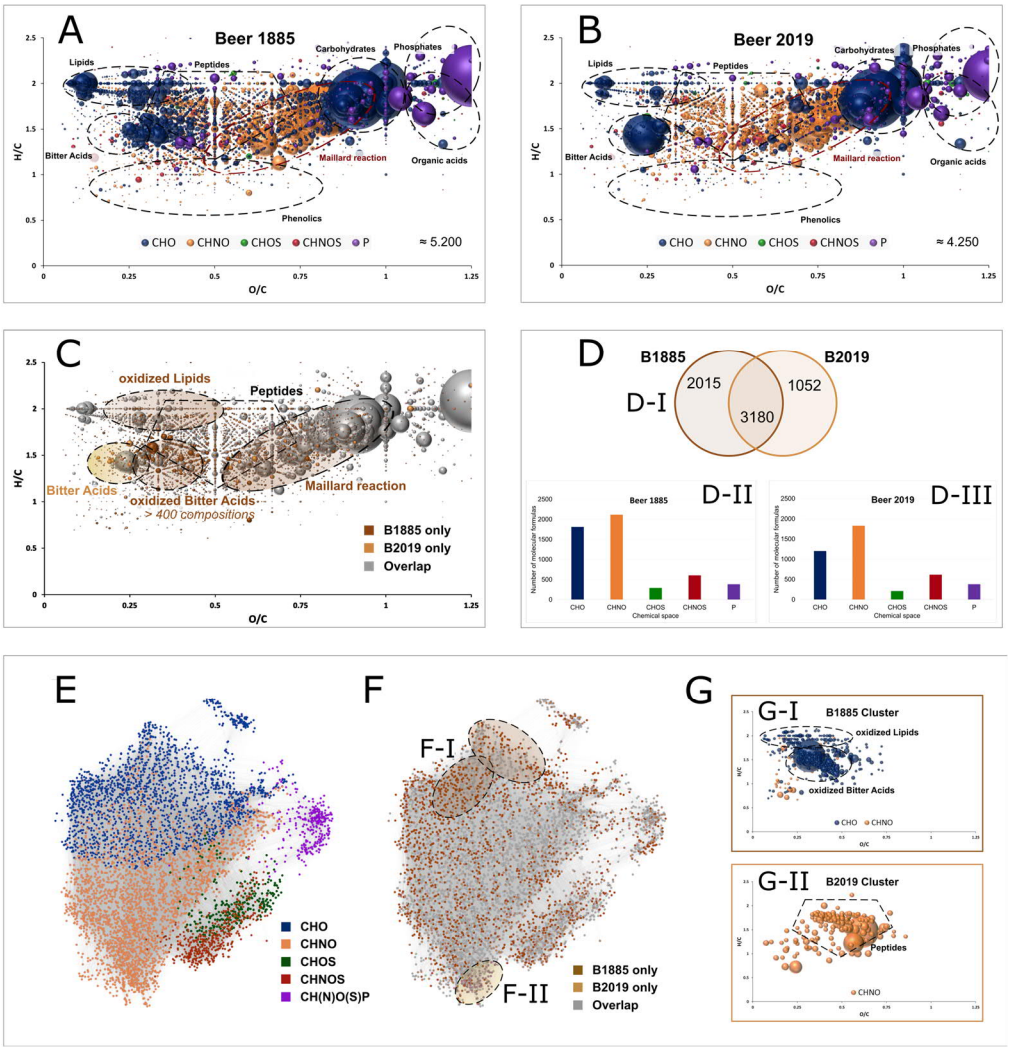

Figure 5.2 | Van Krevelen spectra of compositions found in B1885 (A), B2019 (B), the overlap of the samples (C), respective Venn-diagram (D-I) and chemical spaces for B1885 (D-II) and B2019 (D-III). Mass difference network of annotated compositions colored by the chemical space (E), by presence in sample B1885 and B2019 (F) and clusters of compositions specific to B1885 (F-I) and B2019 (F-II) with their respective position in the van Krevelen diagram (G-I and G-II, respectively).Color code: CHO (blue), CHNO (orange), CHOS (green), CHNOS (red), CH(N)O(S)P (violet). Neutral compositions are depicted. Approximate regions of compound classes are marked (A, B, C, G) and specific areas are highlighted in (F).

The compositions in the area of peptides, more specific to the modern beer, are in agreement with their role in the Maillard reaction. The biggest difference between the samples' metabolic profiles lay in the region of hop bitter acids. These terpeno phenolics, which most significantly contribute to the bitterness of beer, showed great presence in both beers, but markedly differed in the degree of oxygenation. The modern and fresh beer spectra, as expected, contained composition signals for the well-known main bitter acids in hops like humulone [$C_{21}H_{30}O_5$], cohumulone [$C_{20}H_{28}O_5$], lupulone [$C_{26}H_{38}O_4$] and colupulone [$C_{25}H_{36}O_4$]. In contrast, there were hundreds of oxygenated derivatives in the historical beer, shifted to the right in the van Krevelen diagram (Figure 2C). Such an oxidation process could already be indicated [225] but showed an extraordinary extent in this very special sample. Although the bottle was corked and waxed, which led to a largely maintained ethanol content, the oxygen present in the head-space of the bottle has been sufficient to almost completely oxidize the known hop constituents. Consequently, the signal intensity of humulone (1.4 %, compared to fresh beer) and cohumulone (1.6 %) are drastically decreased. Over 400 new derivative compositions unique for the historical beer were observed. Bearing in mind that several isomers are to be expected (e.g. 24 for humulone itself), the richness of the hop metabolite profile likely even goes far beyond hundreds of compounds. The MDiN between the modern beer hop bitter acids and the derivatives only found in the 1885s beer featured mostly compositional changes equivalent to oxidation reaction (O_3, O_2, O_4, are the three most common differences), substantiating the assumption of derivative formation through oxidation. As early as the 1980s, brewing research investigated the degradation of hops on a molecular level to describe the formation of volatile carbonyls, alcohols and esters [406-408] as ultimate breakdown products. Later, Intelmann, et al. [409] elucidated the molecular structures of several more complex cohumulone derivatives in storage model systems. A quantification method including up to 117 bitter acid derivatives (carboxylic acids, epoxides, cyclic, hydroxylated, and peroxided derivatives) was developed to describe oxidation intermediates and products in hops [410], throughout the brewing process [186] and during storage experiments [187]. The beers found in a shipwreck in the Baltic Sea and originating from a similar period were examined using these methods [287]. Comparable to the low signals found in the 1885s beer, negligible amounts of intact α- and β-acids were found. Isomerized humulones were present in minimal amounts. In line with their model experiments, cyclic oxidation products could be identified as a sign of long-term storage. The strong bacterial influence, the impact of low pH and the diffusion of seawater in the Baltic beers surely resulted in special reaction conditions. Nevertheless, it is noticeable that, despite the already comprehensive targeted analytical approach, the compounds found in the Baltic beer represent less than 5 % of the compositions described in our work. The resolved complexity and richness of hop-derived compounds in the well-preserved historical beer of 1885 remains a unique description of the "dark metabolome" of hop oxidation. Overall, compared to the oxidation of wine [400,411] where sulfur compositions play a major role as antioxidants, the differences between the modern and the 130 years aged historical beer are mostly limited to the CHO-chemical space (Figure 2D). With more than 60 % of the around 5,200 compositions overlapping between the found beverage and the modern beer, there should be no doubt that the bottle contains a

beer whose age is reflected in oxidation processes. The allocation of the aging products with regard to their chemical origin could also be traced in the MDiN (Figure 2E-G). It showed distinct areas for the chemical spaces with slight overlapping of the CHO/CHNO and CHOS/CHNOS spheres respectively (Figure 2E). The compositions characteristic of the historical or modern beer (Figure 2F) formed specific clusters in the linked network that corresponded to the described compositional spaces of oxidized lipids, oxidized bitter acids and peptides (Figure 2G). These findings underline the remarkably good preservation of the beer over 130 years and indicate that, apart from extensive oxidation primarily of the hop components, its metabolic signature is very comparable to modern, industrially brewed beers.

5.2.5 Chemometric interpretation of the metabolic signature

The beer attributes, the sensory characterization, microbiological analyses, NMR-profile and FT-ICR compositions of the historical beer overlap in many parts with today's beer. Given these clear similarities, the metabolic fingerprint of the historical beer was statistically compared with that of hundreds of other modern beers conclude about its original nature. For this purpose, OPLS-DA models were developed that put the molecular profiles of up to 400 beers in relation to their beer type, the type of fermentation, compliance with the Purity Law, the grain used and the Maillard signature (Figure 3). All models showed a clear classification power of the samples with regard to the examined criterion. Their statistical relevance concerning the goodness of the fit, quality of prevision and the exclusion of overfitting could be proven with RY2 values between 0.87 and 0.97, Q2 between 0.57 and 0.81 and ANOVA p-values << 0.05 respectively [214,215] (Table E.3 in Supplementary Chapter 5). Based on these models, the most significant compositions could be extracted in the associated loadings plots (Figure E.4 in Supplementary Chapter 5) and visualized in van Krevelen diagrams (Figure E.5 in Supplementary Chapter 5). In the respective score plots, the historical beer and its modern equivalent as a reference could be located in a prediction. The great similarity already shown between the well-preserved bottle and industrially manufactured beer was reflected in the fact that the historical sample did not appear as an outlier in any of the models even after 130 years of storage (Hoteling's T2). It enabled us to use the molecular fingerprint of the beer to conclude about the brewing method in the 19th century when compared to validated metabolic profiles of hundreds of modern beers.

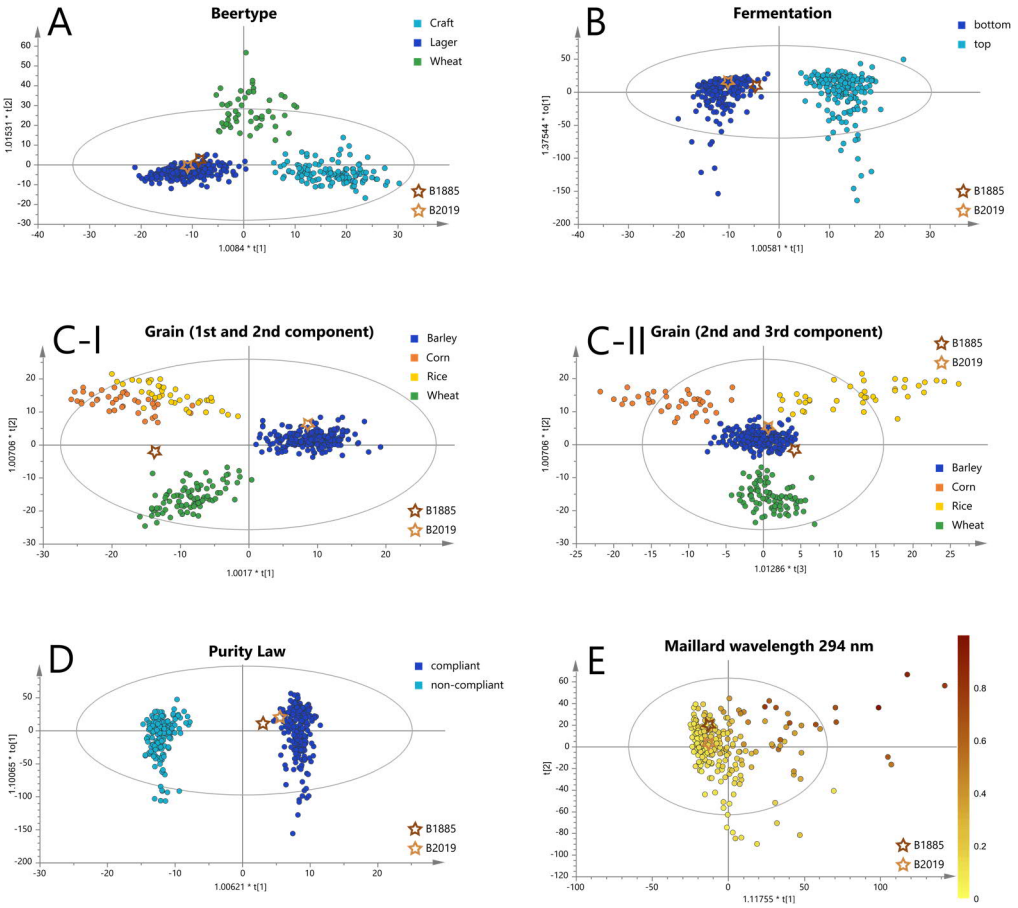

Figure 5.3 | Score plots of the OPLS-DA differentiating beer types (A), fermentation types (B), compliance with the German Purity Law (C), grains used (D) and Maillard signatures (E). The spot for each beer is colored according to its respective class. The position of beers B1885 (dark brown star) and B2019 (light brown star) is based on a prevision based on the statistical model and is indicated by a star.

A typical lager beer. The use of specific yeasts, malts, adjuncts and/or the type of hopping defines the type of beer resulting from the brewing process. These characteristics influence the metabolic signature of the respective way of brewing. As reported earlier [225,228], wheat beers showed a network of compositions that can be traced back to secondary metabolites (phytoanticipines) of the wheat plant. The major difference between the molecular fingerprint of lager and craft beers is due to the different way of hopping. Dry-hopped craft beers featured a variety of oxidized bitter acid derivatives, whereas the lager and wheat beers showed no defined signature of hop components (Figure E.5A in Supplementary Chapter 5). Despite the numerous characteristic oxidation products found in both the craft beers and the historical beer, the latter clearly could be assigned to the lager beer type (Figure 3A). Discrepancy is

to be found in the different oxidation mechanisms coming with dry-hopping compared to long-term storage and the associated extraction of hop polyphenols.

Another fundamental difference between the beer types is the type of yeast. Craft beers are fermented with ale yeasts whereas lager beers are brewed with bottom-fermenting yeasts, which were causative for a metabolite pattern of CHNO compositions in the shared region of lipids and amino acids/peptides in the van Krevelen diagram (Figure E.5A-I in Supplementary Chapter 5). Only 19 of the respective 112 m/z-values showed a database entry (HMDB, YMDB, ChEBi, Metacyc, Lipid maps) with suggested carnitine, ethanolamine and amino acid acyl-conjugates of fatty acids. Despite the yet unknown identity of these compounds, the same signals could be found in both the historical (80%) and modern (87%) beer. The beer of 1885 could be identified as a typical lager beer by the fingerprint of its “dark metabolome”.

Bottom-fermenting yeast. Although no viable yeast cells could be isolated, it was possible to determine the type of yeast used at the time by its influence on the beer metabolome. In general, when it comes to brewing, a distinction is made between top- and bottom-fermenting yeast species (Saccharomyces cerevisiae). They differ in their sprouting and thus the behavior during fermentation [393]. Top-fermenting yeasts in ale or wheat beers form sprouts that rise to the top at the time of the most intensive fermentation. Bottom-fermenting yeasts linger as single cells or cell pairs at the bottom of the fermentation vessel. The biggest differences of brewing-relevance concerning the metabolism are the enzyme expression (e.g. hydrolysis and decarboxylation of ferulic acid to 4-vinylguaiacol [$C_9H_{10}O_2$] for wheat beer yeasts [412]) and their optimum temperature. Top-fermented brewing takes place at around 18°C, whereas the bottom-fermented method prefers cooling to 9°C. Due to the necessity of elaborate cooling with ice in winter and no such possibility in summer, the bottom-fermented lager spent a little pronounced existence until the second half of the 19th century [413]. It was only with the work of Linde leading to the refrigeration apparatus in the 1870s [164] that bottom-fermenting yeast was made practicable all year round. It remains unclear whether this groundbreaking invention has already come into use for the historical beer. Yet, the tradition that the associated brewery already had a Linde refrigeration apparatus in 1881 is substantiated by these findings [414]. The metabolic profile, however, could clearly be assigned to that of a bottom-fermented beer (Figure 3B). The availability of controlled cooling opened up the world of standardized fermentation. The historic brew may be among the first lagers that spread consistent brewing quality and a recognizable taste around the world. It, as well, is questionable whether the yeast used was a pure cultured yeast, as the first isolation of single cells was achieved only a few years before by Hansen [163] during his beer research. [368] report the genome sequence of the first pure cultured Saccharomyces carlsbergensis and report the oldest yet-known beer brewed with this yeast [369]. However, by analyzing similar reference beers (from 1880s to 1990s), the latter authors were able to point out that beer spoilage by wild yeasts was still common in that period.

Simply Barley. The grain used for brewing serves primarily as a starch and enzyme source and thus as a supply of fermentable carbohydrates. Yet, in addition

to these products of primary metabolism, secondary metabolites that are extracted during the brewing process contribute to the molecular diversity of the final beverage. Utilizing the FT-ICR-MS analytical approach, the molecular profiles of barley, wheat, corn and rice could be characterized and potential marker substances identified using UPLC-ToF-MS (55). We used these statistical models to examine the metabolic profile of the beers with regard to the use of the various starch sources that still are very common today. The prediction of the modern beer showed a clear allocation to the beers made from pure barley in the score plots of both the 1st against 2nd (Figure 3C-I) and the 2nd against 3rd (Figure 3C-II) principal components. In contrast, the historical beer was unambiguously identified as beer without wheat, corn or rice added only in the second score plot. For this reason, subsequent UPLC-ToF-MS measurements were carried out. Neither the characteristic benzoxazinones of wheat (e.g. MBOA, HBOA-Glucoside, DIBOA-glucoside, HMBOA-glucoside), the hydroxyoxindoleacetic acid or the lipid profile of corn nor the rice-specific aspartic acid conjugate of N-glucosyl-indoleacetic acid were found in both beer samples (Figure E.6 in Supplementary Chapter 5). Consequently, using complementary and comprehensive mass spectrometric approaches, it could be demonstrated that the historical beer did not show any metabolites or metabolic signatures that would suggest the use of wheat, corn or rice.

Brewed according to the Bavarian Purity Law. Besides the advances in science (Pasteur [364], Hansen [163]) and technology (Enzinger [378], (Linde [164]), the tradition of beer and brewing goes hand in hand with fundamental changes in human culture and jurisprudence. As one of the oldest fermented beverages of ancient origin [159], the historical meaning of brewing lies in the cultural transition towards producing durable beverages from domesticated cereals. To ensure the quality and bacteriostatic property of beer, the Bavarian Purity Law (1516) was established as one of the most significant food legislations of the early modern period. At this time, brewing with wheat was banned in order to have it reserved for bakers. The production of wheat beer was an exclusive right of the duke (from 1602) and was not allowed to be widely practiced until the beginning of the 19th century. To this day, the use of raw grain, additives and adjuncts, starch and sugar or spices is prohibited in Germany and a few other countries. The chemometric classification of the 400 beers analyzed was based on current law. The beers declared as not compliant with the Purity Law were (1) brewed with corn, rice, soy, raw barley / wheat / rye / oat, malt extracts and syrups, sugar, sugar syrups or starch (2) sweetened with one of the above, caramel or sugar substitutes (3) preserved with antioxidants, stabilizers and acidity regulators (4) made by adding green tea, lotus blossoms, hemp, seaweed, whiskey or brandy (5) refined by yuzu, honey, plumb, cherry, orange peel, chestnut or coffee or (6) flavored with coriander, anise or herbs. The chemical profiles of all these attributes were compared to those beers brewed according to the Purity Law have in common (Figure 3D). As the metabolome-based prediction of the historical beer in the score plot shows, it was brewed according to the standards of the Purity Law that is currently in force. Accordingly, in view of the fact that no wheat signature could be identified, it also complied with the regulations of the German imperial era.

Moderate roasting signature. The last OPLS-DA model was created based on a non-binary y-variable. The metadata used was obtained from UV/Vis-measurements like described in an earlier study [226]. The Maillard roasting signature of the historical find was slightly more pronounced, but similar to that of modern pale beers (Figure 3E). The metabolic signature described a typical pale lager beer, whose Maillard chemical imprint originates not in the roasting process, but long-term storage under moderate conditions.

5.3 Conclusion

Every raw material involved in the beer-making, the brewing method itself and all production steps towards the type of storage influence the chemical composition of the beer and preserve a specific metabolite footprint. Through comprehensive archeochemical investigations, we showed that the molecular profile of beer can be revealed and interpreted even after more than a hundred years of natural occurring alterations (Figure 4). The historical brewing process and the changes caused by aging could be described on a molecular level in more detail. We described a hitherto unknown diversity (>400 specific compositions) of oxidized hop bitter acid derivatives and lipid oxidation (FT-ICR-MS), the role of niacin as an indicator compound of insufficient germ removal and undescribed high concentrations of Maillard-reaction marker molecules (NMR). The clear indicators of the ravages of time, however, have not been able to obscure the detailed molecular information left in the brewing of the late 19th century. Despite the over 130 years of storage of the beer under atmospheric pressure and in a standing position, the beer's original nature was unchanged in many parts. (Ultra)high-resolution mass spectrometry enabled the description of the largely unidentified "dark metabolome" of the historical beer and to compare it to modern brewing. In this way, the beer sample could be identified as a typical lager beer, which was subjected to bottom-fermentation even at a time when industrial production with accordant yeasts was still under early development. Following the Bavarian brewing tradition, the Purity Law applicable at the time was complied with, and specific metabolite profiles of adjuncts like wheat, maize or rice could not be detected. Critical points during the historical brewing process could be unraveled by forensic archeochemistry utilizing whole systems' fingerprints and specific molecular indicators.

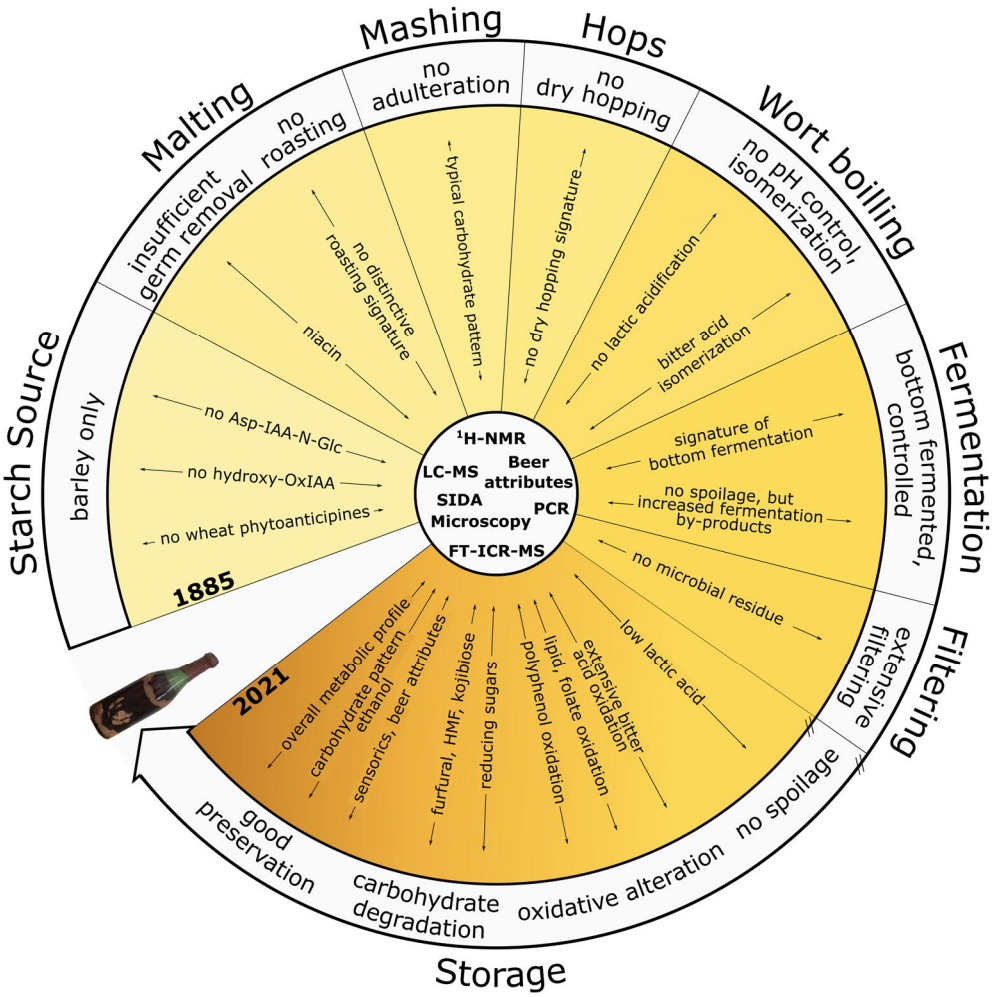

Figure 5.4 | Representation of critical production steps during the putative brewing process of the historical beer of 1885.

5.4 Materials and Methods

5.4.1 Brewing parameters, folate analysis and sensory characterization

Alcohol content and specific gravity were analyzed according to MEBAK WBBM 2.9.6.3 with an Alcolyzer Plus with a DMA 5000 density meter and Xsample 122 sample changer (Anton-Paar GmbH, Ostfildern, Germany) and the pH value according to MEBAK WBBM 2.13. Final attenuation was determined according to MEBAK WBBM 2.8.1. Foam stability was determined according to MEBAK WBBM 2.18.4. Sensory Analysis was performed according to MEBAK II 2.34.3. Samples of the same beer were subjected to forced aging by shaking them overhead for 24 hours and storing them at 40°C for 4 days. The beers were tasted and judged among four certified tasters according to MEBAK II 2.34.3. Folate analysis was performed as described in Pferdmenges, et al. [375] on a Shimadzu Nexera X2 UHPLC system (Shimadzu, Kyoto, Japan), utilizing stable-isotope dilution (Table E.4 in Supplementary Chapter 5).

5.4.2 Microscopy, microbiological analyses, PCR-based methods

25 mL homogenized sample of the 1885 beer were transferred aseptically to a sterile 50 ml cell culture centrifuge tube. 1 mL of the beer each were transferred to broth-based (liquid) and agar-plate (solid) based cultivation methods. A broad range of culture media for cultivation of beer, wort and beverage related microbes were selected for this approach: Wort-Agar, Wort, YM broth, YM-Agar, YGC-Agar, NBB-Agar, NBB broth, MRS broth, MRS-Agar, Micro Inoculum Broth (MIB), DEV-Nutrient-Agar, DEV-Nutrient broth, PCA, TSA, WLN-Agar, WLD-Agar, YPM broth, OSA, VRBD-Agar, Lactose-Peptone broth. Culture techniques, incubation conditions and incubation periods were applied according to MEBAK III 10.3-10.6, 10.1 and according to Back [415,416]. Additionally, the beer sample was analyzed microscopically according to the method MEBAK III 10.11.3 (using a Microscope Nikon Eclipse E200 with 1000-fold magnification as phase-contrast and dark-field microscopic application). After DNA-extraction of the beer sample-specific Real-Time PCR systems for beer-related yeast and bacteria species (e.g. Saccharomyces cerevisiae, Saccharomyces pastorianus, other Saccharomyces species, non-Saccharomyces beer associated yeast species, lactic acid bacteria) and PCR of 16S rDNA (bacteria) and D1/D2 26S rDNA and ITS1-5.8S-ITS2 rDNA (yeast/ fungi) with subsequent Sanger-sequencing were carried out according to Brandl [417], Hutzler [418,419], Koob et al. [420], Riedl et al. [421,422], Sampaio et al. [423], Schneiderbanger et al. [424].

5.4.3 NMR-analysis

The samples of both analyzed beers were diluted 3:1 with D2O containing sodium 3-(trimethylsilyl)propionate-d4 (1.8 mM) as a chemical shift reagent and Di-sodium hydrogen phosphate (1.5 M, pH7) to buffer the sample at pH 7.
Experiments were carried out on an 800MHz Bruker AVANCE lll spectrometer equipped with a 5 mm QCI-probehead at 300K. 1D 1H spectra were recorded using a 1D version of the nuclear Overhauser effect (NOE) experiment with a shaped pulse for off-resonance presaturation of the ethanol and water signal during the relaxation delay and mixing time. 2D-Experiments consisted of a phase-sensitive TOCSY with shaped off-resonance presaturation and a dipsi mixing scheme [425-427]. HSQC spectra were recorded with a phase-sensitive version using Echo/Antiecho-TPPI gradient selection, decoupling during acquisition and off-resonance presaturation with a shaped pulse during the relaxation delay [428-430]. The assignment of the observed signals was carried out based on of 2D NMR experiments considering published information [194,197,297] and spiking of standards, compiled in Table E.2 in Supplementary Chapter 5. Quantification was done by integration of the peaks in the case of isolated peaks and via peak fitting (assuming a Lorentzian peak shape) in the case of overlapping peaks. The obtained areas were used to calculate the corresponding concentration by comparison with the TSP area. Detailed experiment parameters are given in Table E.5 in Supplementary Chapter 5.

5.4.4 Sample set and FT-ICR-measurements

A total of 400 samples of commercially available beers from over 50 different countries were analyzed as a basis for statistical modeling. The sample set represents a cross-section of all possible combinations of beer styles, fermentation types, raw materials, color impressions and alcohol contents available to exclude co-varying metadata. The samples were stored, prepared and measured on a Bruker solariX ion cyclotron resonance Fourier transform mass spectrometer (Bruker Daltonics GmbH, Bremen, Germany) as reported recently [225,226,228] and summarized in Table E.4 in Supplementary Chapter 5. The obtained raw data was processed as reported [228] resulting in 7,700 unambiguous molecular formulae with a mass error of < ±0.15 ppm (at a resolving power of 400,000 at m/z 400) as a basis for statistical modeling. An overview of the sample set is given in the Supplementary (Table E.6 in Supplementary Chapter 5
The sample set was accompanied by a historical beer from 1885 (B1885) and its equivalent from 2019 (B2019) to investigate their molecular signature based on single-spectra comparison and statistical prevision of their metabolite profile. The modern beer was kindly provided by the same brewery to which the old beer is assigned and analyzed immediately upon receipt. The beer from 1885 was sampled through a previously disinfected (MeOH, heat) metal syringe. The sampling was carried out through the cork. Care was taken not to transfer any parts of the wax

coating. Both these individual samples were measured as referenced above (for statistics) and with an increased number of 2000 scans for single spectra comparison.

5.4.5 FT-ICR data visualization and statistical treatment

For each metadata criterion, the beer type, type of fermentation, compliance with the German Purity Law, grains used and wavelength at 294 nm (Maillard signature), we performed a supervised OPLS-DA analysis on the FT-ICR dataset. Based on these models, the position of beers B1885 and B2019 in the score plots were determined by a prevision to investigate the correspondence of their metabolic profile. The statistical parameters of the beer samples (Table E.7 in Supplementary Chapter 5) and OPLS models (Table E.3 in Supplementary Chapter 5) can be found in the Supplementary section. The characteristic composition profile for each observation and the compositions found in the 2000 scan spectra of B1885 and B2019 were plotted in van Krevelen diagrams. By plotting H/C- versus O/C-atomic ratios it is possible to depict common compositional patterns within observations' markers [26,111,126]. By plotting H/C- against O/C-ratios of the annotated molecular formulae, it enables tentative classification of the metabolite signals resolved [26]. Compositions characteristic for certain beer attributes were subjected to database search including HMDB[290], YMDB [294], ChEBi [291], Metacyc [292], and Lipid maps [293]. A mass difference network (MDiN) was applied utilizing the NetCalc approach [237]. The nodes, representing the annotated molecular formulae, were connected by edges that represent compositional changes corresponding to 250 different (bio)chemical reactions.

5.4.6 UHPLC measurements and marker compound comparison

As described earlier [228], the statistical analysis of a sub-sample set (102 beers) revealed compounds characteristic for the use of wheat, corn and rice with identification levels reaching from 1 to 3 [10]. Utilizing the same sample preparation and Shimadzu LCMS-9030 Q ToF (Shimadzu Deutschland GmbH, Duisburg, Germany) analytical system, beers B1885 and B2019 were screened for those marker molecules to verify the carbohydrate source used. For comparison, class-QC samples were analyzed containing all wheat, corn or rice samples respectively. The measurement parameters are summarized in Table E.4 in Supplementary Chapter 5.

Acknowledgments
The authors thank the Private Brewery Ernst Barre GmbH (Lübbecke, Germany) for the access to and exchange about the unique historical beer sample.

Chapter 6 |
Concluding Discussion and Outlook

The thesis reports on the non-targeted analysis of the beer metabolome. Brewing has been of great importance as a source of durable rich beverages for millennia. It evolved over thousands of years leading to scientific investigations and industrial scaling eventually. Yet, the metabolite richness extracted from the raw materials and their alteration during the malting and brewing process remains an unsolved puzzle. This work aims at and contributes to resolving the blurred picture draft. It aims to comprehensively map and structure the small molecules that in their entirety form the exceedingly complex aqueous mixture of organics we know as beer. Many chemical and biological processes result in the molecular diversity of the fermented beverage. When it comes to addressing these processes and their impact, it first is necessary to depict and visualize the richness from which certain signatures can be read. The thesis reports the application of an analytical approach that allows both describing the big picture and searching for marker compounds and molecular networks. As a first step, the requirement of comprehensiveness, which is demanded of metabolomics investigations, was pursued. Where pertinent brewing literature attributes up to two thousand compounds to beer, it was possible to describe already over 8,000 metabolite mass signals based on the mass resolution of the DI-FT-ICR-MS technique. The assignment of unambiguous molecular compositions turned unknown features into interpretable signals. The mass dimension was supplemented by isomeric separation (UPLC-ToF-MS). Hence, the structural space that could be observed expanded considerably, when compared to single instrumentation approaches. With over 20 isomers found for certain exact masses, the metabolic complexity of what defines a beer on the molecular level could be reported to dramatically exceed previously estimated numbers. The holistic approach includes those compositions that are of yet-unknown structure and considered as the “dark metabolome”.

The aim of depicting an overall picture, yet one allowing deep insights, shows in the minimalistic sample preparation. The metabolic signatures remain unharmed. The variety of beer samples represents another key point. In total, close to 500 beer samples from over 50 different countries across the globe were analyzed. They feature all facets of beer brewing and form an exhaustive basis of metabolite information. The presented studies have proven that such an extensive sample set not only comprehensively depicts the metabolome of brewing but enables robust statistical modeling. The decisive advantage is to enable mining for causal metabolic signatures instead of co-varying, correlating information. These fingerprints can be used for sample differentiation, basic research or process guidance. In a further step, they provide a framework to delve deeper into metabolic signatures and networks.

This includes the possibility of structure elucidation (UPLC-ToF-MS / NMR) and quantification (qNMR) of analytical targets. The analytical approach offers a comprehensive and holistic overview of beer metabolites, specific molecular networks and fingerprints, and information about molecular structures of target marker metabolites.

One of the most emerging techniques in modern brewing over the last years is the dry hopping process, where hops is added after wort boiling. This procedure is intended to extract the flavor and aroma compounds of the hops. Alterations due to the influence of heat are avoided. At this appoint it must be said that the analytical approach is not suitable for analyzing very volatile compounds (a different sample transfer and ionization technique would be advantageous to reach that goal) and is more so limited to non-volatile precursor metabolites or flavor compounds. In any case, the signature of dry-hopping could be resolved. It represents the most important specific commonality for all so-called craft beers at the molecular level. The hops was found to imprint a specific compositional pattern dependent on the way it is added to the beer. The probably most characteristic compounds of the plant, the terpeno-phenolics or hop bitter acids, were connected in their biochemical context by mass difference networks. Corresponding chemical changes could be visualized. Where wheat beers have a poor hop signature and that of lager beers is characterized in particular by the classic hop bitter acids (humulones, cohumulones), craft beers showed a variety of highly oxidized derivatives of these compounds. This can be attributed to the large input of oxygen associated with dry-hopping. In addition, the ethanolic extraction medium causes a more pronounced extraction of phenolics, polyphenolics and respective glycosides when compared to hops addition before fermentation. The hitherto undiscovered complexity and richness of these specific compounds could provide a base of knowledge for quality control purposes or process guidance towards flavor and antioxidant properties. Adapting the approach, the closely related field of hop breeding and the characterization of hop varieties and locations could also benefit greatly in future projects. Phenotyping of plants resistant to pests or pathogens and sensomics approaches could profit when hop secondary metabolites are resolved to their fullest, in the plant or final beer product respectively.

A chemical profile that influences the metabolome of beer and beer raw materials to a decisive extent was found to be that of the Maillard reaction (MR). The reaction of amines with carbonyl moieties runs through the entire brewing process. From malting over boiling to storage, it significantly contributes to the diversity of beer molecules and shapes the beer's chemical space of small molecules to a great extent. By unsupervised statistics, over 40 % of all resolved mass signals were found to originate in the reaction of amino compounds and sugars. The characteristic molecular pattern could be described by various visualization techniques emphatically exceeding the fingerprinting level. In beer, the chemical space of the MR was predominantly characterized by CHO and CHNO compounds. A minor (or even inhibiting) role of sulfur-containing amines like cysteine was observed. The MR-derived chemical pattern was shown to be subject to kinetic laws whose regularity is mirrored in the structured chemical compositions. It contrasts the plant (raw materials) or yeast (fermentation) metabolome which is formed by

enzymatic biocatalysis. The systematic distribution of nitrogen and oxygen in Maillard compounds illustrates their origin of chemosynthesis. A specific chemical space in the van Krevelen diagram was characterized. MR products develop from countless possible precursors within the beer matrix. Still, they converge towards shared compositional characteristics by systematic reaction patterns. The degree of saturation of these compounds (the double-bond equivalents) increases with increasing mass. Accordingly, there are a large number of higher-mass molecules that reach a corresponding degree of unsaturation by dehydration cascades. In studies that rely only on model systems and lose sight of the complexity of the actual food, these are oftentimes neglected. Several hundred different beers were analyzed to work out the generally applicable regularities. A representative system of amino acids and sugars, modeled on their composition in beer brewing, showed an overlap in all properties. The investigations were not restricted to the description of about 2,200 compounds carrying the Maillard signature. They also highlighted their chemical relation with regard to possible reaction sequences. Using the color of hundreds of independent beers as a proxy for the progress of the Maillard reaction led to robust, well-interpretable results that are consistent with model systems. Expressed as accurate mass differences, the reaction pattern or rather pattern of compositional change could be extracted. Since hundreds of amino acids and peptides can serve as precursors of the MR, compositional changes that are independent of N-containing steps stood out as the major common denominator. In the mass range of the metabolome, not considering >1000 Da melanoidin polymers, they are characterized as degradation reactions. The reaction sequences could be described in more detail by mass difference networks and evaluation of the pathways from precursor to product. Finally, they were decomposed into individual reactions of the Hodge's scheme. It was shown that the intermediate addition of fission products might lead to a subsequent water elimination cascade and to products of smaller mass eventually.

Follow-up investigations are expected to further increase the knowledge about the MR as occurring in beer brewing. These might include experimental brews to follow the Maillard reaction and resulting products throughout the course of the brewing process. Already the first step of malting, the germination parameters of the green malt, decisively impacts the following MR. By regulation of the enzyme activity, the sugar and amino acid composition available to MR-alterations are defined. We can assume that different malting processes, in particular the parameters of time and temperature, lead to different reaction kinetics and cascades of interest. Plant components that are released by mashing are added to the diverse mixture available for the MR during boiling. The influence of malt's browning degree on the following yeast fermentation is described to some extent but not yet investigated regarding whole Maillard reaction compositional patterns. For long-term storage, as shown with the historical beer, low-temperature reactions favor the building of another subset of Maillard compounds. The final picture of the Maillard reaction network in the finished beer product, therefore, consists of many individual steps. They address different MR environments and kinetics leading to various compositional signatures.

The analytical, data mining and visualization approach described here provide an excellent basis to further explore the Maillard diversity in beer. Alternative ionization methods could enhance the range of the chemical space accessible with the capability of both APPI and APCI to ionize less oxygenated compounds and highly unsaturated MR end products, respectively [126]. A further future approach would be to adapt model systems. The questions of whether certain amino acids, sugars, or other additives make a decisive contribution to the molecular diversity could be tackled. Experimental raw materials or experimental beers rich in certain precursors could subsequently pave the way into practical use. Reaction cascades could be studied in time-resolved representative model sequences [168]. A time-resolved approach of reaction kinetics and sequencing would hark back to the beginnings of metabolomics, to flux analysis on a non-enzymatic and compositional level. The complex interplay of amino acids and sugars could be followed by carbon module labeling (CAMOLA [431]), where isotope-labeled precursors are added to the reaction pool. Traditionally, such an approach is carried out using NMR or LC-MS analytical techniques. Due to the mass resolving power and accuracy of FT-ICR, including isotopologue resolution, a direct-infusion approach could add a holistic picture of carbon label distribution. Building blocks could be identified in the evolving MR through accurate mass annotation and mass difference networking. Structure elucidating approaches such as tandem HILIC- and RP-LC-MS [432] could complementarily be of use to ensure the best possible coverage of compounds. These considerations regarding further areas of application should contribute to a better understanding of the overall picture of MR in beer. It plays an important role not only in terms of basic research but also with regard to quality control and process guidance in the malting and brewing industry. These complex streams of chemical reactions are influenced by a variety of parameters. Metabolomics aims to move away from linear downstream reactions or single compounds (such as desoxyosones or HMF). Those proxies ambiguously mirror the complexity of the reaction pool. Metabolomics aims towards whole unambiguous chemical signatures. By understanding general driving forces and addressing the whole compositional space, malting and brewing processes could be optimized towards desired attributes like organoleptic, physical and chemical properties resulting in an overall quality and shelf-life increase. However, the analytical instrumentation of most current food inspections and industry often is reliant on a few-molecule characterization. It leaves the comprehensive approach to (1) generate deeper knowledge in basic research with the aim of process optimization eventually and (2) extract those compounds out of the holistic metabolic picture that might be suitable for targeted analytical approaches. Such a transfer might be of use for on-site control or inspection purposes.

When considering beer quality and possible alterations, grain adjuncts are of great interest, especially with regard to the German Purity Law. Widely spread across the global landscape, rice and corn grits are used as starch sources due to the competitive price. They alter the brewing and sensory properties of the beer and leave a molecular signature specific to the respective grain. Those fingerprints, both as extensive compositional patterns and single-molecule markers, could be described herein. The metabolic profile of corn as a brewing adjunct consisted on the one hand

of lipids derived from the seedling. On the other hand, it is complemented by a network of secondary metabolites built around the already known marker compound 7-hydroxy-2-oxindole-3-acetic acid. These potential growth-regulating molecules are not well described in literature. Likewise, a network of related compositions was found to be specific for the use of rice. Meeting the requirements for practical food inspection, the aspartic acid conjugate of N-β-D-glucopyronosyl-indole-3-acetic acid was described as a marker for potential monitoring of rice adjuncts in beer. In the commonality that these growth-related secondary metabolites leave a specific deep signature in the beer - including numerous database and literature unknowns – one could see an intrinsic call to transfer the analytical method to plant research.

The use of wheat grain is, according to the German Purity Law, restricted to the eponymous brewing style. Malting of the grain is obligatory. The use of wheat malt in lager beers, although prohibited in Germany, is appealing due to the associated foam stability. It could be shown that the use of wheat does result in the final beer featuring a wide biochemical network of secondary metabolites annotated and identified as phytoanticipines. It allows proving the use of merely pure wheat starch. A differentiation of raw against malted wheat was not investigated in this thesis. Wheat raw grain is widely used for Belgian wit beers and is appealing due to its low price. The main difference between the secondary metabolite imprint of raw and malted wheat, except from Maillard-alterations, might potentially be the germination process. Following on from this work, studies on the alteration of the metabolite pattern of those plant defense compounds during the germination process could provide deeper insights into the authentic use of the wheat raw materials.

Consumers' increasing awareness of the integrity of food is not only reflected in the demand for authentic use of raw materials. The focus is also shifting to a sustainable method of production, which consumer commonly associate with a high quality of the product. The need for more sustainable production has led to increasing demand for organically grown food and food products [433,434]. This trend shows in a selection of organic brews on the beer market. The steadily increasing but relatively low availability of such products indicates a restriction of the analytical approach applied in this work. Undeniably, the extraction of molecular patterns from the abundance of the comprehensively characterized metabolome is a decisive strength of metabolomics. From this, analytical signatures and markers can be further identified. However, a prerequisite either is (1) a comprehensive selection of samples that represent all potentially co-varying factors in the studied populations of equivalent sample size, or (2) a highly controlled and defined selection of samples differing in only one criterion. Concerning the sample set compiled in this work, the first condition was met for all the metadata-based differentiations presented. It was not true for the selection of organic beers [data not part of this thesis]. Although almost fifty commercial organic beers were analyzed, these were limited to a few specialized breweries from Central Europe. A representative sample set is not available at this point in time. The statistical analysis could show a difference between organic and conventional brewing but not at the significance level of the other attributes and not at a predictive level ($R^2Y = 0.859$, $Q^2 = 0.360$). The smaller the effect of the criterion under investigation on the entire metabolome is, the more

difficult it is to answer the question of an appropriate data set. Numerous studies agree that the systematic differences between conventional and organic farming concerning the expression of metabolic pathways of plant raw materials often is not very pronounced [435-440]. Rather, influencing factors such as the year of production [435-437] or the cultivars [437,438] predominate. An approach according to scheme (2) would require the use of experimentally brewed beers including multiple biological replicates. Such an approach would start with a field study of appropriate plant cultivation (barley, hops) and yeast breeding and is beyond the scope of this work. Although the findings would not be transferable to the beer market as a whole in a representative manner, they could provide valid starting points for metabolic pathways that should be particularly focused on.

Tracking such possible chemical signatures of raw materials throughout the brewing process is another question of interest. Although the influence of individual factors on the metabolome of the final product has been answered in a revealing manner, it remains to be seen how metabolic patterns evolve as the brewing process progressed. Investigating the starch sources has already shown that analytical markers can be derivatized over the curse of brewing process (corn lipids). The studies about the Maillard reaction show that the chemical signature of the finished beer surely is more diverse than the parts of its raw materials. Breaking down the chemical, but also biochemical-enzymatic interplay of small molecules to the various process steps of brewing is a goal for the future. It will provide a deeper understanding about the changes of a metabolome within a complex industrial process that leads to a product of consumer's preference. Especially in direct-infusion approaches, the comparability of matrices from the grain over the wort to the final beer is a critical point to be ensured. With regard to metabolic changes during fermentation, the integration of genomic or proteomic data from yeast represents an opportunity for a multi-omics approach. Correlations of beer attributes like sensorics or storage stability not only with chemical profile of the final product but with signatures within the brewing process might open the door for online monitoring techniques. It might bring together the aims of knowledge about our food and the practical implementation concerning food quality. Both of which are somewhat lacking focus in the foodomics focus as defined by A. Cifuentes.

Regardless of its production process, beer and brewing tradition accompany human civilization for millennials shaping its culture and traditions. Under the term archeochemistry, scientists describe the chemical inorganic and organic composition of historical finds to conclude about their nature at that time. In food and fermented beverage analytics, search for specific, yet ambiguous, molecular markers dominate the field. Expanding this field of research through a holistic approach of metabolome analysis proved beneficial in the analysis of a 130-year-old beer. The molecular composition of the beer bottle from the German Empire era represented a unique and rich source about the brewing culture at the end of the 19th century. Comprehensive analytics could certify the unprecedented good condition of the sample on a molecular level. The base of knowledge created throughout the investigations reported in this thesis allowed to decipher molecular fingerprints and markers for technological aspects of historical beer brewing from the raw materials to the storage.

Several critical production steps such as malting and germ treatment, wort preparation and fermentation, filtration and storage, and compliance with the Bavarian Purity Law left detectable molecular imprints.

Authentic aging mechanisms led to an unseen diversity of hop-derived compounds. Long-term chemistry in the sealed bottle resulted in furfural and HMF concentrations previously unknown for beer-like beverages. Analyzing the historical beer, it became evident that the Maillard reaction is one of the main contributors to compositional change in beer staling. Yet, the beer of the German Empire era remains a unique source of information. It represents the ultimate stage of beer aging. Experimentally aged beers could give more reproducible insights into the chemistry of short- to mid-term alteration of the beer metabolome. Such forced aging studies are investigating the stability of the beer during storage and associated changes in beer quality. Utilizing the holistic analytical approach, molecular signatures and analytical targets could be addressed that influence the quality and shelf-life of the brews. Oxidation processes, as shown for lipids and hop bitter acids in case of historical bottling, are aimed to be prevented by modern filling methods. Having a comprehensive picture of metabolites available, the effects of headspace-oxygen could be correlated with changes in the beer metabolome and sensory investigations.

The key challenges in the metabolomics community in mind, the LC-MS data generated during this work was shared at the GNPS [141] open-access metabolomics platform inside the MassIVE environment incorporating the MSI reporting standards as summarized by Goodacre [137].

In Summary, the multi-layered analytical approach allowed to decisively expand our knowledge about beer as a traditional but no less diverse beverage. It points out how complex our everyday foods are at the molecular level and how challenging it is to resolve their whole chemical profiles even with sophisticated instrumentation. Every raw material and every brewing method adds further aspects to the multifaceted metabolome of beer and brewing. Such molecular signatures could be made visible by the developed statistical and data treatment strategies. In addition to a wide variety of raw materials such as grains or hops, this work dealt with the effects of their processing. In the color of the beer, the hidden Maillard reaction network could be discovered. Molecular networking allowed to describe an ordered scope on the rather chaotic chemical interplay and to find structured reaction pathways. It furthermore provided molecular relations of analytical markers that could be identified eventually. The investigations of the historical beer showed that beyond food quality and adulteration control, process guidance and search for hidden molecular markers, the holistic non-targeted approach allows the comprehensive molecular characterization of unknown samples that hide cultural information of the past.

A Supplementary Chapter 1

Review Chapter Supplementary A

Depicting the Molecular Complexity of Beer by Direct-Infusion Fourier Transform Ion Cyclotron Mass Spectrometry (DI-FT-ICR-MS)

As already outlined in previous chapters, beer brewing is determined by several factors, all of which are mirrored in the complex metabolome of beer. Metabolomics aims to use a holistic approach to decipher this diversity, plurality and complexity. Following this top-down concept, a wide variety of analytical techniques were used independently and in complementary applications. The goal is to understand the product beer based on its metabolome and to generate in-depth knowledge of its composition. The direct-infusion or flow injection analysis of a beer in mass spectrometry offers the opportunity to analyze the beer as unchanged as possible and to make the entire molecular diversity tangible. Such an approach, however, needs to involve highest possible mass resolution to differentiate all possible elementary compositions based on the CHNOSP chemical space and the isotopic fine structures. A singularity of beer, compared to wine [111] and whiskey [441], is the complexity of carbohydrate structures. While the sugar compounds in whiskey are largely separated by distillation and play a minor role in wine, the carbohydrate metabolome of beer builds up in a versatile way. This diversity of quantitatively dominant compounds creates an analytical problem that [193] already noted in the direct-infusion of beer into a lower resolution ToF mass spectrometer. In addition to suppression effects during electrospray ionization, there are strong overlaps of signals with lower-resolution mass spectrometry that make the beer challenging for direct-infusion. On the other hand, extraction methods and chromatographic pretreatment limit what can be made analytically visible in terms of polarity and physiochemical properties.

A DI-FT-ICR-MS technique, novel to the field of beer research, can provide simultaneous detection of the numerous diverse molecules of a wide polarity range. Non-targeted metabolic profiling of beer can exceedingly benefit from the unrivaled mass resolution FT-ICR-MS can offer [225]. Resolving thousands of masses simultaneously enables a direct-infusion analysis without overlapping mass peaks. Thus, the measurement of a beer sample is possible without greatly influencing its visible composition by extraction workups or chromatography. Due to its unmatched

mass accuracy, which amounts to 0.1 ppm or rather the mass of a fraction of an electron throughout the whole mass range of metabolomics, it is possible to assign a molecular formula and thus a concrete elemental composition to each signal. It was shown that the holistic approach can provide universal information, that otherwise would remain hidden [442]. This means that well over 40 signals can be detected in a nominal mass; the masses of which differ only in their decimal place, the mass defect. They can be assigned to compound classes like carbo-hydrates (e.g., $C_{10}H_{18}O_9$), hop bitter acids (e.g., $C_{19}H_{26}O_4$), Maillard reaction products (e.g., $C_{16}H_{18}N_2O_5$), peptides (e.g., $C_{14}H_{27}N_3O_5$), polyphenols (e.g., $C_{17}H_{18}O_6$), sulfates (e.g., $C_9H_{18}O_{10}S$), lipids (e.g. $C_{18}H_{34}O_2$) and Phosphates (e.g., $C_8H_{15}O_{11}P$) and thus to the entire diversity of the beer metabolome, even inside one single nominal mass (Figure A.1). Furthermore, the isotopic fine structure of compounds can be

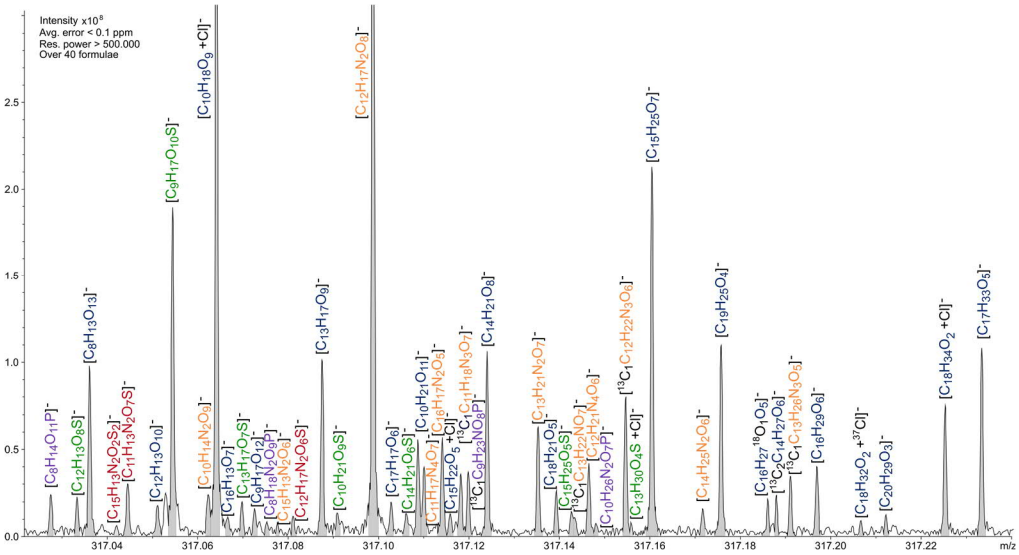

Figure A.1 | The molecular complexity of beer can be resolved in one nominal mass (m/z 317) with 46 annotated formulas by DI-FT-ICR-MS.
resolved (e.g., $C_{16}H_{27}{}^{18}O_1O_5$ and $^{13}C_2C_{14}H_{27}O_6$).

To utilize the compositional information a molecular formula can provide, the van Krevelen diagram is used [126]. By plotting the ratio of hydrogen to carbon atoms of a molecular formula against the O/C-ratio the van Krevelen diagram offers certain regions, which reflect the compositional nature of respective molecules and associated biochemical origins [26]. Here, the tentative classification of structural formulas of beer into substance classes lies in their biosynthetic pathway. In gluconeogenesis, the addition of water to the basic building block pyruvate gives the carbohydrates very saturated and oxygen-rich compositions, which, therefore, are

located in the upper right region (Figure A.2). In contrast, the basic building block of fatty acid synthesis, acetyl-CoA, is obtained via an oxidative decarboxylation of the pyruvate. Another decarboxylation step catalyzed by the ketoacyl synthase during chain expansion has the consequence that lipid species are correspondingly less oxygenated and can therefore be found at the top left [292]. The polyphenols, on the other hand, are significantly more unsaturated and have lower H/C-ratios. The chemical space of the phosphates in beer can be broken down into the corresponding sugar-phosphate, nucleotide and phospholipid spheres. Due to the divergent biosynthetic pathways of the amino acids and the associated different residues on the amino group, a peptide region is difficult to narrow down. The situation is similar with sulfur-containing formulas, which include both sulfates, thiols and heterocyclic sulfur compounds. Small organic acids usually have a very high O/C-ratio that can exceed the value of one. Hence, it is possible to visualize the entire, holistic variety and complexity of the beer in a diagram. When analyzing beer, Pieczonka, et al. [225] characterized the region specific for hop bitter acids. Due to their special biosynthesis, the quite hops-specific compounds have not only the phenolic base structure. They also feature the compositional characteristics of terpenes, which are based on prenyl side chains. Accordingly, these ‘terpeno-phenolics’ show a very characteristic positioning in van Krevelen.

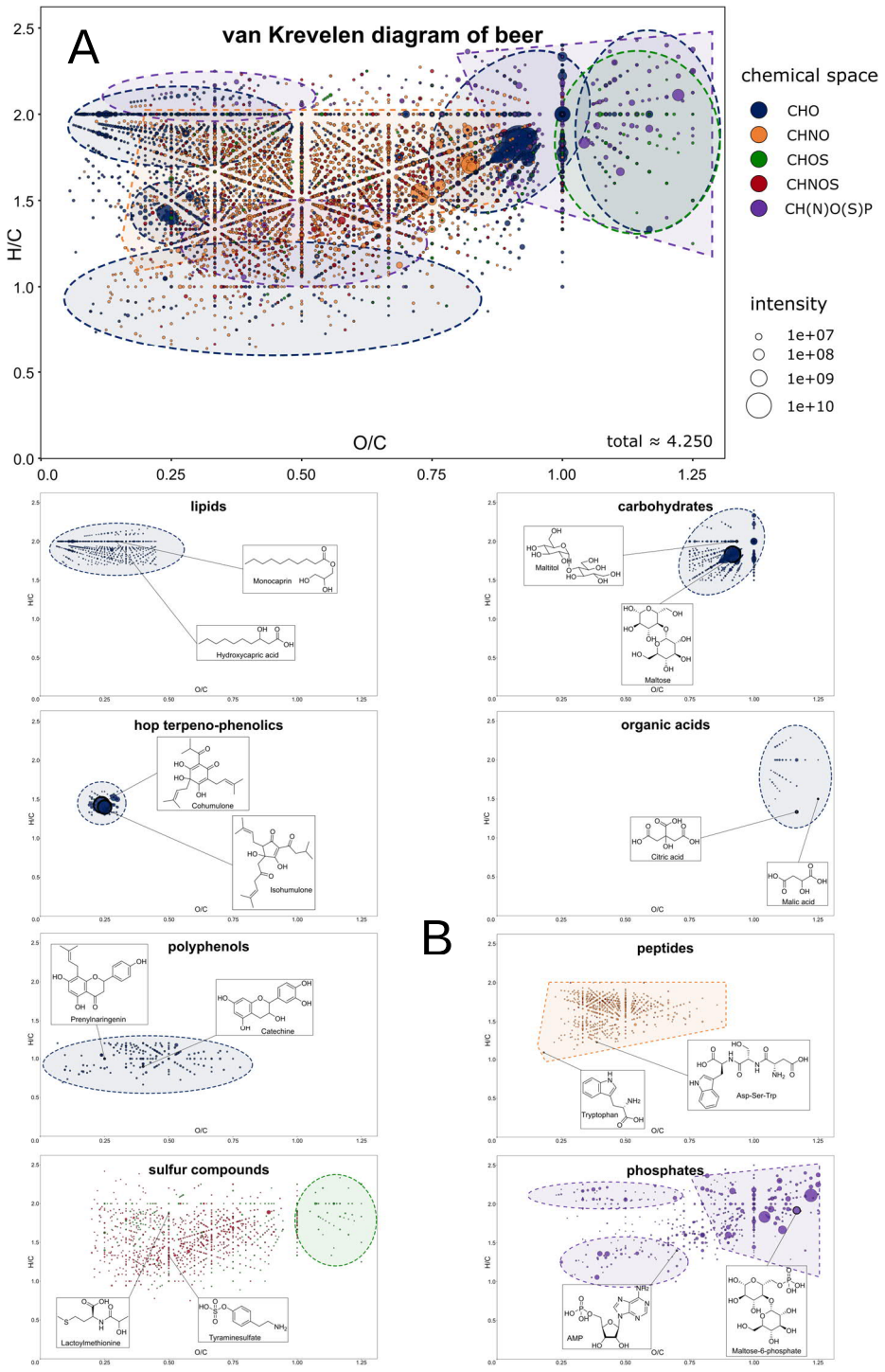

Figure A.2 | The molecular diversity of beer can be classified by the van Krevelen diagram (A). The regions specific for certain compositional classes are marked with dashed lines in the color of the corresponding chemical space. The complexity is broken down in (B).

Moreover, the differences between molecular formulae, i.e. the exact mass differences between molecules, are a tool with which complex DI-FT-ICR-MS data can be interpreted and visualized [237]. Based on known alpha- (humulones) and beta-acids (lupulones), a network can be built that contains well over a hundred molecular formulas. The defined mass differences represent a chemical or biochemical relationship between species. By that, it is for instance possible to trace the metabolic pathway of hop bitter acids [292] in the beer matrix. The mass of phlorisovalerophenone, which is derived from isovalerate and malonate, can be found with a formula of $C_{11}H_{14}O_4$ (Figure A.3). It is subjected to two prenylation steps. With the mass difference of C_5H_8 the 4-prenylphlorisovalerophenone ($C_{16}H_{22}O_4$) is visible; the second prenylation leads to the deoxyhumulone ($C_{21}H_{30}O_4$). Latter can be oxidized to the humulon ($C_{21}H_{30}O_5$, α-acid). Though, if a further prenyl group is transferred, the signal of lupulone ($C_{26}H_{38}O_4$, β-acid) can also be detected. This way, chemical and biochemical processes of hop phytochemicals can be understood, and large networks interpreted on the compositional space projection .

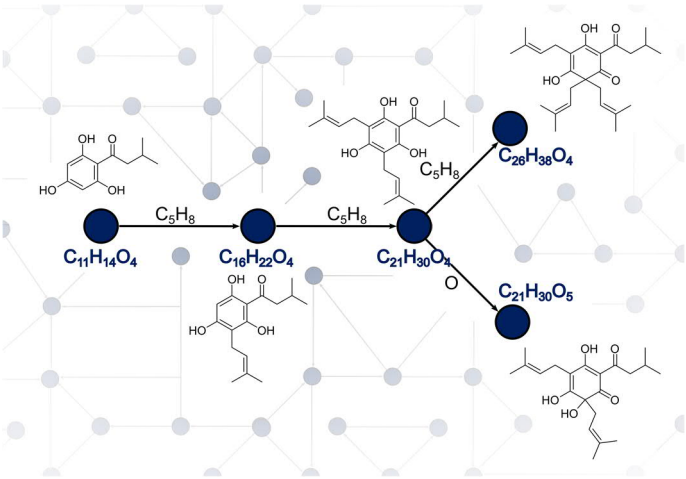

Figure A.3 | The biochemical relation of hop components can be followed by their distinct mass differences on the compositional space projection.

Having access to thousands of diverse chemical compositions and utilizing these tools, which are offered by FT-ICR-MS, it is possible to differentiate beer types based on their deep molecular signatures. With the help of hierarchical clustering, it was possible to distinguish the metabolic profiles of lager, craft, wheat beers and non-alcoholic beers. Using OPLS-DA, characteristic molecular patterns could be extracted, visualized and characterized using the van Krevelen diagram. The van Krevelen diagram of lager beers showed a specific cluster of CHO-molecules in the region specific for hop terpeno-phenolics, the hop bitter acids. Several marker compositions for the rich hopping featured in export and Pilsner type lager beers could be extracted, whereas a majority was described as not having an equivalent molecular structure published. Bearing in mind that these compositions also might feature a multitude of isomeric compounds, it can be assumed that there still is a lot to explore about hop components and their reactions in the brewing process. In

addition, it was possible to chemically and biochemically relate known and unknown characteristic molecules using discrete mass differences. In the craft beers, the focus was also on hops, whereby two special features have been shown. The dry hopping and thus the entry of the whole hop cones and oxygen in the beer favor oxidation processes. The resulting oxidation products of hops were found further to the right in the VK diagram due to the oxygenated (larger O/C-ratio) and were linked to known compounds via corresponding mass differences. The potential of the DI-FT-ICR-MS for deep metabolic profiling and the search for hidden metabolites was shown in terms of the wheat characteristic compounds. The mass difference network of corresponding compositions made it possible to recognize a pattern of related markers. The pattern featured a variety of so-called blepharin derivatives. These phytoanticipins are common and ubiquitous defense molecules of the wheat plant that have antimicrobial, fungicidal and insecticidal properties [282]. These molecules are wheat specific since they are not synthesized by the barley plant. This interpretation of the metabolomic data based on elementary compositions and mass differences was then verified by targeted LC-MS measurements. Hereby the advantages of the complementary use of different mass spectrometric methods was illustrated. The secondary metabolites of the wheat plant were described as marker substances for the use of wheat in the brewing industry, including previously unknown ones.

The attention that multivariate evaluation of big data and the importance that artificial intelligence is getting in this context rises steadily. With regard to interpreting thousands of features, the complementary combination of instrumental approaches follows this development. The holistic and comprehensive concept can address all questions, which are related to the beer's metabolome. Yet, such advanced mass spectrometric techniques are not ready for everyday use in routine quality control or process tuning, due to the high costs related to the technology. Metabolomic studies still are research tools for exploratory investigations and are presently used in the academic field. Inevitably the question arises, how brewers can benefit from the detailed description and understanding of the product beer metabolomics can offer. The medium-term goal in this regard should be that the novel technologies are used to discover new markers and new chemistry. In a second step, these can be followed with cheaper tools, which are available to the brewing industry, accordingly. Yet, the potential in integrating the absolute mass data profiles obtained possibly from thousands of samples across space and time gives a strong motivation to bring this technology into routine.

Tables A

Table A.1 |. Overview of metabolomics research in the field of brewing.

Subject	Objective	Metabolites	Instrumen-tation	(non-) targeted	Data analysis	Reference
Beer	Influence of temperature, yeast strain, brewing site	Acetate esters, alcohols, fatty acids and derivatives	GC-FID	targeted	Factor analysis	Jacobsen, et al. [171]
Hops	Hop varieties	Fatty acids, monoterpenes	GC-MS	non-targeted	NNS, HCA, PCA,	Stenroos and Siebert [178]
Beer	Develop a new beer	Aroma compounds	GC-MS	targeted	PCA	Kimura, et al. [189]
Hops	Genotype and production year	Alcohols, carophyllenes, epoxides, monoterpenes, sesquiterpenes	GC-FID	targeted	Factor analysis	Kralj, et al. [179]
Yeast	Yeast strains	Fatty acids	GC-FID	targeted	PCA	da Silva, et al. [172]
Yeast	Ale vs. lager yeasts	Non-targeted profiling	pyMS	non-targeted	HCA, LDA	Timmins, et al. [173]
Beer	Dark vs. pale, ale vs. lager	Polyphenoles, phenolic acids	LC-MS	targeted	PCA	Whittle, et al. [192]
Beer	Lager vs.Pilsener vs. wheat	Amino acids, acetate esters, small organic acids	Bubbling-burst ESI-MS	non-targeted	PCA	Zhu, et al. [190]
Beer	Ale vs. lager	Aromatic Amino acids, nucleotides, (poly)phenols	^{1}H-NMR	non-targeted	PCA	Duarte, et al. [194]
Beer	Alcohol free vs. ale vs. lager	Aromatics, sugars	^{1}H-NMR	non-targeted	PCA	Duarte, et al. [198]
Beer	Dark vs. pale vs. malt beer	Sugars, humulones	FI-MS	non-targeted	PCA	Araujo, et al. [193]
Beer	Barley vs. wheat, brewing sites, deteriorations	Aromatics, amino acids, fatty acids, small organic acids	FI-^{1}H-NMR	non-targeted	PCA	Lachenmeier, et al. [195]
Beer	Brewing sites	Amino acids, small organic acids, nucleotides	^{1}H-NMR	non-targeted	PCA	Almeida, et al. [196]
Yeast	Ale vs. lager	Non-targeted profiling	FI-MS, GC-MS	non-targeted	HCA, PCA	Pope, et al. [174]

Table A.1 (continued) |. Overview of metabolomics research in the field of brewing.

Subject	Objective	Metabolites	Instrumen-tation	(non-) targeted	Data analysis	Reference
Beer	volatile pattern of lager beers	Additives, higher alcohols, acetate esters	GC-FID	non-targeted	Neur. networks	da Silva, et al. [184]
Beer	Distinguish Rochefort beers	Acetate esters, alcohols, aldehydes, fatty acids	GC-MS	targeted	LDA, PLS, ANN-MLP	Cajka, et al. [278]
Beer	Distinguish Rochefort beers	Non-targeted profiling	LC-MS	non-targeted	PCA, OPLS	Mattarucchi, et al. [112]
Beer	Bitter metabolites	Humulones, prenylated flavonoids	LC-MS	targeted	HCA	Haseleu, et al. [186]
Beer	Beer aging	Small organic acids, higher alcohols, dextrins	1H-NMR	non-targeted	PCA, PLS	Rodrigues, et al. [297]
Beer	Beer aging	MRPs, fatty acids, non-targeted profiling	GC-MS	non-targeted	PCA	Rodrigues, et al. [202]
Beer	Brewing sites, barley vs. wheat	Amino acids, small organic acids, small alcohols, aromatics	^{1}H-NMR	non-targeted	PCA	Rodrigues and Gil [197]
Beer	Bitter metabolites	Humulones & derivatives	LC-MS	targeted	HCA, PCA	Intelmann, et al. [187]
Beer	Distinguish Rochefort beers	Small organic acids, nucleotides, sugars	DART-MS	non-targeted	PCA, PLS	Cajka, et al. [113]
Hops	Varieties and extracts	Non-targeted profiling	LC-MS, ^{1}H-NMR, ICR-MS	non-targeted	PCA	Farag, et al. [175]
Beer	Beer aging	Nucleotides, peptides, chalcones	LC-MS	non-targeted	PCA	Heuberger, et al. [203]
Hops	Hop varieties	Proanthocyanidins	LC-MS	targeted	HCA, PCA	Olšovská, et al. [177]
Beer	Aroma components	Acetate esters, Caryophyllenes, Epoxides, Ketones	GCxGC-MS	non-targeted	PCA	Inui, et al. [185]
Raw materials	Metabolic volatile pattern of raw materials	Aldehydes, fatty acids, furans, ketones, monoterpenes, thiols	GC-MS	targeted	PCA	Goncalves, et al. [181]
Beer	Alcohol free vs. alcohol reduced vs. normal lager	Alcohols, esters, fatty acids, monoterpenes, pyrazines, furans	GC-MS	targeted	PCA	Riu-Aumatell, et al. [200]

Table A.1 (continued) |. Overview of metabolomics research in the field of brewing.

Subject	Objective	Metabolites	Instrumen-tation	(non-) targeted	Data analysis	Reference
Beer	Alcohol free vs. alcohol reduced vs. normal lager	Sugars, humulones, non-targeted profiling	LC-MS	non-targeted	PCA	Andres-Iglesias, et al. [199]
Beer	Ale vs. Pilsner	Non-targeted profiling	LC-MS	non-targeted	PCA	Gallart-Ayala, et al. [191]
Beer	Influence of hop varieties and year of production	Non-targeted profiling	LC-MS	non-targeted	HCA, PCA	Hughey, et al. [204]
Urine, Plasma	Metabolites following beer intake	Amino acids, humulones, non-targeted profiling	LC-MS	non-targeted	PLS, ASCA	Guerdeniz, et al. [207]
Beer	Beer hopping techniques	Amino acids, nucleotides, sugars, fatty acids, small organic acids	^{1}H-NMR	non-targeted	PCA	Spevacek, et al. [188]
Beer	Beer aging	Purine metabolites, non-targeted profiling	LC-MS	non-targeted	PCA	Heuberger, et al. [206]
Urine	Metabolites following beer and non-alcoholic beer intake	Non-targeted profiling	LC-MS	non-targeted	PLS	Quifer-Rada, et al. [208]
Beer	Beer aging	Non-targeted profiling	LC-MS	non-targeted	PCA, PLS	Yao, et al. [205]
Beer, Malt	Malt influence on flavor compounds	Amino acids, fatty acids, small organic acids, sugars, sugar alcohols, purines, phenolics, monoterpenes, non-targeted profiling	LC-MS, GC-MS, ICP-MS	non-targeted	PCA, OPLS	Bettenhausen, et al. [183]
Hops	Hop varieties	Esters, monoterpenes, sesquiterpenes, ketones	GC-MS	targeted	HCA, PCA	Yan, et al. [180]
Beer	Molecular characterization of beer	Non-targeted profiling, phytochemical composition	FT-MS LC-MS	non-targeted	HCA, OPLS	Pieczonka, et al. [225]

Table A.2 | m/z-values of starting compositions $[M-H]^-$ for mass difference network creation in the beer matrix verified by isotopologue patterns.

m/z	Composition	m/z	Composition	m/z	Composition
128.0353	$C_5H_7NO_3$	255.2330	$C_{16}H_{32}O_2$	341.0878	$C_{15}H_{18}O_9$
133.0142	$C_4H_6O_5$	258.0384	$C_6H_{14}NO_8P$	343.1704	$C_{24}H_{24}O_2$
151.0261	$C_5H_4N_4O_2$	259.0224	$C_6H_{13}O_9P$	343.2126	$C_{18}H_{32}O_6$
157.0367	$C_4H_6N_4O_3$	259.1299	$C_{11}H_{20}N_2O_5$	346.0558	$C_{10}H_{14}N_5O_7P$
161.0455	$C_6H_{10}O_5$	266.0881	$C_9H_{17}NO_8$	347.1864	$C_{20}H_{28}O_5$
171.0064	$C_3H_9O_6P$	277.1940	$C_{15}H_{30}O_2$ [a]	349.2151	$C_{18}H_{34}O_4$ [a]
177.0405	$C_6H_{10}O_6$	279.2330	$C_{18}H_{32}O_2$	353.0878	$C_{16}H_{18}O_9$
179.0561	$C_6H_{12}O_6$	281.0878	$C_{10}H_{18}O_9$	353.1394	$C_{21}H_{22}O_5$
202.0721	$C_8H_{13}NO_5$	289.0696	$C_9H_{18}O_8$ [a]	361.2020	$C_{21}H_{30}O_5$
214.0486	$C_5H_{14}NO_6P$	289.0718	$C_{15}H_{14}O_6$	362.0507	$C_{10}H_{14}N_5O_8P$
215.0328	$C_6H_{12}O_6$ [a]	290.0881	$C_{11}H_{17}NO_8$	383.1195	$C_{14}H_{24}O_{12}$
216.0514	$C_8H_{11}NO_6$	292.1402	$C_{12}H_{23}NO_7$	385.0929	$C_{20}H_{18}O_8$
217.0484	$C_6H_{14}O_6$ [a]	302.0662	$C_{10}H_{13}N_5O_4$ [a]	427.2102	$C_{18}H_{37}O_9P$
220.0827	$C_8H_{15}NO_6$	308.0987	$C_{11}H_{19}NO_9$	447.0933	$C_{21}H_{20}O_{11}$
221.0667	$C_8H_{14}O_7$	318.0611	$C_{10}H_{13}N_5O_5$ [a]	453.2259	$C_{20}H_{39}O_9P$
223.0612	$C_{11}H_{12}O_5$	319.2409	$C_{18}H_{36}O_2$ [a]	463.0882	$C_{21}H_{20}O_{12}$
229.0484	$C_7H_{14}O_6$ [a]	321.0493	$C_{10}H_{15}N_2O_8P$	465.3044	$C_{27}H_{46}O_4S$
243.0623	$C_9H_{12}N_2O_6$	322.0446	$C_9H_{14}N_3O_8P$	470.1515	$C_{17}H_{29}NO_{14}$
243.0641	$C_8H_{16}O_6$ [a]	325.0484	$C_{15}H_{14}O_6$ [a]	503.1618	$C_{18}H_{32}O_{16}$
245.1143	$C_{10}H_{18}N_2O_5$	331.1915	$C_{20}H_{28}O_4$		
250.0721	$C_{12}H_{13}NO_5$	333.0592	$C_9H_{19}O_{11}P$		

[a] $[M+Cl]^-$

Table A.3 | Mass difference values (MD), compositional changes and (bio-)chemical reaction equivalents of mass differences connecting the compositions in MDiNs.

MD	Comp. Change	Reaction	MD	Composit. Change	Reaction
0.9840	$H_{-1}N_{-1}O_1$	Amination	130.0089	$C_5H_6O_2S_1$	2-Oxo-4-methylthiobutanoic acid
1.0316	$H_3N_1O_{-1}$	Deamination	130.0419	$C_9H_6O_1$	Cinnamic acid
1.9793	$C_{-1}H_{-2}O_1$	Acetic acid	130.0742	$C_5H_{10}N_2O_2$	Glutamine
2.0157	H_2	(De-)hydrogenation	130.1106	$C_6H_{14}N_2O_1$	Lysine
4.0313	H_4	(De-)hydrogenation	131.0405	$C_5H_9N_1O_1S_1$	Methionine
6.0470	H_6	(De-)hydrogenation	131.0582	$C_5H_9N_1O_3$	Glutamic acid
8.0626	H_8	(De-)hydrogenation	131.0946	$C_6H_{13}N_1O_2$	(Iso)leucine
12.0000	C_1	Glyoxylic acid	132.0423	$C_5H_8O_4$	Pentose
13.0316	$C_1H_3N_1O_{-1}$	Glycine	133.0388	$C_5H_3N_5$	Guanine
13.9793	$H_{-2}O_1$	Epoxidation	133.0561	$C_5H_{11}N_1O_1S_1$	Methionine
14.0157	C_1H_2	Methylation	134.0229	$C_5H_2N_4O_1$	Xanthin
14.0269	$H_2N_2O_{-1}$	Di-Ammonia	136.0160	$C_7H_4O_3$	Siacylic Acid
14.9997	$C_1H_1N_{-1}O_1$	Cytosin to Tymin	136.0273	$C_6H_4N_2O_2$	Imidazole pyruvic acid
15.0109	H_1N_1	Amination	136.0524	$C_8H_8O_2$	4-Hydroxyphenylpyruvic acid
15.0235	C_1H_3	N-Methylation	136.1252	$C_{10}H_{16}$	Di-prenylation
15.9772	$O_{-1}S_1$	Exchange of O with S	137.0589	$C_6H_7N_3O_1$	Histidine
15.9949	O_1	(De-)hydroxylation	138.0065	$C_5H_2N_2O_3$	Orotidin
17.0265	H_3N_1	Amonia	138.1772	$C_{11}H_{22}O_{-1}$	Dodecanoic acid
18.0106	H_2O_1	Hydrolysis/condensation	139.0746	$C_6H_9N_3O_1$	Histidine
25.9793	$C_1H_{-2}O_1$	C=O insertion	140.1201	$C_9H_{16}O_1$	Sebacic acid
26.0157	C_2H_2	Pyruvic acid	140.1565	$C_{10}H_{20}$	Alcohol
26.0520	$C_3H_6O_{-1}$	Butanoic acid	141.0578	$C_{10}H_7N_1$	Indole pyruvic acid
27.0109	$C_1H_1N_1$	Formimino transfer	142.0630	$C_7H_{10}O_3$	Pimelate
27.0473	$C_2H_5N_1O_{-1}$	Alanine	142.0895	$C_{10}H_{10}N_2O_{-1}$	Tryptophan
27.9949	C_1O_1	Formyl transfer	143.0582	$C_6H_9N_1O_3$	Aminoadipate
28.0313	C_2H_4	C2-unit	146.0368	$C_9H_6O_2$	Phenylpyruvic acid
28.9902	$H_{-1}N_1O_1$	Nitrosylation	146.0579	$C_6H_{10}O_4$	Rhamnose
29.9564	$H_{-2}S_1$	Thio-heteroatom	146.1055	$C_6H_{14}N_2O_2$	Lysine
30.0106	$C_1H_2O_1$	Hydroxymethyl	147.0684	$C_9H_9N_1O_1$	Phenylalanine
31.9721	S_1	Thiolation	148.0736	$C_6H_{12}O_4$	Glycerol

Table A.3 (continued) | Mass difference values (MD), compositional changes and (bio-)chemical reaction equivalents of mass differences connecting the compositions in MDiNs.

MD	Comp. Change	Reaction	MD	Composit. Change	Reaction
31.9898	O_2	Hydro-peroxidation	149.0477	$C_8H_7N_1O_2$	Pyridoxal
33.9877	H_2S_1	Hydrogen sulfide	149.0688	$C_5H_{11}N_1O_4$	Pentose schiff base
35.9767	Cl_1	Chloride	149.0841	$C_9H_{11}N_1O_1$	Phenylalanine
36.0000	C_3	DNA-R2	150.0528	$C_5H_{10}O_5$	Pentose
36.0211	H_4O_2	Water	150.0793	$C_8H_{10}N_2O_1$	Pyridoxamine
40.0061	C_1N_2	Guanin to Cytosin	151.0633	$C_8H_9N_1O_2$	Pyridoxine
40.0313	C_3H_4	Acetone	152.0110	$C_7H_4O_4$	Gallic Acid
42.0106	$C_2H_2O_1$	Hydroxypyruvic acid	154.0031	$C_3H_7O_5P_1$	Glycerol-3-phosphate
42.0218	$C_1H_2N_2$	Guanidyl group transfer	154.0046	$C_5H_2N_4Cl_1$	Hypoxanthin
42.0470	C_3H_6	CH2-Chain	154.1358	$C_{10}H_{18}O_1$	Decanoic acid
43.0058	$C_1H_1N_1O_1$	Carbamoyl transfer	154.1722	$C_{11}H_{22}$	Alcohol
43.0422	$C_2H_5N_1$	Serine	155.0695	$C_6H_9N_3O_2$	2-Oxoarginine
43.9898	C_1O_2	(De-)carboxylation	156.0423	$C_7H_8O_4$	Shikimic acid
44.0262	$C_2H_4O_1$	Pyruvic acid	156.0786	$C_8H_{12}O_3$	Suberate
44.9851	$H_{-1}N_1O_2$	Nitration	156.1011	$C_6H_{12}N_4O_1$	Arginine
45.0215	$C_1H_3N_1O_1$	Strecker degradation	158.0215	$C_6H_6O_5$	Ascorbic acid
46.0055	$C_1H_2O_2$	Hydroxy and Methoxy	158.1168	$C_6H_{14}N_4O_1$	Arginine
47.9847	O_3	Oxygenation	159.0684	$C_{10}H_9N_1O_1$	Indole pyruvic acid
53.0629	$C_4H_7N_1O_{-1}$	Proline	159.9327	$H_2O_6P_2$	Pyrophosphate
54.0106	$C_3H_2O_1$	DNA-R1	162.0317	$C_9H_6O_3$	Caffeic acid
54.0470	C_4H_6	2-Ketoisovaleric acid	162.0528	$C_6H_{10}O_5$	Glucose
54.0833	$C_5H_{10}O_{-1}$	Hexanoic acid	163.0633	$C_9H_9N_1O_2$	Tyrosine
55.0786	$C_4H_9N_1O_{-1}$	Valine	164.0685	$C_6H_{12}O_5$	Sugaralcohol
55.9898	C_2O_2	Glyoxylic acid	165.0790	$C_9H_{11}N_1O_2$	Tyrosine
56.0262	$C_3H_4O_1$	3-Hydroxy-2-oxobutanoic acid	166.0633	$C_5H_{13}N_1O_3P_1$	Phosphorylcholine
56.0626	C_4H_8	CH2-Chain	166.1358	$C_{11}H_{18}O_1$	11:1 Fatty acid
56.9799	$C_2H_1S_1$	2-Sulfanylethanone	166.2085	$C_{13}H_{26}O_{-1}$	Tetradecanoic acid
57.0215	$C_2H_3N_1O_1$	Glycine	166.9984	$C_3H_6N_1O_5P_1$	Phosphatidylserine
57.0578	$C_3H_7N_1$	Threonine	168.0059	$C_7H_4O_5$	Gallic acid
57.9877	$C_2H_2S_1$	3-Mercaptopyruvate	168.1514	$C_{11}H_{20}O_1$	11:0 Fatty acid
58.0419	$C_3H_6O_1$	Propionic acid	168.1878	$C_{12}H_{24}$	Alcohol

Table A.3 (continued) | Mass difference values (MD), compositional changes and (bio-)chemical reaction equivalents of mass differences connecting the compositions in MDiNs.

MD	Comp. Change	Reaction	MD	Composit. Change	Reaction
59.0194	$C_2H_5N_1O_{-1}S_1$	Cysteine	170.0943	$C_9H_{14}O_3$	Azelaic acid
59.0371	$C_2H_5N_1O_1$	Glycine	174.0528	$C_7H_{10}O_5$	Quinate
60.0211	$C_2H_4O_2$	Dimethoxylation	176.0321	$C_6H_8O_6$	Glucuronidation
63.9797	O_4	Oxygenation	176.0473	$C_{10}H_8O_3$	Ferulic acid
68.0262	$C_4H_4O_1$	Diacetyl	177.9432	$H_4O_7P_2$	Pyrophosphate cleavage
68.0626	C_5H_8	Prenylation	179.0794	$C_6H_{13}N_1O_5$	Hexose schiff base
69.0215	$C_3H_3N_1O_1$	2-Oxosuccinamic acid	180.0634	$C_6H_{12}O_6$	Hexose
69.0578	$C_4H_7N_1$	5-Amino-2-oxopentanoic acid	182.0123	$C_4H_8N_1O_5S_1$	Threoninephosphate
69.0942	$C_5H_11N_1O_{-1}$	Leucine/Isoleucine	182.1671	$C_{12}H_{22}O_1$	Dodecanoic acid
70.0055	$C_3H_2O_2$	2-Ketosuccinate	182.2035	$C_{13}H_{26}$	Alcohol
70.0419	$C_4H_6O_1$	Butanoic acid	184.1099	$C_{10}H_{16}O_3$	Sebacic acid
70.0531	$C_3H_6N_2$	Asparagine	185.0477	$C_{11}H_7N_1O_2$	Indole pyruvic acid
70.0783	C_5H_{10}	CH2-Chain	186.0793	$C_{11}H_{10}N_2O_1$	Tryptophan
70.0895	$C_4H_{10}N_2O_{-1}$	Ornithine	187.0489	$C_8H_{13}N_1S_2$	Lipoamide
71.0371	$C_3H_5N_1O_1$	Alanine	188.0330	$C_8H_{12}O_1S_2$	Lipoic acid
71.9847	C_2O_3	Oxalate	188.0950	$C_{11}H_{12}N_2O_1$	Tryptophan
72.0211	$C_3H_4O_2$	R1 MDA formation	192.0270	$C_6H_8O_7$	Glucaric acid
72.0575	$C_4H_8O_1$	2-Ketoisovaleric acid	194.2398	$C_{15}H_{30}O_{-1}$	Hexadecanoic acid
73.0164	$C_2H_3N_1O_2$	Indole, Pyruvate, Ammonia	196.0385	$C_{10}H_4N_4O_1$	Isoalloxazine
73.0528	$C_3H_7N_1O_1$	Alanine	196.1827	$C_{13}H_{24}O_1$	13:0 Fatty acid
74.0368	$C_3H_6O_2$	Glycerol	196.2191	$C_{14}H_{28}$	Alcohol
75.0320	$C_2H_5N_1O_2$	Glycine	201.1001	$C_9H_{15}N_1O_4$	Panthothenic acid
75.9983	$C_2H_4O_1S_1$	3-Mercaptopyruvate	204.1878	$C_{15}H_{24}$	Tri-prenylation
77.0299	$C_2H_7N_1S_1$	Cysteamin	208.1827	$C_{14}H_{24}O_1$	14:1 Fatty acid
79.9568	O_3S_1	Sulfonation	210.1984	$C_{14}H_{26}O_1$	Tetradecanoic acid
79.9663	$H_1O_3P_1$	(De-)phosphorylation	210.2348	$C_{15}H_{30}$	Alcohol
79.9746	O_5	Oxygenation	211.0246	$C_5H_{10}N_1O_6P_1$	Phosphoribosylamin
82.1146	$C_7H_{14}O_{-1}$	Octanoic acid	212.0086	$C_5H_9O_7P_1$	Ribose-5-phosphate
83.0371	$C_4H_5N_1O_1$	2-Keto-glutaramic acid	224.2140	$C_{15}H_{28}O_1$	15:0 Fatty acid
83.0735	$C_5H_9N_1$	6-Amino-2-oxohecanoic acid	224.2504	$C_{16}H_{32}$	Alcohol
84.0211	$C_4H_4O_2$	2-Ketoglutarate	225.0750	$C_9H_{11}N_3O_4$	Cytidine

Table A.3 (continued) | Mass difference values (MD), compositional changes and (bio-)chemical reaction equivalents of mass differences connecting the compositions in MDiNs.

MD	Comp. Change	Reaction	MD	Composit. Change	Reaction
84.0575	$C_5H_8O_1$	Adipate	226.0590	$C_9H_{10}N_2O_5$	Uridine
84.0687	$C_4H_8N_2$	Glutamine	226.0776	$C_{10}H_{14}N_2O_2S_1$	Biotin
84.0939	C_6H_{12}	Alcohol	228.0399	$C_6H_{13}O_7P_1$	Phosphoglycerol-Glycerol
84.1051	$C_5H_{12}N_2O_{-1}$	Lysine	236.2140	$C_{16}H_{28}O_1$	16:1 Fatty acid
85.0514	$C_2H_5N_4$	Adenin(Transaminated)	238.2297	$C_{16}H_{30}O_1$	Hexadecanoic acid
85.0528	$C_4H_7N_1O_1$	Glutamic acid	238.2661	$C_{17}H_{34}$	Alcohol
86.0004	$C_3H_2O_3$	Hydroxypyruvic acid	239.0923	$C_8H_{18}N_1O_5P_1$	Phosphatidylcholine
86.0190	$C_4H_6S_1$	2-Oxo-4-methylthiobutanoic acid	242.0192	$C_6H_{11}O_8P_1$	Glucosephosphate
86.0732	$C_5H_{10}O_1$	2-Ketohexanoic acid	244.0280	$C_9H_{10}N_1O_5S_1$	Tyrosinephosphate
87.0320	$C_3H_5N_1O_2$	Serine	244.0348	$C_6H_{13}O_8P_1$	Glycerolphosphatinnositol
87.0507	$C_4H_9N_1O_{-1}S_1$	Methionine	248.0532	$C_9H_{12}O_8$	Malonylglucosid
87.0684	$C_4H_9N_1O_1$	5-Amino-2-oxopentanoic acid	249.0849	$C_9H_{15}N_1O_7$	Neuraminic Acid
88.0160	$C_3H_4O_3$	2-Ketosuccinate	249.0862	$C_{10}H_{11}N_5O_3$	Adenosinen
88.0313	C_7H_4	Benzylaldehyde	252.2453	$C_{17}H_{32}O_1$	17:0 Fatty acid
89.0477	$C_3H_7N_1O_2$	Serine	252.2817	$C_{18}H_{36}$	Alcohol
90.0317	$C_3H_6O_3$	Triose	254.0579	$C_{15}H_{10}O_4$	Naringenin
90.0470	C_7H_6	Benzyl alcohol	258.1984	$C_{18}H_{26}O_1$	18:4 Fatty acid
92.0374	$C_5H_4N_2$	Imidazole pyruvic acid	259.0457	$C_6H_{14}N_1O_8P_1$	Phosphoserin-glycerol
93.0327	$C_4H_3N_3$	Cytosine	260.2140	$C_{18}H_{28}O_1$	18:3 Fatty acid
93.0691	$C_5H_7N_3O_{-1}$	Histidine	262.2297	$C_{18}H_{30}O_1$	18:2 Fatty acid
94.0167	$C_4H_2N_2O_1$	Uracil	264.0845	$C_{10}H_{16}O_8$	Disaccharide (5|5)
95.9695	O_6	Oxygenation	264.2453	$C_{18}H_{32}O_1$	18:1 Fatty acid
97.0528	$C_5H_7N_1O_1$	Proline	265.0811	$C_{10}H_{11}N_5O_4$	Guanosine
97.9769	$H_3O_4P_1$	Phosphate Adduct	266.2610	$C_{18}H_{34}O_1$	18:0 Fatty acid
98.0368	$C_5H_6O_2$	2-Ketoisovaleric acid	266.2974	$C_{19}H_{38}$	Alcohol
98.0732	$C_6H_{10}O_1$	Hexanoic acid	268.0372	$C_{15}H_8O_5$	Kaemperol
98.1096	C_7H_{14}	Alcohol	268.0460	$C_7H_{13}N_2O_7P_1$	Glycinamidribonucleotid
99.0684	$C_5H_9N_1O_1$	Proline	268.2191	$C_{20}H_{28}$	Retinol
100.0160	$C_4H_4O_3$	3-Hydroxy-2-oxobutanoic acid	272.2504	$C_{20}H_{32}$	Tetra-prenylation
101.0477	$C_4H_7N_1O_2$	Threonine	280.2766	$C_{19}H_{36}O_1$	19:0 Fatty acid
101.0841	$C_5H_{11}N_1O_1$	Valine	280.3130	$C_{20}H_{40}$	Alcohol

Table A.3 (continued) | Mass difference values (MD), compositional changes and (bio-)chemical reaction equivalents of mass differences connecting the compositions in MDiNs.

MD	Comp. Change	Reaction	MD	Composit. Change	Reaction
101.9776	$C_3H_2O_2S_1$	3-Mercaptopyruvate	284.0321	$C_{15}H_8O_6$	Quercitin
102.0317	$C_4H_6O_3$	2-Ketoglutarate	284.2140	$C_{20}H_{28}O_1$	20:5 Fatty acid
102.0470	C_8H_6	Phenylpyruvic acid	286.2297	$C_{20}H_{30}O_1$	20:4 Fatty acid
103.0092	$C_3H_5N_1O_1S_1$	Cysteine	289.0732	$C_{10}H_{15}N_3O_5S_1$	Glutathione
103.0633	$C_4H_9N_1O_2$	Threonine	291.0954	$C_{11}H_{17}N_1O_8$	Sialic Acid
103.0786	$C_8H_9N_1O_{-1}$	Phenylalanine	292.2766	$C_{20}H_{36}O_1$	20:1 Fatty acid
104.0262	$C_7H_4O_1$	Salicyl aldehyde	294.0951	$C_{11}H_{18}O_9$	Disaccharide(5|6)
104.0296	$C_4H_8O_1S_1$	2-Oxo-4-methylthiobutanoic acid	294.2923	$C_{20}H_{38}O_1$	20:0 Fatty acid
104.0374	$C_6H_4N_2$	Niacinamide	300.0270	$C_{15}H_8O_7$	Myricetin
105.0215	$C_6H_3N_1O_1$	Niacine	304.0460	$C_{10}H_{13}N_2O_7P_1$	TMP
105.0248	$C_3H_7N_1O_1S_1$	Cysteine	305.0413	$C_9H_{12}N_3O_7P_1$	CMP
106.0419	$C_7H_6O_1$	Salicyl alcohol	305.0682	$C_{10}H_{15}N_3O_6S_1$	Glutathione Disulfid
107.0041	$C_2H_5N_1O_2S_1$	Taurine	306.0253	$C_9H_{11}N_2O_8P_1$	UMP
108.0324	$C_5H_4N_2O_1$	Thymine	308.1107	$C_{12}H_{20}O_9$	Rutinosid
109.0198	$C_2H_7N_1O_2S_1$	Taurine	308.3079	$C_{21}H_{40}O_1$	21:0 Fatty acid
110.0480	$C_5H_6N_2O_1$	Imidazole pyruvic acid	310.2297	$C_{22}H_{30}O_1$	22:6 Fatty acid
110.1459	$C_9H_{18}O_{-1}$	Decanoic acid	312.2453	$C_{22}H_{32}O_1$	22:5 Fatty acid
111.0796	$C_5H_9N_3$	2-Oxoarginine	314.2610	$C_{22}H_{34}O_1$	22:4 Fatty acid
112.0524	$C_6H_8O_2$	2-Ketohexanoic acid	316.0460	$C_{11}H_{13}N_2O_7P_1$	Nicotineamide nucleotide
112.0888	$C_7H_{12}O_1$	Suberate	316.0559	$C_9H_{17}O_{10}P_1$	Glycerolphosphatglucose
112.1113	$C_5H_{12}N_4O_{-1}$	Arginine	318.2923	$C_{22}H_{38}O_1$	22:2 Fatty acid
112.1252	C_8H_{16}	Alcohol	319.1644	$C_{15}H_{21}N_5O_3$	Tyrosyl-arginin
113.0113	$C_4H_3N_1O_3$	2-Oxosuccinamic acid	320.3079	$C_{22}H_{40}O_1$	22:1 Fatty acid
113.0477	$C_5H_7N_1O_2$	5-Amino-2-oxopentanoic acid	322.3236	$C_{22}H_{42}O_1$	22:0 Fatty acid
113.0841	$C_6H_{11}N_1O_1$	Leucine/Isoleucine	324.1057	$C_{12}H_{20}O_{10}$	Disaccharide(6|6)
113.9953	$C_4H_2O_4$	2-Ketosuccinate	329.0525	$C_{10}H_{12}N_5O_6P_1$	AMP
114.0317	$C_5H_6O_3$	Glutarate	336.3392	$C_{23}H_{44}O_1$	23:0 Fatty acid
114.0429	$C_4H_6N_2O_2$	Asparagine	338.0849	$C_{12}H_{18}O_{11}$	Maltose acid
114.0793	$C_5H_{10}N_2O_1$	Ornithine	338.2610	$C_{24}H_{34}O_1$	24:6 Fatty acid
115.0269	$C_4H_5N_1O_3$	Aspartic acid	345.0474	$C_{10}H_{12}N_5O_7P_1$	GMP
115.0633	$C_5H_9N_1O_2$	Proline	348.3392	$C_{24}H_{44}O_1$	24:1 Fatty acid
115.0997	$C_6H_{13}N_1O_1$	Leucine/Isoleucine	350.3549	$C_{24}H_{46}O_1$	24:0 Fatty acid

Table A.3 (continued) | Mass difference values (MD), compositional changes and (bio-)chemical reaction equivalents of mass differences connecting the compositions in MDiNs.

MD	Comp. Change	Reaction	MD	Composit. Change	Reaction
116.0473	$C_5H_8O_3$	Deoxy-pentose	358.1277	$C_{17}H_{18}N_4O_5$	Riboflavin
116.0586	$C_4H_8N_2O_2$	Asparagine	364.3705	$C_{25}H_{48}O_1$	25:0 Fatty acid
116.0950	$C_5H_{12}N_2O_1$	Ornithine	366.3287	$C_{27}H_{42}$	Cholecalciferol
117.0426	$C_4H_7N_1O_3$	Aspartic acid	378.3287	$C_{28}H_{42}$	Ergocalciferol
117.0439	$C_5H_3N_5O_{-1}$	Adenine	378.3862	$C_{26}H_{50}O_1$	26:0 Fatty acid
118.0279	$C_5H_2N_4$	Hypoxanthin	384.0124	$C_{10}H_{14}N_2O_{10}P_2$	TDP
118.0419	$C_8H_6O_1$	4-Hydroxyphenylpyruvic acid	385.0076	$C_9H_{13}N_3O_{10}P_2$	CDP
119.0735	$C_8H_9N_1$	Tyrosine	385.9916	$C_9H_{12}N_2O_{11}P_2$	UDP
120.0211	$C_7H_4O_2$	Salicylic acid	406.3236	$C_{29}H_{42}O_1$	Tocotrienol
120.0423	$C_4H_8O_4$	Erythrose	409.0189	$C_{10}H_{13}N_5O_9P_2$	ADP
120.0575	$C_8H_8O_1$	Phenylpyruvic acid	412.3705	$C_{29}H_{48}O_1$	Tocoferol
121.0198	$C_3H_7N_1O_2S_1$	Cysteine	423.1291	$C_{19}H_{17}N_7O_5$	Folic acid
121.0658	$C_5H_{11}N_1Cl_1$	Choline (chlorid)	425.0138	$C_{10}H_{13}N_5O_{10}P_2$	GDP
123.0085	$C_2H_6N_1O_3P_1$	Phosphoethanolamine	427.1604	$C_{19}H_{21}N_7O_5$	Tetrahydrofolic acid
126.1045	$C_8H_{14}O_1$	Octanoic acid	432.3392	$C_{31}H_{44}O_1$	Phylloquinone
126.1409	C_9H_{18}	Alcohol	434.3549	$C_{31}H_{46}O_1$	Phylloquinol
127.0269	$C_5H_5N_1O_3$	2-Keto-glutaramic acid	455.1553	$C_{20}H_{21}N_7O_6$	Folinic acid
127.0633	$C_6H_9N_1O_2$	6-Amino-2-oxohexanoic acid	463.9787	$C_{10}H_{15}N_2O_{13}P_3$	TTP
128.0110	$C_5H_4O_4$	2-Ketoglutarate	464.9740	$C_9H_{14}N_3O_{13}P_3$	CTP
128.0473	$C_6H_8O_3$	Adipate	465.9580	$C_9H_{13}N_2O_{14}P_3$	UTP
128.0586	$C_5H_8N_2O_2$	Glutamine	488.9852	$C_{10}H_{14}N_5O_{12}P_3$	ATP
128.0950	$C_6H_{12}N_2O_1$	Lysine	504.9801	$C_{10}H_{14}N_5O_{13}P_3$	GTP
129.0426	$C_5H_7N_1O_3$	Glutamic acid			

B Supplementary Chapter 2

Tables B

Table B.1 | Overview of the OPLS-DA models (exclusions, predictions) and statistical parameters (R^2Y, Q^2, CV-ANOVA).

Model	Samples	Exclusion	Prediction	R^2Y	Q^2	ANOVA (p-value)
Beertype	78	Geuze	Triticum dicoccum, Triticum aestivium spelta used for wheat beers; wit beer (raw wheat); sample 85 (typical wheat beer	0.96	0.63	1.13 E-23
Grain	81	-	Triticum dicoccum, Triticum aestivium	0.98	0.73	2.55 E-19

Table B.2 | Overview (beer type, grain used, scores and set type) of the measured samples' characteristics.

Sample no.	Beer type	Grain	Model 1		Model 2		Sample set	Country
			score (x)	score (y)	score (x)	score (y)		
01	Wheat	Wheat	17.93	1.33	-16.17	2.24	model	GER
02	Lager	Barley	-10.95	13.23	7.94	16.76	model	GER
03	Lager	Barley	-10.82	13.55	9.17	13.05	model	GER
04	Abbey	Barley	-1.00	1.21	9.48	-13.03	model	BEL
05	Wheat	Wheat	20.29	-2.80	-17.59	-22.83	model	GER
06	Wheat	Wheat	22.54	-0.60	-16.98	-17.74	model	GER
07	Wheat	Wheat	19.49	-0.07	-17.30	-3.92	model	GER
08	Lager	Barley	-10.09	13.34	11.10	-8.80	model	GER
09	Lager	Barley	-10.62	12.38	9.49	11.52	model	GER
10	Lager	Barley	-10.15	8.21	7.57	20.13	model	GER
11	Wheat	Wheat	17.59	4.94	-12.08	16.53	model	GER
12	Wheat	Wheat	19.04	-2.03	-14.82	-1.58	model	GER
13	Lager	Barley	-10.11	8.49	7.31	13.35	model	GER
14	Lager	Barley	-7.39	10.04	6.67	6.94	model	CZE
15	Lager	Barley	-9.69	13.77	10.08	9.40	model	GER
16	Lager	Barley	-9.54	11.57	10.25	10.47	model	GER
17	Abbey	Barley	-1.82	1.36	10.83	-6.38	model	BEL
18	Wheat	Wheat	20.99	-0.55	-17.32	-10.85	model	USA
19	Wheat	Wheat	19.47	-0.66	-14.74	4.4	model	GER
20	Wheat	Wheat	14.76	0.15	-12.2	6.57	model	GER
21	Lager	Barley	-8.25	6.99	9.61	-3.43	model	GER
22	Lager	Barley	-8.36	10.13	10.1	-0.20	model	GER
23	Lager	Barley	-9.36	6.32	10.34	-3.63	model	GER
24	Wheat	Wheat	16.68	-0.82	-14.7	0.10	model	IRL
25	Lager	Barley	-12.5	11.96	10.24	-19.22	model	GER
26	Lager	Barley	-7.42	12.61	9.65	9.30	model	GER
27	Wheat	Wheat	20.85	0.39	-16.41	-14.00	model	GER
28	Lager	Barley	-9.42	14.09	10.43	6.71	model	GER
29	Wheat	Wheat	18.52	2.04	-16.74	-6.81	model	GER
30	Wheat	Wheat	20.01	-0.63	-15.85	-17.76	model	GER
31	Wheat	Wheat	20.90	-0.99	-17.21	-7.81	model	GER
32	Lager	Barley	-9.32	11.58	8.04	7.88	model	BEL

Table B.2 (continued) | Overview (beer type, grain used, scores and set type) of the measured samples' characteristics.

Sample no.	Beer type	Grain	Model 1		Model 2		Sample set	Country
			score (x)	score (y)	score (x)	score (y)		
33	Lager	Barley	-7.76	11.80	8.70	4.00	model	GER
34	Lager	Barley	-14.35	11.45	11.43	-18.68	model	GER
35	Wheat	Wheat	20.17	1.93	-17.17	-7.20	model	GER
36	Lager	Barley	-7.23	13.64	9.46	-1.9	model	GER
37	Abbey	Barley	-0.01	0.54	8.33	-19.71	model	GER
38	Lager	Barley	-9.38	12.08	11.13	0.91	model	GER
39	Abbey	Barley	-0.16	1.90	8.18	-1.21	model	GER
40	Lager	Barley	-8.36	13.84	10.46	10.75	model	BEL
41	Wheat	Wheat	21.64	1.50	-17.67	-4.25	model	GER
42	Lager	Barley	-10.08	12.75	11.87	7.49	model	GER
43	Lager	Barley	-10.81	7.98	9.22	11.81	model	BEL
44	Lager	Barley	-12.85	8.46	10.08	-28.41	model	GER
45	Craft	Barley	-9.02	-23.15	8.98	30.98	model	GER
46	Lager	Barley	-10.2	8.54	10.04	0.94	model	GER
47	Wheat	Wheat	20.14	-3.26	-16.69	-5.28	model	GER
48	Craft	Barley	-7.91	-21.61	10.10	12.25	model	GER
49	Wheat	Wheat	20.19	1.04	-17.10	-12.99	model	GER
50	Craft	Barley	-7.59	-19.19	9.03	3.44	model	GER
51	Wheat	Wheat	21.67	1.40	-16.46	-1.82	model	GER
52	Craft	Barley	-8.70	-21.01	9.32	21.08	model	GER
53	Craft	Wheat	-7.84	-19.04	-12.98	30.57	model	BEL
54	Craft	Wheat	-7.44	-23.61	-16.42	30.32	model	LTU
55	Wheat	Wheat	18.79	1.47	-15.61	-12.02	model	GER
56	Craft	Barley	-8.16	-18.04	7.47	8.13	model	GER
57	Abbey	Barley	-1.06	3.02	10.65	-9.46	model	GER
58	Abbey	Barley	-0.33	2.45	11.78	-24.42	model	BEL
59	Geuze	Barley	excl.	excl.	11.46	-27.46	model	GER
60	Lager	Barley	-9.2	15.31	10.71	-0.06	model	GER
61	Lager	Barley	-6.95	12.88	10.69	-10.24	model	GER
62	Lager	Barley	-7.6	10.96	10.08	-9.79	model	GER
63	Lager	Barley	-8.52	12.71	9.04	1.1	model	GER
64	Wheat	Wheat	19.22	1.90	-15.32	8.66	model	BEL
65	Wheat	Wheat	20.31	-1.80	-17.33	-8.44	model	BEL

Table B.2 (continued) | Overview (beer type, grain used, scores and set type) of the measured samples' characteristics.

Sample no.	Beer type	Grain	Model 1		Model 2		Sample set	Country
			score (x)	score (y)	score (x)	score (y)		
66	Wheat	Wheat	19.68	0.64	-16.27	1.12	model	GER
67	Craft	Barley	-9.87	-27.03	8.27	5.71	model	GER
68	Lager	Barley	-10.88	7.69	7.80	7.33	model	BEL
69	Lager	Barley	-8.49	8.63	10.41	-4.48	model	NAM
70	Craft	Barley	-10.03	-27.71	7.93	20.05	model	DNK
71	Craft	Barley	-12.03	-21.12	9.26	-6.71	model	GER
72	Craft	Barley	-10.87	-20.19	10.70	-22.94	model	GER
73	Craft	Wheat	-9.76	-24.97	-11.46	26.61	model	GER
74	Craft	Barley	-10.52	-23.65	9.12	22.49	model	GER
75	Craft	Barley	-8.66	-22.2	7.76	-20.98	model	GER
76	Craft	Wheat	-5.50	-19.07	-11.84	15.57	model	GER
77	Abbey	Wheat(starch)[a]	-0.92	3.65	9.27	-11.75	model	GER
78	Craft	Emmer[b]	-10.69	-16.62	5.94	-20.77	model	GER
79	Geuze	Barley	excl.	excl.	14.10	-32.85	model	GER
80	Craft	Wheat	-4.29	-17.34	-15.46	8.86	model	GER
81	excl.	excl.	excl.	excl.	excl.	excl.	model	GER
82	Wheat	Wheat	5.70	-6.08	-14.58	7.15	model	GER
83	Wheat	Wheat	17.07	-0.68	-16.65	-7.00	model	GER
84	Wit	Wheat(raw)[c]	9.18	0.53	-12.73	3.59	model	GER
85	Wheat	Spelt[d]	15.27	0.38	-13.49	-3.76	model	GER
86	Lager	Barley	-2.79	1.07	5.21	-6.72	prediction	CUB
87	Lager	Barley	-2.57	5.82	5.22	-4.98	prediction	CUB
88	Lager	Barley	-6.64	-1.86	6.06	-4.64	prediction	MEX
89	Lager	Barley	-1.71	3.88	2.83	0.84	prediction	MEX
90	Lager	Barley	-3.67	-0.10	4.03	3.09	prediction	CHN
91	Lager	Barley	-6.54	3.26	8.49	-4.32	prediction	PER
92	Lager	Barley	-2.05	0.57	5.53	-6.20	prediction	ARG
93	Lager	Barley	-3.68	-3.77	3.3	-19.06	prediction	PER
94	Lager	Barley	-2.77	0.01	2.91	2.52	prediction	ESP
95	Lager	Barley	-2.70	-1.89	9.35	-14.11	prediction	BRA
96	Craft	Barley	-5.28	-8.41	6.01	5.74	prediction	JPN
97	Wheat	Wheat	5.77	-2.03	-5.43	6.64	prediction	NLD
98	Lager	Barley	-4.91	4.01	7.29	-1.71	prediction	KOR

Table B.2 (continued) | Overview (beer type, grain used, scores and set type) of the measured samples' characteristics.

Sample no.	Beer type	Grain	Model 1		Model 2		Sample set	Country
			score (x)	score (y)	score (x)	score (y)		
99	Abbey	Wheat(raw)[c]	6.79	-0.41	-0.71	-5.15	prediction	BEL
100	Abbey	Wheat	-3.63	-9.37	2.98	-12.19	prediction	NLD
101	Abbey	Wheat(starch)[a]	-1.32	-0.54	5.79	-2.10	prediction	BEL
102	Abbey	Wheat(raw)[c]	10.39	-1.13	-6.06	-1.19	prediction	BEL
103	Craft	Barley	-5.56	-12.21	1.98	-6.02	prediction	BEL
104	Lager	Barley	-8.36	-4.28	7.7	9.01	prediction	NLD
105	Lager	Barley	-7.94	0.27	6.96	7.05	prediction	NLD
106	Craft	Barley	-8.00	-15.59	5.26	15.03	prediction	NLD
107	Lager	Barley	-6.36	-6.18	3.45	5.15	prediction	GER
108	Lager	Barley	-4.74	7.55	7.14	-2.31	prediction	SGP
109	Wheat	Wheat	9.61	-6.5	-7.35	-2.52	prediction	NDL
110	Abbey	Wheat(starch)[a]	0.87	0.13	5.83	-10.34	prediction	BEL
111	Craft	Barley	3.05	1.98	3.19	-7.33	prediction	BEL
112	Craft	Barley	-8.09	-14.45	6.13	-8.40	prediction	NDL
113	Abbey	Barley	-2.15	1.93	5.62	-1.56	prediction	NDL
114	Craft	Wheat	3.10	-6.70	0.35	-18.18	prediction	GER
115	Abbey	Barley	0.35	2.77	6.91	-8.92	prediction	BEL
116	Craft	Barley	-3.87	-12.17	5.19	-15.78	prediction	BEL
117	Lager	Barley	-8.86	-5.33	5.58	-5.06	prediction	GER
118	Craft	Wheat	-1.41	-6.82	2.02	-13.26	prediction	GER
119	Abbey	Barley	-6.81	-12.55	6.47	2.71	prediction	BEL
120	Craft	Wheat(raw)[c]	3.57	-5.55	-1.41	3.94	prediction	BEL

[a] Triticum aestivium starch only

[b] Triticum dicoccum

[c] Triticum aestivium not malted (typical for wit beers)

[d] Triticum aestivium subsp. spelta

Table B.3 | Tentative annotations of markers for rich hopped beers on basis of exact masses.

$m/z_{measured}$	$m/z_{theor.}$	Error [ppm]	Molecular formula	Annotation	Reference
263.12890	263.12888	0.05	$C_{15}H_{20}O_4$	Phenylphlorisobutyro-phenone, hulupinic acid	[292,410]
265.14453	265.14453	0.01	$C_{15}H_{22}O_4$	humulinic acid, adhumulinic acid	[410]
277.14455	277.14453	0.06	$C_{16}H_{22}O_4$	phenylphlorisoalerophenone	[292]
281.13946	281.13945	0.02	$C_{15}H_{22}O_5$	oxyhumulinic acid	[443]
317.17582	317.17583	0.05	$C_{19}H_{26}O_4$	cohulupone	[410]
331.19146	331.19148	0.08	$C_{20}H_{28}O_4$	deoxycohumulone, hulupone, adhulupone	[410]
345.20711	345.20713	0.06	$C_{21}H_{30}O_4$	deoxyhumulone, deoxyadhumulone	[410]
347.18649	347.18640	0.25	$C_{20}H_{28}O_5$	(allo)cohumulone, (allo)iso-cohumulone, (iso)-tricyclocohumene	[410]
349.20203	349.20205	0.05	$C_{20}H_{30}O_5$	dihydrocohumulone	[443]
361.20214	361.20204	0.27	$C_{21}H_{30}O_5$	humulone, (allo)(iso)-(ad)humulone, (iso)-(ad)tricyclohumene	[410]
363.18134	363.18131	0.08	$C_{20}H_{28}O_6$	(iso)cohumulinone, hydroxyl-alloisocohumulone, scorpiocohumol	[410]
363.21771	363.21770	0.03	$C_{21}H_{32}O_5$	dihydrohumulone	[443]
365.19700	365.19696	0.10	$C_{20}H_{30}O_6$	cohumol, tricyclocohumol, (epi)tetracyclocohumol, hydroxyl(iso)cohumulon	[410,444,445]
377.19701	377.19696	0.14	$C_{21}H_{30}O_6$	(iso)humulinone, adhumulinone, hydroxyl-alloiso(ad)humulone, scorpiohumol	[410]
379.21264	379.21261	0.08	$C_{21}H_{32}O_6$	humol, tricyclohumol, tetracyclohumol	[410]
381.19187	381.19188	0.01	$C_{20}H_{30}O_7$	hydroxyl-alloisocohumulonhydroxid	[444]
393.19196	393.19188	0.22	$C_{21}H_{30}O_7$	allosiohumulonhydroperxid	[444]
431.24395	431.24391	0.08	$C_{25}H_{36}O_6$	colupdox, hydroxyperoxytricycloco-lupon	[446,447]
433.25958	433.25956	0.05	$C_{25}H_{38}O_6$	hydroperoxitricyclolupone	[410]
445.25960	445.25956	0.09	$C_{26}H_{38}O_6$	lupdox	[447]

Table B.4 | Structural identification of hops-rich beer type marker masses by means of UHPLC-ToF-MS/MS. Level of identification 2.

$m/z_{measured}$	$m/z_{theor.}$	Error [ppm]	Molecular formula	Rt[a] [min]	Compound	MS/MS fragments [m/z (rel. intensity)]	Reference
251.1289	251.12888	-0.08	$C_{14}H_{20}O_4$	4.8	Cohumulinic acid	71(23), 113(34), 141(100), 165(72), 233(40)	[445]
263.1290	263.12880	-0.76	$C_{15}H_{20}O_4$	4.6	Hulupinic acid	126(21), 151(96), 165(19), 179(37), 193(100)	[446]
317.1760	317.17583	0.54	$C_{19}H_{26}O_4$	5.3	Cohulupone	180(28), 184(23), 205(100), 220(35), 233(69), 248(25)	[186]
347.1863	347.18640	0.29	$C_{20}H_{28}O_5$	6.0	Iso-cohumulone	181(100), 207(11), 209(35), 233(35), 235(10), 251(62), 278(8), 329(4)	[271]
347.1858	347.18640	1.73	$C_{20}H_{28}O_5$	6.5	Cohumulone	207(35), 235(100), 278(84)	[271]
349.2024	349.20205	1.00	$C_{20}H_{30}O_5$	6.6	Dihydrocohumulone	207(11), 209(7), 235(30), 237(24), 278(21), 280(100)	[271] b
361.2032	361.20204	3.21	$C_{21}H_{30}O_5$	6.1	Iso-(ad)humulone	195(100), 221(20), 223(54), 247(59), 265(23), 343(6)	[271]
361.2033	361.20204	3.49	$C_{21}H_{30}O_5$	6.6	(Ad)humulone	221(36), 249(90), 292(100)	[271]
365.1977	365.19696	2.03	$C_{20}H_{30}O_6$	3.8	Tricyclocohumol	165(89), 183(100), 245(8), 277(7), 289(6), 303(9), 347(86)	[409]
365.1976	365.19696	-1.75	$C_{20}H_{30}O_6$	4.2	Hydroxyl(iso)cohumulon	181(38), 193(64), 251(100), 269(71), 296(21)	[444]
365.1972	365.19696	0.66	$C_{20}H_{30}O_6$	4.8	Tetracyclohumol	165(55), 193(100), 289(21), 307(82), 347(3)	[409]
379.2131	379.21261	1.29	$C_{21}H_{32}O_6$	4.2	Tricyclohumol	179(73), 197(100), 277(6), 303(8), 317(6), 361(80)	[409]

[a] retention time

[b] The literature data refers to the dedicated non-hydrated compound. Level of identification 3.

Table B.5 | UHPLC-ToF-MS/MS-data of ambiguous markers for rich hopped beer. Level of identification 3. The five highest fragments are shown.

$m/z_{measured}$	$m/z_{theor.}$	Error [ppm]	Molecular formula	Retention time [min]	MS/MS fragments [m/z (rel. intensity)]
251.1286	251.12888	1.11	$C_{14}H_{20}O_4$	4.4	69(100), 81(6), 98(11), 189(6), 251(6)
251.1289	251.12888	-0.08	$C_{14}H_{20}O_4$	4.8	71(23), 113(34), 141(100), 165(72), 233(40)
251.1289	251.12888	-0.08	$C_{14}H_{20}O_4$	5.8	65(85), 111(28). 152(100), 180(11), 184(62)
263.1288	263.12880	0.00	$C_{15}H_{20}O_4$	5.8	97(40), 163(33), 177(35), 192(100), 205(90)
263.1291	263.12880	-1.14	$C_{15}H_{20}O_4$	6.0	82(14), 124(18), 166(100), 179(22), 198(46)
265.1444	265.14453	0.49	$C_{15}H_{22}O_4$	5.1	69(13), 127(9), 155(100), 179(18), 247(9)
265.1448	265.14453	0.33	$C_{15}H_{22}O_4$	5.7	79(11), 97(100), 177(2), 205(3), 265(20),
277.1451	277.14453	-2.06	$C_{16}H_{22}O_4$	4.4	137(13), 165(100), 175(27), 190(20), 208(29)
279.1239	279.12380	-0.36	$C_{15}H_{20}O_5$	3.5	139(9), 167(100), 181(13), 195(9), 210(18)
279.1237	279.12380	0.36	$C_{15}H_{20}O_5$	3.8	165(100), 167(18), 181(13),.183(9), 210(9)
279.1237	279.12380	0.36	$C_{15}H_{20}O_5$	5.1	139(13), 165(9), 167(100), 210(18), 249(9)
279.1238	279.12380	0.00	$C_{15}H_{20}O_5$	5.3	65(18), 133(9), 151(9), 207(13), 235(100)
279.1236	279.12380	0.72	$C_{15}H_{20}O_5$	5.9	65(18), 151(13), 235(100), 261(9), 279(9)
281.1382	281.13945	4.45	$C_{15}H_{22}O_5$	3.9	73(9), 139(9), 155(18), 165(9), 195(100)
281.1397	281.13945	-0.89	$C_{15}H_{22}O_5$	4.0	66(9), 101(9), 155(9), 177(9), 195(100)
293.1393	293.13945	0.51	$C_{16}H_{22}O_5$	4.1	153(18), 179(100), 195(9), 197(13), 224(9)
295.1552	295.15510	-0.34	$C_{16}H_{24}O_5$	3.6	153(71), 167(33), 181(25), 226(100), 277(30)
305.1395	305.13945	-0.16	$C_{17}H_{22}O_5$	4.3	165(12), 193(14), 231(11), 243(27), 305(100)
305.1394	305.13945	0.16	$C_{17}H_{22}O_5$	5.2	149(14), 193(100), 248(11), 288(7), 303(14)
317.1395	317.13945	-0.16	$C_{18}H_{22}O_5$	4.2	147(90), 161(89), 179(57), 192(71), 233(100)
317.1395	317.13945	-0.16	$C_{18}H_{22}O_5$	4.3	180(100), 192(97), 220(71), 261(43), 289(66)
317.1395	317.13945	-0.16	$C_{18}H_{22}O_5$	5.4	205(43), 262(58), 274(30),302(30), 317(100)
319.1551	319.15510	0.00	$C_{18}H_{24}O_5$	4.6	193(10), 217(8), 235(8), 257(12), 319(100)
319.1551	319.15510	0.00	$C_{18}H_{24}O_5$	4.8	165(9), 193(13), 245(6), 257(14), 319(100)
319.1551	319.15510	0.00	$C_{18}H_{24}O_5$	5.6	165(17), 179(50), 195(17), 207(100), 250(55)
329.1758	329.17583	0.09	$C_{20}H_{26}O_4$	5.2	167(100), 195(41), 201(23), 219(43), 242(29)
331.1917	331.19148	-0.66	$C_{20}H_{28}O_4$	5.5	166(92), 191(44), 194(49), 219(100), 247(68)
331.1915	331.19148	-0.06	$C_{20}H_{28}O_4$	5.6	166(78), 205(100), 219(77), 234(40), 247(76)

Table B.5 (continued) | UHPLC-ToF-MS/MS-data of ambiguous markers for rich hopped beer. Level of identification 3.The five highest fragments are shown.

$m/z_{measured}$	$m/z_{theor.}$	Error [ppm]	Molecular formula	Retention time [min]	MS/MS fragments [m/z (rel. intensity)]
333.1710	333.17075	-0.75	$C_{19}H_{26}O_5$	3.8	205(25), 221(100), 236(27), 247(42), 249(90)
333.1710	333.17075	-0.75	$C_{19}H_{26}O_5$	3.9	152(58), 181(80), 205(69), 233(70), 247(100)
333.1712	333.17075	-1.35	$C_{19}H_{26}O_5$	4.9	169(22), 181(10), 221(11), 237(100), 335(9)
333.1708	333.17075	-0.15	$C_{19}H_{26}O_5$	5.1	151(8), 167(100), 193(13), 195(35), 219(34)
333.1709	333.17075	-0.45	$C_{19}H_{26}O_5$	5.2	163(19), 167(100), 193(9), 195(39), 219(34)
333.1710	333.17075	-0.75	$C_{19}H_{26}O_5$	6.0	179(23), 193(59), 209(24), 221(100), 264(81)
335.1497	335.15001	0.92	$C_{18}H_{24}O_6$	3.3	165(10), 245(7), 251(6), 317(6), 335(100)
335.1499	335.15001	0.33	$C_{18}H_{24}O_6$	3.5	209(4), 245(5), 251(4), 273(7), 335(100)
335.1496	335.15001	1.22	$C_{18}H_{24}O_6$	4.0	181(62), 205(79), 233(80), 247(100), 291(67)
335.1496	335.15001	1.22	$C_{18}H_{24}O_6$	4.5	196(28), 221(32), 247(100), 265(26), 335(29)
335.1496	335.15001	1.22	$C_{18}H_{24}O_6$	6.8	182(17), 195(100), 238(22), 247(29), 263(23)
335.1858	335.18640	1.79	$C_{19}H_{28}O_5$	4.8	59(34), 85(46), 203(87), 219(39), 263(100)
335.1863	335.18640	0.30	$C_{19}H_{28}O_5$	5.0	169(22), 204(21), 237(100), 247(14), 335(67)
335.1864	335.18640	0.00	$C_{19}H_{28}O_5$	5.1	181(100), 231(47), 249(59), 259(51), 265(84)
335.1862	335.18640	0.60	$C_{19}H_{28}O_5$	5.2	85(44), 203(69), 235(34), 263(100), 273(41)
335.1863	335.18640	0.30	$C_{19}H_{28}O_5$	5.3	115(44), 153(23), 167(100), 195(39), 219(35)
335.1858	335.18640	1.79	$C_{19}H_{28}O_5$	5.4	166(44), 187(43), 191(54), 231(100), 235(31)
335.1862	335.18640	0.60	$C_{19}H_{28}O_5$	5.6	166(83), 191(47), 194(47), 219(100), 247(76)
343.1914	343.19148	0.23	$C_{21}H_{28}O_4$	5.0	190(71), 205(65), 231(100), 259(73), 343(50)
343.1915	343.19148	-0.06	$C_{21}H_{28}O_4$	5.5	181(100), 187(56), 191(99), 235(64), 242(52)
343.1918	343.19148	-0.93	$C_{21}H_{28}O_4$	6.0	163(100), 180(99), 247(34), 249(73), 259(36)
345.2073	345.20713	-0.49	$C_{21}H_{30}O_4$	5.6	167(73), 179(65), 191(80), 235(100), 249(40)
347.1495	347.15001	1.47	$C_{19}H_{24}O_6$	4.9	164(81), 191(53), 207(100), 234(48), 305(44)
347.1863	347.18640	0.29	$C_{20}H_{28}O_5$	4.1	219(29), 221(25), 235(26), 261(37), 263(100)
347.1861	347.18640	0.86	$C_{20}H_{28}O_5$	5.3	165(40), 167(49), 181(38), 223(39), 251(100)
349.1657	349.16566	-0.11	$C_{19}H_{26}O_6$	4.0	167(20), 201(32), 235(51), 263(100), 347(24)
349.2020	349.20205	0.14	$C_{20}H_{30}O_5$	4.8	164(34), 207(77), 221(100), 253(92), 305(75)
351.1813	351.18131	0.03	$C_{19}H_{28}O_6$	4.6	166(17), 193(100), 239(11), 263(32), 351(14)
351.1810	351.18131	0.88	$C_{19}H_{28}O_6$	4.9	181(7), 195(9), 209(26), 223(58), 292(100)

Table B.5 (continued) | UHPLC-ToF-MS/MS-data of ambiguous markers for rich hopped beer. Level of identification 3.The five highest fragments are shown.

$m/z_{measured}$	$m/z_{theor.}$	Error [ppm]	Molecular formula	Retention time [min]	MS/MS fragments [m/z (rel. intensity)]
351.1813	351.18131	0.03	$C_{19}H_{28}O_6$	5.0	177(63), 191(100), 207(76), 303(65), 349(79)
359.1868	359.18640	-1.11	$C_{21}H_{28}O_5$	5.3	194(20), 222(17), 233(9), 292(11), 359(100)
359.1866	359.18640	-0.56	$C_{21}H_{28}O_5$	5.5	205(94), 221(32), 249(49), 263(100), 359(28)
359.1866	359.18640	-0.56	$C_{21}H_{28}O_5$	5.6	183(71), 189(75), 195(61), 295(60), 359(100)
359.1867	359.18640	-0.84	$C_{21}H_{28}O_5$	5.8	167(63), 179(42), 191(81), 195(75), 235(100)
359.1867	359.18640	-0.84	$C_{21}H_{28}O_5$	5.9	179(30), 191(28), 195(35), 235(38), 263(100)
359.1867	359.18640	-0.84	$C_{21}H_{28}O_5$	6.1	99(23), 195(100), 223(49), 247(52), 265(23)
359.1865	359.18640	-0.28	$C_{21}H_{28}O_5$	6.2	195(100), 223(35), 247(35), 263(25), 265(15)
363.1815	363.18131	-0.52	$C_{20}H_{28}O_6$	3.8	231(5), 251(3), 345(4), 363(100)
363.1815	363.18131	-0.52	$C_{20}H_{28}O_6$	3.9	165(5), 183(6), 301(3), 347(6), 363(100)
363.1817	363.18131	-1.07	$C_{20}H_{28}O_6$	4.3	164(39), 181(100), 195(39), 233(34), 235(25)
363.1818	363.18131	-1.35	$C_{20}H_{28}O_6$	4.4	167(7), 206(7), 209(15), 225(7), 249(100)
363.1814	363.18131	-0.25	$C_{20}H_{28}O_6$	4.5	181(100), 195(48), 233(34), 249(44), 253(32)
363.1816	363.18131	-0.80	$C_{20}H_{28}O_6$	4.7	85(27), 139(18), 167(41), 209(88), 249(100)
365.1981	365.19696	-3.12	$C_{20}H_{30}O_6$	5.2	195(6), 209(9), 223(28), 237(55). 296(100)
375.1815	375.18131	-1.70	$C_{21}H_{28}O_6$	4.3	64(65), 80(100), 191(86), 277(22), 295(21)
377.1976	377.19696	-1.70	$C_{21}H_{30}O_6$	4.0	245(4), 251(3), 293(2), 359(4), 377(100)
377.1977	377.19696	-1.96	$C_{21}H_{30}O_6$	4.1	245(2). 251(3), 293(3), 315(2), 377(100)
377.1974	377.19696	-1.17	$C_{21}H_{30}O_6$	4.2	80(2), 245(2), 251(2), 315(2), 377(100)
377.1974	377.19696	-1.17	$C_{21}H_{30}O_6$	4.5	152(18), 195(100), 207(24), 265(21), 283(17)
377.1976	377.19696	-1.7	$C_{21}H_{30}O_6$	4.7	195(8), 220(8), 223(14), 239(8), 263(100)
379.2132	379.21261	-1.56	$C_{21}H_{32}O_6$	4.1	179(2), 245(3), 293(4), 315(3), 377(100)
379.2147	379.21261	-5.51	$C_{21}H_{32}O_6$	5.5	223(7), 237(25), 251(52), 254(11), 310(100)
381.1913	381.19188	1.52	$C_{20}H_{30}O_7$	2.9	245(3), 273(3), 275(3), 337(100), 381(63)
381.1921	381.19188	-0.58	$C_{20}H_{30}O_7$	3.1	181(100), 193(24), 361(28), 363(20), 379(18)
381.1920	381.19188	-0.31	$C_{20}H_{30}O_7$	3.3	181(100), 193(18), 233(9), 363(13), 281(70)
381.1913	381.19188	1.52	$C_{20}H_{30}O_7$	3.5	181(85), 193(100), 249(73), 305(6)), 379(84)
381.1922	381.19188	-0.84	$C_{20}H_{30}O_7$	3.7	181(84), 193(40), 265(30), 305(59), 379(100)
383.2072	383.20753	0.86	$C_{20}H_{32}O_7$	3.7	165(60), 183(34), 267(30), 325(100), 281(49)

Table B.5 (continued) | UHPLC-ToF-MS/MS-data of ambiguous markers for rich hopped beer. Level of identification 3.The five highest fragments are shown.

$m/z_{measured}$	$m/z_{theor.}$	Error [ppm]	Molecular formula	Retention time [min]	MS/MS fragments [m/z (rel. intensity)]
389.1964	389.19696	1.44	$C_{22}H_{30}O_6$	5.8	250(50), 261(44), 263(39), 306(100), 389(41)
389.1969	389.19696	0.15	$C_{22}H_{30}O_6$	5.6	249(19), 263(26), 265(11), 277(60), 320(100)
389.1968	389.19696	0.41	$C_{22}H_{30}O_6$	6.1	235(17), 278(100), 285(13), 301(42), 329(72)
389.1968	389.19696	0.41	$C_{22}H_{30}O_6$	6.6	247(56), 263(100), 277(24), 290(28), 302(40)
391.2130	391.21261	-1.00	$C_{22}H_{32}O_6$	4.9	153(73), 205(82), 225(100), 253(48), 263(40)
391.2123	391.21261	0.79	$C_{22}H_{32}O_6$	5.1	209(47), 224(34), 238(100), 277(64), 324(86)
391.2126	391.21261	0.03	$C_{22}H_{32}O_6$	5.3	165(21), 237(52), 248(27), 277(100), 317(31)
391.2119	391.21261	1.81	$C_{22}H_{32}O_6$	6.7	179(15), 195(18), 237(36), 253(13), 277(100)
393.2278	393.22826	1.17	$C_{22}H_{34}O_6$	6.2	181(22), 223(15), 233(11), 237(39), 324(100)
401.2339	401.23335	-1.37	$C_{24}H_{34}O_5$	5.7	221(16), 259(87), 271(42), 289(100), 329(12)
403.2120	403.21261	1.51	$C_{23}H_{32}O_6$	5.2	64(100), 80(66), 167(18), 219(11), 237(21)
403.2158	403.21261	-2.95	$C_{23}H_{32}O_6$	5.9	222(18), 235(11). 247(100), 250(928), 275(9)
405.1923	405.19188	-1.04	$C_{22}H_{30}O_7$	8.3	62(12), 147(3), 157(2), 263(3), 337(100)
407.2074	407.20753	0.32	$C_{22}H_{32}O_7$	4.1	179(12), 183(13), 251(100), 263(26), 273(16)
407.2074	407.20753	0.32	$C_{22}H_{32}O_7$	4.2	183(18), 263(100), 263(24), 277(33), 409(24)
407.2074	407.20753	0.32	$C_{22}H_{32}O_7$	4.3	163(20), 181(54), 221(100), 251(21), 263(22)
419.2072	419.20753	0.79	$C_{23}H_{32}O_7$	5.4	191(7), 247(20), 278(7), 291(6), 291(100), 350(12)
419.2076	419.20753	-0.17	$C_{23}H_{32}O_7$	5.5	192(22), 219(29), 235(18), 247(71), 306(100)
431.2431	431.24391	1.88	$C_{25}H_{36}O_6$	5.1	259(18), 317(23), 329(20), 387(100), 431(26)
431.2437	431.24391	0.49	$C_{25}H_{36}O_6$	5.2	287(98), 303(65), 314(33), 331(100), 431(34)
431.2439	431.24391	0.02	$C_{25}H_{36}O_6$	6.6	265(61), 278(75), 292(100), 329(62), 343(85)
433.2593	433.25956	0.6	$C_{25}H_{38}O_6$	5.3	277(80), 301(100), 321(47), 389(35), 431(32)
433.2598	433.25956	-0.55	$C_{25}H_{38}O_6$	5.6	207(17), 280(22), 289(18), 305(100), 433(66)
445.2595	445.25956	0.13	$C_{26}H_{38}O_6$	5.5	271(36), 301(38), 310(36), 317(100), 445(60)
445.2595	445.25956	0.13	$C_{26}H_{38}O_6$	6.8	265(22), 292(92), 299819), 315(64), 343(100)
447.2392	447.23883	-0.83	$C_{25}H_{36}O_7$	4.1	267(5), 329(6), 361(9), 377(11), 447(100)
447.2392	447.23883	-0.83	$C_{25}H_{36}O_7$	4.9	209(23), 239(12), 265(5), 429(7), 447(100)
447.2386	447.23883	0.51	$C_{25}H_{36}O_7$	5.3	235(31), 247(83), 265(26), 343(32), 351(100)
457.2237	457.22318	-1.14	$C_{26}H_{34}O_7$	5.3	233(100), 249(48), 251(46), 278(80), 329(92)

Table B.6 | Structural identification of wheat grain analytical marker masses by means of UPLC-ToF-MS/MS. Level of identification 2.

$m/z_{measured}$	$m/z_{theor.}$	Error [ppm]	Molecular formula	Rt[a] [min]	Compound	MS/MS fragments [m/z (rel. intensity)]	Collision	Reference
326.0880	326.0881	0.4	$C_{14}H_{17}NO_8$	2.6	HBOA-Hexoside	108(12), 118(4), 136(10), 164(100), 326(1)	30 eV	[283,448]
342.0835	342.0830	1.3	$C_{14}H_{17}NO_9$	1.7	DHBOA/DIBOA-Hex.[b]	124(17), 134(7), 152(49), 162(15), 180(100), 208(22), 342(1)	35 eV	[281]
342.0835	342.0835	0.0	$C_{14}H_{17}NO_9$	2.6	DHBOA/DIBOA-Hex.[b]	134(9), 162(31), 175 (20), 180(30), 342(100)	10 eV	[283]
356.0988	356.0987	0.2	$C_{15}H_{19}NO_9$	2.8	HMBOA-Hexose	138(9), 148(7), 166(34), 179(9), 194(100), 356(1)	30 eV	[281,448]
436.0558	436.0554	0.6	$C_{15}H_{19}NO_{12}S$	2.5	HMBOA-Hexosesulfate	194(65), 356(96), 436(100)	20 eV	[281,448], c
504.1357	504.1359	0.4	$C_{20}H_{27}NO_{14}$	1.9	DHBOA/DIBOA-Dihexoside[c]	162(19), 180(100), 342(15), 504(1)	35 eV	[281]
504.1352	504.1359	1.4	$C_{20}H_{27}NO_{14}$	2.6	DHBOA/DIBOA-Dihexoside[c]	134(7), 162(9), 175(100), 504(1)	35 eV	[281]
518.1514	518.1515	0.3	$C_{21}H_{29}NO_{14}$	2.7	HMBOA-Dihexoside	166(11), 194(100)	35 eV	[281]

[a] retention time

[b] differentiation between DHBOA and DIBOA can't be accomplished with (LC)-MS/MS-data only.

[c] The literature data refers to the dedicated de-sulfated compound. Level of identification 3.

Table B.7 | Instrumental parameters and reagents used for FT-ICR- and UHPLC-ToF-MS measurements.

Reagent	Source
Methanol (MeOH)	FLUKA, Sigma-Aldrich (LC-MS grade, CHROMASOLV, St Louis, MO, USA)
Acetonitrile (ACN)	FLUKA, Sigma-Aldrich (LC-MS grade, CHROMASOLV, St Louis, MO, USA)
Acetic acid	Biosolve (Valkenswaard, NL)
Ultrapure water	Milli-Q Integral Water Purification System (Millipore, Billerica, MA, USA)
L-arginine	Sigma-Aldrich (reagent grade >98%, St Louis, MO, USA)
ESI-L Low Concentration Tuning Mix	Agilent (Santa Clara, CA, United States of America)
FT-ICR-MS	**Value**
Sample preparation	Degassing by ultrasonification (10 °C, 5min.); dilution 1:500 in methanol (v:v); separation of precipitated proteins by centrifugation (10,000 rmp, 3min.)
Direct-infusion flowrate	120 µL.h^{-1}.
ESI capillary voltage	3600 V
Time domain	4 mega words
Accumulation time	0.25 ms
Mass range	m/z 120 to 1000
Accumulated scans	400
Measurement time	10 min.
External calibration	Clusters of arginine (5 mg.L^{-1} in methanol)
Internal calibration	in-house calibration list containing 2000 molecular formulae, which are highly abundant in beers
UHPLC-ToF-MS	**Value**
Sample preparation	Degassing by ultrasonification (10 °C, 5min.); dilution 1:4 in methanol (v:v); separation of precipitated proteins by centrifugation (10,000 rmp, 3min.); evaporation of the supernatant and dissolving in acetonitrile:water (20:80; v:v)
Column	RP (C18: 1.7 µm, 2.1 x 100 mm, Acquity™ UPLC BEH™)
Flow rate	400 µL min^{-1}
Column temperature	40 °C
Injection volume	5 µL (partial loop)

Table B.7 (continued) | Instrumental parameters and reagents used for FT-ICR- and UHPLC-ToF-MS measurements.

UHPLC-ToF-MS	Value
Gradient profile	95 % A (0.1 % formic acid in water) and 5 % B (0.1 % formic acid in
Measurement mode	Data dependent analysis with pre-built preference list (based on FT-ICR data)
Measurement time	10 min.
Internal calibration	ESI-L Low Concentration Tuning Mix
External calibration	ESI-L Low Concentration Tuning Mix (1:4 diluted in 75% acetonitrile) in the first 0.3 min of each LC-MS run; introduced by a switching valve.
ESI ionization mode	Negative
Nitrogen flowrate	10 L min^{-1}
Dry heater	200°C
Nebulizer pressure	2.0 bar
Capillary voltage	4500 V
Endplate offset	500 V
MS/MS fragmentation parameters	Data dependent analysis; collision energy 10 eV to 35 eV

Figures B

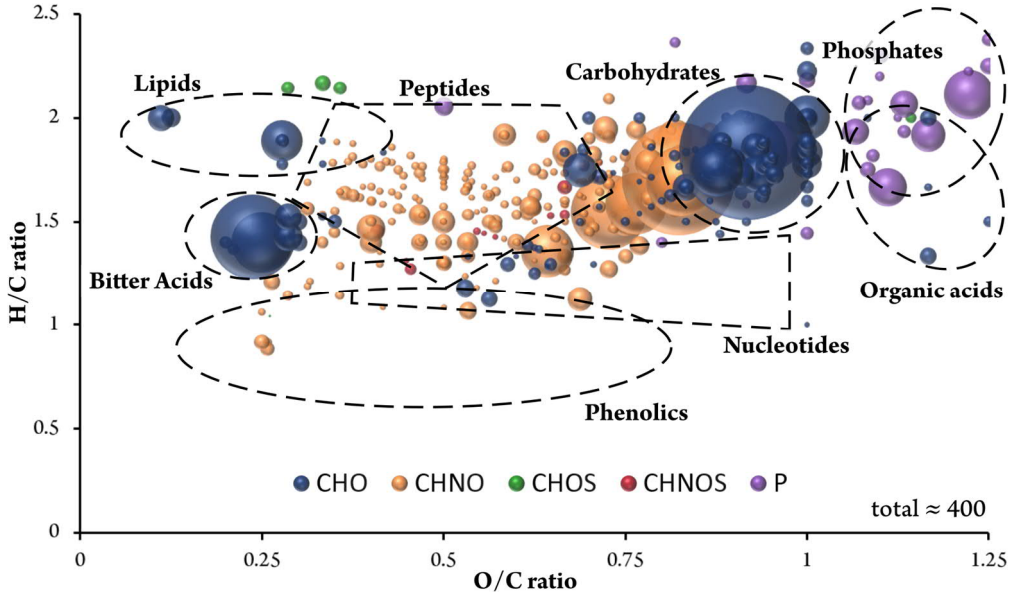

Figure B.1 | Van Krevelen diagram (H/C vs O/C) of the annotated molecular formulae appearing in more than 95 % of all beer samples (B). Areas specific for certain compound classes are marked with dotted lines. Color code of the van Krevelen diagrams: CHO blue; CHNO orange; CHOS green; CHNOS red; P violet; Cl light violet. The bubble size indicates the mean relative intensities of corresponding peaks in the spectra.

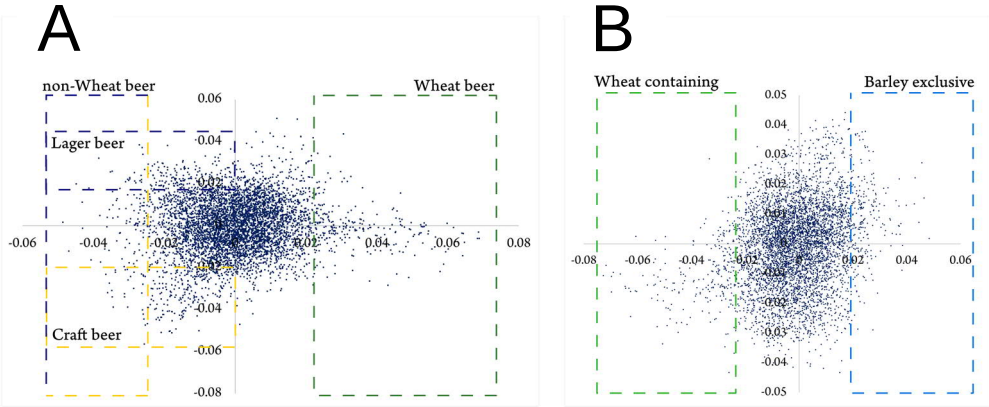

Figure B.2 | OPLS-DA loading plots for the beer type (A) and grain (B) observations. The 95th percentile of the different classes' marker substances is marked by colored areas.

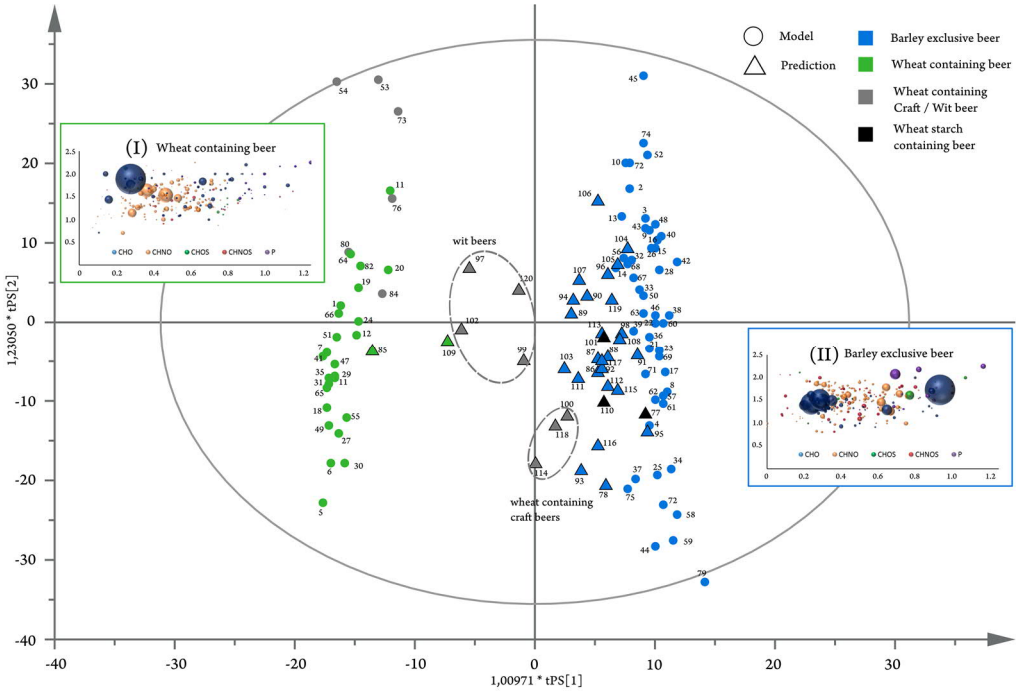

Figure B.3 | OPLS-DA model's score plot for the wheat-containing (green) and beers brewed with barley exclusively (blue) observation. The model sample set is depicted as circles, the prediction set is depicted as triangles. Different grain types are indicated by different colors. The score plots are surrounded by the observations' van Krevelen diagrams. Color code and bubble size of the van Krevelen diagrams see Figure B.2. Samples included in the model calculation are depicted as circles, whereas predicted samples are represented as triangles.

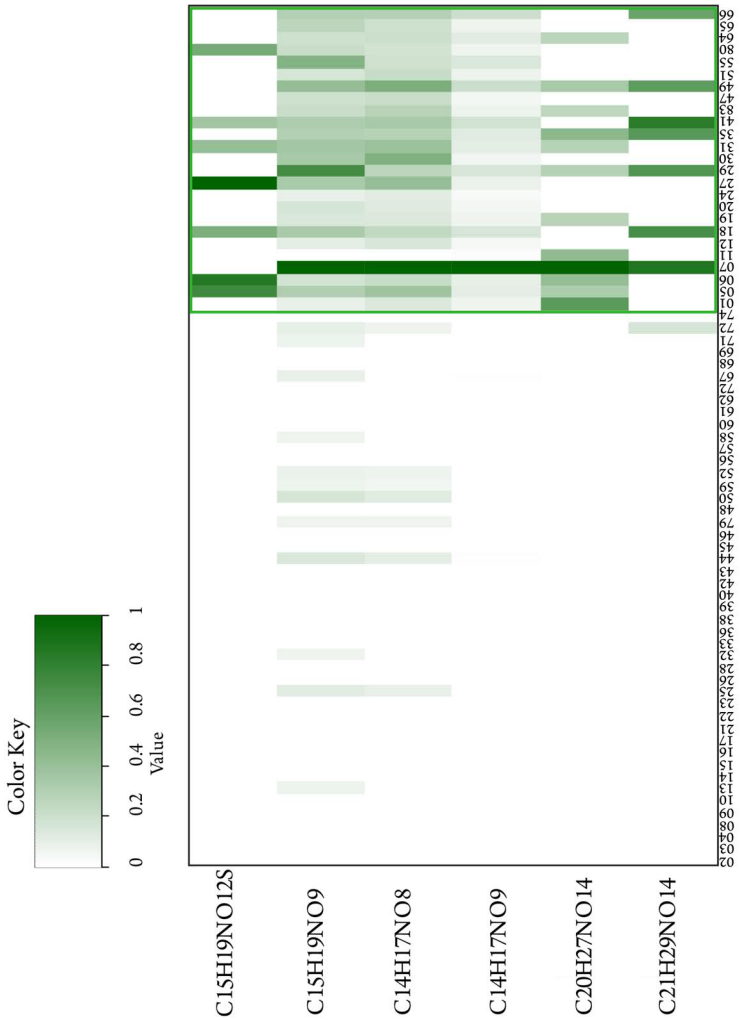

Figure B.4 | Intensity distribution for the wheat grain markers. $C_{14}H_{17}NO_8$ (HBOA-hex.), $C_{14}H_{17}NO_9$ (DHBOA/DIBOA-hex.), $C_{15}H_{19}NO_9$ (HMBOA-hex.), $C_{15}H_{19}NO_{12}S$ (HMBOA-hex.sulfate), $C_{20}H_{27}NO_{14}$ (DHBOA/DIBOA-dihex.), $C_{21}H_{29}NO_{14}$ (HMBOA-dihex.) are depicted. The maximum intensity for every peak is set to 100%. Beers brewed with wheat grain are marked. Trace amounts of the markers' corresponding masses in exclusively barley-containing beers might occur due to isomeric compounds.

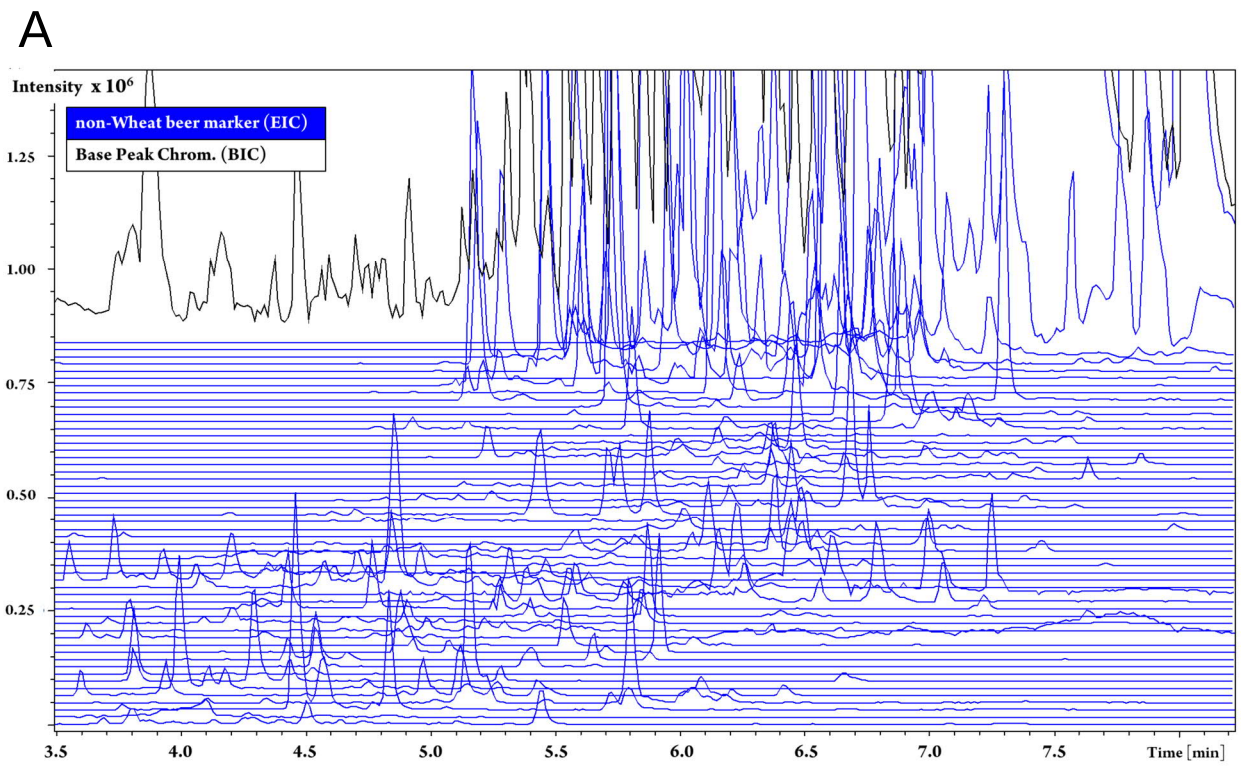

Figure B.5 | UHPLC-ToF-MS chromatogram of samples 52 and 41. Extracted ion chromatograms of markers for rich hopped beers found by FT-ICR-MS (blue) found in sample 52 (A). Extracted ion chromatograms of cohulupone (dark blue; confirmed by MS/MS data, compare Table S4) and humulinone isomeric compounds (light blue) (B). Mass traces of identified hops rich beer type markers (compare Table S4) of sample 52 (hops rich craft beer, blue) and sample 41 (wheat beer, green) in comparison (C). Isomeric compounds are shaded blue (for sample 52). UHPLC-ToF-MS extracted ion chromatograms (sample 41) of wheat grain marker masses and corresponding structures substantiated by MS/MS-data (compare Table S6)(D).

B

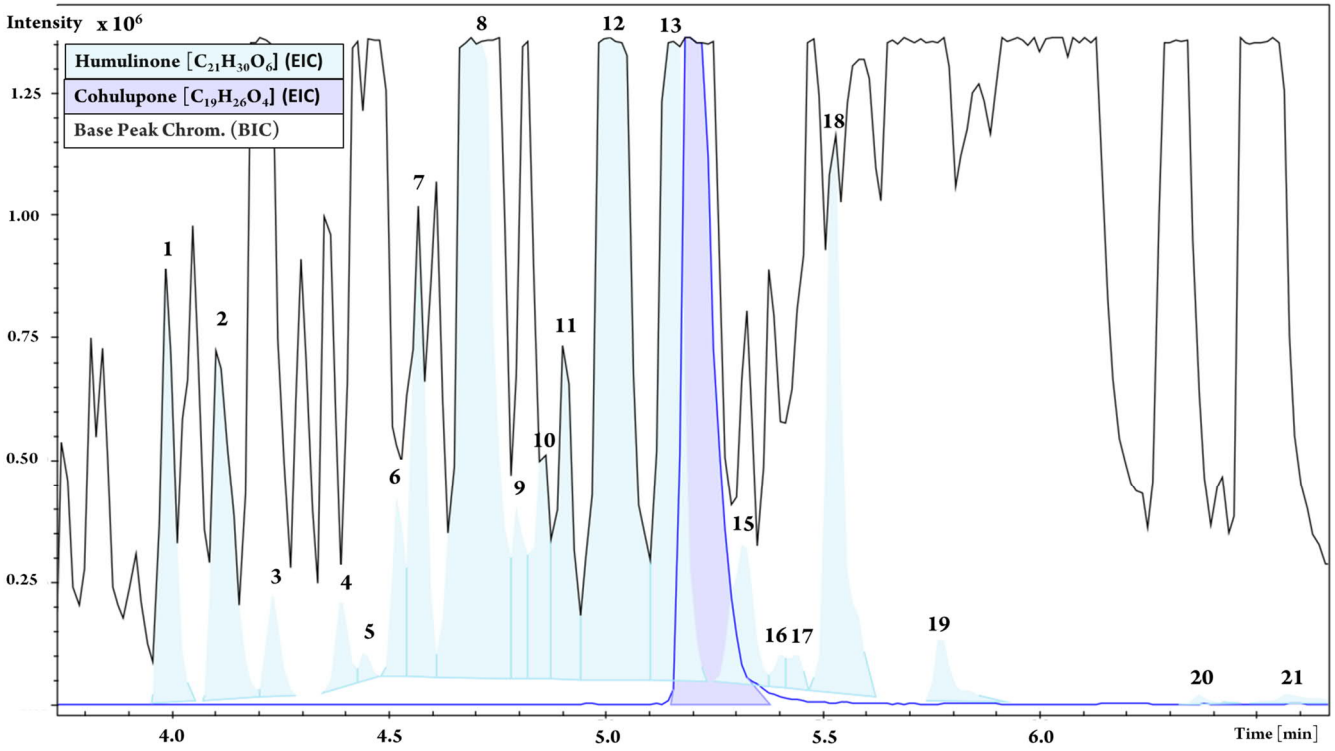

Figure B.5 | continued.

C

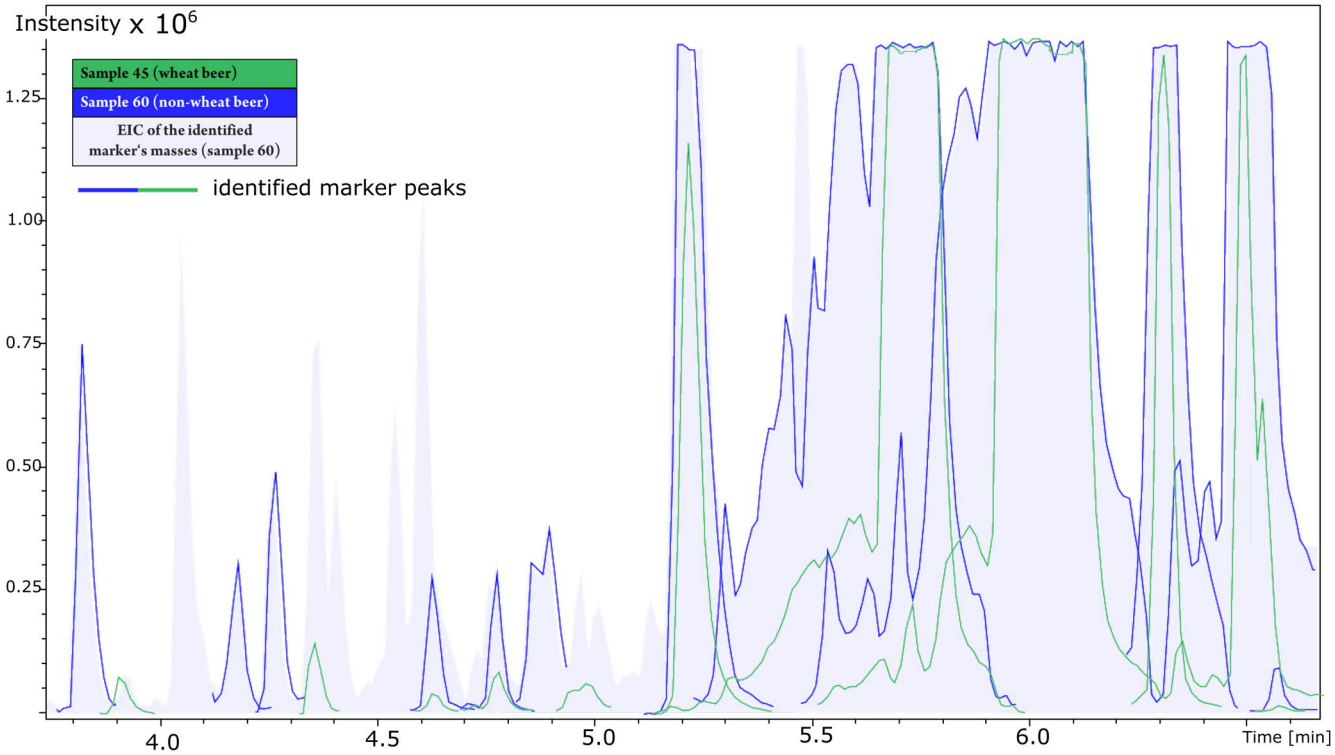

Figure B.5 | continued.

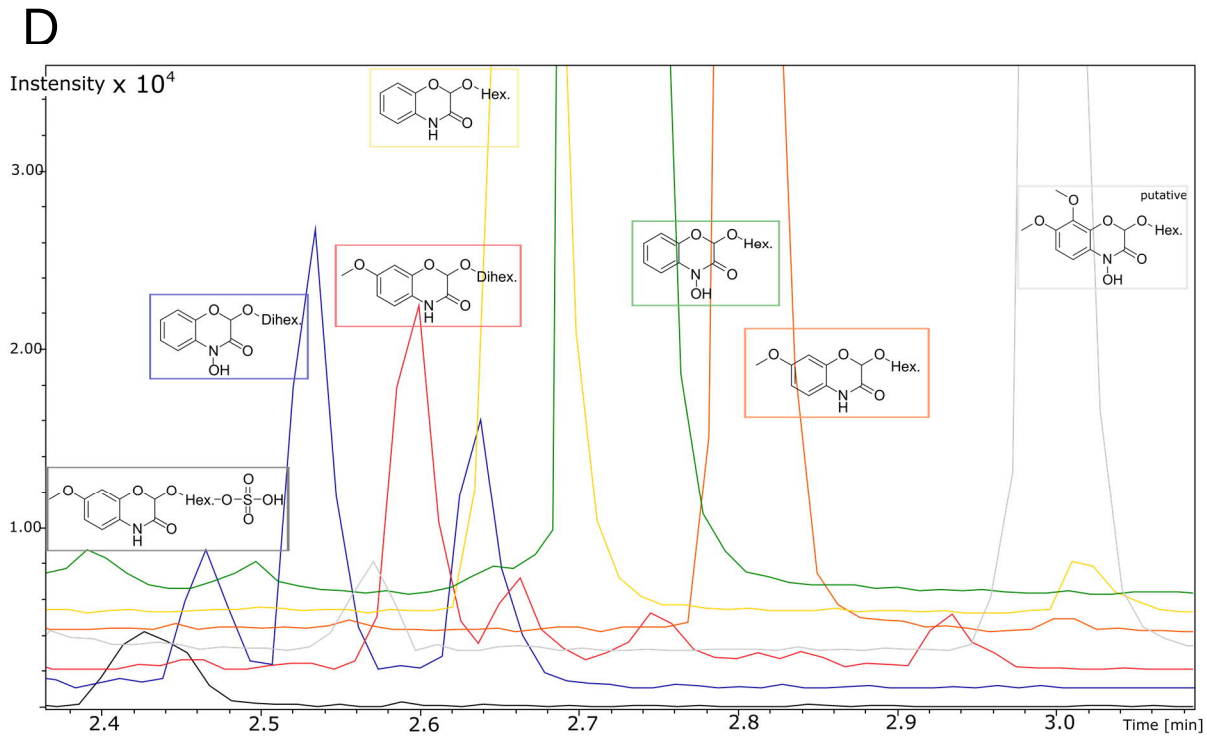

Figure B.5 | UHPLC-ToF-MS chromatogram of samples 52 and 41. Extracted ion chromatograms of hops rich beer type markers found by FT-ICR-MS (blue) found in sample 52 (A). Extracted ion chromatograms of cohulupone (dark blue; confirmed by MS2 data, compare Table S4) and humulinone isomeric compounds (light blue) (B). Mass traces of identified hops rich beer type markers (compare Table S4) of sample 52 (hops rich craft beer, blue) and sample 41 (wheat beer, green) in comparison (C). Isomeric compounds are shaded blue (for sample 52). UHPLC-ToF-MS extracted ion chromatograms (sample 41) of wheat grain marker masses and corresponding structures substantiated by MS2 data (compare Table B6)(D).

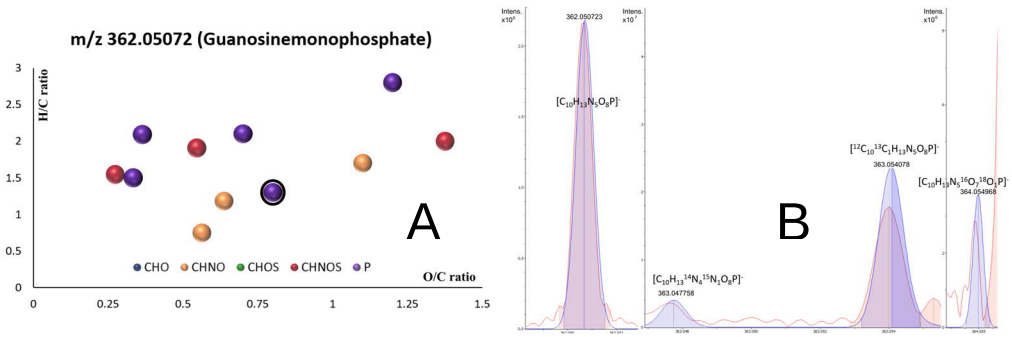

Figure B.6 | Eleven valid compositions for m/z 362.05072 in the error window of 3 ppm in a $C_{1\text{-}50}$ $H_{1\text{-}100}$, $O_{0\text{-}50}$ $N_{0\text{-}10}$, $S_{0\text{-}3}$, $P_{0\text{-}1}$, $Cl_{0\text{-}1}$ chemical space (A). Calculations are based on the FormCalc algorithm [449] and restrictions are given by the 'seven golden rules' [235]. The single correct formula inside a 0.1 ppm window is marked. $[C_{10}H_{13}N_5O_8P]^-$ is additionally validated by the isotopic fine structure of the ^{15}N, ^{13}C and ^{18}O isotopologue (beer measurement in red, prediction in blue) (B).

C Supplementary Chapter 3

Tables C

Table C.1 | Germination parameters, green malt extraction method, EBC-value quantification and analytical approach of the quantification of amino acids and saccharides.

Step	Parameters
Raw material	Barley (Hordeum vulgare) variety Accordine
Germination	5h at 14°C (1st wetstep), 19h at 14°C (1st drystep), 4h at 14°C (2nd wetstep), 20h at 14°C (2nd drystep), 72h at 14°C with continuous flow-through of conditioned air (germination)
Green malt extraction	100g of green malt + 400 ml H_2O, 1h at 20°C, stirring
Amino acid quantification	RP-HPLC-Fluorescence after precolumn-derivatisation with o-phthaldialdehyde [450]
Saccharide quantification	RP-HPLC-ELSD [450,451]
EBC-value-range	Samples with the lowest and highest absorption at 294 nm were analyzed as described in Jacob [451] (WBBM 2.12.1). Low value of 4.10 and high value of 146.00.

Table C.2 | Quantification of amino acids and sugars. Biological triplicates, technical duplicates arithmetic mean and standard deviation and standard's vendor. The amino acid proline was not quantified as it is not accessible for o-phthaldialdehyde derivatization.

Analyte	Biological Replicate 1		BR 2		BR 3		Mean	Stdev	Purity	Vendor
	Technical Replicate 1.1	TR 1.2	TR 2.1	TR 2.2	TR 3.1	TR 3.2				
Asp [a] [mg/100 mL]	13.9	12.9	12.9	11.8	9.2	9.7	11.7	1.9	>98 %	Sigma Aldrich [c]
Glu [mg/100 mL]	4.7	5.6	5.2	3.6	6.0	3.2	4.7	1.1	>99 %	Sigma Aldrich
Asn [mg/100 mL]	13.8	13.1	21.5	19.4	13.8	11.6	15.5	4.0	>99 %	Sigma Aldrich
Ser [mg/100 mL]	7.2	6.1	7.2	8.3	7.0	7.7	7.3	0.7	>99 %	Sigma Aldrich
Gln [mg/100 mL]	42.5	41.8	43.5	45.9	53.1	47.6	45.7	4.2	>98 %	Sigma Aldrich
His [mg/100 mL]	4.0	3.7	4.9	5.4	2.9	3.3	4.0	1.0	>98 %	Sigma Aldrich
Gly [mg/100 mL]	1.9	1.5	1.7	2.3	2.2	1.9	1.9	0.3	>99 %	Sigma Aldrich
Thr [mg/100 mL]	5.9	5.5	5.9	6.8	6.6	7.2	6.3	0.7	>98 %	Sigma Aldrich
Ala [mg/100 mL]	6.3	5.5	7.0	8.0	7.1	6.9	6.8	0.9	>99 %	Sigma Aldrich
Arg [mg/100 mL]	0.5	1.0	1.0	0.5	1.0	0.5	0.8	0.3	>98 %	Sigma Aldrich
GABA [mg/100 mL]	9.8	7.3	8.4	12.4	8.7	10.5	9.5	1.8	>99 %	Sigma Aldrich
Tyr [mg/100 mL]	6.0	5.8	6.2	7.5	4.6	4.9	5.8	1.0	>99 %	Sigma Aldrich
Val [mg/100 mL]	12.4	10.6	12.1	13.3	8.6	8.4	10.9	2.1	>98 %	Sigma Aldrich
Met [mg/100 mL]	2.4	2.4	2.6	3.1	1.2	1.6	2.2	0.7	>98 %	Sigma Aldrich
Ile [mg/100 mL]	7.4	6.8	7.6	8.5	4.4	4.6	6.5	1.7	>98 %	Sigma Aldrich
Trp [mg/100 mL]	3.5	3.5	2.6	3.2	2.4	2.4	2.9	0.5	>99 %	Sigma Aldrich
Phe [mg/100 mL]	10.1	9.2	10.0	11.7	9.6	10.0	10.1	0.9	>99 %	Sigma Aldrich
Leu [mg/100 mL]	11.4	9.4	10.9	12.7	12.3	12.4	11.5	1.3	>99 %	Sigma Aldrich
Lys [mg/100 mL]	5.0	4.3	4.5	5.3	4.8	5.7	4.9	0.5	>98 %	Sigma Aldrich
Fru [g/L]	1.0	1.2	1.0	1.1	0.8	1.0	1.0	0.1	>99 %	FLUKA [d]
Glc [g/L]	3.1	2.8	2.0	2.1	2.2	3.4	2.6	0.6	>99 %	Sigma Aldrich
Sac [g/L]	1.7	1.8	1.0	0.9	1.0	1.8	1.4	0.4	>99 %	Sigma Aldrich
Mal [g/L]	2.1	2.0	1.8	1.9	1.2	2.2	1.9	0.4	>99 %	Sigma Aldrich
Maltotriose [g/L]	bdl. [b]	bdl.	bdl.	bdl.	bdl.	bdl.	-	-	>98 %	Alfa Aesar [e]

[a] Aspartic acid was not included in the model system as it forms disrupting and suppressing clusters in DI-FT-ICR-MS.

[b] Detection limit of the method equals 50 mg/L. Therefore, maltotriose was not included in the model system.

[c] Sigma Aldrich (St Louis, MO, USA)

[d] FLUKA from Sigma Aldrich (St Louis, MO, USA)

[e] Alfa Aesar from Thermo Fisher Scientific

Table C.3 | Instrumental parameters and reagents used for FT-ICR-MS measurements.

Reagent	Parameters
Methanol (MeOH)	FLUKA, Sigma-Aldrich (LC-MS grade, CHROMASOLV, St Louis, MO, USA)
Acetonitrile (ACN)	FLUKA, Sigma-Aldrich (LC-MS grade, CHROMASOLV, St Louis, MO, USA)
Ultrapure water	Milli-Q Integral Water Purification System (Millipore, Billerica, MA, USA)
L-arginine	Sigma-Aldrich (reagent grade >98%, St Louis, MO, USA)
FT-ICR-MS	**Value**
Sample preparation	Degassing by ultrasonification (10 °C, 5min.); dilution 1:500 in methanol (v:v); separation of precipitated proteins by centrifugation (10,000 rmp, 3min.)
Direct-infusion flowrate	120 $\mu L.h^{-1}$.
ESI capillary voltage	3600 V
Time domain	4 mega words
Accumulation time	0.25 ms
Mass range	m/z 120 to 1000
Accumulated scans	400
Measurement time	10 min.
External calibration	Clusters of arginine (5 $mg.L^{-1}$ in methanol)
Internal calibration	in-house calibration list containing 2000 molecular formulae, which are highly abundant in beers (found in 33% of about 500 beers measured over the past years; data not shown)
QC sample	Heineken® lager beer from 2017 as an industrialized beer consistent sample, stored at -20°C

Table C.4 | UV-Vis absorption and positions of the beers samples and model system in the multivariate statistical models.

Sample	Absorption (294nm)	Scores							
		PCA (compositions)		OPLS (compositions)		PCA (mass differences)		OPLS (mass differences)	
		x	y	x	y	x	y	x	y
1	0.048	34.0	-8.2	-24.1	-26.6	-111.8	4.6	-64.5	-74.8
2	0.083	5.0	18.9	-21.8	8.9	23.6	12.7	-45.8	54.1
3	0.105	4.5	18.8	-18.5	7.9	11.4	13.6	-46.9	36.3
4	0.069	19.0	6.4	-16.4	-10.1	-39.5	28.2	-46.6	18.6
5	0.081	6.8	5.8	-16.9	1.7	27.8	6.2	-23.8	27.1
6	0.070	13.5	8.1	-16.9	-4.8	-4.8	20.1	-46.5	20.5
7	0.077	1.7	18.1	-11.5	8.3	33.5	18.4	-27.7	55.5
8	0.162	-1.7	25.7	-14.4	15.8	42.8	21.3	-56.6	81.9
9	0.140	13.2	11.9	-18.3	-1.3	-6.6	6.7	-50.2	33.1
10	0.168	38.3	-5.2	-12.0	-33.3	-170.5	9.1	-31.0	-128.6
11	0.170	-4.4	17.8	-7.5	13.4	69.1	5.8	-34.8	80.6
12	0.143	15.3	0.4	-10.3	-11.1	-13.2	-8.5	-49.3	5.5
13	0.067	30.5	1.1	-13.1	-24.3	-122.0	9.9	-25.2	-82.7
14	0.053	17.2	9.2	-13.2	-10.1	-42.3	9.1	-38.8	-15.3
15	0.135	32.9	-2.0	-7.2	-29.4	-166.3	14.5	-10.3	-126.7
16	0.173	25.7	-7.0	1.2	-26.6	-90.9	8.5	-4.5	-77.7
17	0.136	14.2	5.2	-16.0	-7.5	-10.0	7.1	-29.6	0.2
18	0.149	39.0	-7.0	-9.3	-35.6	-167.5	5.3	-42.2	-136.4
19	0.144	45.2	-10.6	-9.1	-43.0	-274.5	2.5	-31.0	-227.0
20	0.138	42.2	-7.4	-7.8	-39.3	-270.6	13.3	-23.4	-203.0
21	0.298	33.7	-0.3	0.1	-30.9	-155.9	29.0	-48.2	-86.3
22	0.267	38.0	-11.8	6.3	-41.2	-186.4	-34.2	41.4	-215.4
23	0.200	33.4	-13.2	-3.2	-34.0	-133.5	-17.5	-10.5	-142.4
24	0.356	6.4	-6.1	18.0	-13.5	19.5	-19.1	41.2	-31.6
25	0.142	35.7	-0.9	-12.2	-29.1	-175.9	6.7	-44.5	-128.1
26	0.243	47.2	-14.4	-4.5	-48.0	-286.2	-9.6	-11.8	-264.2
27	0.224	38.1	-11.8	-1.7	-39.8	-191.9	-23.4	-23.6	-207.8
28	0.138	41.1	-5.7	-7.3	-38.1	-256.9	7.9	-25.0	-203.4
29	0.127	13.5	-4.2	-0.6	-14.5	-39.0	1.8	-12.3	-32.5

Table C.4 (continued) | UV-Vis absorption and positions of the beers samples and model system in the multivariate statistical models.

Sample	Absorption (294nm)	Scores PCA (compositions) x	PCA (compositions) y	OPLS (compositions) x	OPLS (compositions) y	PCA (mass differences) x	PCA (mass differences) y	OPLS (mass differences) x	OPLS (mass differences) y
30	0.264	-4.1	0.3	1.6	2.2	49.0	3.0	32.7	24.5
31	0.074	25.2	-6.6	-16.6	-21.9	-81.3	4.1	-28.6	-65.3
32	0.136	-3.1	18.1	-15.4	12.0	28.4	20.7	-39.8	58.2
33	0.126	25.6	0.3	-12.6	-20.9	-102.7	12.5	-37.8	-66.3
34	0.420	-31.0	-11.8	29.2	14.9	116.3	-17.6	64.3	46.9
35	0.124	23.3	-5.3	-6.4	-22.3	-45.5	-6.5	-3.2	-63.3
36	0.145	26.5	1.0	-8.3	-22.2	-113.1	19.1	-34.5	-70.6
37	0.268	27.2	-9.1	8.2	-30.8	-89.8	-16.1	-0.4	-110.3
38	0.139	25.1	-8.4	-8.6	-25.1	-101.7	-20.0	-24.5	-107.3
39	0.151	53.6	-17.5	-10.3	-52.3	-343.5	-27.3	-21.0	-319.8
40	0.129	24.9	0.4	-9.7	-21.1	-92.5	15.8	-37.2	-52.1
41	0.122	34.9	-2.7	-12.8	-29.5	-140.4	2.7	-33.6	-110.1
42	0.130	24.2	-1.6	-12.0	-20.6	-54.7	1.7	-19.2	-53.2
43	0.099	52.0	-17.9	-13.0	-50.2	-360.6	-39.8	-14.8	-343.9
44	0.113	53.9	-20.9	-12.5	-53.3	-331.5	-73.6	-10.4	-386.6
45	0.399	26.7	-18.9	16.4	-36.3	-92.7	-48.7	47.5	-185.3
46	0.203	39.0	-5.6	-5.7	-36.7	-157.5	-29.3	-7.5	-165.3
47	0.121	25.2	5.1	-14.9	-15.4	-72.4	5.5	-56.1	-28.2
48	0.197	19.7	4.2	-9.5	-13.1	-39.0	19.9	-43.7	-8.3
49	0.149	20.4	1.0	-8.9	-16.8	-56.6	10.1	-32.9	-40.4
50	0.187	46.7	-18.1	-4.2	-50.1	-292.1	-59.4	-40.2	-313.2
51	0.169	6.1	3.3	-14.3	-1.0	24.7	7.4	-22.5	24.7
52	0.421	-13.4	3.5	23.7	4.7	76.3	-14.9	25.2	37.4
53	0.156	25.2	-0.8	-13.8	-20.4	-86.6	13.4	-26.3	-62.4
54	0.282	-10.2	14.1	7.7	9.4	69.0	-3.9	-10.0	57.0
55	0.191	35.5	-16.3	-5.1	-37.1	-127.1	-56.5	16.1	-179.4
56	0.174	12.5	4.8	-6.6	-9.5	-10.3	3.1	-26.1	0.5
57	0.296	10.4	2.6	7.3	-11.9	-13.5	14.3	3.2	1.7
58	0.330	30.8	-17.0	14.9	-39.5	-140.1	-20.3	29.3	-155.8
59	0.167	16.3	0.9	-8.9	-13.1	-8.4	-5.2	-23.8	-22.7
60	0.218	21.2	-17.2	13.4	-29.8	-54.5	-39.3	55.7	-140.6
61	0.095	15.2	3.8	-10.9	-11.1	-35.6	10.3	-25.1	-15.9
62	0.048	23.8	5.9	-15.8	-16.2	-74.6	15.9	-25.5	-42.1

Table C.4 (continued) | UV-Vis absorption and positions of the beers samples and model system in the multivariate statistical models.

Sample	Absorption (294nm)	Scores							
		PCA (compositions)		OPLS (compositions)		PCA (mass differences)		OPLS (mass differences)	
		x	y	x	y	x	y	x	y
63	0.108	40.4	-6.9	-17.1	-34.7	-196.8	8.3	-39.6	-146.4
64	0.279	23.2	-6.1	-0.7	-24.1	-58.7	0.6	-34.7	-56.9
65	0.275	15.5	-1.4	6.5	-18.1	-7.2	-24.5	-1.4	-38.5
66	0.178	22.7	1.9	-5.6	-19.9	-46.2	-7.3	-20.1	-45.5
67	0.112	39.7	-4.2	-10.8	-34.3	-192.7	-0.1	-30.4	-153.2
68	0.222	32.9	-6.8	0.2	-33.8	-121.5	-44.8	10.8	-156.7
69	0.243	22.8	-5.4	1.7	-23.6	-33.2	-25.0	1.4	-69.6
70	0.477	23.1	-13.4	22.0	-31.7	-69.3	-37.6	37.8	-136.6
71	0.238	31.0	0.9	-4.6	-28.1	-119.8	-11.7	-42.7	-105.9
72	0.904	24.3	-19.1	33.6	-38.8	-93.1	-53.2	104.8	-192.9
73	0.297	36.1	-12.4	7.5	-39.5	-170.6	-8.4	-9.2	-157.2
74	0.136	17.9	-9.2	-9.9	-11.6	-50.5	-32.0	-22.2	-70.6
75	0.099	-66.4	46.4	-13.0	88.2	161.5	24.8	-14.8	174.0
76	0.063	-59.0	45.3	-13.0	81.0	160.3	23.7	-16.1	176.3
77	0.232	-107.0	22.6	3.8	108.9	214.1	4.1	27.4	184.1
78	0.134	-76.0	51.3	-12.9	95.4	164.1	20.1	-24.0	175.3
79	0.086	-42.2	34.7	-20.5	62.8	137.5	26.4	-41.1	171.1
80	0.160	-74.5	58.2	-2.6	93.5	159.5	17.5	-3.9	154.0
81	0.100	-43.2	33.3	-11.5	58.6	129.1	19.2	-17.4	140.9
82	0.137	-95.1	55.2	-21.3	111.8	193.7	12.7	9.0	183.0
83	0.189	-85.1	30.3	-16.6	90.9	183.6	1.6	-1.1	164.5
84	0.116	-20.7	22.3	-25.5	33.9	86.1	13.0	-28.3	98.6
85	0.104	-20.7	35.1	-20.3	40.6	71.0	24.7	-14.7	103.5
86	0.121	-4.9	10.8	-16.8	13.5	36.0	7.7	-17.8	45.6
87	0.360	-51.0	-22.3	28.1	30.5	142.6	-26.5	59.7	68.7
88	0.192	-23.2	20.5	-4.2	29.9	96.8	8.7	-21.8	99.7
89	0.107	-12.0	13.2	-21.6	22.1	65.3	20.8	-35.4	100.3
90	0.368	-32.9	-25.5	33.7	8.2	109.2	-34.1	67.0	36.0
91	0.204	-36.0	22.0	-5.9	40.1	133.1	-1.4	-3.6	112.8
92	0.134	-38.9	35.5	-17.6	54.8	110.9	26.1	-29.4	135.8
93	0.219	-21.8	20.1	-2.8	25.9	108.9	-4.5	-8.0	89.0
94	0.167	-31.9	17.9	-4.6	34.7	114.2	1.1	-9.2	97.4
95	0.127	7.5	11.2	-15.8	2.0	-26.0	31.8	-32.4	26.2

Table C.4 (continued) | UV-Vis absorption and positions of the beers samples and model system in the multivariate statistical models.

Sample	Absorption (294nm)	Scores PCA (compositions)		OPLS (compositions)		PCA (mass differences)		OPLS (mass differences)	
		x	y	x	y	x	y	x	y
96	0.136	-1.9	1.1	-13.8	4.7	29.9	5.7	-34.1	37.6
97	0.238	-0.7	5.3	1.5	1.6	29.9	7.2	-5.6	33.9
98	0.167	-9.7	13.3	-6.5	13.3	50.3	9.8	-1.5	46.3
99	0.709	-43.3	-33.1	62.4	7.0	131.5	-44.3	99.2	30.8
100	0.170	5.5	9.4	-6.8	-1.2	-9.5	15.5	-14.3	7.5
101	0.132	-1.1	7.7	-9.4	4.7	30.6	1.1	-15.4	37.3
102	0.418	-33.2	-33.7	43.2	2.7	96.9	-42.9	124.9	-8.6
103	0.276	-4.1	7.8	6.3	4.5	48.0	18.8	-13.0	72.9
104	0.334	-62.6	-6.0	21.4	49.1	195.8	-10.2	50.0	149.8
105	0.657	-108.7	-52.5	58.3	61.9	225.8	-13.9	104.0	150.8
106	0.197	16.8	-15.3	-5.9	-16.8	-12.8	-27.8	-14.2	-27.4
107	0.353	-6.2	-24.6	25.1	-12.4	33.5	-48.0	78.2	-36.8
108	0.144	9.9	-0.4	-9.9	-7.2	-2.5	-6.5	-34.3	11.8
109	0.183	-0.6	-4.3	0.8	-3.2	14.3	-8.3	-4.2	6.8
110	0.187	-1.6	4.9	-7.9	2.8	25.7	1.1	-22.7	28.2
111	0.187	-14.9	9.7	4.4	16.7	66.2	20.1	-2.1	81.2
112	0.095	4.6	13.3	-16.3	11.4	14.8	19.1	-51.6	57.9
113	0.076	10.5	4.6	-24.1	2.3	-3.0	6.0	-46.6	33.8
114	0.128	-38.0	21.6	-12.7	50.3	120.4	24.7	-25.7	138.5
115	0.288	-32.1	6.4	13.3	30.2	109.9	-5.0	40.5	69.9
116	0.409	-60.9	-10.3	28.8	47.5	172.1	-9.4	56.4	111.6
117	0.177	-2.6	-2.3	8.3	0.4	56.3	0.4	41.1	26.6
118	0.137	4.6	21.2	-9.8	9.2	-56.5	22.9	-32.2	-15.5
119	0.086	25.0	4.7	-13.7	-16.9	-91.7	21.9	-28.0	-42.9
120	0.102	20.0	3.3	-9.3	-13.9	-77.8	33.9	-25.7	-19.2
121	0.095	17.4	11.6	-16.9	-6.5	-52.1	21.1	-29.1	-4.7
122	0.326	-23.8	-3.2	18.9	15.2	109.3	-11.1	47.2	56.5
123	0.153	2.6	11.8	-9.8	4.6	16.0	14.3	-29.4	39.1
124	0.190	22.5	-5.5	-1.4	-23.6	-97.9	1.5	-23.1	-75.8
125	0.189	21.2	-6.2	-0.2	-21.9	-87.9	16.1	-30.0	-46.5
126	0.118	12.0	-6.4	-8.0	-13.5	-21.3	-1.6	-18.5	-30.7
127	0.147	5.0	4.3	-10.2	1.4	13.8	15.2	-40.3	49.5
128	0.146	18.1	6.7	-9.4	-10.2	-69.8	26.2	-35.8	-21.2

Table C.4 (continued) | UV-Vis absorption and positions of the beers samples and model system in the multivariate statistical models.

Sample	Absorption (294nm)	Scores							
		PCA (compositions)		OPLS (compositions)		PCA (mass differences)		OPLS (mass differences)	
		x	y	x	y	x	y	x	y
129	0.349	-13.1	2.7	7.4	10.1	59.1	6.9	3.9	45.7
130	0.287	14.5	-11.7	10.8	-21.3	-44.3	-6.4	25.5	-55.0
131	0.184	7.0	9.3	-9.3	0.2	0.8	26.9	-22.2	38.7
132	0.123	-51.3	42.3	-20.2	70.2	146.7	23.8	-36.5	167.8
133	0.118	-29.7	18.0	-9.7	37.3	125.8	16.5	-26.4	139.6
134	0.120	-28.3	35.0	-8.9	44.4	96.7	31.3	-15.8	122.0
135	0.112	18.3	9.0	-16.6	-4.9	-40.5	29.8	-48.0	30.4
136	0.115	23.2	0.6	-13.1	-14.9	-76.9	18.7	-44.4	-7.9
137	0.137	-13.5	24.7	-14.5	28.6	95.6	21.1	-41.4	126.5
138	0.126	4.3	13.1	-15.2	8.7	10.7	40.3	-51.7	82.4
139	0.124	15.9	6.3	-15.0	-3.7	-29.1	33.0	-56.3	53.9
140	0.114	15.4	7.9	-12.1	-6.1	-37.8	20.7	-36.3	19.9
141	0.132	21.4	5.7	-16.2	-10.3	-61.5	34.1	-56.1	21.2
142	0.088	29.2	2.5	-14.9	-21.3	-135.7	41.2	-29.9	-49.1
143	0.088	11.2	15.0	-16.5	0.4	-41.9	46.2	-19.6	23.8
144	0.089	30.8	-2.1	-12.7	-24.5	-151.0	24.7	-17.6	-83.0
145	0.084	16.9	7.1	-17.6	-7.0	-63.1	38.2	-34.6	9.0
146	0.153	-24.1	16.2	-1.8	25.5	118.0	-2.4	-8.0	96.0
147	0.103	28.4	1.7	-10.6	-23.0	-115.6	29.8	-32.4	-50.5
148	0.172	27.0	-7.0	-1.7	-27.5	-82.3	-24.1	20.6	-107.7
149	0.331	-30.0	-9.3	23.6	13.8	127.3	-28.1	53.2	59.4
150	0.108	29.4	0.2	-17.0	-21.9	-113.7	14.6	-45.3	-59.6
151	0.123	31.0	-4.2	-8.0	-28.1	-149.2	27.3	1.3	-93.8
152	0.188	15.9	-5.7	-3.2	-16.0	-49.1	20.7	-58.4	-0.6
153	0.177	29.4	-1.2	-10.9	-24.6	-122.9	28.5	-37.9	-53.1
154	0.183	-67.8	14.3	-15.1	69.1	176.7	-16.8	13.4	130.3
155	0.096	-14.8	21.2	-15.7	27.1	69.8	27.3	-27.7	99.9
156	0.110	-16.7	21.1	-13.4	28.0	71.3	21.4	-30.7	103.0
157	0.536	-115.9	-49.1	41.0	87.9	220.7	-13.1	74.3	154.9
158	0.193	-49.4	21.2	-11.3	51.8	142.1	-13.3	3.1	108.8
159	0.207	-42.6	17.4	0.1	42.6	147.5	-10.0	2.0	118.1
160	0.129	3.1	10.4	-9.2	4.4	2.8	18.7	-14.6	30.6
161	0.184	-0.2	7.7	-6.6	4.1	38.7	12.5	-19.7	55.5

Table C.4 (continued) | UV-Vis absorption and positions of the beers samples and model system in the multivariate statistical models.

Sample	Absorption (294nm)	Scores PCA (compositions)		OPLS (compositions)		PCA (mass differences)		OPLS (mass differences)	
		x	y	x	y	x	y	x	y
162	0.135	-15.4	25.9	-12.0	29.2	71.7	31.7	-36.0	114.6
163	0.121	-90.6	-33.4	-15.7	76.7	202.1	-12.0	60.4	138.1
164	0.525	-112.6	-59.5	39.1	70.5	231.8	-24.4	107.4	135.0
165	0.196	-3.6	6.4	-8.5	6.6	63.2	-12.5	7.4	45.8
166	0.262	-21.6	7.3	6.5	20.7	99.2	8.9	8.9	90.7
167	0.152	5.4	-0.4	-18.1	-0.3	21.2	7.6	-12.9	26.1
168	0.098	-3.6	25.6	-16.9	19.1	43.9	35.9	-36.5	98.4
169	0.155	-6.3	8.9	-11.7	9.3	51.1	-9.0	-7.1	41.7
170	0.168	-23.6	23.8	-6.4	32.8	85.1	16.8	-12.8	99.5
171	0.108	8.5	10.1	-12.9	0.7	0.4	26.1	-23.7	49.0
172	0.127	7.5	14.1	-13.2	3.6	19.4	36.9	-46.1	85.0
173	0.966	-71.3	-68.9	105.3	9.9	175.8	-46.5	161.1	51.8
174	0.781	-86.9	-131.5	70.6	6.8	168.2	-50.6	175.2	39.1
175	0.163	12.1	7.0	-8.0	-6.6	-30.4	8.2	9.3	-16.1
176	0.193	-17.0	7.5	-3.0	17.6	103.2	-1.4	-15.1	100.2
177	0.890	-60.5	-112.1	91.2	-15.8	144.2	-50.2	187.6	7.0
178	0.155	-12.8	20.4	-9.9	22.3	85.0	17.5	-38.2	115.4
179	0.145	-3.2	18.0	-6.8	15.7	44.3	29.3	-24.0	92.7
180	0.168	5.4	7.9	-5.2	-0.5	19.0	11.3	-29.0	35.9
181	0.185	-38.9	24.7	-1.1	44.1	134.8	16.3	-16.6	142.1
182	0.157	-34.1	23.5	-6.1	40.6	120.2	6.0	1.4	107.1
183	0.249	-12.8	0.0	3.9	11.5	90.9	-10.6	20.2	48.0
184	0.134	-2.4	9.7	-10.3	6.9	71.9	-6.2	-31.7	72.8
185	0.270	-2.5	9.6	-9.5	6.7	71.7	-6.3	-31.5	72.5
186	0.208	-23.5	20.6	2.1	26.6	104.1	3.5	5.3	87.7
187	0.132	-19.1	10.9	-11.8	22.0	114.7	-11.6	-2.7	82.3
188	0.114	-9.1	15.2	-8.1	17.8	60.9	19.3	-25.5	94.5
189	0.569	-39.4	-8.4	48.5	21.3	131.4	-11.2	88.8	70.8
190	0.211	-13.7	17.1	1.7	20.0	78.0	16.3	-6.0	86.6
191	0.225	38.9	-19.9	-1.1	-39.5	-195.2	-39.0	4.8	-203.5
192	0.238	-25.3	12.1	9.0	24.3	103.8	-2.8	29.1	73.6
193	0.207	-15.0	-4.6	0.6	11.4	81.9	-5.4	38.9	47.4
194	0.140	7.3	10.6	-9.1	1.0	1.7	27.8	-42.2	49.4

Table C.4 (continued) | UV-Vis absorption and positions of the beers samples and model system in the multivariate statistical models.

Sample	Absorption (294nm)	Scores							
		PCA (compositions)		OPLS (compositions)		PCA (mass differences)		OPLS (mass differences)	
		x	y	x	y	x	y	x	y
195	0.158	19.5	1.6	-9.7	-13.1	-73.4	14.4	-33.0	-27.6
196	0.143	16.3	7.6	-9.2	-9.0	-43.6	27.5	-24.3	8.3
197	0.096	23.9	3.3	-11.0	-10.6	-76.0	25.3	-39.9	6.6
198	0.193	0.6	15.2	-0.7	5.9	16.7	19.3	-5.2	39.6
199	0.387	2.3	1.0	15.0	-5.5	24.7	0.5	44.7	0.8
200	0.330	-69.1	-12.0	13.7	58.5	181.7	-5.4	39.5	141.3
201	0.167	34.8	-19.2	-2.7	-36.2	-140.8	-50.4	27.1	-191.9
202	0.166	16.9	10.3	-14.3	-7.4	-51.9	22.3	-34.7	-3.9
203	0.133	3.6	21.6	-11.4	11.6	21.1	22.5	-35.0	75.0
204	0.145	-0.7	18.6	-14.1	9.9	19.6	27.0	-26.7	55.1
205	0.115	29.5	3.1	-18.3	-19.9	-119.9	14.5	-26.1	-68.9
206	0.129	12.5	12.2	-15.4	-2.1	-34.6	31.1	-33.5	22.8
207	0.186	22.6	1.0	-9.5	-17.7	-90.6	23.0	-14.5	-44.4
208	0.111	38.2	-4.8	-13.2	-32.9	-203.0	5.4	-22.2	-141.7
209	0.172	15.8	5.0	-10.4	-9.2	-21.8	22.2	-42.9	30.8
210	0.158	19.3	-3.8	-11.4	-16.1	-45.2	4.7	-34.7	-26.1
211	0.180	6.6	0.7	-5.3	-4.7	18.1	10.8	6.2	22.5
212	0.129	21.7	6.9	-16.5	-11.3	-58.9	27.9	-49.4	9.0
213	0.137	12.7	-1.1	-14.7	-9.2	17.9	12.3	-43.3	40.7
214	0.122	29.4	-6.5	-6.4	-27.9	-84.3	-2.4	-12.8	-60.4
215	0.159	24.9	-9.2	-8.5	-24.6	-68.4	8.6	-46.7	-44.5
216	0.137	30.7	-6.5	-15.2	-26.2	-118.3	25.2	-49.7	-52.8
217	0.156	28.6	-4.1	-13.6	-22.0	-95.3	24.3	-35.0	-35.9
218	0.185	20.7	-6.9	-9.7	-19.4	-37.5	8.3	-20.9	-24.3
219	0.235	16.0	-17.1	5.5	-23.5	-19.8	-16.6	7.2	-62.6
220	0.177	25.9	-1.3	-8.6	-21.9	-73.7	-4.6	-4.6	-65.1
221	0.167	16.3	1.4	-5.4	-13.5	-34.6	8.7	-23.7	-9.1
222	0.358	3.8	-3.3	10.9	-5.4	13.7	-7.8	13.8	-7.0
223	0.139	16.5	8.4	-14.2	-5.6	-16.0	34.5	-32.4	56.9
224	0.386	-24.2	-28.4	32.4	-0.4	110.7	-35.2	96.4	29.6
225	0.222	20.2	-14.1	7.0	-27.5	-49.8	-25.9	33.1	-70.2
226	0.160	8.3	3.4	-4.0	-4.6	0.8	21.2	-22.8	33.7
227	0.169	9.1	-7.9	2.5	-12.3	4.2	-6.5	0.4	-1.0

Table C.4 (continued) | UV-Vis absorption and positions of the beers samples and model system in the multivariate statistical models.

Sample	Absorption (294nm)	Scores							
		PCA (compositions)		OPLS (compositions)		PCA (mass differences)		OPLS (mass differences)	
		x	y	x	y	x	y	x	y
228	0.130	7.1	7.9	-13.6	0.6	13.7	18.4	-22.3	51.7
229	0.270	-22.3	-1.5	14.0	16.6	106.3	0.6	29.1	83.0
230	0.252	-33.2	-22.1	26.3	14.5	129.9	-21.3	75.1	61.6
231	0.627	6.1	-30.0	46.8	-31.5	31.0	-49.6	113.9	-66.2
232	0.709	-26.8	-22.8	59.3	-2.1	111.4	-37.6	109.1	25.7
233	0.460	1.1	-14.4	30.9	-16.2	46.6	-57.3	79.0	-65.2
234	0.391	28.2	-17.5	17.7	-38.6	-78.9	-52.0	91.3	-153.2
235	0.247	-4.5	-3.6	13.4	-3.7	71.9	-19.2	36.6	16.4
236	0.685	-2.9	-28.0	47.9	-22.8	50.0	-53.2	118.6	-50.0
237	0.456	-17.4	-34.0	46.8	-12.2	90.7	-47.7	124.5	-12.5
238	0.457	12.4	-20.9	31.7	-28.9	-16.1	-49.6	106.5	-105.7
239	0.367	-35.1	-11.3	31.7	14.6	145.4	-20.2	78.1	72.6
240	0.435	17.3	-20.3	25.0	-31.8	-52.2	-53.8	71.9	-138.4
241	0.613	-33.9	-10.8	52.3	11.3	129.1	-25.0	107.4	43.5
242	0.537	-23.2	-5.8	38.1	7.8	126.3	-19.6	43.4	75.6
243	0.687	-42.9	-53.3	70.0	-4.3	147.6	-46.2	123.7	31.8
244	0.432	-44.5	-42.4	33.0	13.0	151.3	-33.1	93.8	79.0
245	0.804	3.1	-23.2	50.2	-26.5	37.7	-40.6	125.7	-65.3
246	0.196	27.4	-7.2	3.7	-30.3	-66.6	-19.9	7.4	-95.8
247	0.180	12.3	6.9	-6.4	-6.3	-4.8	12.8	-3.1	14.3
248	0.393	32.0	-25.1	22.4	-46.8	-128.7	-82.2	118.3	-241.1
249	0.466	12.9	-18.1	30.5	-28.3	18.4	-33.2	109.3	-62.9
250	0.679	-54.9	-42.7	66.5	11.2	161.6	-32.3	129.3	60.5
MR	0.395	-	-	216.1	32.2	-	-	474.4	-139.0

Table C.5 | Statistical parameters of the multivariate data analysis.

Statistical model	R2Y	R2X	Q2	ANOVA
PCA (compositions)	0.619	-	0.239	-
OPLS (compositions)	0.928	0.261	0.794	<< 0.05
PCA (mass differences)	0.974	-	0.959	-
OPLS (mass differences)	0.974	0.293	0.811	<< 0.05

Table C.6 | Typical MR intermediate phase reactions and their respective mass differences and molecular formulae.

Reaction	Mass difference	Molecular formula
(De)amination (Strecker)	(-)1.03163	$H_{-3}O_1N_{-1}$
(De)hydrogenation	(-)2.01565	$-H_2/H_2$
Ammonia elimination	-17.02655	$-NH_3$
(De)hydration	(-)18.01065	$-H_2O/H_2O$
Oxidation	31.98983	O_2
Decarboxylation	-43.98983	$-CO_2$
Acetaldehyde	(-)44.02622	$-C_2H_4O/C_2H_4O$
Glyoxal	(-)58.00548	$-C_2H_2O_2/C_2H_2O_2$
Methylglyoxal	(-)72.02113	$-C_3H_4O_2/C_3H_4O_2$
Diacetyl	(-)86.03678	$-C_4H_6O_2/C_4H_6O_2$
Hexose	(-)162.05283	$-C_6H_{10}O_5/C_6H_{10}O_5$

Figures C

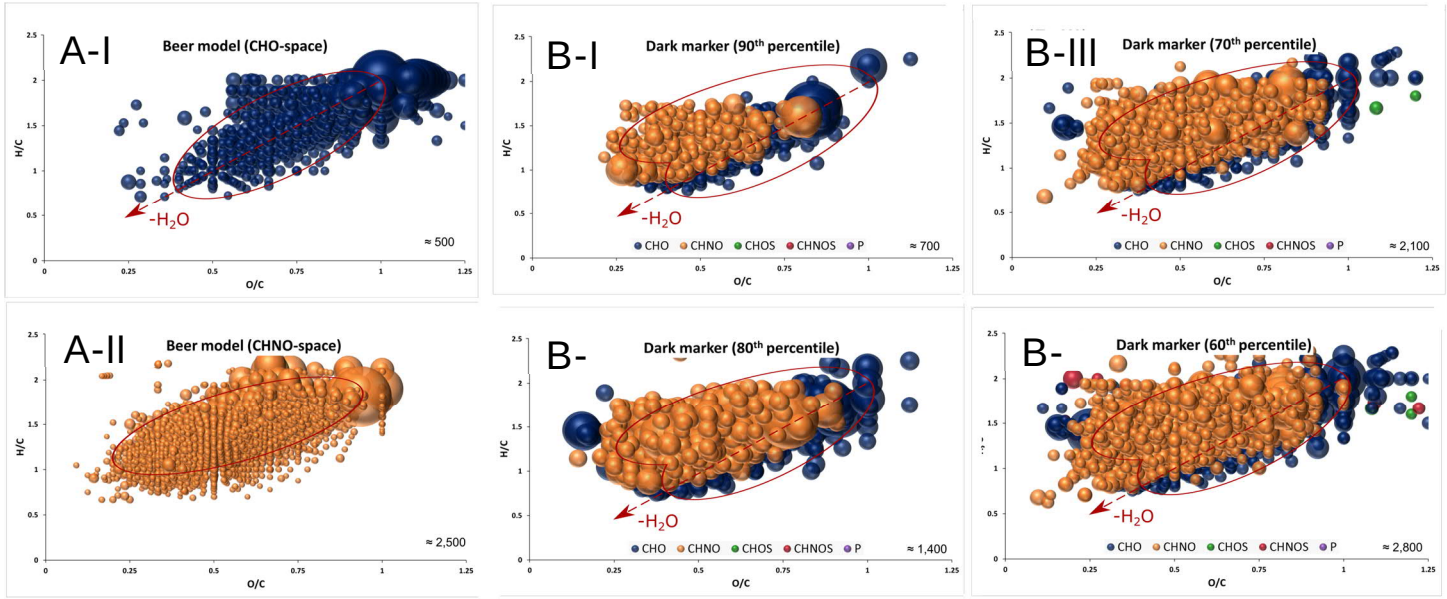

Figure C.1 | Van Krevelen diagram of molecular formula annotations found in the model system (A) and marker formula found in beer (B). Model annotations are divided in the CHO (A-I) and CHNO (A-II) chemical space. The van Krevelen diagram of marker formula annotations (B) is divided into steps of 10-percentiles (I-IV). Color code: CHO blue; CHNO orange; CHOS green; CHNOS red; P purple. Neutral molecular formulae are plotted. The bubble size indicates the mean relative intensities of corresponding peaks in the spectra. The characteristic pattern of compounds derived from the MR is marked in red and can be recognized to the 60th percentile. The line that houses compositions that differ by H_2O is indicated.

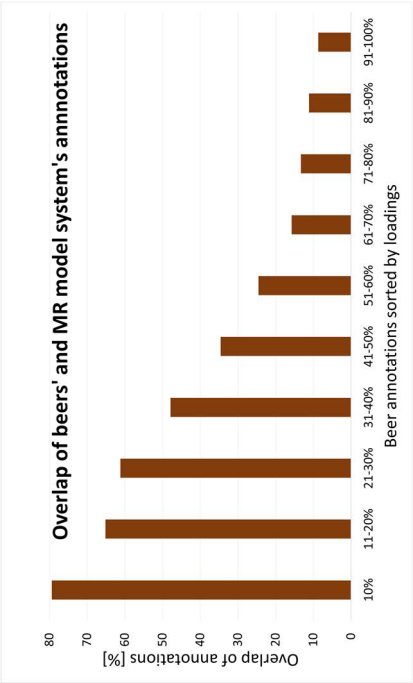

Figure C.2 | Overlap of the annotations found in beer samples and the annotations of the MR model system. Sorted by loadings of the OPLS model and itemized in 10 % sections.

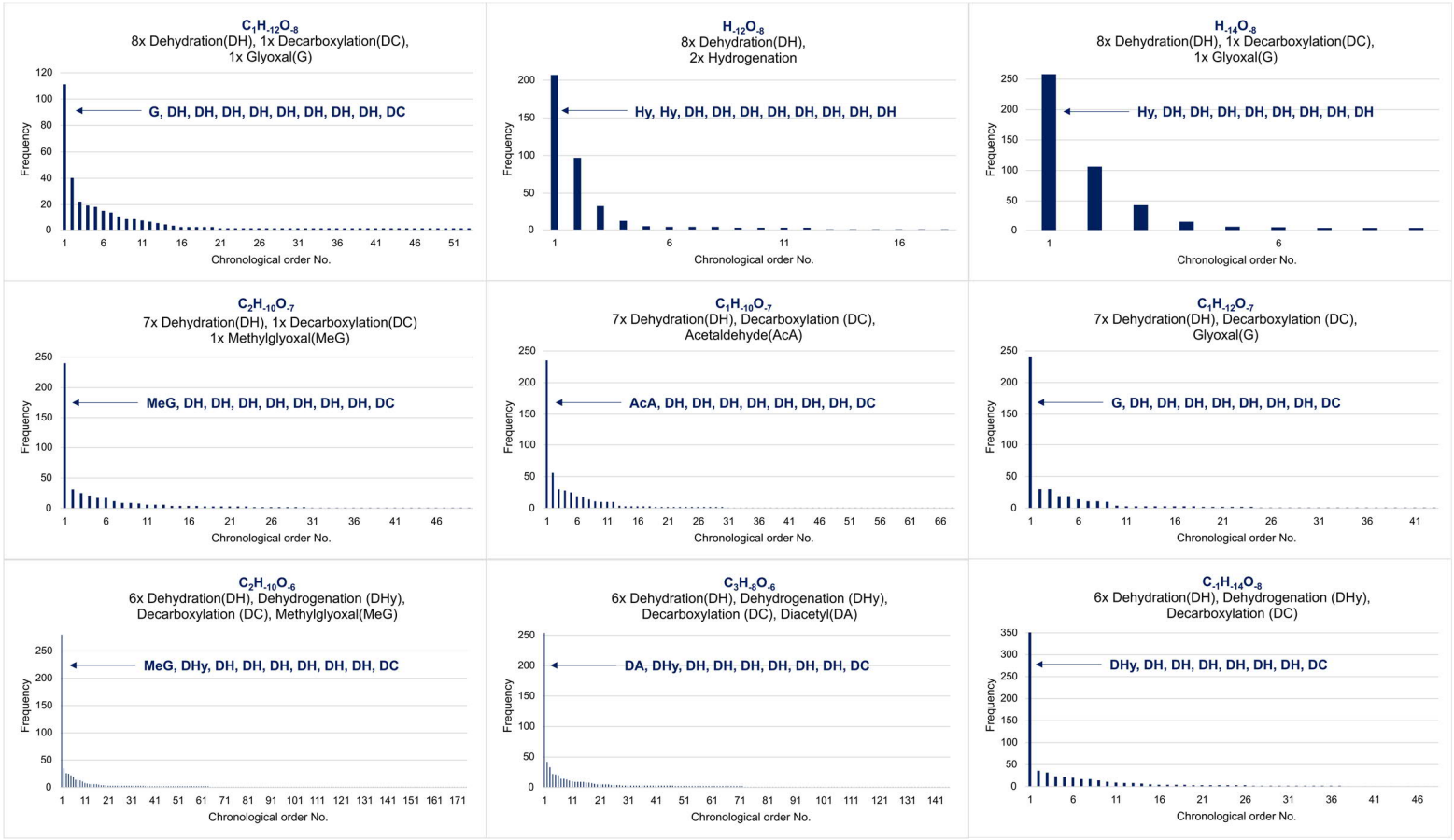

Figure C.3 | Frequency distribution of the different reaction sequences building up the statistically significant mass differences. For each of the mass differences, a dominant reaction sequence could be observed.

D Supplementary Chapter 4

Tables D

Table D.1 | Carbohydrate source and positions of the beer samples in the multivariate statistical models.

Sample	Starch source [a]	OPLS scores						Sample	Starch source	OPLS scores					
		DI-FT-ICR-MS components			UHPLC-ToF components					DI-FT-ICR-MS components			UHPLC-ToF components		
		1st	2nd	3rd	1st	2nd	3rd			1st	2nd	3rd	1st	2nd	3rd
1	W	-10.17	-15.51	-2.89	-	-	-	231	C	-18.73	14.39	-16.69	-	-	
2	B	12.52	3.04	-3.47	-	-	-	232	R	-11.69	11.14	12.47	-13.66	-0.16	
3	B	12.51	2.05	-3.08	-	-	-	233	B	15.53	4.47	-5.73	7.38	29.16	
4	B	6.82	3.37	-2.66	-	-	-	234	W	-4.74	-10.08	0.88	27.13	-15.15	
5	W	-9.66	-21.02	1.51	-	-	-	235	C	-20.27	10.05	-13.60	-	-	
6	W	-12.96	-19.25	1.08	27.39	-12.75	0.05	236	C	-24.31	12.45	-17.40	-12.69	-5.66	
7	W	-13.62	-15.55	-1.76	-	-	-	237	C	-22.00	13.69	-19.97	-15.62	-4.96	
8	B	12.91	4.77	-4.67	-	-	-	238	B	10.52	2.65	-4.97	-	-	
9	B	13.78	4.32	-4.56	-	-	-	239	R	-12.59	14.95	2.21	-6.62	-5.41	
10	B	13.24	0.79	1.53	-	-	-	241	R	-14.15	15.10	5.54	-13.13	-1.42	
11	W	-11.85	-15.11	-3.19	-	-	-	242	B	10.23	4.35	-3.22	-	-	
12	W	-6.94	-12.22	0.18	-	-	-	243	B	12.32	1.20	-3.64	-	-	
13	B	10.69	2.44	-1.17	-	-	-	244	B	9.94	-0.01	-4.07	-	-	
14	B	4.84	-1.02	-4.54	-	-	-	245	B	6.98	2.75	-1.56	-	-	
15	B	9.63	0.54	-2.98	-	-	-	246	B	11.09	2.66	-1.81	-	-	
16	B	13.28	-0.06	-1.19	-	-	-	247	B	4.44	2.31	-2.85	-	-	

Table D.1 (continued) | Carbohydrate source and positions of the beer samples in the multivariate statistical models.

Sample	Starch source [a]	OPLS scores						Sample	Starch source	OPLS scores					
		DI-FT-ICR-MS components			UHPLC-ToF components					DI-FT-ICR-MS components			UHPLC-ToF components		
		1st	2nd	3rd	1st	2nd	3rd			1st	2nd	3rd	1st	2nd	3rd
17	C	-	-	-	-8.71	1.66	-14.58	248	B	7.12	1.09	0.79	-	-	
18	B	9.44	4.01	-1.21	-	-	-	249	B	8.45	2.16	-2.83	-	-	
19	W	-8.94	-20.70	-1.25	-	-	-	250	W	-10.91	-15.63	-1.58	-	-	
20	W	-8.29	-13.93	-0.91	-	-	-	251	W	-4.11	-14.67	0.77	-	-	
21	W	-5.72	-11.01	-0.84	-	-	-	252	B	11.06	2.68	0.88	-0.25	16.35	
22	B	5.59	2.60	-1.54	-	-	-	253	W	-7.29	-21.55	3.42	-	-	
23	B	10.77	2.02	-1.73	-	-	-	254	B	1.65	3.04	1.81	-	-	
24	B	6.21	0.44	-0.81	-	-	-	255	W	-8.84	-14.53	0.45	-	-	
25	W	-8.52	-9.14	-0.51	-	-	-	256	W	-9.50	-11.05	-0.38	23.39	-6.41	
26	B	11.81	2.94	0.07	-	-	-	257	W	-7.11	-18.75	1.59	26.72	-12.49	
27	B	11.68	1.50	-0.93	-	-	-	258	W	-6.13	-16.23	3.18	23.75	-5.50	
28	W	-3.74	-10.63	-0.47	-	-	-	259	W	-5.89	-15.65	1.40	-	-	
29	W	-6.59	-16.52	2.29	-	-	-	260	B	6.65	-0.04	2.13	-	-	
30	B	7.55	0.96	-0.91	-	-	-	261	B	8.70	1.69	-0.05	-	-	
31	W	-5.18	-12.49	-0.94	-	-	-	262	B	8.90	3.73	-0.92	-	-	
32	B	1.61	2.12	-2.80	-	-	-	263	W	-14.09	-19.62	-0.87	-	-	
33	W	-8.42	-18.95	1.37	29.37	-8.02	0.55	264	C	-18.04	16.07	-13.07	-12.75	-7.06	
34	W	-8.56	-15.34	0.73	-	-	-	265	C	-18.25	15.63	-7.33	-	-	
35	B	11.10	1.40	-1.66	-	-	-	266	C	-19.50	10.38	-7.71	-7.04	-1.53	
36	B	11.28	-0.62	0.93	3.78	18.89	4.94	267	C	-22.09	13.46	-8.36	-	-	
37	B	11.82	0.07	-3.80	-	-	-	268	R	-3.17	10.93	9.68	-13.01	2.67	
38	W	-4.43	-14.77	0.92	-	-	-	269	C	-15.07	7.01	-7.50	-2.73	-2.25	
39	B	8.18	0.82	-2.30	0.72	22.17	-1.55	270	C	-18.38	11.25	-11.27	-10.04	-6.96	
40	B	15.51	5.52	-2.47	-	-	-	271	C	-13.62	8.49	-9.38	-7.67	-1.82	
41	W	-8.66	-15.30	-1.60	-	-	-	272	R	-13.05	15.52	6.69	-	-	
43	B	1.12	0.01	-1.47	-	-	-	273	B	9.04	1.41	-0.96	-	-	
44	B	10.74	-0.49	-0.77	-	-	-	274	R	-14.59	19.35	13.50	-6.33	-3.95	
45	W	-5.70	-16.65	0.41	-	-	-	275	C	-19.59	17.30	-4.08	-10.47	2.57	
46	B	4.31	-2.46	-1.22	-	-	-	276	C	-17.75	15.12	-15.38	-8.17	-3.43	
47	W	-1.26	-9.82	-1.79	-	-	-	277	C	-13.69	13.55	-9.19	-	-	
48	B	5.37	-0.88	0.19	-	-	-	278	B	4.31	2.80	2.08	-	-	
49	B	6.75	-0.21	0.41	-	-	-	279	B	2.03	5.58	-1.27	-	-	
50	B	11.93	4.27	-0.35	-	-	-	280	C	-16.13	12.93	-8.09	-	-	

Table D.1 (continued) | Carbohydrate source and positions of the beer samples in the multivariate statistical models.

Sam-ple	Starch source [a]	OPLS scores DI-FT-ICR-MS components 1st	2nd	3rd	UHPLC-ToF components 1st	2nd	3rd	Sam-ple	Starch source	OPLS scores DI-FT-ICR-MS components 1st	2nd	3rd	UHPLC-ToF components 1st	2nd	3rd
51	W	-11.96	-15.43	-0.48	32.21	-3.54	-0.86	281	B	8.57	1.49	0.65	-	-	
52	W	-10.10	-17.32	1.61	23.18	-16.85	1.09	282	B	11.96	3.77	-1.13	-	-	
53	B	10.06	2.68	-4.19	-	-	-	283	C	-8.18	11.86	-6.99	-	-	
54	B	1.92	-2.42	-0.51	-	-	-	284	B	6.75	2.50	-0.07	-	-	
55	W	-0.89	-12.12	0.45	-	-	-	285	C	-13.94	12.29	-10.30	-12.19	-1.67	
56	W	-7.74	-17.72	-2.61	-	-	-	286	B	8.14	2.27	2.19	-	-	
57	B	8.26	0.26	0.81	-	-	-	287	B	6.20	0.83	0.18	-	-	
58	W	-6.63	-16.50	0.35	-	-	-	288	B	2.87	0.95	-0.59	7.48	21.97	
59	B	3.16	0.01	-1.76	-	-	-	289	W	-13.96	-8.64	-2.65	-	-	
60	B	11.52	1.58	-1.34	-	-	-	290	W	-7.47	-12.76	4.01	-	-	
61	W	-3.40	-13.26	-2.84	-	-	-	291	B	4.15	1.00	1.80	-	-	
62	W	-9.37	-18.90	-2.35	-	-	-	292	B	10.22	2.35	1.84	-	-	
63	W	-8.04	-21.04	3.15	-	-	-	293	B	6.47	3.31	-1.90	2.28	19.01	
64	B	11.89	-1.60	1.09	-	-	-	294	B	6.19	2.17	1.11	8.50	20.45	
65	B	9.29	-0.12	0.73	-	-	-	295	B	4.80	1.29	0.87	-	-	
66	B	9.30	2.13	-0.63	-	-	-	296	C	-16.08	9.57	-6.27	-11.31	-6.81	
67	W	-6.47	-15.98	3.09	-	-	-	297	R	-	-	-	-11.43	-1.23	
68	B	5.74	0.03	-0.18	-	-	-	298	B	2.58	1.79	3.13	-	-	
69	W	-3.11	-11.65	0.29	12.73	-2.80	-1.55	299	W	-3.28	-9.13	1.20	-	-	
70	B	13.47	-0.21	0.69	-	-	-	300	B	9.72	2.18	-0.03	-	-	
71	B	7.36	3.29	1.51	5.70	26.70	1.50	301	B	13.75	2.65	3.39	-	-	
72	B	7.49	3.97	-1.99	-	-	-	302	B	2.10	5.39	-0.98	-	-	
73	B	6.77	-0.09	0.13	-	-	-	303	W	-7.36	-17.79	2.39	-	-	
76	W	-6.77	-17.28	0.80	-	-	-	304	B	15.52	3.11	-0.48	-	-	
78	B	8.18	1.00	3.24	-	-	-	305	W	-10.36	-18.80	2.24	-	-	
80	R	-6.24	10.88	6.59	-	-	-	306	B	9.92	4.81	3.83	-	-	
81	B	3.03	-1.42	0.85	-	-	-	307	R	-6.02	14.42	7.21	-7.62	-3.97	
83	B	7.43	0.08	0.52	-	-	-	308	W	-16.52	-19.82	7.12	-	-	
85	W	-2.96	-8.99	-0.42	-	-	-	309	R	-16.87	7.67	18.03	-12.54	-5.16	
86	B	11.70	-0.15	0.00	11.72	27.44	-0.79	310	B	8.56	1.59	2.23	-	-	
90	B	11.99	0.92	-5.30	-	-	-	311	R	-3.01	9.01	2.04	-9.40	-1.09	
91	B	11.55	2.63	-5.10	-	-	-	312	R	-1.14	8.32	3.64	-7.04	0.99	
92	B	10.77	1.89	-0.03	-	-	-	313	R	-5.85	13.48	2.55	-14.13	-0.69	
93	B	6.00	3.35	-2.48	-	-	-	314	W	-11.41	-22.25	-0.10	-	-	

Table D.1 (continued) | Carbohydrate source and positions of the beer samples in the multivariate statistical models.

Sam-ple	Starch source [a]	OPLS scores DI-FT-ICR-MS components 1st	2nd	3rd	UHPLC-ToF components 1st	2nd	3rd	Sam-ple	Starch source	OPLS scores DI-FT-ICR-MS components 1st	2nd	3rd	UHPLC-ToF components 1st	2nd	3rd
94	B	3.62	0.19	-1.35	-	-	-	315	B	11.94	1.34	-2.65	-	-	
95	?[b]	14.62	11.13	-2.73	-8.45	-5.69	-12.26	317	R	-14.49	15.44	5.75	-12.39	-5.66	
96	B	9.06	0.08	-2.87	-	-	-	318	R	-14.19	19.57	19.00	-	-	
97	C	-24.39	13.00	-14.70	-9.50	-1.96	0.40	319	C	-24.18	17.38	-18.15	-13.85	-4.52	
98	B	6.07	1.04	-2.13	-	-	-	320	C	-22.83	15.17	-9.88	-11.34	-10.16	
99	B	13.66	8.35	-0.52	-	-	-	321	R	-7.26	13.50	6.68	-4.63	1.92	
101	R	-18.30	18.25	26.14	-	-	-	322	R	-12.18	18.63	15.72	-9.45	-3.64	
102	W	-13.43	-19.55	1.58	-	-	-	323	C	-19.29	13.68	-15.29	-	-	
103	B	10.37	-1.35	-2.45	-	-	-	324	R	-19.93	21.34	13.25	-12.77	-1.50	
104	B	11.51	2.16	-6.88	-	-	-	325	R	-4.86	10.68	19.95	-9.04	-1.23	
105	W	-7.88	-17.88	-0.44	-	-	-	326	B	4.65	1.47	-3.18	-	-	
106	W	-7.41	-16.59	-1.48	-	-	-	327	R	-16.93	19.47	9.50	-	-	
107	B	8.99	1.26	-2.46	-	-	-	328	C	-24.98	13.26	-10.93	-	-	
108	W	-9.76	-18.63	1.97	-	-	-	329	C	-20.38	14.34	-12.91	-14.79	-6.03	
109	B	7.39	2.91	-2.80	-	-	-	330	C	-25.39	16.05	-14.58	-	-	
110	B	9.67	-2.63	0.83	-	-	-	331	R	-10.67	16.73	17.68	-13.69	-7.56	
111	B	12.12	-0.35	-4.84	-	-	-	333	B	2.03	7.34	-1.75	-	-	
112	B	6.44	0.04	3.26	-	-	-	334	R	-14.52	18.71	21.59	-5.18	-2.40	
113	B	9.44	-2.37	1.11	6.51	30.10	1.62	335	R	-19.21	19.18	24.29	-	-	
114	B	3.20	3.05	-1.83	-	-	-	336	R	-12.99	14.46	19.36	-3.84	-5.22	
115	W	-10.76	-11.56	-0.27	13.73	-12.35	-1.54	337	R	-15.92	19.22	23.25	-14.85	-8.10	
116	B	8.62	-0.29	-1.57	-	-	-	345	C	-11.27	15.93	-9.72	-10.17	-3.06	
117	W	-9.03	-18.22	1.82	-	-	-	351	W	-4.01	-11.76	-1.26	18.45	-10.12	
118	W	-8.42	-15.82	1.77	22.76	-6.06	5.83	352	W	-4.89	-19.97	2.63	24.34	-7.36	
119	B	5.09	-0.66	-0.43	-	-	-	354	W	1.01	-1.06	-5.06	20.63	-11.14	
121	W	-7.53	-11.73	-1.18	-	-	-	357	W	-13.40	-19.18	3.30	-	-	
123	W	-3.10	-8.23	-0.23	-	-	-	358	B	8.75	3.20	-0.77	0.37	20.15	
124	W	-7.25	-13.71	-0.73	-	-	-	360	C	-	-	-	-7.91	-9.04	
125	B	13.47	1.49	2.76	-	-	-	364	W	-9.00	-8.69	6.60	-	-	
126	W	-7.98	-16.55	-0.03	-	-	-	365	B	10.60	1.37	0.56	-	-	
127	B	11.73	2.54	-2.62	-	-	-	366	R	-13.41	20.07	11.36	-15.25	-5.07	
128	B	11.24	-2.33	0.81	-	-	-	367	W	-11.53	-17.33	5.13	17.05	-10.23	
129	B	9.33	-3.86	-1.26	-	-	-	368	B	9.30	6.87	-6.00	-	-	

Table D.1 (continued) | Carbohydrate source and positions of the beer samples in the multivariate statistical models.

Sample	Starch source [a]	OPLS scores DI-FT-ICR-MS components 1st	2nd	3rd	UHPLC-ToF components 1st	2nd	3rd	Sample	Starch source	OPLS scores DI-FT-ICR-MS components 1st	2nd	3rd	UHPLC-ToF components 1st	2nd	3rd
130	B	9.75	1.07	-0.19	-	-	-	369	B	9.96	3.89	-0.58	-	-	
131	B	4.16	-1.38	2.16	-	-	-	370	B	13.14	-0.16	0.87	-	-	
132	B	10.36	0.48	1.06	-	-	-	371	W	-7.97	-18.90	3.10	28.88	-14.24	
133	W	-1.99	-15.74	4.15	-	-	-	372	W	-14.11	-19.18	4.57	-	-	
134	B	12.90	4.48	-4.32	-	-	-	375	B	12.13	4.14	-1.52	-	-	
136	B	5.58	2.42	-5.36	-	-	-	376	B	8.95	0.28	-7.38	-	-	
137	W	-5.15	-17.09	-3.08	-	-	-	379	C	-24.06	15.98	-21.73	-3.64	0.86	
138	W	-4.78	-16.36	3.84	-	-	-	380	B	14.42	4.03	-0.11	-	-	
139	B	13.74	-3.22	-0.44	-	-	-	381	R	-11.35	14.83	13.09	-	-	
140	B	14.51	1.68	-2.39	-	-	-	382	R	-9.97	13.37	15.02	-3.77	-8.10	
141	B	11.58	0.72	-5.31	-	-	-	383	C	-21.36	16.40	-10.11	-	-	
142	B	10.11	2.96	1.34	-	-	-	385	B	17.54	-2.41	-7.06	-	-	
143	B	15.90	0.31	-1.23	-	-	-	387	B	13.67	2.95	-2.59	-	-	
144	B	10.23	3.85	-0.46	-	-	-	389	B	10.63	3.91	0.88	-	-	
145	B	4.53	2.71	1.64	-	-	-	390	B	9.44	4.00	1.33	-	-	
146	B	6.76	1.44	-0.38	10.08	26.56	-6.01	391	R	-15.60	16.05	13.59	-	-	
147	B	10.92	0.71	-2.59	-	-	-	392	B	12.10	3.02	3.06	-	-	
148	B	9.12	0.00	-1.85	8.01	26.50	2.20	393	B	6.72	0.34	0.63	-	-	
149	- [b]	10.16	-1.77	-14.73	5.07	7.07	-14.59	394	B	-	-	-	6.79	19.17	
151	C	-13.99	7.89	-11.48	-	-4.83	-11.33	395	W	-12.37	-17.87	-0.90	-	-	
152	W	-7.77	-18.24	4.39	16.65	-9.37	0.81	396	B	9.02	3.26	2.59	-	-	
153	B	4.09	2.67	-2.73	-	-	-	397	W	-7.40	-16.13	2.27	-	-	
154	B	7.68	5.30	-2.03	-	-	-	398	B	9.61	1.26	0.30	-	-	
155	W	-13.21	-21.20	3.11	28.79	-13.35	3.49	399	B	10.69	-2.68	2.02	-	-	
156	C	-13.20	6.74	-11.84	-	-	-	400	W	-9.85	-20.28	5.49	-	-	
157	B	9.92	3.12	-1.17	-	-	-	401	B	7.38	-2.79	2.23	-	-	
159	B	16.03	0.63	-5.86	-	-	-	402	W	-9.82	-15.69	2.45	-	-	
160	C	-22.79	12.01	-18.87	-	-	-	404	W	-1.33	-7.90	0.53	-	-	
162	B	12.62	0.13	2.43	-	-	-	405	W	-9.34	-13.19	3.55	-	-	
163	B	10.66	1.75	-0.25	-	-	-	406	B	8.65	-1.72	2.57	-	-	
164	C	-23.51	11.99	-13.87	-6.80	-7.15	-5.68	407	R	-13.66	14.27	13.77	-	-	
165	B	5.99	5.31	0.68	-	-	-	408	C	-	-	-	-12.23	-1.76	
166	- [b]	-9.18	15.07	2.27	-	-1.74	1.23	409	W	-13.37	-23.69	-0.99	-	-	

Table D.1 (continued) | Carbohydrate source and positions of the beer samples in the multivariate statistical models.

Sample	Starch source [a]	OPLS scores DI-FT-ICR-MS components 1st	2nd	3rd	UHPLC-ToF components 1st	2nd	3rd	Sample	Starch source	OPLS scores DI-FT-ICR-MS components 1st	2nd	3rd	UHPLC-ToF components 1st	2nd	3rd
167	C	-16.64	13.28	-4.16	-8.34	3.76	1.24	410	R	-13.06	17.89	20.86	-11.96	-4.11	
168	R	-10.77	12.65	13.34	-	-	-	411	C	-25.87	13.57	-18.47	-8.17	-5.90	
169	C	-13.20	12.15	-8.45	-	-	-	412	W	-12.11	-16.23	4.34	-	-	
170	R	-3.89	11.07	6.34	-	-	-	413	R	-12.62	16.33	17.63	-	-	
171	R	-7.03	14.15	7.27	-	-	-	414	B	11.63	2.17	-1.84	-	-	
172	C	-14.62	13.55	-8.73	-	-	-	416	B	9.41	-1.47	-0.23	-	-	
173	R	-11.25	13.81	5.86	-9.02	-0.90	8.04	417	B	7.80	1.33	1.51	-	-	
174	B	9.87	0.80	3.86	10.40	26.11	2.35	418	B	12.42	4.72	0.82	-	-	
175	B	4.61	1.46	0.81	9.14	17.90	9.28	419	B	8.57	4.09	1.11	-	-	
177	B	10.19	-1.01	2.80	-	-	-	420	B	10.35	2.25	-2.12	-	-	
178	B	7.37	4.22	-0.11	-	-	-	421	B	7.86	-0.69	-2.28	-	-	
179	B	3.79	3.96	0.57	-	-	-	422	B	6.91	1.13	1.47	-	-	
180	B	6.84	0.26	-4.08	-	-	-	424	B	6.87	1.49	4.28	-	-	
182	B	9.41	3.02	4.40	-	-	-	425	B	6.28	1.54	1.85	-	-	
191	C	-13.70	11.39	-12.70	-	-1.73	-8.99	426	B	19.33	-0.64	-3.71	-	-	
192	B	13.19	2.03	3.89	-	-	-	427	B	9.24	3.69	0.75	11.34	19.01	
193	B	10.37	-0.50	-3.57	-	-	-	428	B	8.73	0.75	1.76	-	-	
194	W	-10.53	-15.45	-4.21	-	-	-	429	B	5.78	5.34	-0.68	-	-	
197	B	4.59	0.53	-0.75	-	-	-	430	B	9.81	1.43	0.33	-	-	
198	W	-6.23	-8.59	-0.74	14.31	-8.58	-5.95	431	B	4.95	1.52	-0.15	-	-	
199	B	12.61	1.55	2.35	-	-	-	432	B	9.38	1.65	-0.95	-	-	
200	W	-15.96	-18.50	0.21	24.60	-17.21	0.77	433	B	16.87	6.85	-5.87	-	-	
201	B	8.63	5.08	-1.72	-	-	-	434	B	14.37	3.77	3.53	-	-	
202	W	-12.53	-20.72	4.45	19.55	-7.58	-0.22	435	B	10.42	-1.48	1.29	8.84	22.96	
203	B	10.40	3.99	1.49	-	-	-	436	B	10.74	-0.94	1.62	-	-	
204	C	-18.32	6.75	-9.53	-	-0.04	-1.84	437	R	-12.37	17.13	18.95	-	-	
205	B	4.91	5.83	2.46	-	-	-	438	B	12.49	4.63	-3.96	-	-	
206	B	5.92	0.71	-2.09	-	-	-	439	W	-1.64	-11.50	0.67	-	-	
207	W	-6.77	-17.18	4.71	-	-	-	440	B	7.11	2.96	-4.13	-	-	
208	B	10.39	4.06	0.52	-	-	-	441	W	-14.15	-21.57	2.26	-	-	
209	B	5.74	2.54	2.11	-	-	-	442	W	-11.55	-14.12	-0.68	-	-	
210	B	13.12	7.44	-1.10	-	-	-	443	B	8.27	2.67	-2.84	-	-	
211	B	13.72	3.06	1.74	-	-	-	444	B	5.46	-1.93	-1.57	-	-	

Table D.1 (continued) | Carbohydrate source and positions of the beer samples in the multivariate statistical models.

Sam-ple	Starch source [a]	OPLS scores DI-FT-ICR-MS components			UHPLC-ToF components			Sam-ple	Starch source	OPLS scores DI-FT-ICR-MS components			UHPLC-ToF components		
		1st	2nd	3rd	1st	2nd	3rd			1st	2nd	3rd	1st	2nd	3rd
212	B	4.96	-2.26	1.92	-	-	-	445	B	13.72	4.17	-5.14	4.37	21.39	
213	R	-12.88	19.82	17.69	-	-4.99	11.49	446	W	-9.56	-13.93	-1.58	-	-	
214	B	6.87	2.54	-3.27	-	-	-	447	B	9.14	1.58	1.14	-	-	
215	B	12.25	1.89	0.52	-	-	-	448	B	7.70	0.46	-0.44	-	-	
216	B	9.76	2.12	-2.14	-	-	-	449	W	-6.07	-13.26	3.26	10.42	-8.71	
217	W	-12.08	-19.90	2.43	27.19	-12.02	1.09	450	W	-8.42	-15.81	3.65	16.48	-0.98	
218	B	11.81	1.46	-0.90	-	-	-	451	B	7.74	5.49	-3.52	12.86	25.64	
219	B	11.69	1.35	-0.79	-	-	-	452	R	-8.67	9.82	13.53	-	-	
220	B	11.00	-0.35	-3.86	-	-	-	453	W	-6.69	-16.87	5.69	-	-	
221	W	-7.45	-13.45	-1.66	-	-	-	454	B	6.08	3.42	2.69	-	-	
222	R	-5.91	15.26	11.57	-	-7.45	10.75	455	B	10.54	7.25	2.85	-	-	
223	B	10.33	3.44	-4.12	-	-	-	456	B	5.42	2.35	0.10	-	-	
224	B	10.64	3.28	1.18	-	-	-	457	B	13.21	1.41	2.34	-	-	
226	B	8.56	1.12	-4.46	-	-	-	458	B	7.66	0.81	2.74	-	-	
227	W	-13.81	-20.03	1.48	-	-	-	459	B	9.85	6.32	2.27	-	-	
228	C	-19.75	12.60	-15.16	-	-6.11	-12.60	464	R	-8.90	14.38	14.69	-	-	
229	C	-18.34	11.72	-12.58	-	-1.58	-13.79	465	R	-5.39	13.22	9.88	-	-	
230	C	-8.36	9.60	-9.01	-	-8.35	-9.21	467	R	-5.40	14.15	13.61	-	-	

[a] Barley (B), Wheat (W), Corn (C) and Rice (R)

[b] The sample was excluded from the models because of contradicting information on the beer bottle and unambiguous positions in the score plots (FT-ICR and UPLC-MS). Only predicted score values are available for the sample.

Table D.2 | SPE work-up of the beer samples for UHPLC-ToF-MS analysis.

Cartridge	Bond Elut PPL, 1 mL and 100 mg (Agilent Santa Clara, CA, USA)
Conditioning	1000 µL MeOH 2x 1000 µL Milli-Q Water + 2 % FA
Sample	1000 µL acidified sample (2 % FA)
Washing	500 µL Milli-Q Water + 2 % FA
Dry vacuum	
Elution	2x 500 µL MeOH

Table D.3 | Parameters for UHPLC-separation and ToF-measurements.

Parameter	Value
Sample preparation	Table D.2 in Supplementary Chapter 4
Column	RP (C18: 1.7 µm, 2.1 x 100 mm, Acquity™ UPLC BEH™)
Flow rate	400 µL min^{-1}
Column temperature	40 °C
Injection volume	5 µL (partial loop)
Gradient profile	95 % A (0.1 % formic acid in water) and 5 % B (0.1 % formic acid in
Measurement time	10 min.
Internal calibration	ESI-L Low Concentration Tuning Mix
External calibration	Sodium iodide solution clusters
ESI ionization mode	negative
Nitrogen flowrate	10 L min^{-1}
Interface temperature	300°C
Nebulizer gas flow	1 L min^{-1}
Interface voltage	-4 kV
DL temperature	250 °C
Heat block temperature	400 °C
Drying gas flow	10 L min^{-1}
Detector voltage	2 kV
MS^1 parameters	5 Hz event cycle time
	Ion accumulation on
MS^2 fragmentation parameters	DDA (3 dependent events)
	CE spread 20 eV ± 15 eV

Table D.4 | Parameters of the UHPLC-ToF-MS and FT-ICR-MS data treatment using the MS-Dial and SIMCA software.

Parameter (LC-MS-data treatment)	Value
Minimum peak height	1800 ampl.
Minimum peak width	10 scans
RT tolerance	3 sec.
m/z tolerance	0.005 Da
Sample Intensity / blank Intensity	>10 fold change
Filter	>33 % of the samples within the given class
Normalization (compensation for intensity fluctuations)	LOWESS, based on 22 QCs
MS/MS network similarity	65% cutoff
Zero filling	Random value between average minimum peak intensity for each sample ± σ, (LC-MS and FT-MS)
Normalization	Z-scores (LC-MS and FT-MS)
Scaling	Unit-Variance (UV) scaling (LC-MS and FT-MS)
Transformation	Logarithmize (only applied to FT-MS)

Table D.5 | Statistical parameters of the multivariate data analysis.

Statistical model	n	Features	Components (predictive + orthogonal)	R2Y	R2X	Q^2	ANOVA
OPLS (FT-ICR-MS)	392	7697	3+9	0.881	0.378	0.601	<< 0.05
OPLS (UHPLC-ToF-MS)	98	1776	3+5	0.862	0.528	0.641	<< 0.05

Table D.6 | Mass features resolved by FT-ICR-MS within the nominal mass m/z 385 throughout the whole sample set.

m/z	Neutral Formula	Mean intensity	Loadings 3rd component	Loadings 2nd component	Marker
385.02360	$C_{15}H_{14}O_{10}S$	5.8E+06	-0.054	0.020	Corn
385.03811	$C_{11}H_{18}N_2O_9S_2$	3.9E+06	-0.025	0.006	Corn
385.04461	$C_{12}H_{18}O_{12}S$	6.9E+06	-0.005	0.001	
385.04604	$C_{13}H_{14}N_4O_8S$	5.8E+06	0.003	0.000	
385.04932	$C_{10}H_{18}N_4O_8S_2$	4.8E+06	-0.021	0.002	Corn
385.05412	$C_{12}H_{19}O_{12}P$	1.2E+07	-0.001	-0.010	
385.07459	$C_{12}H_{22}N_2O_8S_2$	1.1E+07	-0.006	-0.002	
385.07764	$C_{16}H_{18}O_{11}$	8.3E+06	0.015	-0.017	Wheat
385.08091	$C_{13}H_{22}O_{11}S$	4.6E+06	-0.020	0.001	Corn
385.08888	$C_{15}H_{18}N_2O_{10}$	8.3E+06	0.007	0.020	Corn&Rice
385.09291	$C_{20}H_{18}O_8$	6.8E+06	0.013	0.001	
385.09876	$C_{13}H_{22}O_{13}$	8.2E+06	-0.001	-0.005	
385.10023	$C_{14}H_{18}N_4O_9$	7.9E+06	0.002	0.000	
385.10179	$C_{12}H_{23}N_2O_{10}P$	1.0E+07	-0.007	-0.007	
385.11404	$C_{17}H_{22}O_{10}$	6.6E+07	0.001	-0.018	Wheat
385.11547	$C_{18}H_{18}N_4O_6$	2.2E+07	0.048	0.009	Rice
385.11733	$C_{14}H_{26}O_{10}S$	6.9E+06	-0.007	0.006	
385.12525	$C_{16}H_{22}N_2O_9$	6.9E+06	-0.002	-0.010	
385.13259	$C_{18}H_{26}O_7S$	1.6E+07	0.004	0.021	Corn&Rice
385.13496	$C_{14}H_{26}O_{12}$	1.3E+07	0.000	0.003	
385.13649	$C_{15}H_{22}N_4O_8$	4.1E+07	-0.001	-0.008	
385.13816	$C_{13}H_{27}N_2O_9P$	6.2E+07	0.027	0.015	Rice
385.14634	$C_{13}H_{26}N_2O_{11}$	9.3E+06	0.008	-0.018	Wheat
385.14941	$C_{12}H_{27}N_4O_8P$	6.8E+06	0.003	-0.016	Wheat
385.15042	$C_{18}H_{26}O_9$	6.4E+06	-0.003	-0.006	
385.16161	$C_{17}H_{26}N_2O_8$	8.7E+06	-0.001	-0.010	
385.16563	$C_{22}H_{26}O_6$	6.6E+06	0.013	0.009	
385.17140	$C_{15}H_{30}O_{11}$	1.3E+07	-0.009	-0.022	Wheat

Table D.6 (continued) | Mass features resolved by FT-ICR MS within the nominal mass m/z 385 throughout the whole sample set.

m/z	Neutral Formula	Mean intensity	Loadings		Marker
			3rd component	2nd component	
385.17288	$C_{16}H_{26}N_4O_7$	2.3E+07	0.008	0.024	Corn&Rice
385.17867	$C_{20}H_{30}O_5Cl$	6.6E+06	-0.005	0.008	
385.18676	$C_{19}H_{30}O_8$	6.8E+06	0.006	-0.001	
385.19801	$C_{18}H_{30}N_2O_7$	5.1E+06	0.029	0.003	Rice
385.20201	$C_{23}H_{30}O_5$	4.3E+06	0.001	0.001	
385.20923	$C_{17}H_{30}N_4O_6$	9.1E+06	0.005	0.032	Corn&Rice
385.22314	$C_{20}H_{34}O_7$	2.3E+07	-0.007	0.005	
385.23840	$C_{24}H_{34}O_4$	9.2E+06	0.005	-0.010	
385.24560	$C_{18}H_{34}N_4O_5$	4.8E+06	-0.011	0.009	Corn
385.25953	$C_{21}H_{38}O_6$	7.5E+06	0.021	0.009	Rice
385.29592	$C_{22}H_{42}O_5$	8.0E+06	0.015	0.001	
385.33232	$C_{23}H_{46}O_4$	6.4E+06	0.009	0.006	
385.02360	$C_{15}H_{14}O_{10}S$	5.8E+06	-0.054	0.020	Corn
385.03811	$C_{11}H_{18}N_2O_9S_2$	3.9E+06	-0.025	0.006	Corn
385.04461	$C_{12}H_{18}O_{12}S$	6.9E+06	-0.005	0.001	
385.04604	$C_{13}H_{14}N_4O_8S$	5.8E+06	0.003	0.000	
385.04932	$C_{10}H_{18}N_4O_8S_2$	4.8E+06	-0.021	0.002	Corn
385.05412	$C_{12}H_{19}O_{12}P$	1.2E+07	-0.001	-0.010	
385.07459	$C_{12}H_{22}N_2O_8S_2$	1.1E+07	-0.006	-0.002	
385.07764	$C_{16}H_{18}O_{11}$	8.3E+06	0.015	-0.017	Wheat
385.08091	$C_{13}H_{22}O_{11}S$	4.6E+06	-0.020	0.001	Corn
385.08888	$C_{15}H_{18}N_2O_{10}$	8.3E+06	0.007	0.020	Corn&Rice
385.09291	$C_{20}H_{18}O_8$	6.8E+06	0.013	0.001	
385.09876	$C_{13}H_{22}O_{13}$	8.2E+06	-0.001	-0.005	
385.10023	$C_{14}H_{18}N_4O_9$	7.9E+06	0.002	0.000	
385.10179	$C_{12}H_{23}N_2O_{10}P$	1.0E+07	-0.007	-0.007	
385.11404	$C_{17}H_{22}O_{10}$	6.6E+07	0.001	-0.018	Wheat
385.11547	$C_{18}H_{18}N_4O_6$	2.2E+07	0.048	0.009	Rice
385.11733	$C_{14}H_{26}O_{10}S$	6.9E+06	-0.007	0.006	

Table D.6 (continued) | Mass features resolved by FT-ICR MS within the nominal mass m/z 385 throughout the whole sample set.

m/z	Neutral Formula	Mean intensity	Loadings		Marker
			3rd component	2nd component	
385.12525	$C_{16}H_{22}N_2O_9$	6.9E+06	-0.002	-0.010	
385.13259	$C_{18}H_{26}O_7S$	1.6E+07	0.004	0.021	Corn&Rice
385.13496	$C_{14}H_{26}O_{12}$	1.3E+07	0.000	0.003	
385.13649	$C_{15}H_{22}N_4O_8$	4.1E+07	-0.001	-0.008	
385.13816	$C_{13}H_{27}N_2O_9P$	6.2E+07	0.027	0.015	Rice
385.14634	$C_{13}H_{26}N_2O_{11}$	9.3E+06	0.008	-0.018	Wheat
385.14941	$C_{12}H_{27}N_4O_8P$	6.8E+06	0.003	-0.016	Wheat
385.15042	$C_{18}H_{26}O_9$	6.4E+06	-0.003	-0.006	
385.16161	$C_{17}H_{26}N_2O_8$	8.7E+06	-0.001	-0.010	
385.16563	$C_{22}H_{26}O_6$	6.6E+06	0.013	0.009	
385.17140	$C_{15}H_{30}O_{11}$	1.3E+07	-0.009	-0.022	Wheat
385.17288	$C_{16}H_{26}N_4O_7$	2.3E+07	0.008	0.024	Corn&Rice
385.17867	$C_{20}H_{30}O_5Cl$	6.6E+06	-0.005	0.008	
385.18676	$C_{19}H_{30}O_8$	6.8E+06	0.006	-0.001	
385.19801	$C_{18}H_{30}N_2O_7$	5.1E+06	0.029	0.003	Rice
385.20201	$C_{23}H_{30}O_5$	4.3E+06	0.001	0.001	
385.20923	$C_{17}H_{30}N_4O_6$	9.1E+06	0.005	0.032	Corn&Rice
385.22314	$C_{20}H_{34}O_7$	2.3E+07	-0.007	0.005	
385.23840	$C_{24}H_{34}O_4$	9.2E+06	0.005	-0.010	
385.24560	$C_{18}H_{34}N_4O_5$	4.8E+06	-0.011	0.009	Corn
385.25953	$C_{21}H_{38}O_6$	7.5E+06	0.021	0.009	Rice
385.29592	$C_{22}H_{42}O_5$	8.0E+06	0.015	0.001	
385.33232	$C_{23}H_{46}O_4$	6.4E+06	0.009	0.006	

Table D.7 | Identification of compounds characteristic for wheat, corn and rice-based on UPLC-ToF-MS fragmentation spectra.

m/z $[M-H]^-$	Ret. time	Starch source	Identification		MS^2-fragm. (neg.) [x/y][a]	MS^2-fragm. (pos.) [x/y][a]	Literature
			potential structure [molecular formula]	Level [10]			
164.0348	3.79	wheat	MBOA [$C_8H_7NO_3$]	2	121(18), 149(100), 164(25) [2/2]	67(26), 95(40), 106(19), 107(26), 110(64), 122(17),	[349]
326.0886	3.00	wheat	HBOA-Glc [$C_{14}H_{17}NO_8$]	2	108(47), 149(17), 164(100), 236(61) [3/3]	-	[225,281,349]
342.0831	3.03	wheat	DIBOA-Glc [$C_{14}H_{17}NO_9$]	2	134(100), 162(11), 180(9), 342(22) [3/3]	-	[225,281]
356.0991	3.14	wheat	HMBOA-Glc [$C_{15}H_{19}NO_9$]	2	123(10), 138(26), 166(9), 194(100), 356(32) [4/4]	-	[225,281]
421.2710	4.40	wheat	N-Acylglutamine [$C_{23}H_{38}N_2O_5$]	3	243(10), 357(100), 375(8) [3/3]	-	in silico [262,347]
423.2867	4.62	wheat	N-Acylglutamine [$C_{23}H_{40}N_2O_5$]	3	157(5), 209(27), 221(9), 245(4), 359(100), 377(15), 423(14)	-	in silico
431.2916	4.49	wheat	N-Acylglutamine [$C_{25}H_{40}N_2O_4$]	3	209(17), 221(16), 245(36), 359(56), 431(100) [4/4]	-	in silico
437.2653	4.32	wheat	N-Acylglutamine [$C_{23}H_{38}N_2O_6$]	3	243(20), 373(100), 391(42), 437(9) [NA]	120(29), 121(100), 133(79), 439(62) [NA]	in silico
439.2820	4.50	wheat	N-Acylglutamine [$C_{23}H_{40}N_2O_6$]	3	164(4), 173(10), 225(11), 237(4), 245(8), 375(100),	-	in silico
206.0458	3.02	corn	Hydroxyoxindol-acetic acid [$C_{10}H_9NO_4$]	2	147(11), 162(100), 188(17), 206(36) [3/3]	85(21), 89(20), 116(52), 144(51), 162(100), 208(25) [5/5]	in silico, [342]
337.2382	6.04	corn	Lipid (DiHEtrE) [$C_{20}H_{34}O_4$]	3	169(3), 183(4), 197(4), 211(7), 225(7), 239(16), 276(4),	79(22), 81(65), 93(31), 95(100), 105(34), 107(23), 109(54),	in silico, [350,351]
337.2381	6.09	corn	Lipid (DiHEtrE) [$C_{20}H_{34}O_4$]	3	169(3), 183(3), 197(3), 211(8), 225(7), 239(18), 276(3),		in silico

Table D.7 (continued) | Identification of compounds characteristic for wheat, corn and rice based on UPLC ToF MS fragmentation spectra.

m/z $[M-H]^-$	Ret. time	Starch source	Identification potential structure [molecular formula]	Level [10]	MS^2-fragm. (neg.) [x/y][a]	MS^2-fragm. (pos.) [x/y][a]	Literature
351.2182	6.57	corn	Lipid (TriHETE) $[C_{20}H_{32}O_5]$	3	181(3), 209(6), 211(5), 235(10), 239(13), 253(12), 264(3),	91(25), 95(26), 113(546), 163(43), 181(54), 241(66),	in silico [350,351]
351.2182	6.62	corn	Lipid (TriHETE) $[C_{20}H_{32}O_5]$	3	181(3), 209(6), 211(4), 235(9), 239(11), 253(11), 264(3),		in silico
351.2538	6.34	corn	Lipid $[C_{21}H_{36}O_4]$	3	183(4), 211(5), 225(3), 239(11), 253(9), 290(4), 333(17),	107(27), 279(35), 335(100), 353(31) [NA]	in silico
351.2544	6.26	corn	Lipid $[C_{21}H_{36}O_4]$	3	183(4), 211(6), 225(3), 235(2), 239(11), 253(9), 290(5),		in silico
365.2332	7.17	corn	Lipid $[C_{21}H_{34}O_5]$	3	183(2), 211(2), 223(3), 239(6), 249(4), 250(5), 253(6), 267(5),	127(37), 195(68), 255(72), 265(29), 269(30), 349(100),	in silico
365.2334	6.87	corn	Lipid $[C_{21}H_{34}O_5]$	3	195(2), 211(4), 223(6), 239(10), 249(11), 253(11), 267(12),		in silico
365.2337	6.80	corn	Lipid $[C_{21}H_{34}O_5]$	3	224(4), 240(5), 250(9), 251(5), 253(7), 267(3), 268(7), 322(6),		in silico
237.0768	3.39	corn grits	Coumaroyl glycerol $[C_{12}H_{14}O_5]$	2	117(100), 119(38), 145(76), 163(11), 237(71) [4/4]	65 (13), 91(54), 119(37), 147(100), 239(13) [4/4]	in silico, [343]
253.0718	3.15	corn grits	Caffeoyl glycerol $[C_{12}H_{14}O_6]$	2	105(10), 133(87), 135(46), 161(82), 179(12), 253(100)	63(11), 77(8), 89(80), 107(4), 117(31), 135(23), 145(25),	in silico, [343]
451.1380	2.95	rice	N-Glc-IAA-Asp $[C_{20}H_{24}N_2O_{10}]$	1	132(35), 173(43), 292(15), 335(18), 433(7), 451(100) [5/5]	130(100), 134(14), 147(18), 172(17), 291(63), 453(23) [5/5]	Co-Chrom.
539.2845	3.50	rice	$[C_{24}H_{40}N_6O_8]$	-	127(3), 167(7), 215(12), 255(10), 424(2), 539(100) [NA]	-	-
542.2621	3.88	rice	Peptide (Glu-Trp-Leu/Ile-Pro) $[C_{27}H_{37}N_5O_7]$	3	127(3), 171(3), 222(7), 240(13), 542(100) [4/4]	116(46), 120(93), 144(32), 159(28), 173(98), 284(34), 316(35), 320(48), 429(47),	in silico
544.2257	2.96	rice	$[C_{22}H_{35}N_5O_{11}]$	-	128(21), 185(6), 215(7), 241(6), 544(100) [NA]	-	-

Table D.7 (continued) | Identification of compounds characteristic for wheat, corn and rice based on UPLC ToF MS fragmentation spectra.

m/z $[M-H]^-$	Ret. time	Starch source	Identification potential structure [molecular formula]	Level [10]	MS^2-fragm. (neg.) [x/y][a]	MS^2-fragm. (pos.) [x/y][a]	Literature
599.2831	3.77	rice	Peptide (Asp-Ser-Val-Leu-Trp, cyclic) [$C_{29}H_{40}N_6O_8$]	3	240(6), 369(3), 387(28), 599(100) [3/3]	217(11), 227(11), 245(13), 339(15), 340(11), 486(34), 601(100) [6/6]	in silico

[a] x: fragment ions found for the compound; y: fragment ions described in the reference

Table D.8 | Presence of the compounds characteristic for wheat, corn and rice in respective grain foodstuff.

m/z [M-H]⁻	RT	Compound	CG[a]	CS	CF	CO	WG	WS	WF	HWF	RG	RS	RF
164.0348	3.79	MBOA [$C_8H_7NO_3$]	-	-	-	-	-	-	-	pos.	-	-	-
326.0886	3.00	HBOA-Glc [$C_{14}H_{17}NO_8$]	-	-	-	-	-	-	neg.	neg.	-	-	-
342.0831	3.03	DIBOA-Glc [$C_{14}H_{17}NO_9$]	-	-	-	-	neg.	-	-	-	-	-	-
356.0991	3.14	HMBOA-Glc [$C_{15}H_{19}NO_9$]	-	-	-	-	-	-	neg.	neg.	-	-	-
421.2710	4.40	N-Acylglutamine [$C_{23}H_{38}N_2O_5$]	-	-	-	-	-	-	-	-	-	-	-
423.2867	4.62	N-Acylglutamine [$C_{23}H_{40}N_2O_5$]	-	-	-	-	neg.	-	neg.	neg.	-	-	-
431.2916	4.49	N-Acylglutamine [$C_{25}H_{40}N_2O_4$]	-	-	-	-	neg.	-	-	-	-	-	-
437.2653	4.32	N-Acylglutamine [$C_{23}H_{38}N_2O_6$]	-	-	-	-	neg. pos.	-	pos.	pos.	-	-	-
439.2820	4.50	N-Acylglutamine [$C_{23}H_{40}N_2O_6$]	-	-	-	-	neg.	-	-	-	-	-	-
206.0458	3.02	Hydroxyoxindol-acetic acid [$C_{10}H_9NO_4$]	neg.[b] pos.	neg. pos.	neg. pos.	-	-	-	-	-	-	-	-
337.2382	6.04	Lipid (DiHEtrE) [$C_{20}H_{34}O_4$]	-	-	-	neg.	-	-	-	-	-	-	-
337.2381	6.09	Lipid (DiHEtrE) [$C_{20}H_{34}O_4$]	-	-	-	neg.	-	-	-	-	-	-	-
351.2182	6.57	Lipid (TriHETE) [$C_{20}H_{32}O_5$]	-	-	-	-	-	-	-	-	-	-	-
351.2182	6.62	Lipid (TriHETE) [$C_{20}H_{32}O_5$]	-	-	-	-	-	-	-	-	-	-	-
351.2538	6.34	Lipid [$C_{21}H_{36}O_4$]	-	-	-	neg. pos.	-	-	-	-	-	-	-
351.2544	6.26	Lipid [$C_{21}H_{36}O_4$]	-	-	-	neg. pos.	-	-	-	-	-	-	-
365.2332	7.17	Lipid [$C_{21}H_{34}O_5$]	-	-	-	-	-	-	-	-	-	-	-
365.2334	6.87	Lipid [$C_{21}H_{34}O_5$]	-	-	-	-	-	-	-	-	-	-	-
365.2337	6.80	Lipid [$C_{21}H_{34}O_5$]	-	-	-	-	-	-	-	-	-	-	-
451.1380	2.95	N-Glc-IAA-Asp [$C_{20}H_{24}N_2O_{10}$]	-	-	-	-	-	-	-	-	neg.	neg. pos.	neg.
539.2845	3.50	[$C_{24}H_{40}N_6O_8$]	-	-	-	-	-	-	-	-	-	-	neg.
542.2621	3.88	Glu-Trp-Leu/Ile-Pro	-	-	-	-	-	-	-	-	-	neg.	neg.

Table D.8 (continued) | Presence of the compounds characteristic for wheat, corn and rice in respective grain foodstuff.

m/z [M-H]$^-$	RT	Compound	CG[a]	CS	CF	CO	WG	WS	WF	HWF	RG	RS	RF
544.2257	2.96	[$C_{22}H_{35}N_5O_{11}$]	-	-	-	-	-	-	-	-	-	neg.	-
599.2831	3.77	Asp-Ser-Val-Leu-Trp (cyclic)	-	-	-	-	-	-	-	-	-	-	-

[a] CG: corn grits, CS: corn starch, CF: corn flour, CO: corn oil, WG: wheat grits, WS: wheat starch, WF: wheat flour, HWF: whole wheat flour, RG: rice grits, RS: rice starch, RF: rice flour

[b] the respective compound was found in negative (neg.) and/or positive (pos.) ionization mode.

Figures D

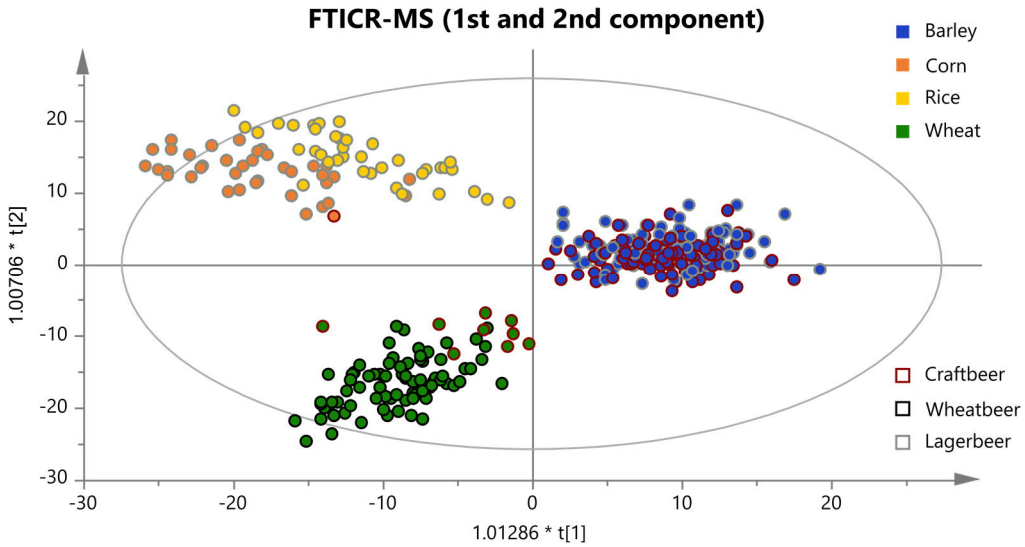

Figure D.1 | Score plot of FT-ICR-MS data (1st and 2nd component) shows the overlap of barley beers (carbohydrate source) with craft beers (beer type). All measured samples are colored according to their carbohydrate source. The color of the frame is defined by the beer type. Most of the craft beers are brewed with barley as the only carbohydrate source.

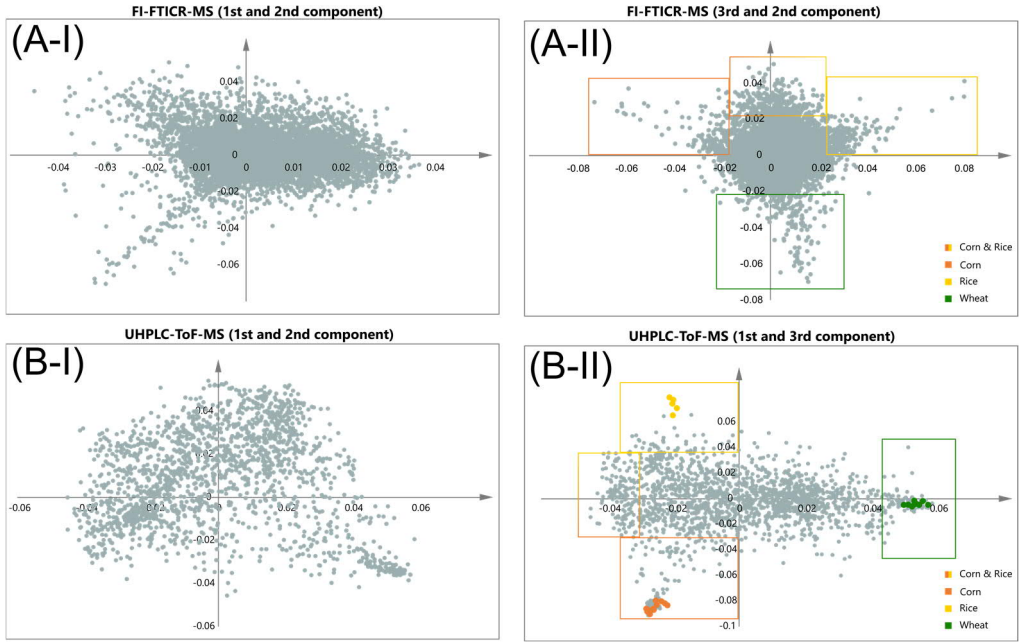

Figure D.2 | Loadings plots of the OPLS-DA of the DI-FT-ICR-MS (A) and UPLC-ToF-MS (B) data differentiating the carbohydrate sources used. The position of mass features (grey) indicates their separation significance regarding the beer characteristics given in the score plot (Figure 4.2). The most significant marker compositions are highlighted in the corresponding color. The first and second components are shown in (A-I) and (B-I). The third against the second and the first against the third component are shown in (A-II) and (B-II) respectively. Colored dots in (B-II) could be identified (identification level 1-3).

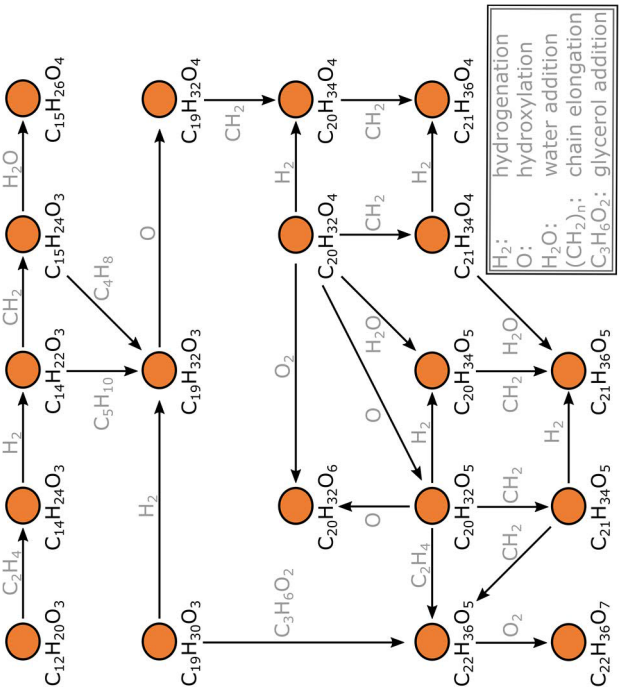

Figure D.3 | Mass difference network excerpt of lipids characteristic for corn. The nodes representing annotations are connected by edges representing potential biochemical reactions. Some connections are neglected for reasons of clarity.

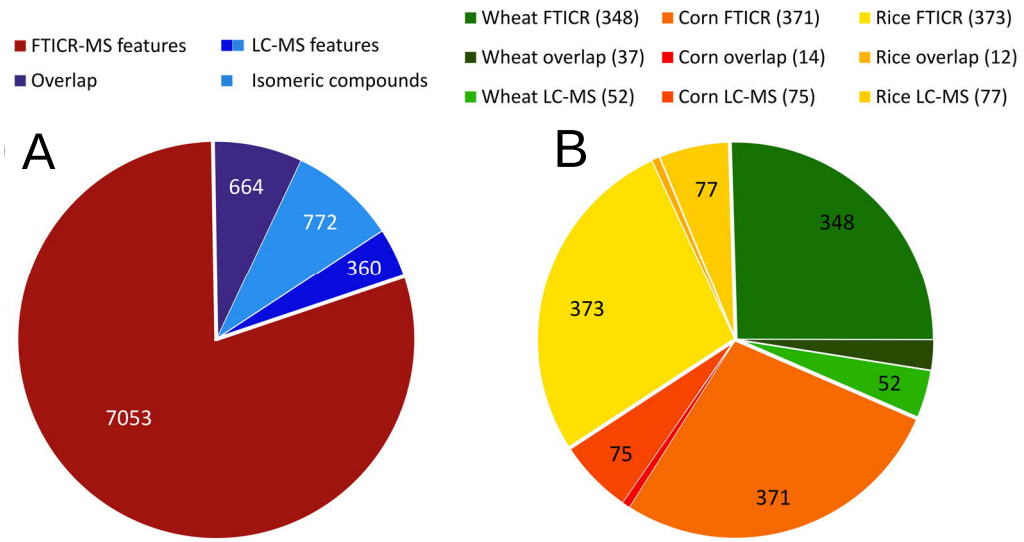

Figure D.4 | Overlap of mass features found in RP-UPLC-ToF-MS (LC-MS) and DI-FT-ICR-MS (FT-ICR) within a mass tolerance of ±10 ppm with regard to overall peaks (A) and peaks found as potential markers for carbohydrate sources (B). The analytical approaches are differentiated by color in (A). The colors in (B) are based on the different carbohydrate sources.

E Supplementary Chapter 5

Tables E

Table E.1 | Regular beer attributes and folate contents of Barre Pilsener from 1885 and 2019 compared to Vienna, Bohemian and Bavarian beer from 1888.

Beer attribute	Unit	Barre Pilsner 1885	Vienna Beer [373]	Bohemian Beer [373]	Bavarian Beer [373]	Barre Pilsner 2019
Original gravity	w/w%	10.36	10.39-13.26	12.45	14.71	11.195
Alcohol	w/w%	3.12	2.9-3.7	3.43	3.94	3.94
Real extract	w/w%	4.26	4.4-5.7	5.4	6.7	3.6
Attenuation limit,	%	58.8	57	56.2	54.3	68
pH	-	4.42	-	-	-	4.21
Bitter units	EBC	18.4	-	-	-	28.7
Color	EBC	12.5	-	-	-	7.7
Folate analysis						
PteGlu	[µg/100g]	n.d.	-	-	-	n.d.
H_4Holate	[µg/100g]	n.d.	-	-	-	n.d.
5-CH_3-H_4Folate	[µg/100g]	0.58	-	-	-	1.10
5-CHO-H_4Folate	[µg/100g]	n.d.	-	-	-	2.06
10-CHO-PteGlu	[µg/100g]	n.d.	-	-	-	3.91
Total Folates	[µg/100g]	0.58	-	-	-	7.08

Table E.2 | ^{1}H and ^{13}C chemical Shifts, Proton Multiplicities for identified metabolites in the beer samples.

Compound (No.)	Assigned group	σ ^{1}H	Multiplicity	σ ^{13}C
2-Methyl-1-propanol (1)	2xCH_3	0.88	d	21.0
	$(CH_3)_2CHCH_2OH$	1.76	m	27.0
	$(CH_3)_2CHCH_2OH$	3.38		
3-Methyl-1-butanol (2)	2xCH_3	0.89	d	24.8
	$(CH_3)_2CH(CH_2)_2OH$	1.44	m	43.0
	$(CH_3)_2CHCH_2CH_2OH$	1.66	m	27.2
	$(CH_3)_2CHCH_2CH_2OH$	3.64		
Propanol (3)	$CH_3CH_2CH_2OH$	0.89	t	n.d.
	$CH_3CH_2CH_2OH$	1.56	m	
	$CH_3CH_2CH_2OH$	3.57	t	
Valine (4)	2xCH_3	1.05, 0.99 2.27	d, d	19.7
	$(CH_3)_2CH$		m	
Lactic acid (5)	$CH_3(CHOH)COOH$	1.33	d	19.33
	$CH_3(CHOH)COOH$	4.11	q	71.6
Alanine (6)	CH_3	1.48	d	19.4
	CH	3.79	q	
Acetic acid (7)	CH_3	1.92	s	26.3
Proline (8)	γ-CH_2	2.00	m	26.6
	β-CH_2	2.06	m	31.7
	β-CH_2	2.33	m	31.7
	σ-CH_2	3.32	m	48.9
	σ-CH_2	3.41	m	48.9
	α-CH	4.11	dd	64.1
GABA (9)	CH_2COO	2.30	t	37.3
	$(CH_2)CH_2(CH_2$	1.90	m	26.7
	NH_2CH_2	3.02	t	42.3
Pyruvate (10)	CH_3	2.37	s	29.5

Table E.2 (continued) | 1H and 13C chemical Shifts, Proton Multiplicities for identified metabolites in the beer samples.

Compound (No.)	Assigned group	**σ** ^{1}H	Multiplicity	**σ** ^{13}C
Succinic acid (11)	$(CH_2)_2$	2.40	s	37.4
Citrate (12)	CH'_2	2.53	d	48.8
	CH''_2	2.66	d	48.8
(13) – (20)	Compound classes			
Uridine (21)	2x C=CH	5.92, 7.88	d, d	90.7 , 144.8
Adenosin/ Inosine (22)	N=CH′	8.27	s	155.7
	N=CH′′	8.36	s	143.5
	OCHN	6.07	d	91.3
Tyrosol (23)	2x C=CH′	6.87	m	118.6
	2x C=CH′′	7.19	m	133.4
Tyrosine (24)	2x C=CH′	6.91	m	119.0
	2x C=CH′′	7.20	m	133.7
Phenylalanine (25)	$CH'_{aromatic}$	7.34	m	132.1
	$CH''_{aromatic}$	7.43	m	131.1
Histidine (26)	N=CH	8.00	s	140.7
	C=CH	7.06	s	119.5
Cytidine (27)	C=CH′	6.07	d	99.2
	C=CH′′	7.85	d	144.7
Formic acid (28)	HCOOH	8.46	s	174.0
Niacin (29)	4x C=CH	8.95, 8.62 8.27, 7.54	m	n.d.
HMF (30)	CHO	9.46	s	183.7
	2x C=CH	7.55	d	n.d
	CH_2OH	6.69	m	n.d.
Furfural (31)	CHO	9.50	s	n.d.
	3x C=CH	7.94, 7.60, 6.78	m	n.d.
Acetaldehyde (32)	CHO	9.68	q	n.d.
	CH_3	2.21	d	n.d.

Table E.3 | General statistical and model parameters of the multivariate data analysis.

Parameter	
Outlier detection	Hotelling's T^2 (95 %)
Goodness of fit	R2
Goodness of prediction	Q2
Overfitting	CV-ANOVA
Significant features	95th percentile of features with most characteristic loadings (385 compositions)
Metadata	As given on the beers' label. The UV/Vis measurements were executed as described in [226]
Sample exclusion	For the grain model, 23 samples were excluded due to ambiguous information of the grains used ("rice and/or corn", "cereals")
Statistics software	SIMCA 13.0.3.0 (Umetrics, Umeå, Sweden)

Statistical model (OPLS)	n	R2Y	R2X	Q^2	ANOVA
Beer type	400	0.865	0.294	0.752	<< 0.05
Fermentation	400	0.936	0.274	0.792	<< 0.05
Purity Law	400	0.971	0.325	0.569	<< 0.05
Grain	377	0.881	0.373	0.601	<< 0.05
Maillard (Abs. 294 nm)	221	0.941	0.239	0.806	<< 0.05

Table E.4 | Instrumental parameters and reagents used for FT-ICR-MS, UPLC-ToF-MS and HPLC-Triple Quad (Folates) measurements.

Reagent	Source
Methanol (MeOH)	FLUKA, Sigma-Aldrich (LC-MS grade, CHROMASOLV, St Louis, MO, USA)
Acetonitrile (ACN)	FLUKA, Sigma-Aldrich (LC-MS grade, CHROMASOLV, St Louis, MO, USA)
Ultrapure water	Milli-Q Integral Water Purification System (Millipore, MA, Billerica, USA)
L-arginine	Sigma-Aldrich (reagent grade >98%, St Louis, MO, USA)
Formic acid (FA)	VWR HiPerSolv CHROMANORM® (LC-MS grade; ≥99%)

FT-ICR-MS	Value
Sample preparation	degassing by ultrasonification (10 °C, 5min.); dilution 1:500 in methanol (v:v); separation of precipitated proteins by centrifugation (10,000 rpm, 3min.)
Direct injection flowrate	120 µL.h^{-1}.
ESI capillary voltage	3600 V
Time domain	4 mega words
Accumulation time	0.25 ms
Mass range	m/z 120 to 1000
Accumulated scans	400
Measurement time	10 min.
External calibration	clusters of arginine (5 mg.L^{-1} in methanol)
Internal calibration	in-house calibration list containing 2000 molecular formulae, which are highly abundant in beers

UPLC-ToF-MS	Value
Sample preparation	SPE: Bond Elut PPL, 1 mL and 100 mg (Agilent Santa Clara, CA, USA); conditioning: 100 µL MeOH, 2x1000µL Mili-Q-Water + 2% Formic acid (FA); 1000 µL acidified sample (2% FA); washing: 500 µL Mili-Q-Water + 2%FA; dry vacuum; elution: 2x500µL MeOH)
Column	RP (C18: 1.7 µm, 2.1 x 100 mm, Acquity™ UPLC BEH™)
Flow rate	400 µL min^{-1}
Column temperature	40 °C
Injection volume	5 µL (partial loop)

Table E.4 (continued) | Instrumental parameters and reagents used for FT-ICR-MS, UPLC-ToF-MS and HPLC-Triple Quad (Folates) measurements.

UPLC-ToF-MS	Value
Gradient profile	95 % A (0.1 % formic acid in water) and 5 % B (0.1 % formic acid in acetonitrile) for 1 min; decreasing to 0.5 % A in 5 min; held for 4 min.
Measurement time	10 min.
Internal calibration	ESI-L Low Concentration Tuning Mix
External calibration	Sodium iodide solution clusters
ESI ionization mode	negative
Nitrogen flowrate	10 L min^{-1}
Interface temperature	300°C
Nebulizer gas flow	1 L min^{-1}
Interface voltage	-4 kV
DL temperature	250 °C
Heat block temperature	400 °C
Drying gas flow	10 L min^{-1}
Detector voltage	2 kV
MS^1 parameters	5 Hz event cycle time Ion accumulation on
MS^2 fragmentation parameters	DDA (3 dependent events) CE spread 20 eV ± 15 eV

UHPLC-Triple Quad-MS	Value
Sample preparation	The sample preparation of Striegel, et al. [452] was modified by adding the suitable $^{13}C_5$ labelled isotopologue standard of 10-CHO-PteGlu for quantification. As described in Pferdmenges, et al. [375]
Column	Raptor™ ARC-18 (2.7 µm, 100 x 2.1 mm)
Precolumn	Raptor™ EXP Guard Column (2.7 µm, 5 x 2.1 mm)
Flow rate	400 µL min^{-1}
Column temperature	30 °C
Injection volume	10 µL

Table E.4 (continued) | Instrumental parameters and reagents used for FT-ICR-MS, UPLC-ToF-MS and HPLC-Triple Quad (Folates) measurements.

UHPLC-Triple Quad-MS	Value
Gradient profile	97 % A (0.1 % formic acid in water) and 3 % B (0.1 % formic acid in acetonitrile) for 1 min; increasing to 10% B in 2 min; held for 2.5 min; increasing to 15 % B in 5 min; increasing to 50 % B in 1 min; held for 1 min; decrease to 3 % B in 1 min; equilibrate for 4 min.
Measurement time	17.5 min
ESI ionization mode	Positive (MRM-multiple reaction monitoring)
Interface temperature	300 °C
Nebulizer gas flow	3 L min^{-1}
Heating gas flow	10 L min^{-1}
Interface voltage	4 kV
DL temperature	250 °C
Heat block temperature	400 °C
Drying gas flow	10 L min^{-1}
CID gas	270 kPa

Table E.5 | Instrumental parameters and reagents used for NMR measurements.

Reagent	Source (Purity)
D_2O	Armar chemicals (99.8 atom%, Döttingen, CH)
Di-natriumhydrogenphosphate	Merck Millipore (99 %, Billerica, MA, USA)
3-(trimethylsilyl)propionic-	Sigma Aldrich (98 atom%, MO, St Louis, USA)

Standard	Source (Purity)
Furfural	Sigma Aldrich (99 %, MO, St Louis, USA)
Niacin	Sigma Aldrich (≥ 98 %, MO, St Louis, USA)
Histidine	Merck Millipore (≥ 98 %, MA, Billerica, USA)
Xylose	Sigma Aldrich (≥ 99 %, MO, St Louis, USA)

NMR	Value
1D-NOE-experiment	
Pulse sequence	90° pulse (12.4 µs), mixing time (100 ms), relaxation delay (16 s)
Cycle time	20 s (AQ = 4 s)
Data acquisition	32 transients, 102562 data points
Spectral width	12,820 Hz
2D-TOCSY	
Pulse sequence	90° pulse (12.4 µs), mixing time (70 ms), relaxation delay (2.4 s)
Data acquisition	16 scans, 1024 increments, 48074 data points
Spectral width	12,000 Hz (both dimensions)
HSQC	
Pulse sequence	90° pulse (12.4 µs), relaxation delay (1.25 s)
Data acquisition	128 transients, 300 increments
Spectral width	12,000 Hz (F2), 46,300 Hz (F1)

Table E.6 | Metadata of the analyzed beer samples.

Sample	Beer style	Fermen-tation	Purity Law	Grain	Abs. 294 nm	Origin	Sample	Beer style	Fermen -tation	Purity Law	Grain	Abs. 294nm	Origin
1	Wheat	top	yes	Wheat	0.048	GER	238	Lager	bottom	yes	Barley	0.330	GER
2	Lager	bottom	yes	Barley	0.083	GER	239	Lager	bottom	no	Rice	-	ESP
3	Lager	bottom	yes	Barley	0.105	GER	241	Lager	bottom	no	Rice	-	ESP
4	Craft	top	no	Barley	0.069	BEL	242	Lager	bottom	yes	Barley	0.166	GER
5	Wheat	top	yes	Wheat	0.081	GER	243	Lager	bottom	yes	Barley	0.133	GER
6	Wheat	top	yes	Wheat	0.07	GER	244	Lager	bottom	yes	Barley	0.145	GER
7	Wheat	top	yes	Wheat	-	GER	245	Lager	bottom	yes	Barley	0.115	GER
8	Lager	bottom	yes	Barley	0.077	GER	246	Lager	bottom	yes	Barley	0.129	GER
9	Lager	bottom	yes	Barley	0.162	GER	247	Lager	bottom	yes	Barley	0.186	GER
10	Lager	bottom	yes	Barley	0.14	GER	248	Lager	bottom	yes	Barley	0.111	GER
11	Wheat	top	yes	Wheat	-	GER	249	Lager	bottom	yes	Barley	0.172	GER
12	Wheat	top	yes	Wheat	0.168	GER	250	Wheat	top	yes	Wheat	0.158	GER
13	Lager	top	yes	Barley	0.17	GER	251	Wheat	top	yes	Wheat	0.18	GER
15	Lager	bottom	yes	Barley	0.067	GER	252	Lager	bottom	yes	Barley	0.129	GER
16	Lager	bottom	yes	Barley	0.053	GER	253	Wheat	top	yes	Wheat	0.137	GER
19	Wheat	top	yes	Wheat	0.136	GER	254	Lager	bottom	no	Barley	0.122	CZE
20	Wheat	top	yes	Wheat	0.149	GER	255	Wheat	top	yes	Wheat	0.159	GER
21	Wheat	top	yes	Wheat	0.144	GER	256	Wheat	top	yes	Wheat	0.137	GER
22	Lager	bottom	yes	Barley	0.138	GER	257	Wheat	top	yes	Wheat	0.156	GER
23	Lager	bottom	yes	Barley	0.298	GER	258	Wheat	top	yes	Wheat	0.185	GER
24	Lager	bottom	no	Barley	0.267	IRL	259	Wheat	top	yes	Wheat	0.235	GER
25	Wheat	top	yes	Wheat	0.2	GER	260	Lager	bottom	yes	Barley	0.177	GER
26	Lager	bottom	yes	Barley	0.356	GER	261	Lager	bottom	yes	Barley	0.167	GER
27	Lager	bottom	yes	Barley	0.142	GER	262	Lager	bottom	yes	Barley	-	GER
28	Wheat	top	yes	Wheat	0.243	GER	263	Wheat	top	yes	Wheat	-	GER
29	Wheat	top	yes	Wheat	0.224	GER	264	Lager	bottom	no	Corn	-	ESP
30	Lager	bottom	yes	Barley	0.138	GER	265	Lager	bottom	no	Corn	-	ESP
31	Wheat	top	yes	Wheat	-	GER	266	Lager	bottom	no	Corn	-	ESP
32	Craft	top	no	Barley	0.127	BEL	267	Lager	bottom	no	Corn	-	ESP

Table E.6 (continued) | Metadata of the analyzed beer samples.

Sample	Beer style	Fermen-tation	Purity Law	Grain	Abs. 294 nm	Origin	Sample	Beer style	Fermen -tation	Purity Law	Grain	Abs. 294nm	Origin
33	Wheat	top	yes	Wheat	0.264	GER	268	Lager	bottom	no	-	-	ESP
34	Wheat	top	yes	Wheat	0.074	GER	269	Lager	bottom	no	Corn	-	ESP
35	Lager	top	yes	Barley	0.136	GER	270	Lager	bottom	no	Corn	-	ESP
36	Lager	bottom	yes	Barley	0.126	GER	271	Lager	bottom	no	Corn	-	ESP
37	Lager	bottom	yes	Barley	0.42	GER	272	Lager	bottom	no	Rice	0.358	ESP
38	Wheat	top	yes	Wheat	0.124	GER	273	Craft	top	yes	Barley	-	ESP
39	Lager	bottom	yes	Barley	0.145	GER	274	Lager	bottom	no	Rice	-	ESP
41	Wheat	top	yes	Wheat	0.139	GER	275	Lager	bottom	no	Corn	0.139	ESP
43	Craft	top	yes	Barley	0.129	BEL	276	Lager	bottom	no	Corn	-	ESP
44	Lager	bottom	yes	Barley	0.122	GER	277	Lager	bottom	no	Corn	-	ESP
45	Wheat	top	yes	Wheat	0.13	GER	278	Craft	top	yes	Barley	-	ESP
46	Lager	bottom	yes	Barley	0.099	GER	279	Lager	bottom	yes	Barley	-	ESP
47	Lager	bottom	yes	Wheat	0.113	GER	280	Lager	bottom	no	Corn	-	ESP
48	Lager	bottom	yes	Barley	0.399	GER	281	Craft	top	yes	Barley	-	ESP
49	Craft	top	yes	Barley	0.203	GER	282	Craft	top	yes	Barley	0.386	ESP
50	Lager	bottom	yes	Barley	0.121	GER	283	Lager	bottom	no	Corn	-	ESP
51	Wheat	top	yes	Wheat	0.197	GER	284	Craft	top	yes	Barley	0.222	ESP
52	Wheat	top	yes	Wheat	0.149	GER	285	Lager	bottom	no	Corn	0.16	ESP
53	Lager	bottom	yes	Barley	-	GER	286	Craft	top	yes	Barley	-	ESP
54	Craft	top	no	Barley	-	BEL	287	Craft	top	yes	Barley	-	ESP
55	Craft	top	no	Wheat	0.187	LTU	288	Craft	top	no	Barley	-	BEL
56	Wheat	top	yes	Wheat	0.169	GER	289	Craft	top	no	Wheat	-	BEL
57	Craft	top	yes	Barley	0.421	GER	290	Wheat	top	no	Wheat	0.169	NLD
58	Wheat	top	yes	Wheat	0.156	GER	291	Lager	top	no	Barley	-	BEL
59	Craft	top	no	Barley	-	BEL	292	Craft	top	no	Barley	0.13	BEL
60	Craft	top	yes	Barley	0.282	GER	293	Lager	bottom	yes	Barley	0.27	HRV
61	Craft	top	yes	Wheat	0.191	GER	294	Lager	bottom	yes	Barley	-	SLO
62	Craft	top	yes	Wheat	-	GER	295	Lager	bottom	yes	Barley	-	HRV
63	Wheat	top	yes	Wheat	-	GER	296	Lager	bottom	no	Corn	-	HRV

Table E.6 (continued) | Metadata of the analyzed beer samples.

Sample	Beer style	Fermen-tation	Purity Law	Grain	Abs. 294 nm	Origin	Sample	Beer style	Fermen -tation	Purity Law	Grain	Abs. 294nm	Origin
64	Craft	top	yes	Barley	0.174	GER	297	Lager	bottom	yes	-	-	HRV
65	Craft	top	no	Barley	0.296	BEL	298	Craft	top	yes	Barley	-	HRV
66	Craft	top	no	Barley	0.33	BEL	299	Craft	top	yes	Wheat	-	HRV
67	Wheat	top	no	Wheat	0.167	GER	300	Lager	bottom	yes	Barley	0.252	HRV
68	Lager	bottom	yes	Barley	0.218	GER	301	Craft	top	yes	Barley	-	HRV
69	Wheat	top	no	Wheat	0.095	BEL	302	Lager	bottom	no	Barley	-	HRV
70	Lager	bottom	yes	Barley	0.048	NAM	303	Wheat	top	yes	Wheat	-	HRV
71	Lager	bottom	yes	Barley	-	DNK	304	Lager	bottom	yes	Barley	-	HRV
72	Lager	bottom	yes	Barley	-	GER	305	Wheat	top	yes	Wheat	-	HRV
73	Lager	bottom	yes	Barley	-	GER	306	Lager	bottom	yes	Barley	-	JPN
76	Wheat	top	yes	Wheat	0.279	GER	307	Lager	bottom	no	Rice	-	JPN
78	Craft	top	yes	Barley	0.275	GER	308	Lager	top	yes	Wheat	-	JPN
80	Lager	bottom	no	Rice	0.112	GER	309	Lager	bottom	no	Rice	-	JPN
81	Craft	top	yes	Barley	0.222	GER	310	Craft	top	yes	Barley	-	USA
83	Lager	bottom	yes	Barley	0.243	GER	311	Lager	bottom	no	Rice	-	JPN
85	Craft	top	yes	Wheat	-	GER	312	Lager	bottom	no	Rice	-	JPN
86	Craft	top	yes	Barley	0.238	GER	313	Lager	bottom	no	Rice	-	JPN
90	Craft	top	yes	Barley	0.136	GER	314	Wheat	top	no	Wheat	-	FRA
91	Lager	bottom	no	Barley	0.099	CUB	315	Lager	top	no	Barley	-	FRA
92	Lager	bottom	no	Barley	0.063	CUB	317	Lager	bottom	no	-	-	ESP
93	Lager	bottom	yes	Barley	0.232	MEX	318	Lager	bottom	no	Rice	-	ESP
94	Lager	bottom	yes	Barley	0.134	MEX	319	Lager	bottom	no	Corn	-	ESP
95	Lager	bottom	no	Rice	0.086	CHN	320	Lager	bottom	no	Corn	-	ESP
96	Lager	bottom	yes	Barley	0.16	PER	321	Lager	bottom	no	Rice	-	ESP
97	Lager	bottom	no	Corn	0.1	ARG	322	Lager	bottom	no	-	-	ESP
98	Lager	bottom	yes	Barley	-	PER	323	Lager	bottom	no	Corn	-	ESP
99	Lager	bottom	no	Barley	0.137	ESP	324	Lager	bottom	no	Rice	-	ESP
100	Craft	top	no	-	-	BRA	325	Lager	bottom	no	-	-	ESP
101	Craft	top	no	Rice	0.189	JPN	326	Lager	bottom	yes	Barley	-	ESP
102	Wheat	top	no	Wheat	0.116	NDL	327	Lager	bottom	no	Rice	-	ESP

Table E.6 (continued) | Metadata of the analyzed beer samples.

Sample	Beer style	Fermen-tation	Purity Law	Grain	Abs. 294 nm	Origin	Sample	Beer style	Fermen -tation	Purity Law	Grain	Abs. 294nm	Origin
103	Lager	bottom	no	Barley	0.104	KOR	328	Lager	bottom	no	Corn	-	ESP
104	Craft	top	yes	Barley	-	GER	329	Lager	bottom	no	Corn	-	ESP
105	Craft	top	no	Wheat	0.121	BEL	330	Lager	bottom	no	Corn	-	ESP
106	Craft	top	yes	Wheat	0.36	BEL	331	Lager	bottom	no	Rice	-	ESP
107	Craft	top	no	Barley	0.192	BEL	333	Lager	bottom	yes	Barley	-	ESP
108	Craft	top	no	Wheat	0.107	BEL	334	Lager	bottom	no	Rice	-	PHL
109	Craft	top	yes	Barley	0.368	BEL	335	Lager	bottom	no	Rice	-	THA
110	Craft	top	yes	Barley	0.204	NDL	336	Lager	bottom	no	Rice	-	TWN
111	Lager	bottom	yes	Barley	0.134	NDL	337	Lager	bottom	no	Rice	-	SGP
112	Craft	top	yes	Barley	0.219	NDL	357	Craft	top	yes	Wheat	-	GER
113	Lager	bottom	yes	Barley	0.167	GER	358	Lager	bottom	yes	Barley	-	GER
114	Lager	bottom	yes	Barley	0.127	SGP	360	Craft	top	no	-	-	MEX
116	Craft	top	no	Barley	0.238	BEL	361	Lager	bottom	no	-	-	MEX
117	Craft	top	yes	Wheat	0.167	BEL	362	Lager	bottom	no	-	-	MEX
118	Craft	top	yes	Wheat	-	BEL	363	Lager	bottom	yes	-	-	MEX
119	Craft	top	yes	Barley	0.709	NDL	364	Craft	top	no	Wheat	-	ZAF
121	Craft	top	yes	Wheat	-	BEL	365	Craft	top	no	Barley	-	USA
123	Craft	top	no	Wheat	0.132	NDL	366	Lager	bottom	no	-	-	EGY
124	Craft	top	yes	Wheat	0.418	GER	367	Wheat	top	yes	Wheat	-	NAM
125	Craft	top	no	Barley	0.276	BEL	368	Craft	top	yes	Barley	-	ZAF
126	Craft	top	yes	Wheat	-	BEL	369	Lager	bottom	yes	Barley	-	ZAF
127	Lager	bottom	yes	Barley	0.334	GER	370	Craft	top	yes	Barley	-	USA
128	Craft	top	yes	Barley	0.657	GER	371	Wheat	top	yes	Wheat	-	GER
129	Lager	bottom	yes	Barley	0.197	NDL	372	Wheat	top	yes	Wheat	-	ZAF
130	Craft	top	no	Barley	0.353	BEL	373	Lager	bottom	no	-	-	ARG
131	Craft	top	yes	Barley	0.144	BEL	374	Lager	bottom	no	-	-	ARG
132	Craft	top	no	Barley	0.183	BEL	375	Lager	bottom	yes	Barley	-	ZAF
133	Craft	top	no	Wheat	0.187	BEL	376	Lager	bottom	yes	Barley	-	BRA
134	Craft	top	no	Barley	-	BEL	377	Lager	bottom	no	-	-	BRA

Table E.6 (continued) | Metadata of the analyzed beer samples.

Sample	Beer style	Fermen-tation	Purity Law	Grain	Abs. 294 nm	Origin	Sample	Beer style	Fermen -tation	Purity Law	Grain	Abs. 294nm	Origin
136	Lager	bottom	yes	Barley	0.095	FRA	378	Lager	bottom	no	-	-	MEX
137	Wheat	top	yes	Wheat	-	GER	379	Lager	bottom	no	Corn	-	MEX
138	Craft	top	no	Wheat	0.076	BEL	380	Craft	top	yes	Barley	-	USA
139	Lager	bottom	no	Barley	0.128	IND	381	Lager	bottom	no	Rice	-	JPN
140	Lager	bottom	yes	Barley	0.288	GER	382	Lager	bottom	no	Rice	-	CHN
141	Lager	bottom	yes	Barley	0.409	GER	383	Lager	bottom	no	Corn	-	BRA
142	Lager	bottom	yes	Barley	0.177	GER	385	Lager	bottom	yes	Barley	-	CHE
143	Lager	bottom	yes	Barley	0.137	GER	386	Craft	top	yes	-	-	CHN
144	Lager	bottom	yes	Barley	0.086	GER	387	Craft	top	yes	Barley	-	USA
145	Lager	bottom	no	Barley	0.102	MEX	388	Lager	bottom	no	-	-	BRA
146	Lager	bottom	yes	Barley	0.095	BEL	389	Craft	top	no	Barley	0.627	ESP
147	Lager	bottom	yes	Barley	0.326	GER	390	Craft	top	no	Barley	-	ESP
148	Lager	bottom	yes	Barley	0.153	GER	391	Lager	bottom	no	Rice	-	MEX
149	Craft	top	no	Barley	0.19	BEL	392	Lager	bottom	yes	Barley	-	FRA
151	Craft	top	no	Corn	0.189	FRA	393	Craft	top	yes	Barley	-	ITA
152	Wheat	top	yes	Wheat	0.118	GER	394	Craft	top	no	Rice	0.709	ITA
153	Lager	bottom	yes	Barley	0.147	GER	395	Craft	top	no	Wheat	-	ITA
154	Lager	bottom	yes	Barley	0.146	GER	396	Craft	top	yes	Barley	-	ITA
155	Wheat	top	yes	Wheat	0.349	GER	397	Craft	top	yes	Wheat	-	ITA
156	Craft	top	no	Corn	0.287	FRA	398	Craft	top	yes	Barley	0.46	ESP
157	Lager	bottom	yes	Barley	0.184	GER	399	Craft	top	yes	Barley	-	CRO
159	Lager	bottom	yes	Barley	0.123	GER	400	Craft	top	no	Wheat	-	ESP
160	Lager	bottom	no	Corn	-	CHN	401	Craft	top	yes	Barley	-	GRE
161	Lager	bottom	no	-	0.118	ITA	402	Craft	top	no	Wheat	-	EST
162	Lager	bottom	no	Barley	0.12	PHL	404	Craft	top	no	Wheat	-	GRE
163	Lager	bottom	yes	Barley	0.112	GER	405	Craft	top	no	Wheat	-	CAT
164	Lager	bottom	no	-	0.115	GBR	406	Craft	top	yes	Barley	-	POR
165	Lager	bottom	yes	Barley	0.137	GER	407	Lager	bottom	no	Rice	-	CHN
166	Lager	bottom	no	Rice	0.126	THA	408	Lager	bottom	no	-	-	ITA
167	Lager	bottom	no	Corn	0.124	ITA	409	Craft	top	no	Wheat	-	FRA

Table E.6 (continued) | Metadata of the analyzed beer samples.

Sample	Beer style	Fermen-tation	Purity Law	Grain	Abs. 294 nm	Origin	Sample	Beer style	Fermen -tation	Purity Law	Grain	Abs. 294nm	Origin
168	Lager	bottom	no	Rice	0.114	CHN	410	Lager	bottom	no	Rice	-	VAT
169	Lager	bottom	no	Corn	0.132	ITA	411	Lager	bottom	no	Corn	-	CHN
170	Lager	bottom	no	Rice	0.088	GTM	412	Lager	bottom	no	Wheat	-	NLD
171	Lager	bottom	no	Rice	0.088	GTM	413	Lager	bottom	no	Rice	-	CHN
172	Lager	bottom	no	Corn	0.089	CRI	414	Lager	bottom	yes	Barley	-	GER
173	Lager	bottom	no	Rice	0.084	NIC	416	Craft	top	yes	Barley	0.247	GER
174	Craft	top	yes	Barley	0.153	FIN	417	Craft	top	yes	Barley	0.685	NDL
175	Lager	bottom	no	Barley	0.103	FIN	418	Craft	top	yes	Barley	0.456	GBR
177	Craft	top	yes	Barley	0.331	FIN	419	Craft	top	yes	Barley	0.457	GBR
178	Lager	bottom	yes	Barley	0.108	LUX	420	Craft	top	no	Barley	0.367	GER
179	Lager	bottom	yes	Barley	0.123	FRA	421	Craft	top	no	Barley	0.435	GBR
180	Lager	bottom	yes	Barley	0.188	LUX	422	Craft	top	no	Barley	0.613	GER
182	Craft	top	yes	Barley	0.183	NZL	424	Craft	top	no	Barley	0.687	BEL
191	Lager	bottom	no	Corn	0.135	BEL	425	Craft	top	no	Barley	0.432	GBR
192	Lager	bottom	yes	Barley	-	GER	426	Craft	top	yes	Barley	-	GER
193	Lager	bottom	yes	Barley	0.121	GER	427	Craft	top	yes	Barley	0.804	GER
194	Lager	bottom	yes	Wheat	0.525	GER	428	Craft	top	yes	Barley	0.196	GER
197	Craft	top	no	Barley	0.262	GER	429	Lager	bottom	yes	Barley	0.18	GER
198	Craft	top	no	Wheat	-	POL	430	Craft	top	yes	Barley	0.393	GBR
199	Craft	top	no	Barley	-	POL	431	Craft	top	yes	Barley	0.466	BEL
200	Wheat	top	yes	Wheat	0.152	GER	432	Craft	top	yes	Barley	0.679	GER
201	Lager	bottom	yes	Barley	0.098	CHE	433	Lager	bottom	yes	Barley	-	GER
202	Craft	top	no	Wheat	0.155	POL	434	Lager	bottom	yes	Barley	-	GER
203	Lager	bottom	yes	Barley	0.168	ZAF	435	Lager	bottom	yes	Barley	-	GER
205	Lager	bottom	yes	Barley	0.127	CHE	436	Lager	bottom	yes	Barley	-	GER
206	Lager	bottom	no	Barley	0.966	POL	437	Craft	top	no	Rice	-	BEL
207	Craft	top	no	Wheat	0.781	POL	438	Craft	top	yes	Barley	-	BEL
208	Lager	bottom	yes	Barley	0.163	GER	439	Craft	top	no	Wheat	-	BEL
209	Lager	bottom	yes	Barley	0.193	POL	440	Craft	top	yes	Barley	-	NLD

Table E.6 (continued) | Metadata of the analyzed beer samples.

Sample	Beer style	Fermen-tation	Purity Law	Grain	Abs. 294 nm	Origin	Sample	Beer style	Fermen -tation	Purity Law	Grain	Abs. 294nm	Origin
210	Craft	top	no	Barley	-	POL	441	Craft	top	no	Wheat	-	NLD
211	Craft	top	yes	Barley	0.89	POL	442	Wheat	top	no	Wheat	-	NLD
212	Craft	top	yes	Barley	0.155	HUN	443	Lager	bottom	yes	Barley	-	NLD
213	Lager	bottom	no	Rice	0.145	ESP	444	Lager	bottom	yes	Barley	-	BEL
214	Lager	bottom	yes	Barley	0.168	GER	445	Craft	top	yes	Barley	-	NLD
215	Craft	top	yes	Barley	0.185	GER	446	Craft	top	no	Wheat	-	BEL
216	Lager	bottom	yes	Barley	0.157	GER	447	Craft	top	yes	Barley	-	GER
217	Wheat	top	yes	Wheat	0.249	GER	448	Craft	top	yes	Barley	-	NLD
218	Craft	top	yes	Barley	0.134	GER	449	Craft	top	no	Wheat	-	BEL
219	Craft	top	yes	Barley	0.27	GER	450	Lager	bottom	yes	Wheat	-	GER
220	Craft	top	yes	Barley	0.208	GER	451	Craft	top	no	Barley	-	BEL
221	Craft	top	yes	Wheat	0.132	GER	452	Craft	top	no	Rice	-	BEL
222	Lager	bottom	no	-	0.114	JPN	453	Wheat	top	yes	Wheat	-	GER
223	Lager	bottom	yes	Barley	0.569	GER	454	Craft	top	no	Barley	-	BEL
224	Lager	bottom	yes	Barley	0.211	GER	455	Lager	bottom	no	Barley	-	IRL
226	Lager	bottom	yes	Barley	0.238	GER	456	Craft	top	no	Barley	-	BEL
227	Wheat	top	yes	Wheat	0.207	GER	457	Lager	bottom	yes	Barley	-	GER
228	Lager	bottom	no	Corn	0.14	ESP	458	Lager	bottom	yes	Barley	-	GER
229	Lager	bottom	no	Corn	0.158	ESP	459	Lager	bottom	yes	Barley	-	ISR
230	Lager	bottom	no	Corn	0.143	ESP	460	Lager	bottom	yes	-	-	ISR
231	Lager	bottom	no	Corn	0.096	ESP	464	Lager	bottom	no	Rice	-	THA
232	Lager	bottom	no	-	0.193	ESP	465	Lager	bottom	no	Rice	-	THA
235	Lager	bottom	no	Corn	-	ESP	467	Lager	bottom	no	Rice	-	THA
236	Lager	bottom	no	Corn	-	ESP	B1885	-	-	-	-	-	GER
237	Lager	bottom	no	Corn	-	ESP	B2019	Lager	bottom	no	Barley	-	GER

Table E.7 | Score values of the samples.

Sample	Beer style		Fermentation		Purity Law		Grain			Abs. 294nm	
	PC1	PC2	PC1	PC2	PC1	PC2	PC1	PC2	PC3	PC1	PC2
1	-2.49	18.71	8.09	19.04	10.21	37.73	-10.17	-15.51	-2.89	-23.81	-27.70
2	-12.73	-3.39	-10.99	12.35	9.92	14.49	12.52	3.04	-3.47	-21.97	8.11
3	-12.17	-4.88	-10.78	10.09	8.98	12.79	12.51	2.05	-3.08	-18.21	7.10
4	7.31	-1.20	9.23	22.08	-11.14	22.15	6.82	3.37	-2.66	-15.56	-11.13
5	-4.45	38.37	15.09	20.97	9.73	17.99	-9.66	-21.02	1.51	-19.03	2.17
6	-0.45	37.37	16.56	27.06	8.07	20.35	-12.96	-19.25	1.08	-19.08	-4.65
7	0.23	33.60	12.43	16.11	6.86	6.03	-13.62	-15.55	-1.76	-	-
8	-11.47	-0.62	-9.81	8.70	10.17	10.93	12.91	4.77	-4.67	-12.76	7.19
9	-11.93	-1.82	-7.94	12.82	8.74	8.83	13.78	4.32	-4.56	-14.46	15.44
10	-6.12	-5.86	-5.67	16.65	11.82	22.02	13.24	0.79	1.53	-16.11	-3.10
11	-4.87	16.82	7.72	24.42	6.92	56.56	-11.85	-15.11	-3.19	-	-
12	-3.01	22.54	9.88	31.99	7.25	43.59	-6.94	-12.22	0.18	-12.31	-34.56
13	-3.71	-0.12	8.86	13.28	7.1	5.14	10.69	2.44	-1.17	-6.44	12.25
15	-11.67	-3.13	-11.46	14.76	10.72	35.14	9.63	0.54	-2.98	-14.69	-25.25
16	-8.58	-3.32	-8.04	13.01	10.81	23.79	13.28	-0.06	-1.19	-15.27	-11.26
19	-2.69	30.88	13.74	22.81	12.02	22.16	-8.94	-20.70	-1.25	-16.06	-9.15
20	-2.83	19.92	7.45	26.28	8.81	41.92	-8.29	-13.93	-0.91	-9.33	-37.09
21	-4.69	16.65	4.44	29.15	8.31	48.9	-5.72	-11.01	-0.84	-10.77	-44.02
22	-9.52	0.92	-9.08	21.46	6.83	46.27	5.59	2.60	-1.54	-8.76	-40.99
23	-8.54	0.15	-9.53	20.43	8.83	37.36	10.77	2.02	-1.73	5.03	-32.73
24	-2.70	0.61	-4.22	18.73	-12.6	10.23	6.21	0.44	-0.81	4.31	-41.97
25	1.37	14.36	8.32	17.12	8.91	36.83	-8.52	-9.14	-0.51	-2.84	-35.34
26	-7.95	2.08	-7.10	-5.85	9.56	14.23	11.81	2.94	0.07	15.86	-14.37
27	-10.64	-0.43	-10.67	17.31	10.49	40.15	11.68	1.50	-0.93	-13.04	-30.83
28	-0.74	15.59	7.07	29.31	8.29	49.96	-3.74	-10.63	-0.47	-5.76	-49.19
29	3.23	19.77	11.63	27.09	8.2	40.03	-6.59	-16.52	2.29	-2.76	-40.17

Table E.7 (continued) | Score values of the samples.

Sample	Beer style		Fermentation		Purity Law		Grain			Abs. 294nm	
	PC1	PC2	PC1	PC2	PC1	PC2	PC1	PC2	PC3	PC1	PC2
30	-7.55	0.74	-6.40	23.19	7.84	44.88	7.55	0.96	-0.91	-8.95	-39.33
31	-3.77	19.29	5.48	22.72	7.86	42.17	-5.18	-12.49	-0.94	-	-
32	7.89	-0.18	8.09	12.46	-10.38	15.85	1.61	2.12	-2.80	-1.88	-15.79
33	4.99	26.91	18.02	9.88	9	3.35	-8.42	-18.95	1.37	2.32	0.87
34	1.49	26.47	14.26	25.64	7.94	31.34	-8.56	-15.34	0.73	-15.55	-23.69
35	-1.97	-3.74	6.78	12.85	6.38	3.7	11.10	1.40	-1.66	-15.67	11.34
36	-7.11	-1.89	-6.28	15.89	7.49	30.83	11.28	-0.62	0.93	-13.08	-22.63
37	-9.70	-4.30	-9.55	-43.99	8.86	-22.05	11.82	0.07	-3.80	26.69	14.41
38	-4.10	21.09	8.05	16.41	9.85	28.66	-4.43	-14.77	0.92	-7.65	-23.43
39	-13.38	0.77	-11.25	13.37	9.72	32.69	8.18	0.82	-2.30	-9.73	-23.64
41	2.66	23.31	12.59	21.74	6.61	28.66	-8.66	-15.30	-1.60	-9.36	-26.09
43	5.53	2.23	8.31	22.83	8.67	-23.58	1.12	0.01	-1.47	-10.17	-22.29
44	-9.24	-0.42	-8.54	16.77	10.45	39.04	10.74	-0.49	-0.77	-13.01	-31.16
45	-2.76	25.17	10.93	23.33	9.5	29.8	-5.70	-16.65	0.41	-13.30	-21.83
46	-4.10	0.60	-7.18	19.67	8.26	54.12	4.31	-2.46	-1.22	-14.38	-51.72
47	0.27	1.67	-2.86	19.98	7.59	54.02	-1.26	-9.82	-1.79	-12.16	-54.36
48	-5.43	4.40	-5.55	1.98	8.28	30.96	5.37	-0.88	0.19	12.43	-36.68
49	12.35	-4.37	9.19	25.73	7.98	39.96	6.75	-0.21	0.41	-5.39	-37.84
50	-8.37	-0.53	-6.27	20.81	8.49	33.3	11.93	4.27	-0.35	-14.11	-17.22
51	-4.16	30.37	11.54	24.81	6.93	25.99	-11.96	-15.43	-0.48	-10.74	-13.69
52	-0.31	30.03	14.26	25.42	8.21	25.46	-10.10	-17.32	1.61	-9.98	-17.49
53	-12.59	-7.15	-9.17	5.91	9.9	-17.51	10.06	2.68	-4.19	-	-
54	12.35	4.06	9.89	17.73	-6.77	37.4	1.92	-2.42	-0.51	-	-
55	16.90	-3.53	12.23	28.42	-13.1	-12.56	1.71	-10.12	0.45	-4.31	-51.46
56	-3.20	29.92	12.31	16.32	11.21	15.23	-7.74	-17.72	-2.61	-11.90	-2.91
57	20.63	-8.00	17.04	-0.56	7.75	-8.37	8.26	0.26	0.81	24.15	2.90
58	-1.36	21.58	10.60	24.09	6.97	29.61	-6.63	-16.50	0.35	-12.79	-22.32
59	19.47	-4.47	11.01	6.11	-12.62	20.23	3.16	0.01	-1.76	-	-
60	16.95	-10.89	13.97	5.44	10.84	-4.37	11.52	1.58	-1.34	7.90	7.91
61	12.47	-2.92	8.22	14.03	10.13	37.72	-3.40	-13.26	-2.84	-5.00	-37.91

Table E.7 (continued) | Score values of the samples.

Sample	Beer style		Fermentation		Purity Law		Grain			Abs. 294nm	
	PC1	PC2	PC1	PC2	PC1	PC2	PC1	PC2	PC3	PC1	PC2
62	17.28	2.41	13.95	15.51	9.8	16.62	-9.37	-18.90	-2.35	-	-
63	1.95	38.48	8.99	19.05	8.6	2	-8.04	-21.04	3.15	-	-
64	10.88	-5.03	9.99	16.79	9.15	17.82	11.89	-1.60	1.09	-6.50	-11.08
65	22.76	-5.07	18.52	19.54	-13.98	10.38	9.29	-0.12	0.73	7.67	-13.49
66	21.18	-2.42	16.33	20.51	-9.03	31.95	9.30	2.13	-0.63	16.03	-41.61
67	2.54	18.29	11.88	17.72	-13.96	5.19	-6.47	-15.98	3.09	-11.22	-13.44
68	-7.48	4.30	-8.37	-2.92	7.84	26	5.74	0.03	-0.18	10.33	-30.25
69	6.32	12.31	13.12	21.92	-5.89	17.11	-3.11	-11.65	0.29	-11.67	-12.10
70	-8.38	-0.90	-6.92	17.51	10.2	29.75	13.47	-0.21	0.69	-16.96	-17.33
71	-9.69	0.03	-7.87	15.80	5.01	28.84	7.36	3.29	1.51	-	-
72	-13.46	-0.58	-12.35	16.73	7.22	35.93	7.49	3.97	-1.99	-	-
73	-11.69	-0.29	-11.41	12.10	9.22	35.9	6.77	-0.09	0.13	-	-
76	2.47	23.28	13.95	20.77	6.94	27.51	-6.77	-17.28	0.80	-1.61	-25.14
78	15.57	-4.52	12.33	13.58	8.83	18.92	8.18	1.00	3.24	7.10	-19.26
80	-6.51	1.53	-8.55	22.47	-8.81	41.04	-6.24	9.88	5.59	-13.73	-34.93
81	18.50	-5.15	13.07	22.02	7.33	32.54	3.03	-1.42	0.85	0.29	-35.04
83	-0.91	-1.04	-5.08	7.10	9.22	25.71	7.43	0.08	0.52	0.66	-23.88
85	8.48	1.52	8.58	20.20	8.19	36.46	-2.96	-8.99	-0.42	-	-
86	12.85	-6.87	9.67	24.77	10.41	33.05	11.70	-0.15	0.00	-4.88	-29.43
90	21.13	-8.34	15.99	5.82	7.87	22.74	11.99	0.92	-5.30	-7.23	-12.27
91	-9.52	-5.74	-9.07	-20.94	-11.07	-54.1	11.55	2.63	-5.10	-11.47	91.02
92	-12.89	-5.46	-11.22	-16.75	-12.74	-44.83	10.77	1.89	-0.03	-13.31	83.30
93	-17.47	-4.68	-13.26	-75.35	9.65	-87.94	6.00	3.35	-2.48	4.71	115.18
94	-13.40	-1.88	-10.28	-23.77	8.87	-53.57	3.62	0.19	-1.35	-10.99	98.66
95	-16.81	-4.29	-14.50	-13.73	-12.55	-29.81	-14.49	15.68	21.56	-18.96	62.05
96	-11.74	-8.64	-10.40	-19.03	9.06	-52.37	9.06	0.08	-2.87	-4.52	97.57
97	-9.67	-4.26	-11.80	-9.41	-12.01	-31.78	-24.39	13.00	-14.70	-13.51	59.39
98	-6.23	-4.21	-11.15	-32.93	9.65	-11.11	6.07	1.04	-2.13	-	-
99	-21.19	-1.34	-20.06	-40.91	-10.62	-96.16	13.66	8.35	-0.52	-22.13	120.42

Table E.7 (continued) | Score values of the samples.

Sample	Beer style		Fermentation		Purity Law			Grain		Abs. 294nm	
	PC1	PC2	PC1	PC2	PC1	PC2	PC1	PC2	PC3	PC1	PC2
100	21.90	-5.67	13.86	19.87	-11.28	36.31	-	-	-	-	-
101	23.45	-4.20	14.83	-26.95	-11.26	-81.44	-18.30	18.25	26.14	-11.44	95.13
102	5.70	23.88	14.56	13.88	-11.88	-17.9	-13.43	-19.55	1.58	-23.96	33.81
103	-7.59	-5.73	-12.96	11.03	-13.21	-11.83	10.37	-1.35	-2.45	-18.51	41.82
104	23.15	-8.47	16.18	8.85	6.03	27.6	11.51	2.16	-6.88	-	-
105	20.77	5.00	16.62	20.73	-14.26	-2.84	-7.88	-17.88	-0.44	-15.50	12.74
106	21.41	-2.24	13.30	-46.70	11	-44.98	-7.41	-16.59	-1.48	23.71	30.93
107	14.14	-7.99	13.14	4.18	-12.5	-16.67	8.99	1.26	-2.46	-2.53	28.73
108	20.62	9.49	17.98	20.29	-11.49	-8.57	-9.76	-18.63	1.97	-19.78	22.44
109	20.27	-8.74	11.81	-38.07	9.24	-26.19	7.39	2.91	-2.80	30.66	8.53
110	14.91	-10.65	12.05	-6.72	8.2	-28.12	9.67	-2.63	0.83	-3.80	39.01
111	-10.62	-6.53	-10.85	-8.40	7.64	-26.6	12.12	-0.35	-4.84	-16.64	55.60
112	21.24	-11.42	14.68	4.49	9.23	-14.94	6.44	0.04	3.26	-1.97	24.84
113	-9.09	-6.27	-10.10	-19.08	9.2	-21.14	9.44	-2.37	1.11	-6.36	33.97
114	-9.41	-5.82	-9.82	10.38	6.59	20.65	3.20	3.05	-1.83	-13.86	-0.22
116	10.96	-4.08	11.34	9.72	-9.74	3.61	8.62	-0.29	-1.57	0.21	1.68
117	22.81	-2.24	14.00	12.41	8.68	17.16	-9.03	-18.22	1.82	-8.82	13.30
118	19.85	-2.24	11.02	22.26	10.26	25.39	-8.42	-15.82	1.77	-	-
119	23.64	-7.28	15.28	-51.34	10.7	-39.59	5.09	-0.66	-0.43	65.38	6.25
121	22.04	-4.52	13.03	8.73	7.44	24.18	-7.53	-11.73	-1.18	-	-
123	10.61	-6.65	8.18	8.02	-11.82	-0.15	-3.10	-7.00	-0.23	-10.17	3.90
124	13.98	4.70	12.53	-46.04	9.23	-29.77	-7.25	-13.71	-0.73	42.16	3.04
125	25.04	-6.73	19.27	15.39	-13.35	-1.87	13.47	1.49	2.76	7.81	2.60
126	25.91	-7.60	12.24	-2.90	10.37	10.18	-7.98	-16.55	-0.03	-	-
127	-7.66	-7.68	-11.38	-59.61	8.6	-54.21	11.73	2.54	-2.62	18.61	51.27
128	18.38	-4.93	18.46	-120.22	8.6	-102.19	11.24	-2.33	0.81	59.31	63.90
129	-4.21	-1.11	-9.26	-3.63	11.74	23.02	9.33	-3.86	-1.26	-4.02	-17.39
130	25.35	-3.73	14.98	-8.19	-12.03	-5.14	9.75	1.07	-0.19	25.45	-13.53
131	11.93	-4.37	9.16	14.54	7.93	-31.16	4.16	-1.38	2.16	-8.50	-8.64
132	20.36	-8.44	13.77	5.28	-14.2	-0.56	10.36	0.48	1.06	0.54	-4.60

Table E.7 (continued) | Score values of the samples.

Sample	Beer style		Fermentation		Purity Law		Grain			Abs. 294nm	
	PC1	PC2	PC1	PC2	PC1	PC2	PC1	PC2	PC3	PC1	PC2
133	22.58	0.29	18.52	16.60	-9.59	-1.13	-1.99	-16.74	4.15	-6.35	1.14
134	27.70	-10.25	13.69	-15.80	-13.88	-26.37	12.90	4.48	-4.32	-	-
136	-10.51	-8.68	-12.67	11.12	9.86	13.22	5.58	2.42	-5.36	-11.34	10.41
137	10.40	28.94	15.78	-102.03	8.32	-124.5	-5.15	-17.09	-3.08	-	-
138	12.32	5.29	11.82	25.05	-11.27	14.21	-4.78	-16.36	3.84	-19.21	1.70
139	-17.01	-7.52	-13.57	-24.49	-14.69	-28.51	13.74	-3.22	-0.44	-11.68	50.97
140	-8.56	-4.24	-10.70	-26.77	8.17	-16.66	14.51	1.68	-2.39	12.70	29.44
141	-18.12	-7.64	-17.34	-75.98	5.72	-50.19	11.58	0.72	-5.31	26.87	47.36
142	-9.20	-2.81	-8.28	-9.62	5.77	7.21	10.11	2.96	1.34	7.39	-0.99
143	-13.07	-5.51	-12.07	15.84	11.82	20.39	15.90	0.31	-1.23	-8.98	6.68
144	-15.29	-4.86	-14.69	13.60	7.36	32.13	10.23	3.85	-0.46	-14.60	-18.97
145	-11.92	-4.66	-13.46	11.93	-12.52	21.61	4.53	2.71	1.64	-11.46	-14.60
146	-6.93	-5.35	-9.40	17.72	7.62	-9.68	6.76	1.44	-0.38	-18.19	-7.67
147	-9.96	-1.97	-9.49	-29.86	8.67	-13.9	10.92	0.71	-2.59	17.54	14.65
148	-13.71	-3.42	-12.43	2.48	8.9	10.86	9.12	0.00	-1.85	-10.45	3.31
149	18.16	-6.68	14.70	20.24	-12.11	22.18	4.98	-1.50	-1.68	-0.74	-25.19
151	6.29	-4.09	5.59	13.36	-11.52	23.27	-13.99	7.89	-11.48	0.48	-23.95
152	8.04	24.93	15.37	18.04	7.7	15.43	-7.77	-18.24	4.39	-8.55	-14.59
153	-16.49	-5.03	-16.12	-3.16	7.49	24.17	4.09	2.67	-2.73	-10.22	-0.65
154	-10.98	-5.60	-10.69	12.71	5.3	26.19	7.68	5.30	-2.03	-9.67	-12.10
155	5.08	32.30	16.50	5.95	9.85	-7.06	-13.21	-21.20	3.11	8.94	9.10
156	12.42	-3.18	11.09	6.79	-10.05	16.82	-13.20	6.74	-11.84	11.27	-23.09
157	-11.53	-4.61	-10.16	6.35	5.4	14.5	9.92	3.12	-1.17	-8.77	-0.99
159	-14.18	-6.38	-13.05	-13.03	11.48	-36.2	16.03	0.63	-5.86	-18.25	70.40
160	-15.14	-2.41	-16.52	-29.24	-10.75	-56.76	-22.79	12.01	-18.87	-	-
161	-12.10	-7.33	-11.91	-15.52	-12.49	-87.17	-	-	-	-9.62	35.76
162	-14.64	-4.68	-12.65	-3.69	-13.02	-18.4	12.62	0.13	2.43	-10.64	43.18
163	-16.50	-4.40	-11.53	13.99	9.23	27.76	10.66	1.75	-0.25	-14.64	-5.94
164	-5.81	-0.45	-6.23	19.14	-12.63	26.88	-	-	-	-11.53	-17.07

Table E.7 (continued) | Score values of the samples.

Sample	Beer style		Fermentation		Purity Law		Grain			Abs. 294nm	
	PC1	PC2	PC1	PC2	PC1	PC2	PC1	PC2	PC3	PC1	PC2
165	-16.99	-7.57	-13.88	0.23	5.56	-2.25	5.99	5.31	0.68	-13.07	26.77
166	-17.99	-4.19	-15.74	7.34	-13.13	12.03	-12.87	17.61	11.63	-13.69	6.15
167	-14.19	-4.29	-13.19	13.32	-11.06	21.33	-16.64	13.28	-4.16	-12.80	-5.68
168	-10.33	-6.41	-11.73	12.89	-12.66	19.14	-10.77	12.65	13.34	-10.41	-8.20
169	-15.61	-2.63	-13.24	15.16	-7.59	28.01	-13.20	12.15	-8.45	-14.33	-12.67
170	-13.48	-1.59	-12.03	17.79	-7.97	32.5	-3.89	10.07	5.34	-15.40	-23.30
171	-15.24	-2.64	-11.95	12.71	-10.73	16.23	-7.03	13.15	6.27	-17.97	-0.79
172	-14.39	-2.50	-14.89	14.42	-9.05	33.67	-14.62	13.55	-8.73	-13.35	-26.43
173	-12.03	0.68	-10.88	13.62	-11.83	19.92	-11.25	12.81	4.86	-18.96	-8.87
174	12.41	-9.62	9.99	-4.51	9.71	-18.52	9.87	0.80	3.86	-4.74	25.71
175	-7.48	0.43	-8.08	19.96	-8.08	30.55	4.61	1.46	0.81	-13.02	-23.40
177	21.50	-9.50	17.15	-26.26	8.24	-25.61	10.19	-1.01	2.80	24.15	12.80
178	-10.72	-3.55	-11.03	14.24	4.77	33.66	7.37	4.22	-0.11	-17.43	-23.85
179	-8.99	0.09	-7.91	16.90	8.17	39.19	3.79	3.96	0.57	-8.93	-29.61
180	-4.50	-5.14	-8.14	2.28	9.42	22.05	6.84	0.26	-4.08	-3.74	-17.58
182	14.68	-7.56	10.78	-39.48	10.15	-62.65	9.41	3.02	4.40	-12.81	73.81
191	-10.47	-4.69	-8.56	5.02	-12.51	-6.63	-13.70	11.39	-12.70	-11.41	27.72
192	-8.46	-6.77	-9.44	7.60	8.78	10.76	13.19	2.03	3.89	-	-
193	-17.01	-5.40	-12.84	-115.35	5.91	-79.49	10.37	-0.50	-3.57	-22.50	80.91
194	-19.78	-6.80	-12.17	-154.41	8.59	-105.39	-10.53	-15.45	-4.21	36.33	73.14
197	12.11	-0.75	12.36	-8.03	-9.95	-17.68	4.59	0.53	-0.75	6.64	18.76
198	12.83	-4.34	7.73	21.50	-10.96	30.61	-6.23	-8.59	-0.74	-	-
199	18.29	-5.17	11.09	5.36	-10	2.13	12.61	1.55	2.35	-	-
200	0.99	36.42	17.57	18.50	7.16	12.05	-15.86	-21.90	0.21	-16.19	-1.67
201	-11.68	-7.04	-11.96	9.82	5	5.37	8.63	5.08	-1.72	-17.52	17.00
202	22.36	-0.21	15.61	15.90	-11.77	-8.14	-12.53	-20.72	4.45	-11.37	8.31
203	-14.17	-8.17	-11.16	-7.52	9.89	-9.1	10.40	3.99	1.49	-6.57	30.79
205	-13.42	-4.14	-11.62	11.62	3.4	15.3	4.91	5.83	2.46	-13.32	1.99
206	-11.35	-5.19	-15.40	-121.66	-11.55	-74.66	5.92	0.71	-2.09	106.76	9.93
207	10.61	0.02	15.55	-165.02	-12.81	-92.85	-6.77	-17.18	4.71	73.99	8.55

Table E.7 (continued) | Score values of the samples.

Sample	Beer style		Fermentation		Purity Law		Grain			Abs. 294nm	
	PC1	PC2	PC1	PC2	PC1	PC2	PC1	PC2	PC3	PC1	PC2
208	-9.40	-5.42	-9.79	8.42	6.77	19.53	10.39	4.06	0.52	-7.46	-8.92
209	-2.06	-3.79	-3.57	-8.04	8.68	-8.43	5.74	2.54	2.11	-1.73	15.53
210	19.24	-5.80	9.74	-28.22	-11.66	-16.41	13.12	7.44	-1.10	-	-
211	18.50	-4.96	16.40	-127.68	10.4	-64.07	13.72	3.06	1.74	93.77	-14.44
212	13.53	-8.31	12.19	10.65	7.97	-5.84	4.96	-2.26	1.92	-8.56	21.95
213	-9.55	-5.38	-11.78	4.98	-12.22	3.27	-12.88	19.82	17.69	-4.58	13.00
214	-5.05	-5.38	-7.89	7.37	8.19	14.19	6.87	2.54	-3.27	-3.96	-1.85
215	14.02	-11.11	11.87	-5.64	8.89	-26.37	12.25	1.89	0.52	1.88	42.92
216	-11.17	-6.04	-9.75	-18.62	5.57	-22.89	9.76	2.12	-2.14	-6.89	40.03
217	8.06	33.98	18.20	0.19	8.26	-7.28	-12.08	-19.90	2.43	4.41	9.45
218	17.29	-9.08	14.00	11.63	9.26	3.57	11.81	1.46	-0.90	-6.56	5.20
219	17.34	-9.09	13.93	11.60	9	3.52	11.69	1.35	-0.79	-6.70	5.23
220	11.38	-8.10	11.22	-2.19	8.25	-16.85	11.00	-0.35	-3.86	1.61	25.86
221	18.53	5.13	16.41	0.52	9.58	-14.29	-7.45	-13.45	-1.66	-11.62	21.16
222	-8.77	-6.28	-11.56	1.28	-14.44	-3.22	-	-	-	-8.93	16.63
223	-10.25	-0.68	-12.37	-44.28	8.75	-28.6	10.33	3.44	-4.12	47.42	20.14
224	-9.51	-5.99	-11.14	-4.24	9.14	-2.16	10.64	3.28	1.18	0.37	18.65
226	-14.63	-1.73	-13.42	-22.99	8.99	-15.11	8.56	1.12	-4.46	5.77	23.35
227	2.00	36.92	15.28	-0.85	9.63	-6.03	-13.81	-20.03	1.48	1.20	10.08
228	-13.47	-3.57	-14.38	5.79	-13.42	10.52	-19.75	12.60	-15.16	-10.23	-0.25
229	-10.95	-4.50	-13.37	9.35	-12.52	21.41	-18.34	11.72	-12.58	-8.59	-14.96
230	-12.65	-4.93	-13.69	11.41	-9.1	19.69	-8.36	9.60	-9.01	-9.09	-10.10
231	-15.00	-3.65	-11.91	19.59	-13.19	28.86	-18.73	14.39	-16.69	-7.99	-11.93
232	-12.62	-3.65	-13.90	2.92	-10.74	4.77	-	-	-	-0.86	3.08
235	-6.74	0.26	-8.36	12.61	-14.36	25.02	-20.27	10.05	-13.60	-	-
236	-11.93	-2.31	-12.83	12.06	-12.76	17.02	-24.31	12.45	-17.40	-	-
237	-15.15	-3.01	-14.02	8.54	-12.47	13.27	-22.00	13.69	-19.97	-	-
238	-18.11	-5.41	-13.60	-79.36	5.93	-56.08	10.52	2.65	-4.97	13.15	57.65
239	-11.47	-5.67	-13.34	15.87	-11.18	29.27	-12.59	14.95	2.21	-	-

Table E.7 (continued) | Score values of the samples.

Sample	Beer style		Fermentation		Purity Law		Grain			Abs. 294nm	
	PC1	PC2	PC1	PC2	PC1	PC2	PC1	PC2	PC3	PC1	PC2
241	-12.90	-2.49	-13.34	14.06	-11.12	29.43	-14.15	15.10	4.54	-	-
242	-13.59	-3.96	-12.06	13.22	8.69	24.2	10.23	4.35	-3.22	-14.09	-9.01
243	-11.32	-10.21	-9.56	17.38	10.1	14.16	12.32	1.20	-3.64	-9.06	9.63
244	-6.87	-3.78	-6.41	8.29	7.18	4.12	9.94	-0.01	-4.07	-15.64	9.88
245	-15.11	-2.29	-14.95	14.95	8.21	35.53	6.98	2.75	-1.56	-19.12	-21.47
246	-15.19	-4.80	-15.18	10.65	8.95	19.72	11.09	2.66	-1.81	-16.01	-3.42
247	-12.30	-1.96	-12.88	11.21	6.94	27.77	4.44	2.31	-2.85	-9.22	-19.27
248	-9.03	-2.06	-10.52	19.71	7.73	42.13	7.12	1.09	0.79	-14.95	-34.29
249	-9.42	-1.93	-10.81	13.93	7.96	21.91	8.45	2.16	-2.83	-9.58	-10.74
250	-1.03	25.17	11.26	21.13	8.41	24.95	-10.91	-15.63	-1.58	-10.93	-17.70
251	1.49	21.83	13.35	14.88	6.83	13.02	-4.11	-14.67	0.77	-6.08	-5.75
252	-14.04	-3.08	-12.72	14.71	8.98	29.19	11.06	2.68	0.88	-16.04	-13.59
253	-1.00	32.68	13.70	20.57	11.1	18.88	-7.29	-21.55	3.42	-13.19	-11.25
254	-9.54	-0.13	-9.14	12.32	7.42	20.17	1.65	3.04	1.81	-7.38	-29.57
255	-1.52	23.26	9.30	20.15	8.05	29.25	-8.84	-14.53	0.45	-6.64	-26.61
256	-3.28	20.25	7.86	25.59	6.68	34.92	-9.50	-11.05	-0.38	-13.28	-28.41
257	-3.06	25.55	11.97	30.14	9.28	35.18	-7.11	-18.75	1.59	-12.54	-23.97
258	-1.45	26.89	12.73	19.68	9.47	26.56	-6.13	-16.23	3.18	-8.38	-21.51
259	3.68	23.03	13.68	8.17	8.4	20.06	-5.89	-15.65	1.40	6.03	-25.07
260	-7.18	-2.84	-8.07	12.29	8.7	30.56	6.65	-0.04	2.13	-8.45	-23.79
261	-14.05	0.01	-11.26	6.57	9.7	23.62	8.70	1.69	-0.05	-5.96	-15.42
262	-14.69	-5.75	-16.19	9.40	7.88	17.16	8.90	3.73	-0.92	-	-
263	-5.29	35.14	11.22	18.46	8.87	16.83	-14.09	-19.62	-0.87	-	-
264	-13.75	-6.84	-14.89	9.81	-13.25	5.93	-18.04	16.07	-13.07	-	-
265	-11.13	-4.97	-13.57	11.38	-13.17	18.26	-18.25	15.63	-7.33	-	-
266	-3.39	-1.34	-6.40	19.41	-11.69	36.69	-19.50	10.38	-7.71	-	-
267	-11.83	-4.74	-14.08	6.64	-13.77	13.49	-22.09	13.46	-8.36	-	-
268	-9.52	-5.15	-11.59	-0.56	-11.86	-3.05	-	-	-	-	-
269	-9.18	-0.42	-8.53	8.86	-11.76	12.22	-15.07	7.01	-7.50	-	-
270	-7.47	-1.85	-10.36	19.55	-12.37	37.55	-18.38	11.25	-11.27	-	-

Table E.7 (continued) | Score values of the samples.

Sample	Beer style		Fermentation		Purity Law		Grain			Abs. 294nm	
	PC1	PC2	PC1	PC2	PC1	PC2	PC1	PC2	PC3	PC1	PC2
271	-4.89	1.33	-6.79	22.18	-8.27	55.42	-13.62	8.49	-9.38	-	-
272	-3.59	-0.83	-8.10	-1.00	-10.84	6.85	-13.05	14.52	5.69	13.66	-7.59
273	23.21	-9.32	15.78	-71.77	10.01	-85.37	9.04	1.41	-0.96	-	-
274	-4.67	-0.55	-11.04	-11.45	-12.37	-11.29	-14.59	19.35	13.50	-	-
275	-16.02	-3.71	-15.97	10.63	-11.86	20.39	-19.59	17.30	-4.08	-12.94	-8.29
276	-13.83	-5.48	-12.55	5.39	-9.04	6.12	-17.75	15.12	-15.38	-	-
277	-12.16	-3.39	-12.25	7.23	-10.14	14.28	-13.69	13.55	-9.19	-	-
278	23.55	-7.65	17.09	-15.95	7.55	-27.51	4.31	2.80	2.08	-	-
279	-4.32	-3.41	-5.99	19.52	6.42	28.42	2.03	5.58	-1.27	-	-
280	-12.41	-2.65	-13.26	11.12	-10.13	22.87	-16.13	12.93	-8.09	-	-
281	13.17	-5.33	11.90	7.85	6.43	8.59	8.57	1.49	0.65	-	-
282	16.47	-3.74	10.60	-32.89	11.51	-22.61	11.96	3.77	-1.13	32.12	-0.53
283	-10.94	-5.74	-11.40	9.36	-9.59	16.51	-8.18	11.86	-6.99	-	-
284	12.41	-4.99	9.90	11.44	5.7	22.79	6.75	2.50	-0.07	9.90	-30.05
285	-9.72	-2.55	-9.68	5.55	-10.11	12.75	-13.94	12.29	-10.30	-3.05	-7.19
286	7.87	-6.35	7.10	8.77	7.12	12.11	8.14	2.27	2.19	-	-
287	12.31	-4.92	10.21	11.05	10.51	21.5	6.20	0.83	0.18	-	-
288	13.58	-4.43	10.05	18.82	-12.13	24.67	2.87	0.95	-0.59	-	-
289	7.61	6.38	8.79	24.42	-11.85	29.51	-13.96	-8.64	-2.65	-	-
290	8.88	15.73	14.27	13.16	-7.79	11.59	-7.47	-12.76	4.01	1.76	-13.91
291	0.52	-2.36	6.39	14.31	-10.43	10.62	4.15	1.00	1.80	-	-
292	7.76	-7.16	6.34	17.72	-10.94	10.9	10.22	2.35	1.84	-13.80	-0.77
293	-11.21	-1.60	-11.26	-23.09	6.57	-12.61	6.47	3.31	-1.90	12.45	15.12
294	-2.88	-8.51	-5.50	1.61	7.92	7.49	6.19	2.17	1.11	-	-
295	-6.26	-2.70	-7.18	2.58	9.24	15.35	4.80	1.29	0.87	-	-
296	-6.73	-0.03	-7.45	18.93	-13.31	31.44	-16.08	9.57	-6.27	-	-
297	-8.54	-2.81	-10.12	14.14	8.06	40.19	-	-	-	-	-
298	19.51	-8.88	11.65	-16.89	9.75	-42.06	2.58	1.79	3.13	-	-
299	16.77	-2.25	15.40	-10.21	7.84	-19.3	-3.28	-9.13	1.20	-	-

Table E.7 (continued) | Score values of the samples.

Sample	Beer style		Fermentation		Purity Law		Grain			Abs. 294nm	
	PC1	PC2	PC1	PC2	PC1	PC2	PC1	PC2	PC3	PC1	PC2
300	-8.53	-1.11	-11.69	-48.24	9.53	-24.51	9.72	2.18	-0.03	22.71	13.42
301	8.95	-3.78	9.74	0.06	10.04	6.84	13.75	2.65	3.39	-	-
302	-7.99	-2.79	-8.92	-5.12	-9.53	-3.28	2.10	5.39	-0.98	-	-
303	1.81	40.99	7.94	-20.29	9.62	-36.63	-7.36	-17.79	2.39	-	-
304	-11.65	-7.12	-12.11	-18.87	8.48	-35.23	15.52	3.11	-0.48	-	-
305	1.16	36.72	14.86	-8.65	7.98	-27.76	-10.36	-18.80	2.24	-	-
306	-16.42	-9.54	-14.64	-8.95	7.87	-11.12	9.92	4.81	3.83	-	-
307	-4.78	-7.49	-8.06	-6.94	-10.81	-14.48	-6.02	13.42	6.21	-	-
308	-17.80	-9.48	24.75	48.75	12.91	9.42	-15.13	-24.82	7.12	-	-
309	-13.94	-8.09	-1.55	28.73	-10.09	8.87	-16.87	7.67	18.03	-	-
310	15.33	-11.03	15.06	-27.40	9.09	-50.14	8.56	1.59	2.23	-	-
311	-7.69	-2.94	-8.18	14.34	-6.08	29.87	-3.01	9.01	2.04	-	-
312	-10.34	-4.04	-9.76	9.24	-5.64	21.79	-1.14	8.32	3.64	-	-
313	-10.85	-5.10	-11.50	7.15	-9.15	15.7	-5.85	13.48	2.55	-	-
314	9.81	30.03	13.26	29.97	-11.28	30.59	-11.41	-22.25	-0.10	-	-
315	-3.30	-3.59	9.43	6.67	-13.52	-15.46	11.94	1.34	-2.65	-	-
317	-13.70	-6.46	-13.72	4.21	-11.53	5.4	-	-	-	-	-
318	-12.80	-7.88	-11.91	7.82	-10.91	5.45	-14.19	19.57	19.00	-	-
319	-19.15	-8.17	-16.97	-7.83	-12.3	-8.66	-24.18	17.38	-18.15	-	-
320	-9.77	-3.60	-13.27	10.47	-13.9	20.7	-22.83	15.17	-9.88	-	-
321	-10.88	-5.28	-12.19	13.59	-8.63	26.02	-7.26	12.50	5.68	-	-
322	-14.14	-4.68	-14.42	11.73	-13	21.3	-	-	-	-	-
323	-11.49	-8.16	-10.38	-1.76	-12.14	-14.7	-19.29	13.68	-15.29	-	-
324	-14.01	-5.77	-14.48	9.52	-13.95	18.38	-19.93	21.34	13.25	-	-
325	-8.27	-5.64	-12.41	-0.15	-11.77	15.1	-	-	-	-	-
326	-13.82	-0.69	-12.67	18.49	8.31	50.39	4.65	1.47	-3.18	-	-
327	-11.07	-4.57	-11.69	7.57	-13.82	15.44	-16.93	19.47	9.50	-	-
328	-5.54	-2.75	-9.35	14.94	-12.94	28.59	-24.98	13.26	-10.93	-	-
329	-13.56	-4.55	-14.69	9.76	-12.79	11.77	-20.38	14.34	-12.91	-	-
330	-14.28	-3.12	-14.13	10.57	-15.14	18.49	-25.39	16.05	-14.58	-	-

Table E.7 (continued) | Score values of the samples.

Sample	Beer style		Fermentation		Purity Law		Grain			Abs. 294nm	
	PC1	PC2	PC1	PC2	PC1	PC2	PC1	PC2	PC3	PC1	PC2
331	-12.64	-2.74	-13.71	5.99	-12.41	8.42	-10.67	16.73	17.68	-	-
333	-15.99	-6.89	-14.35	-1.98	-13.19	19.86	2.03	7.34	-1.75	-	-
334	-6.11	-2.71	-10.76	-2.05	-11.4	-18.75	-14.52	18.71	21.59	-	-
335	-14.27	-3.37	-13.17	10.23	-10.96	-2.41	-19.21	19.18	24.29	-	-
336	-7.59	0.97	-15.12	1.57	-13.91	-24.55	-12.99	14.46	19.36	-	-
337	-12.46	-3.52	-13.48	4.00	-9.97	-17.13	-15.92	19.22	23.25	-	-
357	19.40	13.52	14.04	13.18	7.42	2.19	-13.40	-19.18	3.30	-	-
358	-10.38	-6.24	-12.47	-30.71	9.09	-41.97	8.75	3.20	-0.77	-	-
360	17.57	-4.91	9.70	12.76	-13.45	8.46	-	-	-	-	-
361	-7.74	-3.55	-12.59	-9.17	-11.01	-26.53	-	-	-	-	-
362	-6.42	-2.43	-12.55	4.02	-9.98	-15.61	-	-	-	-	-
363	-7.60	0.84	-12.59	12.98	8.49	-19.42	-	-	-	-	-
364	18.93	7.41	5.20	-13.77	-7.79	-81.12	-9.00	-8.69	7.60	-	-
365	17.17	-5.18	11.96	-40.16	-11.28	-80.56	10.60	1.37	0.56	-	-
366	-8.37	-0.76	-13.17	5.40	-12.91	-26.23	-	-	-	-	-
367	7.34	35.10	15.51	19.24	8.75	-7.28	-11.53	-17.33	5.13	-	-
368	20.00	-7.62	15.50	-22.80	9.27	-96.44	9.30	6.87	-6.00	-	-
369	-13.58	-4.79	-13.62	-13.07	9.61	-42.94	9.96	3.89	-0.58	-	-
370	16.05	-2.26	10.84	-61.43	10.15	-99.04	13.14	-0.16	0.87	-	-
371	0.54	60.45	12.83	-3.56	4.88	-35.26	-7.97	-18.90	3.10	-	-
372	1.76	42.19	12.57	3.61	9.71	-28.21	-14.11	-19.18	4.57	-	-
373	-16.56	-2.54	-13.74	12.04	-9.83	-1.91	-	-	-	-	-
374	-11.72	-2.00	-12.74	14.10	-13.09	7.47	-	-	-	-	-
375	-12.69	-4.46	-13.71	0.93	11.13	-17.45	12.13	4.14	-1.52	-	-
376	-9.23	-4.56	-12.34	-5.15	8.24	-38.97	8.95	0.28	-7.38	-	-
377	-9.50	-3.59	-10.95	17.54	-12.52	20.48	-	-	-	-	-
378	-12.93	-2.97	-12.16	11.42	-11.79	5.47	-	-	-	-	-
379	-17.78	-7.18	-8.55	4.77	-12.63	-33.09	-24.06	15.98	-21.73	-	-
380	19.59	-8.22	13.64	-30.64	7.71	-40.61	14.42	4.03	-0.11	-	-

Table E.7 (continued) | Score values of the samples.

Sample	Beer style		Fermentation		Purity Law		Grain			Abs. 294nm	
	PC1	PC2	PC1	PC2	PC1	PC2	PC1	PC2	PC3	PC1	PC2
381	-6.82	-4.16	-9.74	8.99	-10.39	22.03	-11.35	14.83	13.09	-	-
382	-11.65	-0.65	-11.63	7.21	-9.33	11.53	-9.97	13.37	15.02	-	-
383	-12.04	-3.71	-12.66	19.32	-12.57	28.68	-21.36	16.40	-10.11	-	-
385	-3.77	-2.55	-15.32	-7.51	7.89	-46.39	17.54	-2.41	-7.86	-	-
386	21.40	-8.33	13.68	-13.28	9.97	-15.6	-	-	-	-	-
387	19.84	-4.93	12.92	-77.69	10.55	-96.34	13.67	2.95	-2.59	-	-
388	-11.05	-4.30	-13.62	16.24	-10.82	11.49	-	-	-	-	-
389	19.50	-6.16	14.38	-10.16	-7.55	5.01	10.63	3.91	0.88	49.60	-33.06
390	20.13	-5.27	15.77	-27.31	-11.57	-15.49	9.44	4.00	1.33	-	-
391	-11.54	-4.68	-13.07	-12.06	-13.62	-22.36	-15.60	16.05	13.59	-	-
392	-14.91	-3.05	-11.51	-14.52	9.35	-27.07	12.10	3.02	3.06	-	-
393	11.38	-5.59	9.31	17.69	6.46	28.81	6.72	0.34	0.63	-	-
394	23.90	-4.10	17.01	-27.68	-14.73	-27.58	-9.00	10.52	9.36	63.23	-4.26
395	20.14	-2.30	14.25	17.35	-13.11	-12.34	-12.37	-17.87	-0.90	-	-
396	16.41	-6.87	13.23	-3.29	8.97	4.14	9.02	3.26	2.59	-	-
397	14.68	-0.10	16.21	42.16	6.48	10.49	-7.40	-16.13	2.27	-	-
398	19.33	-6.02	14.37	-6.18	9.31	4.65	9.61	1.26	0.30	31.98	-18.31
399	11.87	-2.07	12.39	16.91	9.16	16.11	10.69	-2.68	2.02	-	-
400	24.26	3.84	11.05	16.86	-12.14	-9.56	-9.85	-20.28	5.49	-	-
401	19.57	-9.41	13.32	-4.03	9.68	-14.44	7.38	-2.79	2.23	-	-
402	23.68	-6.70	17.38	6.70	-12.83	-14.12	-9.82	-15.69	2.45	-	-
404	21.82	-5.47	15.29	-0.87	-12.72	6.49	-1.33	-7.90	0.53	-	-
405	21.51	-10.77	14.24	12.71	-11.03	-5.73	-9.34	-13.19	3.55	-	-
406	20.08	-9.04	16.62	16.78	5.98	15.64	8.65	-1.72	2.57	-	-
407	-8.81	4.35	-7.30	11.85	-13.21	15.81	-13.66	14.27	13.77	-	-
408	-15.83	-4.66	-15.76	-20.48	-13.02	-29.84	-	-	-	-	-
409	20.53	-6.37	12.33	-88.67	-11.55	-95.92	-13.37	-23.69	-0.99	-	-
410	-18.88	-6.53	-13.92	-15.58	-11.17	-27.15	-13.06	17.89	20.86	-	-
411	-9.76	-7.07	-14.21	-18.77	-11.31	-34.72	-25.87	13.57	-18.47	-	-
412	-10.82	0.81	-14.32	-19.88	-11.29	-52.56	-12.11	-16.23	4.34	-	-

Table E.7 (continued) | Score values of the samples.

Sample	Beer style		Fermentation		Purity Law		Grain			Abs. 294nm	
	PC1	PC2	PC1	PC2	PC1	PC2	PC1	PC2	PC3	PC1	PC2
413	-10.02	-7.67	-13.10	-0.28	-14.16	-8.08	-12.62	16.33	17.63	-	-
414	-20.22	-5.81	-14.19	-14.99	7.85	-33.57	11.63	2.17	-1.84	-	-
416	12.86	-0.48	13.39	-1.56	10.28	1.68	9.41	-1.47	-0.23	13.97	-5.52
417	21.73	-5.58	15.92	-14.67	6.45	-0.69	7.80	1.33	1.51	48.73	-24.17
418	18.50	-6.55	14.19	-33.78	8.27	-12.36	12.42	4.72	0.82	46.64	-13.90
419	11.19	-2.76	8.51	-2.18	6.6	16.61	8.57	4.09	1.11	31.06	-30.57
420	19.82	-6.39	14.13	-28.94	-11.67	-36.26	10.35	2.25	-2.12	29.20	16.49
421	16.57	-4.95	10.76	3.05	8.06	32.48	7.86	-0.69	-2.28	27.16	-33.86
422	14.01	0.17	13.02	-31.53	-11.41	-32.06	6.91	1.13	1.47	51.61	10.79
424	26.03	-7.54	15.71	-65.94	-11.14	-49.78	6.87	1.49	4.28	71.43	-4.75
425	19.30	-6.36	13.52	-57.59	-11.67	-41.25	6.28	1.54	1.85	32.73	12.70
426	21.94	-13.26	14.91	-146.17	7.3	-152.44	19.33	-0.64	-3.71	-	-
427	12.57	-2.88	9.86	-10.87	7.4	6.92	9.24	3.69	0.75	50.94	-28.36
428	8.85	-3.31	8.44	16.64	7.41	30.09	8.73	0.75	1.76	4.23	-32.21
429	-9.42	-4.42	-9.70	8.20	3.85	18.16	5.78	5.34	-0.68	-6.53	-7.96
430	17.03	-4.63	13.13	12.82	5.27	32.86	9.81	1.43	0.33	23.26	-48.90
431	10.87	-0.64	9.87	0.92	-14.09	18.42	4.95	1.52	-0.15	29.76	-29.98
432	21.71	-8.60	15.29	-73.04	8.91	-56.37	9.38	1.65	-0.95	67.59	10.76
433	-12.92	-4.28	-14.09	-40.52	7.48	-56.75	16.87	6.85	-5.87	-	-
434	-14.03	-11.99	-13.64	-3.34	7.67	-18.25	14.37	3.77	3.53	-	-
435	-8.14	-10.48	-12.58	1.76	7.62	0.52	10.42	-1.48	1.29	-	-
436	-7.07	-11.17	-9.78	0.77	8.04	-1.01	10.74	-0.94	1.62	-	-
437	27.92	-8.77	18.48	17.04	-12.6	-19.78	-12.37	17.13	18.95	-	-
438	23.77	-16.78	18.63	37.91	7.2	-14.95	12.49	4.63	-3.96	-	-
439	15.22	1.62	14.23	23.87	-6.42	20.45	-1.64	-11.50	0.67	-	-
440	15.03	-3.66	10.03	-43.85	9.72	-41.63	7.11	2.96	-4.13	-	-
441	18.43	1.30	11.23	-11.80	-10.93	-29.95	-14.15	-21.57	2.26	-	-
442	6.24	18.99	15.13	22.81	-8.68	16.82	-11.55	-14.12	-0.68	-	-
443	-1.78	-5.44	-6.28	-30.63	6.94	-23.53	8.27	2.67	-2.84	-	-

Table E.7 (continued) | Score values of the samples.

Sample	Beer style		Fermentation		Purity Law		Grain			Abs. 294nm	
	PC1	PC2	PC1	PC2	PC1	PC2	PC1	PC2	PC3	PC1	PC2
444	-2.00	-3.43	-6.68	10.65	10.53	31.22	5.46	-1.93	-1.57	-	-
445	29.00	-9.42	20.25	-27.16	9.27	-75.19	13.72	4.17	-5.14	-	-
446	21.44	-4.15	9.89	-70.99	-10.2	-83.34	-9.56	-13.93	-1.58	-	-
447	16.64	-7.29	12.08	2.11	8.15	-6.59	9.14	1.58	1.14	-	-
448	18.60	-7.28	15.73	5.97	9.17	-100.2	7.70	0.46	-0.44	-	-
449	11.27	6.46	12.54	31.45	-9.29	12.08	-6.07	-13.26	3.26	-	-
450	-7.05	5.12	-8.90	3.44	7.73	-7.3	-8.42	-15.81	3.65	-	-
451	27.53	-1.93	14.19	-9.90	-11.37	-6.76	7.74	5.49	-3.52	-	-
452	9.55	-3.80	6.70	24.23	-12.16	19.01	-8.67	9.82	13.53	-	-
453	3.63	24.35	14.72	17.80	9.9	20.92	-6.69	-16.87	5.69	-	-
454	10.83	-2.05	8.81	13.28	-13.82	12.2	6.08	3.42	2.69	-	-
455	-1.54	-5.20	-5.76	-4.39	-9.9	6.25	10.54	8.25	3.55	-	-
456	18.37	-3.45	14.68	9.91	-12.35	9.89	5.42	2.35	0.10	-	-
457	-13.03	-3.52	-11.92	-16.90	9.68	-19.33	13.21	1.41	2.34	-	-
458	-11.68	-4.61	-12.98	-31.08	8.98	-27.63	7.66	0.81	2.74	-	-
459	-14.86	-7.19	-13.27	-5.11	7.5	-5.26	9.85	6.32	2.27	-	-
460	-13.73	-4.25	-11.45	15.76	7.38	25.43	-	-	-	-	-
464	-15.30	-2.52	-12.67	12.67	-10.15	22.77	-8.90	14.38	14.69	-	-
465	-7.41	-2.32	-9.22	18.33	-12.76	37.03	-5.39	13.22	9.88	-	-
467	-16.88	-6.17	-15.94	-1.55	-8.72	5.29	-5.40	14.15	13.61	-	-
B1885	-9.28	2.74	-5.54	10.89	3.82	12.14	-14.17	-2.56	4.19	-16.69	20.60
B2019	-12.41	-1.52	-10.01	14.94			5.38	20.19	3.41		

Figures E

Figure E.1 | Phase contrast microscopy of amorphous organic particles of 1885 beer. Typical particles that occur during the aging of filtered beers due to polyphenol-protein complexation.

Figure E.2 | FT-ICR mass spectrum excerpt of beer B1885 (A) and B2019 (B) showing over 40 different compositions in the nominal mass m/z 317. Chemical space color code: CHO (blue), CHNO (orange), CHOS (green), CHNOS (red), CH(N)O(S)P (violet).

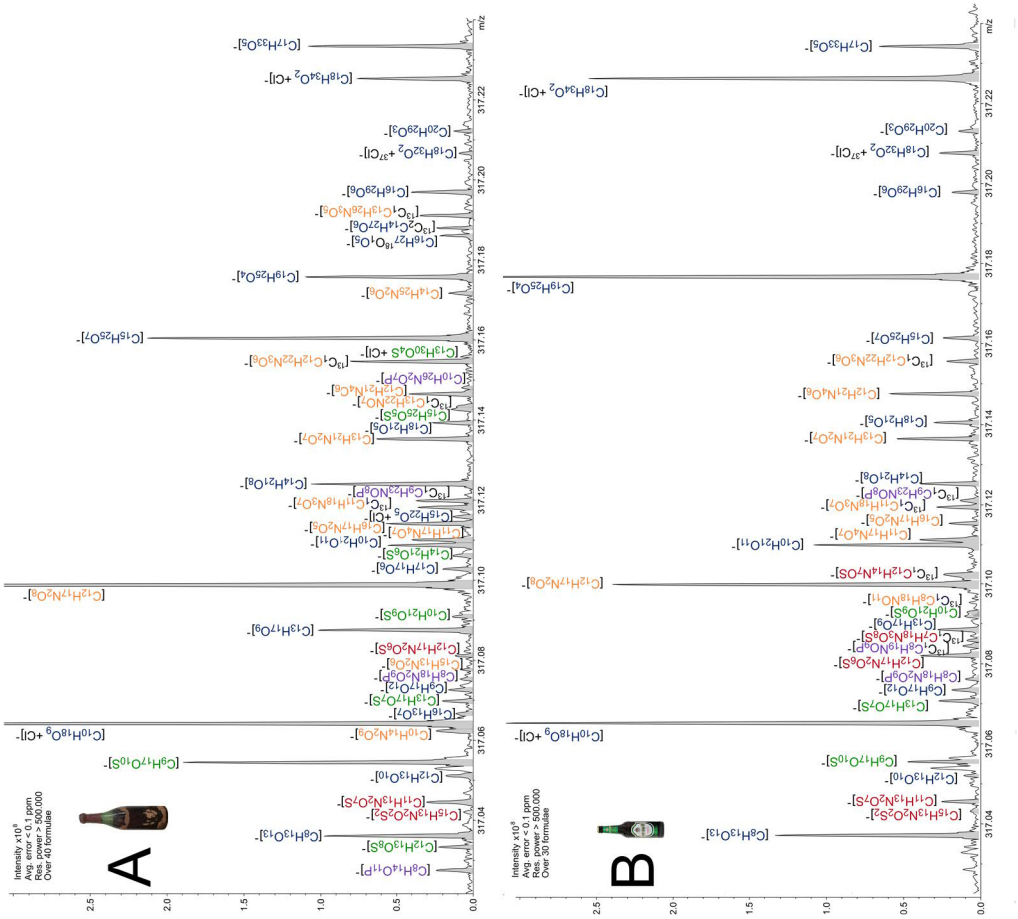

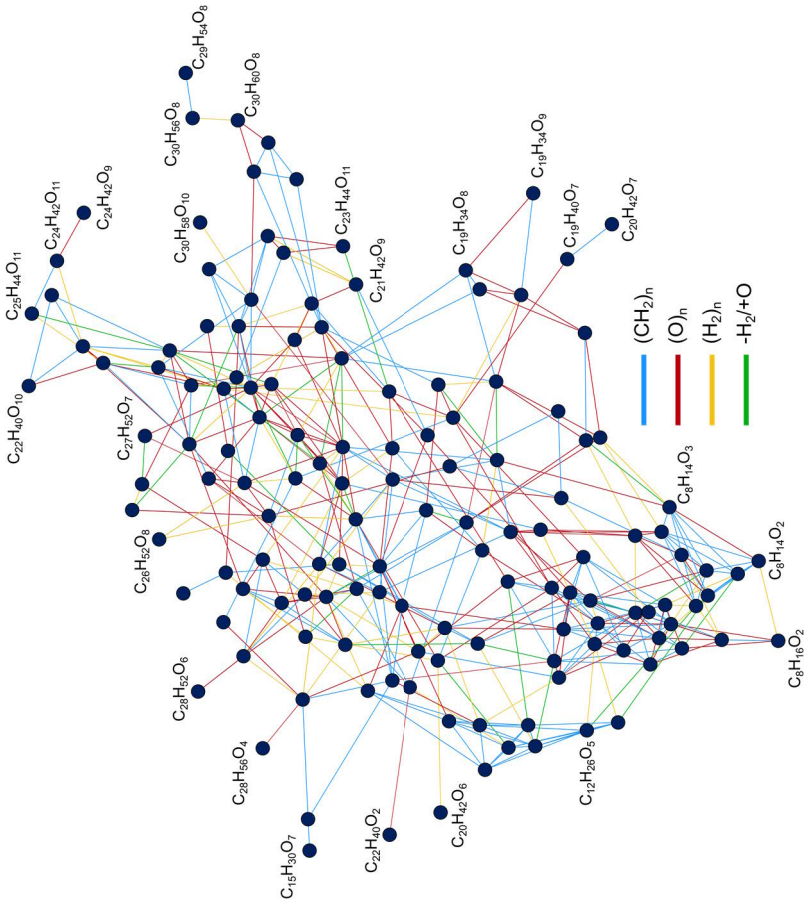

Figure E.3 | Mass difference network of lipid-type compositions specific for the historical beer. The compositions are represented as nodes that are connected by edges, representing changes in the molecular formula equivalent to (bio-)chemical redox processes.

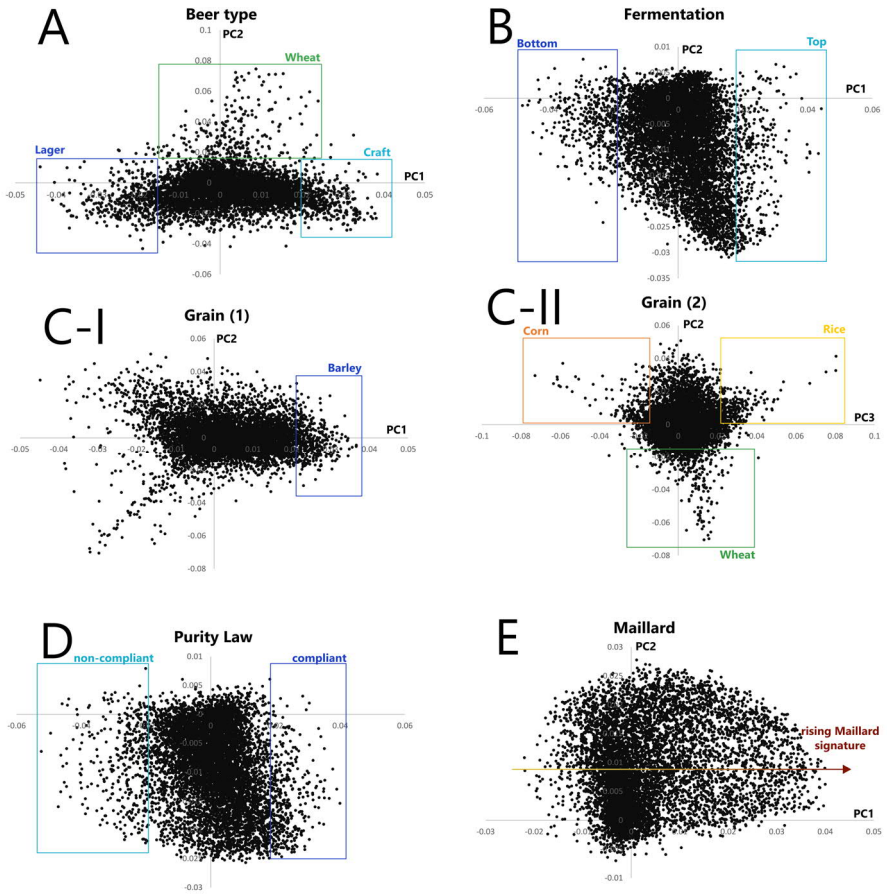

Figure E.4 | Loading plots including 7,700 compositions for the OPLS-DA differentiating beer types (A), fermentation types (B), grains used (C), compliance with the German purity Law (D) and Maillard signatures by the absorption at 294 nm (E). The features specific for an attribute are highlighted.

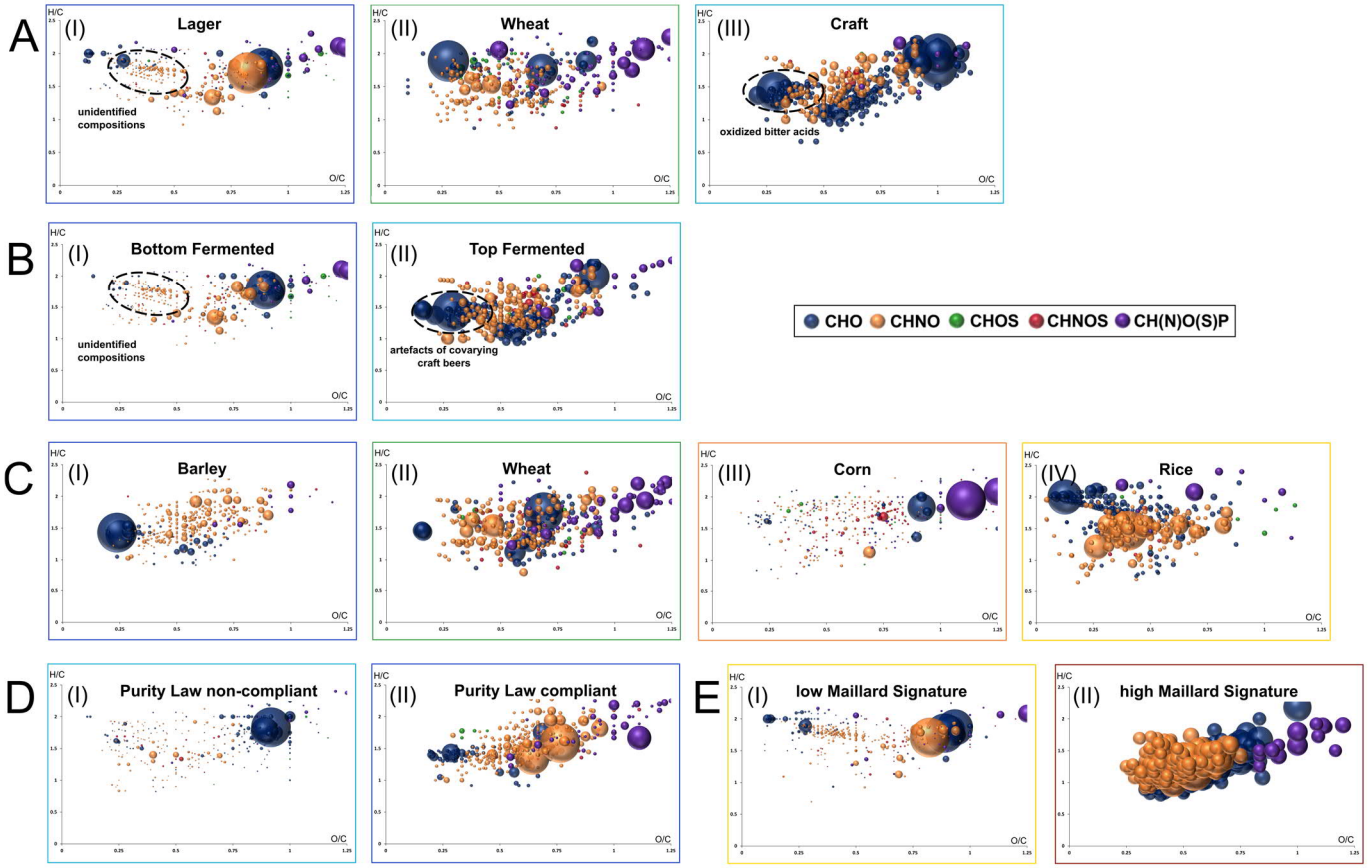

Figure E.5 | Van Krevelen diagrams of the characteristic compositional profiles for beer types (A), fermentation types (B), grains used (C), compliance with the German Purity Law (D) and Maillard signatures (E). Color code: CHO (blue), CHNO (orange), CHOS (green), CHNOS (red), CH(N)O(S)P (violet). Neutral compositions are depicted. Specific areas are highlighted.

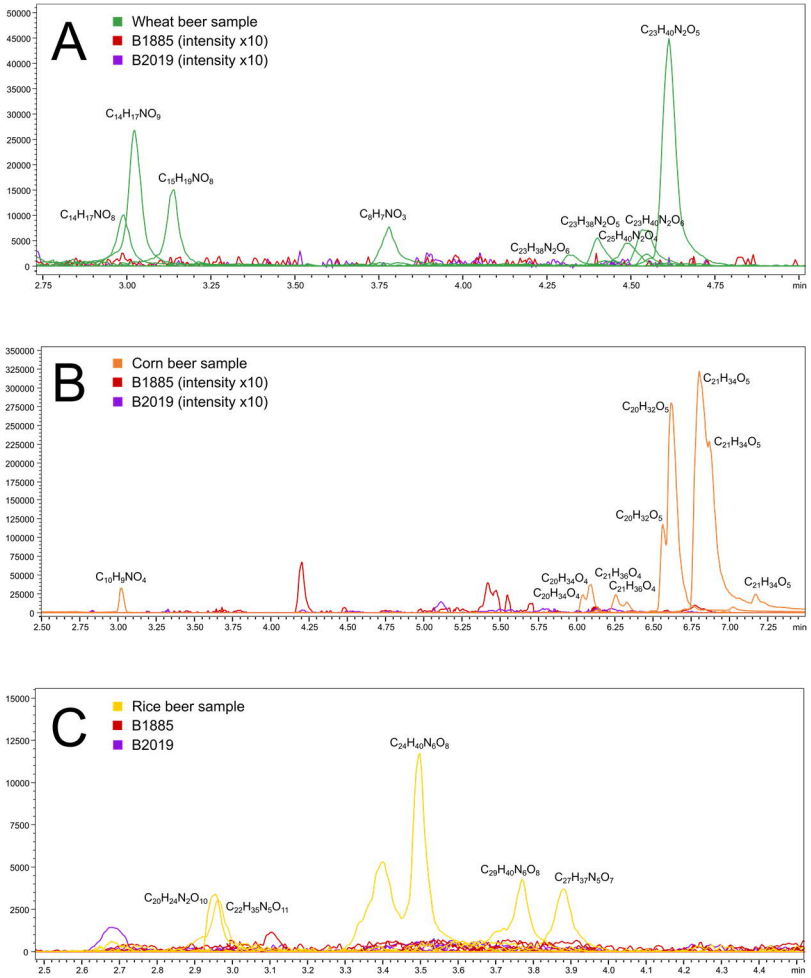

Figure E.6 | Extracted Ion chromatograms of compound masses found to be specific for wheat (A), corn (B) and rice (C) including a respective grain-containing sample, sample B1885 and sample B2019. No overlap of reported marker molecules [228] between the grain-containing samples and samples B1885 and B2019 was observed.

Bibliography

1 Kacser, H. & Burns, J. A. The control of flux. Symp Soc Exp Biol. 27, 65-104 (1973).

2 Heinrich, R. & Rapoport, T. A. A linear steady-state treatment of enzymatic chains. General properties, control and effector strength. Eur. J. Biochem. 42, 89-95 (1974).

3 Oliver, S. G., Winson, M. K., Kell, D. B. & Baganz, F. Systematic functional analysis of the yeast genome. Trends Biotechnol 16, 373-378 (1998).

4 Fiehn, O. Metabolomics - the link between genotypes and phenotypes. Plant Mol. Biol. 48, 155-171 (2002).

5 Nicholson, J. K., Lindon, J. C. & Holmes, E. 'Metabonomics': Understanding the metabolic responses of living systems to pathophysiological stimuli via multivariate statistical analysis of biological NMR spectroscopic data. Xenobiotica 29, 1181-1189 (1999).

6 Roberts, L. D., Souza, A. L., Gerszten, R. E. & Clish, C. B. Targeted Metabolomics. Curr. Protoc. Mol. Biol. 98, 1-34 (2012).

7 Keurentjes, J. J. B. et al. The genetics of plant metabolism. Nat. Genet. 38, 842-849 (2006).

8 Defernez, M. & Colquhoun, I. J. Factors affecting the robustness of metabolite fingerprinting using ^{1}H-NMR spectra. Phytochemistry 62, 1009-1017 (2003).

9 Kell, D. B. et al. Metabolic footprinting and systems biology: the medium is the message. Nat. Rev. Microbiol. 3, 557-565 (2005).

10 Sumner, L. W. et al. Proposed minimum reporting standards for chemical analysis. Metabolomics 3, 211-221 (2007).

11 Moritz, F., Hemmler, D., Schnitzler, J.-P. & Schmitt-Kopplin, P. Mass differences in metabolome analyses of untargeted direct infusion ultra-high resolution MS data in Fundamentals and applications of Fourier transform mass spectrometry (eds B. Kanawati & P. Schmitt-Kopplin) Ch. 12, (Elsevier, 2019).

12 Schmitt-Kopplin, P. & Kanawati, B. Fundamentals and application of Fourier transform mass spectrometry. 1st edn, (Elsevier, 2019).

13 The Metabolomics Society Inc. Statement on the field of metabolomics, <http://metabolomicssociety.org/metabolomics> accessed July 2021

14 Patterson, S. D. & Aebersold, R. H. Proteomics: the first decade and beyond. Nat. Genet. 33, 311-323 (2003).

15 Wilkins, M. R. et al. Progress with proteome projects: Why all proteins expressed by a genome should be identified and how to do it. Biotech. Gen. Eng. Rev. 13, 19-50 (1995).

16 Sanger, F. et al. Nucleotide sequence of bacteriophage ϕX174 DNA. Nature 265, 687-695 (1977).

17 Kuska, B. Beer, Bethesda, and biology: How "Genomics" came into being. J. Natl. Cancer Inst. 90, 93 (1998).

18 Oliver, S. G. et al. The complete DNA sequence of yeast chromosome III. Nature 357, 38-46 (1992).
19 Velculescu, V. E. et al. Characterization of the yeast transcriptome. Cell 88, 243-251 (1997).
20 Kell, D. B. & Oliver, S. G. The metabolome 18 years on: A concept comes of age. Metabolomics 12, 1-8 (2016).
21 Fiehn, O. et al. Metabolite profiling for plant functional genomics. Nat. Biotechnol. 18, 1157-1161 (2000).
22 Jenkins, H. et al. A proposed framework for the description of plant metabolomics experiments and their results. Nat. Biotechnol. 22, 1601-1606 (2004).
23 Xiao, J. F., Zhou, B. & Ressom, H. W. Metabolite identification and quantitation in LC-MS/MS-based metabolomics. Trends Anal. Chem. 32, 1-14 (2012).
24 Kanehisa, M. & Goto, S. KEGG: Kyoto Encyclopedia of Genes and Genomes. Nucleic Acids Res. 28, 27-30 (2000).
25 Alseekh, S. & Fernie, A. R. Metabolomics 20 years on: what have we learned and what hurdles remain? Plant J. 94, 933-942 (2018).
26 Schmitt-Kopplin, P. et al. Systems chemical analytics: introduction to the challenges of chemical complexity analysis. Faraday Discuss. 218, 9-28 (2019).
27 Aherne, S. A. & O'Brien, N. M. Dietary flavonols: chemistry, food content, and metabolism. Nutrition 18, 75-81 (2002).
28 Maier, T. V. et al. Impact of dietary resistant starch on the human gut microbiome, metaproteome, and metabolome. mBio 8, 1-16 (2017).
29 Oliver, S. G. Guilt-by-association goes global. Nature 403, 601-603 (2000).
30 Teusink, B., Baganz, F., Westerhoff, H. V. & Oliver, S. G. Metabolic control analysis as a tool in the elucidation of the function of novel genes. Methods Microbiol. 26, 297-335 (1998).
31 Raamsdonk, L. M. et al. A functional genomics strategy that uses metabolome data to reveal the phenotype of silent mutations. Nature Biotechnol. 19, 45-50 (2001).
32 Allen, J. et al. High-throughput classification of yeast mutants for functional genomics using metabolic footprinting. Nature Biotechnol. 21, 692-696 (2003).
33 Vaidyanathan, S., Rowland, J. J., Kell, D. B. & Goodacre, R. Discrimination of aerobic endospore-forming bacteria via elctrospray-ionization mass spectrometry of whole cell suspensions. Anal. Chem. 73, 4134-4144 (2001).
34 Goodacre, R., Vaidyanathan, S., Bianchi, G. & Kell, D. B. Metabolic profiling using direct infusion electrospray ionisation mass spectrometry for the characterisation of olive oils. Analyst 127, 1457-1462 (2002).
35 Dunn, W. B. et al. Serum metabolomics reveals many novel metabolic markers of heart failure, including pseudouridine and 2-oxoglutarate. Metabolomics 4, 413-426 (2007).
36 Kenny, L. C. et al. Novel biomarkers for pre-eclampsia detected using metabolomics and machine learning. Metabolomics 1, 227-234 (2005).
37 Zamboni, N., Fendt, S.-M., Rühl, M. & Sauer, U. ^{13}C-based metabolic flux analysis. Nat. Protoc. 4, 878-891 (2009).

38 Herrgård, M. J. et al. A consensus yeast metabolic network reconstruction obtained from a community approach to systems biology. Nat. Biotechnol. 26, 1155-1160 (2008).
39 Goodacre, R. et al. Proposed minimum reporting standards for data analysis in metabolomics. Metabolomics 3, 231-241 (2007).
40 Salek, R. M., Steinbeck, C., Viant, M. R., Goodacre, R. & Dunn, W. B. The role of reporting standards for metabolite annotation and identification in metabolomic studies. GigaScience 2, 1-3 (2013).
41 Weininger, D. SMILES, a chemical language and Information System. 1. Introduction to methodology and encoding rules. J. Chem. Inf. Comput. Sci. 28, 31-36 (1988).
42 Heller, S., McNaught, A., Stein, S., Tchekhovskoi, D. & Pletnev, I. InChI - the worldwide chemical structure identifier standard. J. Chemometrics 5, 1-9 (2013).
43 Wang, D. & Bodovitz, S. Single cell analysis: the new frontier in 'Omics'. Trends Biotechnol. 28, 281-290 (2010).
44 King, R. D. et al. The automation of science. Science 384, 85-89 (2009).
45 Mendez, K. M., Broadhurst, D. I. & Reinke, S. N. The application of artificial neural networks in metabolomics: a historical perspective. Metabolomics 15, 1-14 (2019).
46 Kumar, R., Bohra, A., Pandey, A. K., Pandey, M. K. & Kumar, A. Metabolomics for plant improvement: Status and prospects. Front. Plant Sci. 8, 1-27 (2017).
47 Sulpice, R. Closing the yield gap: can metabolomics be of help? J. Exp. Bot. 71, 461-464 (2020).
48 Ainalidou, A. et al. Integrated analysis of metabolites and proteins reveal aspects of the tissue-specific function of synthetic cytokinin in kiwifruit development and ripening. J. Proteom. 143, 318-333 (2016).
49 Hatoum, D., Annaratone, C., Hertog, M. L. A. T. M., Geeraerd, A. H. & Nicolai, B. M. Targeted metabolomics study of 'Braeburn' apples during long-term storage. Postharvest Biol. Technol. 96, 33-41 (2014).
50 Toubiana, D. et al. Metabolic profiling of a mapping population exposes new insights in the regulation of seed metabolism and seed, fruit, and plant relations. PLoS Genet. 8, 1-22 (2012).
51 Nardozza, S. et al. Metabolic analysis of kiwifruit (Actinidia deliciosa) berries from extreme genotypes reveals hallmarks for fruit starch metabolism. J. Exp. Bot. 64, 5049-5063 (2013).
52 Matsuda, F. et al. Dissection of genotype–phenotype associations in rice grains using metabolome quantitative trait loci analysis. Plant J. 70, 624-636 (2012).
53 Wen, W. et al. Metabolome-based genome-wide association study of maize kernel leads to novel biochemical insights. Nat. Commun. 5, 1-10 (2014).
54 Obata, T. et al. Metabolite profiles of maize leaves in drought, heat, and combined stress field trials reveal the relationship between metabolism and grain yield. Plant Physiol. 169, 2665-2683 (2015).
55 Jorge, T. F. et al. Mass spectrometry-based plant metabolomics: Metabolite responses to abiotic stress. Mass Spectrom. Rev. 35, 620-649 (2015).
56 Son, H.-S. et al. Characterization of wines from grape varieties through multivariate statistical analysis of ^{1}H-NMR spectroscopic data. Food Res. Int. 42, 1483-1491 (2009).

57 Roullier-Gall, C., Boutegrabet, L., Gougeon, R. D. & Schmitt-Kopplin, P. A grape wine chemodiversity comparison of different appellations in burgundy: Vintage vs terroir effects. Food Chem. 152, 100-107 (2014).
58 Bundy, J. G., Davey, H. M. & Viant, M. R. Environmental metabolomics: A critical review and future perspectives. Metabolomics 5, 3-21 (2009).
59 Cook, D., Fowler, S., Fiehn, O. & Thomashow, M. F. A prominent role for the CBF cold response pathway in configuring the low-temperature metabolome of Arabidopsis. PNAS 101, 15243-15248 (2004).
60 Malmendal, A. et al. Metabolomic profiling of heat stress: Hardening and recovery of homeostasis in Drosophila. Am. J. Physiol. Regul. Integr. Comp. Physiol. 291, 205-212 (2006).
61 Pinheiro, C., Passarinho, J. A. & Ricardo, C. P. Effect of drought and rewatering on the metabolism of Lupinus albus organs. J. Plant Physiol. 161, 1203-1210 (2004).
62 Sanchez, D. H., Siahpoosh, M. R., Roessner, U., Udvardi, M. & Kopka, J. Plant metabolomics reveals conserved and divergent metabolic responses to salinity. Physiol. Plant. 132, 209-2019 (2008).
63 Rosenblum, E. S. et al. Characterizing the metabolic actions of natural stresses in the California red abalone, Haliotis rufescens using ^{1}H-NMR metabolomics. Metabolomics 1, 199-209 (2005).
64 van Meter, R. J., Glinski, D. A., Purucker, S. T. & Henderson, W. M. Influence of exposure to pesticide mixtures on the metabolomic profile in post-metamorphic green frogs (Lithobates clamitans). Sci. Total Environ. 624, 1348-1359 (2018).
65 Goodacre, R., York, E. V., Heald, J. K. & Scott, I. M. Chemometric discrimination of unfractionated plant extracts analyzed by electrospray mass spectrometry. Phytochemistry 62, 859-863 (2003).
66 Merino, N. et al. Living at the extremes: Extremophiles and the limits of life in a planetary context. Front. Microbiol. 10, 1-25 (2019).
67 Krulwich, T. A., Sachs, G. & Padan, E. Molecular aspects of bacterial pH sensing and homeostasis. Nat. Rev. Microbiol. 9, 330-343 (2011).
68 Anton, J. et al. High metabolomic microdiversity within co-occurring isolates of the extremely halophilic bacterium Salinibacter ruber. PLOS One 8, 1-14 (2013).
69 Steinle, L. et al. Life on the edge: Active microbial communities in the Kryos $MgCl_2$-brine basin at very low water activity. ISME J. 12, 1414-1426 (2018).
70 Amend, J. P. & Shock, E. L. Energetics of overall metabolic reactions of thermophilic and hyperthermophilic Archaea and Bacteria. FEMS Microbiol. Rev. 25, 175-243 (2001).
71 Oger, P. M. & Jebbar, M. The many ways of coping with pressure. Res. Microbiol. 161, 799-809 (2010).
72 Krisko, A. & Radman, M. Biology of extreme radiation resistance: The way of Deinococcus radiodurans. CHS Perspect. Biol. 5, 1-11 (2013).
73 Ksionzek, K. B. et al. Dissolved organic sulfur in the ocean: Biogeochemistry of a petagram inventory. Science Re 354, 456-459 (2016).
74 Neogi, S. B. et al. Biogeochemical controls on the bacterial populations in the eastern Atlantic Ocean. Biogeosciences 8, 3747-3759 (2011).
75 Peiris, D. et al. Metabolite profiles of interacting mycelial fronts differ for pairings of the wood decay basidiomycete fungus, Stereum hirsutum with its

competitors Coprinus micaceus and Coprinus disseminatus. Metabolomics 4, 52-62 (2008).
76 Jansen, J. J. et al. Metabolomic analysis of the interaction between plants and herbivores. Metabolomics 5, 150-161 (2009).
77 Kumaraswamy, K. G., Kushalappa, A. C., Choo, T. M., Dion, Y. & Rioux, S. Mass spectrometry based metabolomics to identify potential biomarkers for resistance in barley against fusarium head blight (Fusarium graminearum). J. Chem. Ecol. 37, 846-856 (2011).
78 Jones, O. A. H. et al. Using metabolic profiling to assess plant-pathogeninteractions: an example using rice (Oryza sativa) and the blast pathogen Magnaporthe grisea. Eur. J. Plant Pathol. 129, 539-554 (2011).
79 Schweiger, R. & Müller, C. Leaf metabolome in arbuscular mycorrhizal symbiosis. Plant Biol. 26, 120-126 (2015).
80 Ankrah, N. Y. D., Wilkes, R. A., Zhang, F. Q., Aristilde, L. & Douglas, A. E. The metabolome of associations between xylem-feeding insects and their bacterial symbionts. J. Chem. Ecol. 46, 735-744 (2020).
81 Chen, F., Ma, R. & Chen, X.-L. Advances of metabolomics in fungal pathogen–plant interactions. Metabolites 9, 1-19 (2019).
82 Zhou, J. et al. Metabolome profiling reveals metabolic cooperation between Bacillus megaterium and Ketogulonicigenium vulgare during induced swarm motility. Appl. Environ. Microbiol. APPL 77, 7023-7030 (2011).
83 Viant, M. R., Rosenblum, E. S. & Tjeerdema, R. S. NMR-based metabolomics: A powerful approach for characterizing the effects of environmental stressors on organism health. Environ. Sci. Technol. 37, 4982-4989 (2003).
84 Stentiford, G. D. et al. Liver tumors in wild flatfish: A histopathological, proteomic, and metabolomic study. OMICS 9, 281-299 (2005).
85 Zhang, A., Sun, H., Yan, G., Wang, P. & Wang, X. Metabolomics for biomarker discovery: Moving to the clinic. BioMed Res. Int. (2015).
86 Tomita, M. & Kami, K. Systems biology, metabolomics, and cancer metabolism. Science 336, 990-991 (2012).
87 Jain, M. et al. Metabolite profiling identifies a key role for glycine in rapid cancer cell proliferation. Science 336, 1040-1044 (2012).
88 Denkert, C. et al. Metabolomics of human breast cancer: new approaches for tumor typing and biomarker discovery. Genome Med. 4, 1-9 (2012).
89 Jansson, J. et al. Metabolomics reveals metabolic biomarkers of Crohn's disease. PLOS One 4, 1-10 (2009).
90 Dobson, P. D., Patel, Y. & Kell, D. B. 'Metabolite-likeness' as a criterion in the design and selection of pharmaceutical drug libraries. Drug Discov. 14, 31-40 (2009).
91 Sheridan, R. P. & Kearsley, S. K. Why do we need so many chemical similarity search methods? Drug Discov. 7, 903-911 (2002).
92 Liu, R., Li, X. & Lam, K. S. Combinatorial chemistry in drug discovery. Curr. Opin. Chem. Biol. 38, 117-126 (2017).
93 Müller, C. et al. Advanced identification of global bioactivity hotspots via screening of the metabolic fingerprint of entire ecosystems. Sci. Rep. 10, 1-13 (2020).
94 Alvarez-Rivera, G., Valdes, A., Leon, C. & Cifuentes, A. Foodomics - Fundamentals, state of the art and future trends in Foodomics: Omic Strategies and Applications in Food Science (ed J. Barros-Velázquez) 1-53 (RSC, 2021).

95 Cifuentes, A. Food analysis and foodomics. J. Chromatogr. A 1216, 7109 (2009).
96 Ehler, L. E. Perspective integrated pest management (IPM): definition, historical development and implementation, and the other IPM. Pest Manag. Sci. 62, 797-789 (2006).
97 Aöiferis, K. A. & Jabaji, S. Metabolomics – A robust bioanalytical approach for the discovery of the modes-of-action of pesticides: A review. Pestic. Biochem. Phys. 100, 105-117 (2011).
98 Hertog, M. L. A. T. M. et al. Where systems biology meets postharvest. Postharvest Biol. Technol. 62, 223-237 (2011).
99 Garcia-Canas, V., Simo, C., Leon, C., Ibanez, E. & Cifuentes, A. MS-based analytical methodologies to characterize genetically modified crops. Mass Spectrom. Rev. 30, 396-416 (2011).
100 Lacina, O., Urbanova, J., Poustka, J. & Hajslova, J. Identification/quantification of multiple pesticide residues in food plants by ultra-high-performance liquid chromatography-time-of-flight mass spectrometry. J. Chromatogr. A 1217, 648-659 (2010).
101 Diez-Simon, C., Mumm, R. & Hall, R. D. Mass spectrometry-based metabolomics of volatiles as a new tool for understanding aroma and flavour chemistry in processed food products. Metabolomics 15, 1-20 (2019).
102 Dunkel, A. et al. Nature's chemical signatures in human olfaction: A foodborne perspective for future biotechnology. Angew. Chem. Int. Ed. 53, 7124-7143 (2014).
103 Cubero-Leon, E., Penalver, R. & Maquet, A. Review on metabolomics for food authentication. Food Res. Int. 60, 95-107 (2014).
104 European Commission. Regulation (EC) No 2065/2001 of 22 October 2001 laying down detailed rules for the application of Council Regulation (EC) No 104/2000 as regards informing consumers about fishery and aquaculture products. OJEC L278, 6-8 (2002).
105 Spiteri, M. et al. Fast and global authenticity screening of honey using ^{1}H-NMR profiling. Food Chem. 189, 60-66 (2015).
106 Schievano, E., Stocchero, M., Morelato, E., Facchin, C. & Mammi, S. An NMR-based metabolomic approach to identify the botanical origin of honey. Metabolomics 8, 679-690 (2012).
107 Tabuenca, J. M. Toxic-allergic syndrome caused by ingestion of rapeseed oil denatured with aniline. Lancet 318, 567-568 (1981).
108 Lioupi, A., Nenadis, N. & Theodoridis, G. Virgin olive oil metabolomics: A review. J. Chromatogr. B 1150, 1-19 (2020).
109 Santos, P. M., Pereira-Filho, E. R. & Rodriguez-Saona, L. E. Rapid detection and quantification of milk adulteration using infrared microspectroscopy and chemometrics analysis. Food Chem. 138, 19-24 (2013).
110 Sen, C., Ray, P. R. & Bhattacharyya, M. A critical review on metabolomic analysis of milk and milk products. Int. J. Dairy Technol. 74, 17-31 (2021).
111 Gougeon, R. D. et al. The chemical diversity of wines can reveal a metabologeography expression of cooperage oak wood. PNAS 106, 9174-9179 (2009).
112 Mattarucchi, E. et al. Authentication of trappist beers by LC-MS fingerprints and multivariate data analysis. J. Agric. Food Chem. 58, 12089-12095 (2010).
113 Cajka, T., Riddellova, K., Tomaniova, M. & Hajslova, J. Ambient mass spectrometry employing a DART ion source for metabolomic

fingerprinting/profiling: a powerful tool for beer origin recognition. Metabolomics 7, 500-508 (2011).

114 Dai, W. et al. Nontargeted analysis using ultraperformance liquid chromatography–quadrupole time-of-flight mass spectrometry uncovers the effects of harvest season on the metabolites and taste quality of tea (Camellia sinensis L.). 63, 9869-9878 (2015).

115 Fraser, K. et al. Analysis of metabolic markers of tea origin by UHPLC and high resolution mass spectrometry. Food Res. Int. 53, 827-835 (2012).

116 Jumhawan, U. et al. Selection of discriminant markers for authentication of Asian palm civet coffee (Kopi Luwak): A metabolomics approach. J. Agric. Food Chem. 61, 7994-8001 (2013).

117 Garrett, R., Vaz, B. G., Hovell, A. M. C., Eberlin, M. N. & Rezende, C. M. Arabica and robusta coffees: Identification of major polar compounds and quantification of blends by direct-infusion electrospray ionization–mass spectrometry. J. Agric. Food Chem. 60, 4253-4258 (2012).

118 Trivedi, D. K. et al. Meat, the metabolites: an integrated metabolite profiling and lipidomics approach for the detection of the adulteration of beef with pork. Analyst 141, 2075-2320 (2016).

119 Corella, D. et al. A high intake of saturated fatty acids strengthens the association between the fat mass and obesity-associated gene and BMI. J. Nutr. 141, 2219-2225 (2011).

120 Kau, A. L., Ahern, P. P., Griffin, N. W., Goodman, A. L. & Gordon, J. I. Human nutrition, the gut microbiome, and immune system: envisioning the future. Nature 474, 327-336 (2012).

121 Smirnov, K. S. et al. Challenges of metabolomics in human gut microbiota research. Int. J. Med. Microbiol. Suppl. 306, 266-279 (2016).

122 Ulaszewska, M. M. et al. Nutrimetabolomics: An integrative action for metabolomic analyses in human nutritional studies. Mol. Nutr. Food Res. 63, 1-38 (2019).

123 Guasch-Ferre, M., Bhupathiraju, S. N. & Hu, F. B. Use of metabolomics in improving assessment of dietary intake. Clin. Chem. 64, 82-98 (2018).

124 Trewavas, A. A brief history of systems biology. Plant Cell 18, 2420-2430 (2006).

125 Hänsch, T. W. Nobel Lecture: "Passion for Precision", <https://www.nobelprize.org/prizes/physics/2005/hansch/lecture/> accessed July 2021

126 Hertkorn, N. et al. Natural organic matter and the event horizon of mass spectrometry. Anal. Chem. 80, 8908-8919 (2008).

127 Smith, D. F., Podgorski, D. C., Rodgers, R. P., Blakney, G. T. & Hendrickson, C. L. 21 Tesla FT-ICR mass spectrometer for ultrahigh-resolution analysis of complex organic mixtures. Anal. Chem. 90, 2041-2057 (2018).

128 van Agthoven, M. A., Lam, Y. P. Y., O'Connor, P. B., Rolando, C. & Delsuc, M.-A. Two-dimensional mass spectrometry: New perspectives for tandem mass spectrometry. Eur. Biophys. J. 48, 213-229 (2019).

129 Venable, J. D., Dong, M.-Q., Wohlschlegel, J., Dillin, A. & Yates, J. R. Automated approach for quantitative analysis of complex peptide mixtures from tandem mass spectra. Nat. Methods 1, 39-45 (2004).

130 Rychlik, M. & Schmitt-Kopplin, P. Reading from the crystal ball: The Laws of Moore and Kurzweil applied to mass spectrometry in food analysis. Front. Nutr. 7, 1-7 (2020).

131 Keifer, D. Z. & Jarrold, M. F. Single-molecule mass spectrometry. Mass Spectrom. Rev. 36, 715-733 (2016).
132 Iwata, K. et al. Chemical structure imaging of a single molecule by atomic force microscopy at room temperature. Nat. Commun. 6, 1-7 (2015).
133 Duncan, K. D., Fyrestam, J. & Lanekoff, I. Advances in mass spectrometry based single-cell metabolomics. Analyst 144, 782-793 (2019).
134 Fiehn, O. et al. The metabolomics standards initiative (MSI). Metabolomics 3, 175-178 (2007).
135 Haug, K. et al. MetaboLights - An open-access general-purpose repository for metabolomics studies and associated meta-data. Nucleic Acids Res. 41, D781-D786 (2013).
136 Sud, M. et al. Metabolomics Workbench: An international repository for metabolomics data and metadata, metabolite standards, protocols, tutorials and training, and analysis tools. Nucleic Acids Res. 44, D463-D470 (2016).
137 Goodacre, R. Water, water, every where, but rarely any drop to drink. Metabolomics 10, 5-7 (2014).
138 Spicer, R. A., Salek, R. M. & Steinbeck, C. Analysis: Compliance with minimum information guidelines in public metabolomics repositories. Sci. Data 4, 1-8 (2017).
139 Wang, M. et al. Sharing and community curation of mass spectrometry data with Global Natural Products Social Molecular Networking. Nat. Biotechnol. 34, 828-837 (2015).
140 Quinn, R. A. et al. Global chemical effects of the microbiome include new bile-acid conjugations. Nature 579, 123-129 (2020).
141 Aron, A. et al. Reproducible molecular networking of untargeted mass spectrometry data using GNPS. Nat. Protoc. 15, 1954-1991 (2020).
142 Gauglitz, J. M. et al. Reference data based insights expand understanding of human metabolomes (Preprint). bioRxiv (2020).
143 Domingo-Almenara, X. et al. The METLIN small molecule dataset for machine learning-based retention time prediction. Nat. Commun., 1-9 (2019).
144 Liebal, U. W., Phan, A. N. T., Sudhakar, M., Raman, K. & Blank, L. M. Machine learning applications for mass spectrometry-based metabolomics. Metabolites 10, 1-25 (2020).
145 Kell, D. B. Metabolomics, machine learning and modelling: towards an understanding of the language of cells. Biochem. Soc. Trans. 33, 520-524 (2005).
146 Valdés, A. et al. Foodomics: Analytical opportunities and challenges. Anal. Chem. (in print) (2021).
147 Bengio, Y., Courville, A. & Vincent, P. Representation learning: A review and new perspectives. IEEE PAMI 35, 1798-1828 (2013).
148 Cappon, G., Acciaroli, G., Vettoretti, M., Facchinetti, A. & Sparacino, S. Wearable continuous glucose monitoring sensors: Revolution in diabetes treatment. Electronics 6, 1-16 (2017).
149 Clish, C. B. Metabolomics: An emerging but powerful tool for precision medicine. Cold Spring Harb. Mol. Case Stud. 1, 1-6 (2015).
150 Shao, Y. & Le, W. Recent advances and perspectives of metabolomics-based investigations in Parkinson's disease. Mol. Neurodegener. 14, 1-12 (2019).
151 Wild, C. P. Complementing the genome with an ''exposome'': The outstanding challenge of environmental exposure measurement in molecular epidemiology. Cancer Epidemiol. Biomark. Prev. 14, 1847-1850 (2005).

152 Barabasi, A.-L.-., Menichetti, G. & Loscalzo, J. The unmapped chemical complexity of our diet. Nat. Food 1, 33-37 (2020).

153 FooDB. <www.foodb.ca> accessed July 2021

154 McGrath, T. F. et al. What are the scientific challenges in moving from targeted to non-targeted methods for food fraud testing and how can they be addressed? – Spectroscopy case study. Trends Food Sci. Technol. 76, 38-55 (2018).

155 Gao, B. et al. Opportunities and challenges using non-targeted methods for food fraud detection. J. Agric. Food Chem. 67, 8425-8430 (2019).

156 Ashton, K. That 'Internet of Things' thing, <https://www.rfidjournal.com/that-internet-of-things-thing> accessed July 2021

157 Ellis, D. I., Muhamadali, H., Haughey, S. A., Elliot, C. T. & Goodacre, R. Point-and-shoot: rapid quantitative detection methods for on-site food fraud analysis –moving out of the laboratory and into the food supply chain. Anal. Methods 7, 9401-9414 (2015).

158 McGovern, P. E. Uncorking the past: The quest for wine, beer, and other alcoholic beverages. (University of California Press, 2009).

159 Michel, R. H. & McGovern, P. E. The first wine & beer. Chemical detection of ancient fermented beverages. Anal. Chem. 65, 408-413 (1993).

160 Meußdoerffer, F. & Zarnkow, M. Das Bier. Eine Geschichte von Hopfen und Malz. Vol. 2nd Ed. (Beck, 2014).

161 Duke Wilhelm, I. D. L., X. Bayerische Landesverordnung. Chapter 2, Row 13-17 (1516).

162 Pasteur, L. Comptes rendus des séances de l'Académie des sciences. Vol. 52 1260-1264 (1861).

163 Hansen, E. C. Recherches sur la physiologie et la morphologie des ferments alcooliques. V. Methodes pour obtenir des cultures pures de Saccharomyces et de microorganismes analogous. Compt. Rend. Trav. Lab. Carlsberg 2, 92-105 (1883).

164 Linde, C. P. G. Refrigerating and ice making apparatus. US patent US 10522 (1884).

165 Herzsprung, P. et al. Variations of DOM quality in inflows of a drinking water reservoir: Linking of van Krevelen diagrams with EEMF spectra by rank correlation. Environ. Sci. Technol. 46, 5511-5518 (2012).

166 Narziss, L. Die Bierbrauerei, Band II: Die Technologie der Würzebereitung. (Enke Verlag, 1992).

167 Basarova, G., Savel, J., Basar, P., Basarova, P. & Lejsek, T. The comprehensive guide to brewing. From raw material to packaging. (Hans Carl Verlag, 2017).

168 Hemmler, D. et al. Evolution of complex Maillard chemical reactions, resolved in time. Sci. Rep. 7, 3227-3233 (2017).

169 Thorn, J. Yeast autolysis and its effect on beer. Brewer's Dig. 46, 110-113 (1971).

170 Jacobsen, T. New aspect of chemical analysis: Chemometrics - variations in trace elements in malt as shown by factor analysis. Brygmesteren 37, 149-158 (1980).

171 Jacobsen, T., Volden, R., Engan, S. & Aubert, O. A chemometric study of some beer flavour components. J. Inst. Brew. 85, 265-270 (1979).

172 da Silva, M. M., Malfeito-Ferreira, M. & Loureiro, V. Long-chain fatty acid composition as a criterion for yeast distinction in the brewing industry. J. Inst. Brew. 100, 17-22 (1994).
173 Timmins, E. M., Quain, D. E. & Goodacre, R. Differentiation of brewing yeast strains by pyrolysis mass spectrometry and Fourier transform infrared spectroscopy. Yeast 14, 885-893 (1998).
174 Pope, G. A. et al. Metabolic footprinting as a tool for discriminating between brewing yeasts. Yeast 24, 667-679 (2007).
175 Farag, M. A., Porzel, A., Schmidt, J. & Wessjohann, L. A. Metabolite profiling and fingerprinting of commercial cultivars of Humulus lupulus L. (hop): a comparison of MS and NMR methods in metabolomics. Metabolomics 8, 492-507 (2012).
176 Sommella, E. et al. Chemical profiling of bioactive constituents in hop cones and pellets extracts by online comprehensive two-dimensional liquid chromatography with tandem mass spectrometry and direct infusion Fourier transform ion cyclotron resonance mass spectrometry. J. Spe. Sci. 41, 1548-1557 (2017).
177 Olšovská, J., Kameník, Z., Čejka, P., Jurková, M. & Mikyška, A. Ultra-high-performance liquid chromatography profiling method for chemical screening of proanthocyanidins in Czech hops. Talanta, 919-926 (2013).
178 Stenroos, L. E. & Siebert, K. J. Application of pattern-recognition techniques to the essential oil of hops. J. Am. Soc. Brew. Chem. 42, 54-61 (1984).
179 Kralj, D., J., Z., Vasilj, D., Kralj, S. & Psenicnik, J. Variability of essential oils of hops, Humulus Lupulus L. J. Inst. Brew. 97, 197-206 (1991).
180 Yan, D. et al. Assessment of the phytochemical profiles of novel hop (Humulus lupulus L.) cultivars: A potential route to beer crafting. Food Chem. 275, 15-23 (2019).
181 Goncalves, J. L. et al. A powerful methodological approach combining headspace solid phase microextraction, mass spectrometry and multivariate analysis for profiling the volatile metabolomic pattern of beer starting raw materials. Food Chem. 160, 266-280 (2014).
182 White, F. H. & Wainwright, T. The presence of tow dimethyl sulphide precursors in malt, their control by malt kilning conditions, and their effect on beer DMS levels. J. Inst. Brew. 83, 224-230 (1977).
183 Bettenhausen, H. M. et al. Influence of malt source on beer chemistry, flavor, and flavor stability. Food Res. Int. 113, 487-504 (2018).
184 da Silva, G. A., Augusto, F. & Poppi, R. J. Exploratory analysis of the volatile profile of beers by HS–SPME–GC. Food Chem. 111, 1057–1063 (2008).
185 Inui, T., Tsuchiya, F., Ishimaru, M., Oka, K. & Komura, H. Different beers with different hops. Relevant compounds for their aroma characteristics. J. Agric. Food Chem. 61, 4758–4764 (2013).
186 Haseleu, G. et al. Quantitative sensomics profiling of hop-derived bitter compounds throughout a full-scale beer manufacturing process. J. Agric. Food Chem. 58, 7930-7939 (2010).
187 Intelmann, D. et al. Comprehensive sensomics analysis of hop-derived bitter compounds during storage of beer. J. Agric. Food Chem. 59, 1939-1953 (2011).
188 Spevacek, A. R., Benson, K. H., Bamforth, C. W. & Slupsky, C. M. Beer metabolomics: molecular details of the brewing process and the differential

effects of late and dry hopping on yeast purine metabolism. J. Inst. Brew. 122, 21-28 (2016).

189 Kimura, Y., Hashimoto, N., Nagashima, Y. & Yoshioka, K. Systematic design of flavor quality of a light beer - "Kirin beer light". J. Agr. Chem. Soc. Jpn. 61 (1987).

190 Zhu, L. et al. Simultaneous sampling of volatile and non-volatile analytes in beer for fast fingerprinting by extractive electrospray ionization mass spectrometry. Analy. Bioanal. Chem. 398, 405-413 (2010).

191 Gallart-Ayala, H., Kamleh, M. A., Hernández-Cassou, S. S., J. & Checa, A. Ultra-high-performance liquid chromatography–high-resolution mass spectrometry based metabolomics as a strategy for beer characterization. J. Inst. Brew. 122, 430-436 (2016).

192 Whittle, N., Eldridge, H. & Bartley, J. Identification of the polyphenols in barley and beer by HPLC/MS and HPLC/electrochemical detection. J. Inst. Brew. 105 (1999).

193 Araujo, A. S. et al. Electrospray ionization mass spectrometry fingerprinting of beer. Analyst 130, 884-889 (2005).

194 Duarte, I. et al. High-resolution nuclear magnetic resonance spectroscopy and multivariate analysis for the characterization of beer. J. Agric. Food Chem. 50, 2475-2481 (2002).

195 Lachenmeier, D. W. et al. Quality control of beer using high-resolution nuclear magnetic resonance spectroscopy and multivariate analysis. Eur. Food Res. Technol. 220, 215-221 (2005).

196 Almeida, C. et al. Composition of beer by ^{1}H-NMR spectroscopy: effects of brewing site and date of production. J. Agric. Food Chem. 54, 700-706 (2006).

197 Rodrigues, J. E. & Gil, A. M. NMR methods for beer characterization and quality control. Magn. Reson. Chem. 49, 37-45 (2011).

198 Duarte, I. F., Barros, A., Almeida, C., Spraul, M. & Gil, A. M. Multivariate analysis of NMR and FTIR data as a potential tool for the quality control of beer. J. Agric. Food Chem. 52, 1031-1038 (2004).

199 Andres-Iglesias, C., Blanco, C. A., Blanco, J. & Montero, O. Mass spectrometry-based metabolomics approach to determine differential metabolites between regular and non-alcohol beers. Food Chem. 157, 205-212 (2014).

200 Riu-Aumatell, M., Miro, P., Serra-Cayuela, A., Buxaderas, S. & Lopez-Tamames, E. Assessment of the aroma profiles of low-alcohol beers using HS-SPME-GC-MS. Food Res. Int. 57, 196-202 (2014).

201 TRACE. Tracing Food Commodities in Europe. Tracing the origin of food. EU FP6–006942. (2005-2009).

202 Rodrigues, J. A. et al. Evaluation of beer deterioration by gas chromatography-mass spectrometry/multivariate analysis: A rapid tool for assessing beer composition. J. Chromatogr. A 7, 990-996 (2011).

203 Heuberger, A. L. et al. Metabolomic profiling of beer reveals effect of termperature on non-volatile small molecules during short-term storage. Food Chem. 135, 1284-1289 (2012).

204 Hughey, C. A., McMinn, C. M. & Phung, J. Beeromics: From quality control to identification of differentially expressed compounds in beer. Metabolomics 12 (2016).

205 Yao, J., Zong, X., Cui, C., Mu, L. & Zhao, H. Metabonomics analysis of nonvolatile small molecules of beers during forced ageing. J. Food Sci. Tech. 53, 1698–1704 (2018).
206 Heuberger, A. L. et al. Evaluation of non-volatile metabolites in beer stored at high temperature and utility as an accelerated method to predict flavour stability. Food Chem. 200, 301-307 (2016).
207 Guerdeniz, G. et al. Detecting beer intake by unique metabolite patterns. J. Proteome Res. 15, 4544–4556 (2016).
208 Quifer-Rada, P., Chiva-Blanch, G., Jauregui, O., Estruch, R. & Lamuela-Ravento, R. M. A discovery-driven approach to elucidate urinary metabolome changes after a regular and moderate consumption of beer and nonalcoholic beer in subjects at high cardiovascular risk. Mol. Nutr. Food Res. 61 (2017).
209 van der Greef, J. & Smilde, A. K. Symbiosis of chemometrics and metabolomics: past, present, and future. J. Chemometrics 19, 376-386 (2005).
210 Wold, S. Chemometrics; What do we mean with it, and what do we want from it? Chemom. Intell. Lab. Syst. 30, 109-115 (1995).
211 Gromski, P. S. et al. A tutorial review: Metabolomics and partial least squares-discriminant analysis – a marriage of convenience or a shotgun wedding. Anal. Chim. Acta 879, 10-23 (2015).
212 Wold, S., Sjöström, M. & Eriksson, L. PLS-regression: A basic tool of chemometrics. Chemom. Intell. Lab. Syst. 58, 109-130 (2001).
213 Henseler, J. & Sarstedt, M. Goodness-of-fit indices for partial least squares path modeling. Comput. Stat. 28, 565-580 (2013).
214 Golbraikh, A. & Tropsha, A. Beware of q2! J. Mol. Graph. Model. 20, 269-276 (2002).
215 Westerhuis, J. A. et al. Assessment of PLSDA cross validation. Metabolomics 4, 81-89 (2008).
216 Eriksson, L., Trygg, J. & Wold, S. CV-ANOVA for significance testing of PLS and OPLS models. J. Chemometrics 22, 594-600 (2008).
217 Anderssen, E., Dyrstad, K., Westad, F. & Martens, H. Reducing over-optimism in variable selection by cross-model validation. Chemom. Intell. Lab. Syst. 84, 69-74 (2006).
218 Broadhurst, D. I. & Kell, D. B. Statistical strategies for avoiding false discoveries in metabolomics and related experiments. Metabolomics 2, 171-196 (2006).
219 Trygg, J. & Wold, S. Orthogonal projections to latent structures (O-PLS). J. Chemometrics 16, 119-128 (2002).
220 Whelehan, O. P., Earll, M. E., Johansson, E., Toft, M. & Eriksson, L. Detection of ovarian cancer using chemometric analysis of proteomic profiles. Chemom. Intell. Lab. Syst. 84 (2006).
221 Stenlund, H., Gorzsas, A., Persson, P., Sundberg, B. & Trygg, J. Orthogonal projections to latent structures discriminant analysis modeling on in situ FT-IR spectral imaging of liver tissue for identifying sources of variability. Anal. Chem. 80, 6898-6906 (2008).
222 Mahadevan, S., Shah, S. L., Marrie, T. J. & Slupsky, C. M. Analysis of metabolomic data using support vector machines. Anal. Chem. 80, 7562-7570.
223 Tapp, H. S. & Kemsley, E. K. Notes on the practical utility of OPLS. Trends Anal. Chem. 28, 1322-1327 (2009).

224 Pieczonka, S. A. et al. Archeochemistry reveals the first steps into modern industrial brewing. PNAS (in review) (2021).
225 Pieczonka, S. A., Lucio, M., Rychlik, M. & Schmitt-Kopplin, P. Decomposing the molecular complexity of brewing. NPJ Sci. Food 4, 1-10 (2020).
226 Pieczonka, S. A. et al. Hidden in its color: A molecular-level analysis of the beer's Maillard reaction network. Food Chem. 361 (130112), 1-9 (2021).
227 Pieczonka, S. A., Rychlik, M. & Schmitt-Kopplin, P. Metabolomics in brewing research in Comprehensive foodomics Vol. 1st (ed A. Cifuentes) Ch. 2.08, 116-128 (Elsevier, 2021).
228 Pieczonka, S. A., Paravicini, S., Rychlik, M. & Schmitt-Kopplin, P. On the trail of the German Purity Law: Distinguishing the metabolic signatures of wheat, corn and rice in beer. Front. Chem. 9, 1-12 (2021).
229 Easterling, M. L. & Agar, J. N. Fundamentals, strengths, and future directions for Fourier transform ion cyclotron resonance mass spectrometry in Fundamentals and applications of Fourier transform mass spectrometry (eds B. Kanawati & P. Schmitt-Kopplin) Ch. 3, 63-89 (Elsevier, 2019).
230 Lorentz, H. A. Versuch einer Theorie der electrischen und optischen Erscheinungen in bewegten Körpern. (E. J. Brill, 1895).
231 Lawrence, E. O. & Livingston, M. S. The production of high speed light ions without the use of high voltages. Phys. Rev. 50, 19-35 (1932).
232 Doroshenko, V. M. & Cotter, R. J. Ideal velocity focusing in a reflectron Time-of-Flight mass spectrometer. J. Am. Soc. Mass Spectrom. 10, 992-999 (1999).
233 Chen, R., Guan, S. & Marshall, A. G. Generation and detection of coherent magnetron motion in Fourier transform ion cyclotron resonance mass spectrometry. J. Chem. Phys. 100, 2258-2266 (1994).
234 Marshall, A. G. & Guan, S. Advantages of high magnetic field for Fourier transform ion cyclotron resonance mass spectrometry. Rapid Commun. Mass Spectrom. 10, 1819-1823 (1996).
235 Kind, T. & Fiehn, O. Seven golden rules for heuristic filtering of molecular formulas obtained by accurate mass spectrometry. BMC Bioinform. 8, 1-20 (2007).
236 Schmitt-Kopplin, P. et al. High molecular diversity of extraterrestrial organic matter in Murchison meteorite revealed 40 years after its fall. PNAS 107, 2763-2768 (2010).
237 Tziotis, D., Hertkorn, N. & Schmitt-Kopplin, P. Kendrick-analogous network visualization of ion cyclotron resonance Fourier transform mass spectra: improved options for the assignment of elemental compositions and the classification of organic molecular complexity. Eur. J. Mass Spectrom. 17, 415-421 (2011).
238 Kim, S., Rodgers, R. P. & Marshall, A. G. Truly “exact” mass: Elemental composition can be determined uniquely from molecular mass measurement at ~0.1 mDa accuracy for molecules up to ~500 Da. Int. J. Mass Spectrom. 251, 260-265 (2006).
239 Makarov, A. & Scigelova, M. Coupling liquid chromatography to Orbitrap mass spectrometry. J. Chromatogr. A 1217, 3938-3945 (2010).
240 Eliuk, S. & Makarov, A. Evolution of orbitrap mass spectrometry instrumentation. Annu. Rev. Anal. Chem. 8, 61-80 (2015).

241 Zhurov, K. O., Kozhinov, A. N. & Tsybin, Y. O. Evaluation of high-field Orbitrap Fourier transform mass spectrometer for Petroleomics. Energy Fuels 27, 2974-2983 (2013).
242 Marshall, A. G., Hendrickson, C. L. & Jackson, G. S. Fourier transform ion cyclotron resonance mass spectrometry: A primer. Mass Spectrom. Rev. 17, 1-35 (1998).
243 Webb, K. J., Xu, T., Park, S. K. & Yates, J. R. Modified MuDPIT separation identified 4488 proteins in a system-wide analysis of ouiescence in yeast. J. Proteome Res. 12, 2177-2184 (2013).
244 Geiger, T., Cox, J. & Mann, M. Proteomics on an orbitrap benchtop mass spectrometer using all-ion fragmentation. Mol. Cell. Proteom. 9, 2252-2261 (2010).
245 Guan, S. & Marshall, A. G. Resolution and chemical formula identification of aromatic hydrocarbons and aromatic compounds containing sulfur, nitrogen, or oxygen in petroleum distillates and refinery streams. Anal. Chem. 68, 46-71 (1996).
246 Marshall, A. G. & Rodgers, R. P. Petroleomics: Chemistry of the underworld. PNAS 105, 18090-18095 (2008).
247 Marshall, A. G. & Rodgers, R. P. Petroleomics: The next grand challenge for chemical analysis. Acc. Chem. Res. 37, 53-59 (2004).
248 Zhu, J. & Cole, R. B. Ranking of gas-phase acidities and chloride affinities of monosaccharides and linkage specificity in collision-induced decompositions of negative ion electrospray-generated chloride adducts of oligosaccharides. J. Am. Soc. Mass Spectrom. 12, 1193-1204 (2001).
249 Boutegrabet, L. et al. Attachment of chloride anion to sugars: Mechanistic investigation and discovery of a new dopant for efficient sugar ionization/detection in mass spectrometers. Chem. Eur. J. 18, 13059-13067 (2012).
250 Wan, E. C. H. & Yu, J. Z. Analysis of sugars and sugar polyols in atmospheric aerosols by chloride attachment in liquid chromatography/negative ion electrospray mass spectrometry. Environ. Sci. Technol. 41, 2459-2466 (2007).
251 King, R. C., Bonfiglio, R., Fernandez-Metzler, C., Miller-Stein, C. & Olah, T. V. Mechanistic investigation of ionization suppression in electrospray ionization. J. Am. Soc. Mass Spectrom. 11, 942-950 (2000).
252 Annesley, T. M. Ion suppression in mass spectrometry. Clin. Chem. 49, 1041-1044 (2003).
253 Bonfiglio, R., King, R. C., Olah, T. V. & Merkle, K. The effects of sample preparation methods on the variability of the electrospray ionization response for model drug compounds. Rapid Commun. Mass Spectrom. 13, 1175-1185 (1999).
254 Taylor, P. K. & Amster, I. J. Space charge effects on mass accuracy for multiply charged ions in ESI–FT-ICR. Int. J. Mass Spectrom 222, 351-361 (2003).
255 Jefries, J. B., Barlow, S. E. & Dunn, G. H. Theory of space-charge shift of ion cyclotron resonance frequencies. Int. J. Mass Spectrom 54, 169-187 (1983).
256 Francl, T. J. et al. Experimental determination of the effects of space charge on ion cyclotron resonance frequencies. Int. J. Mass Spectrom 54, 189-199 (1983).

257 Easterling, M. L., Mize, T. H. & Amster, I. J. Routine part-per-million mass accuracy for high-mass ions: Space-charge effects in MALDI FT-ICR. Anal. Chem. 71, 624-632 (1999).

258 Masselon, C., Tolmachev, A. V., Anderson, G. A., Harkewicz, R. & Smith, R. D. Mass measurement errors caused by “local” frequency perturbations in FT-ICR mass spectrometry. J. Am. Soc. Mass. Spectrom. 13, 99-106 (2002).

259 Smirnov, K. S., Forcisi, S., Moritz, F., Lucio, M. & Schmitt-Kopplin, P. Mass difference maps and their application for the recalibration of mass spectrometric data in nontargeted metabolomics. Anal. Chem. 91, 3350-3358 (2019).

260 Kind, T. et al. Lipidblast in silico tandem mass spectrometry database for lipid identification. Nat. Methods 10, 755-758 (2013).

261 Wolf, S., Schmidt, S., Müller-Hannemann, M. & Neumann, S. In silico fragmentation for computer assisted identification of metabolite mass spectra. BMC Bioinform. 11, 1-12 (2010).

262 Ruttkies, C., Schymanski, E. L., Wolf, S., Hollender, J. & Neumann, S. MetFrag relaunched: incorporating strategies beyond in silico fragmentation. J. Cheminform. 8 (2016).

263 Tsugawa, H. et al. Hydrogen rearrangement rules: Computational MS/MS fragmentation and structure elucidation using MS-FINDER Software. Anal. Chem. 88, 7946-7958 (2016).

264 Allen, F., Greiner, R. & Wishart, D. Competitive fragmentation modeling of ESI-MS/MS spectra for putative metabolite identification. Metabolomics 11, 89-110 (2015).

265 Blazenovic, I. et al. Comprehensive comparison of in silico MS/MS-fragmentation tools of the CASMI contest: database boosting is needed to achieve 93% accuracy. J. Cheminform. 9, 1-12 (2017).

266 Vaniya, A. & Fiehn, O. Using fragmentation trees and mass spectral trees for identifying unknown compounds in metabolomics. Trends Anal. Chem. 69, 52-61 (2015).

267 Shannon, P. et al. Cytoscape: a software environment for integrated models of biomolecular interaction networks. Genome Res. 13, 2498-2504 (2003).

268 Mirabelli, M. F., Wolf, J.-C. & Zenobi, R. Direct coupling of solid-phase microextraction with mass spectrometry: Sub-pg/g sensitivity achieved using a dielectric barrier discharge ionization source. Anal. Chem. 88, 7252-7258 (2016).

269 Wang, J. et al. Revealing a 5,000-y-old beer recipe in China. PNAS 113, 6444-6448 (2016).

270 Quifer-Rada, P. et al. A comprehensive characterisation of beer polyphenols by high resolution mass spectrometry (LC-ESI-LTQ-Orbitrap-MS). Food Chem. 169, 336-343 (2015).

271 Intelmann, D., Haseleu, G. & Hofmann, T. LS-MS/MS quantitation of hop-derived bitter compounds in beer using the ECHO technique. J. Agric. Food Chem. 57, 1172-1182 (2009).

272 Rakete, S., Klaus, A. & Glomb, M. A. Investigations on the Maillard reaction of dextrins during aging of pilsner type beer. J. Agric. Food Chem. 62, 9876-9884 (2014).

273 Hellwig, M., Witte, S. & Henle, T. Free and protein-bound Maillard reaction products in beer: Method development and a survey of different beer types. J. Agric. Food Chem. 64, 7234-7243 (2016).

274 Rossi, S., Sileoni, V., Perretti, G. & Marconi, O. Characterization of the volatile profiles of beer using headspace solid-phase microextraction and gas chromatography-mass spectrometry. J. Sci. Food Agric. 94, 919-928 (2014).
275 Junot, C., Fenaille, F. C., B. & Becher, F. High resolution mass spectrometry based techniques at the crossroads of metabolic pathways. Mass Spectrom. Rev. 33, 471-500 (2014).
276 Worley, B. & Powers, R. Multivariate analysis in metabolomics. Curr. Metabolomics 1, 92-107 (2013).
277 Piazzon, A., Forte, M. & Nardini, M. Characterization of phenolics content and antioxidant activity of different beer types. J. Agric. Food Chem. 58, 10677-10683 (2010).
278 Cajka, T., Riddellova, K., Tomaniova, M. & Hajslova, J. Recognition of beer brand based on multivariate analysis of volatile fingerprint. J. Chromatogr. A 1217, 4195-4203 (2010).
279 Gougeon, R. D. et al. Expressing forest origins in the chemical composition of cooperage oak woods and corresponding wines by using FT-ICR-MS. Chem. Eur. J. 15, 600-611 (2009).
280 Tanwir, F., Fredholm, M., Gregersen, P. L. & Fomsgaard, I. S. Comparison of the levels of bioactive benzoxazinoids in different wheat and rye fractions and the transformation of these compounds in homemade foods. Food Chem. 141, 444-450 (2013).
281 de Bruijn, W. J. C., Vincken, J.-P., Duran, K. & Gruppen, H. Mass spectrometric characterization of benzoxazinoid glycosides from rhizopus-elicited wheat (Triticum aestivum) seedlings. J. Agric. Food Chem. 64, 6267-6276 (2016).
282 Sicker, D., Frey, M., Schulz, M. & Gierl, A. Role of natural benzoxazinones in the survival strategy of plants. Int. Rev. of Cytology 198, 319-346 (2000).
283 Pihlava, J.-M. & Kurtelius, T. Determination of benzoxazinoids in wheat and rye beers by HPLC-DAD and UPLC-QTOF MS. Food Chem. 204, 400-408 (2016).
284 Oladokun, O. et al. The impact of hop bitter acid and polyphenol profiles on the perceived bitterness of beer. Food Chem. 205, 212-220 (2016).
285 Savolainen, O., Pekkinen, J., Katina, K., Poutanen, K. & Hanhineva, K. Glycosylated benzoxazinoids are degraded during fermentation of wheat bran. J. Agric. Food Chem. 63, 5943-5949 (2015).
286 Farag, M. A., Elmassry, M. M., Baba, M. & Friedman, R. Revealing the constituents of Egypt's oldest beer using infrared and mass spectrometry. Sci. Rep. 9, 1-9 (2019).
287 Londesborough, J. et al. Analysis of beer from an 1840s' shipwreck. J. Agric. Food Chem. 63, 2525-2536 (2015).
288 Bastian, M., Heymann, S. & Jacomy, M. Gephie: an open source software for exploring and manipulating networks in International AAAI Conference on Weblogs and Social Media.
289 Suhre, K. & Schmitt-Kopplin, P. MassTRIX: Mass TRanslator Into Pathways. Nucleic Acids Res. 36 (2008).
290 Wishart, D. S., Feunang, Y. D., Marcu, A., Gua, A. C. & Liang, K. HMDB 4.0 - The Human Metabolome Database for 2018. Nucleic Acids Res. 46, 608-617 (2018).

291 Hastings, J. et al. The ChEBI reference database and ontology for biogically relevant chemistry: Enhancements for 2013. Nucleic Acids Res. 41, 456-463 (2013).
292 Caspi, R. et al. The MetaCyc database of metabolic pathways and enzymes. Nucleic Acids Res. 46, 633-639 (2018).
293 Sud, M. et al. LMSD: LIPID MAPS structure database. Nucleic Acids Res. 35, 527-532 (2006).
294 Ramirez-Guana, M. et al. YMDB 2.0: A significantly expanded version of the Yeast Metabolome Database. Nucleic Acids Res. 45, 440-445 (2017).
295 FiehnLab. MoNA - MassBank of North America, <https://mona.fiehnlab.ucdavis.edu/> accessed July 2021
296 Dietrich, L. et al. Investigating the function of pre-pottery neolithic stone troughs from Göbekli Tepe – An integrated approach. J. Archaeol. Sci. Rep 34, 1-20 (2020).
297 Rodrigues, J. A., Barros, A. S., Carvalho, B., Brandão, T. & Gil, A. M. Probing beer aging chemistry by nuclear magnetic resonance and multivariate analysis. Anal. Chim. Acta 702, 178-187 (2011).
298 Capuano, E. & Fogliano, V. Acrylamide and 5-hydroxymethylfurfural (HMF): A review on metabolism, toxicity, occurrence in food and mitigation strategies. LWT-Food Sci. Technol. 44, 793-810 (2011).
299 Yaylayan, V. A. & Mandeville, S. Stereochemical control of maltol formation in Maillard reaction. J. Agric. Food Chem. 42, 771-775 (1994).
300 Mavric, E. & Henle, T. Isolation and identification of 3,4-dideoxypentosulose as specific degradation product of oligosaccharides with 1,4-glycosidic linkages. Eur. Food Res. Technol. 223, 803-810 (2006).
301 Hellwig, M. & Henle, T. Formyline, a new glycation compound from the reaction of lysine and 3-deoxypentosone. Eur. Food Res. Technol. 230, 903-914 (2010).
302 Kuntcheva, M. T. & Obretenov, T. D. Isolation and characterization of melanoidins from beer. Z. Lebensm. Unters. Forsch. 202, 238-243 (1996).
303 Obretenov, T. D. et al. Flavor release in the presence of melanoidins prepared from L-(+)-ascorbic acid and amino acids. J. Agric. Food Chem. 50, 4244-4250 (2002).
304 Lusk, L. T., Goldstein, H. & Ryder, D. Independent role of beer proteins, melanoidins and polysaccharides in foam formation. J. Am. Soc. Brew. Chem. 53, 93-103 (1995).
305 Spreng, S. & Hofmann, T. Activity-guided identification of in vitro antioxidants in beer. J. Agric. Food Chem. 66, 720-731 (2018).
306 Dack, R. E., Black, G. W., Koutsidis, G. & Usher, S. J. The effect of Maillard reaction products and yeast strain on the synthesis of key higher alcohols and esters in beer fermentations. Food Chem. 232, 595-601 (2017).
307 Hemmler, D. et al. Simulated sunlight selectively modifies Maillard reaction products in a wide array of chemical reactions. Chem. Eur. J. (2019).
308 Lucio, M., Fekete, A., Frommberger, M. & Schmitt-Kopplin, P. Metabolomics: High-resolution tools offer to follow bacterial growth on a molecular level in Handbook of Molecular Microbial Ecology I: Metagenomics and Complementary Approaches (ed F. J. de Bruijn) 683-695 (John Wiley & Sons, 2001).
309 Hodge, J. E. Dehydrates foods, chemistry of browning reactions in model systems. J. Agric. Food Chem. 1, 928-943 (1953).

310 Hagberg, A. A., Schult, D. A. & Swart, P. J. Exploring network structure, dynamics, and function using networkx in Proceedings of the 7th Python in Science Conference (SciPy2008). 11-16.
311 Kim, S., Kramer, R. W. & Hatcher, P. G. Graphical method for analysis of ultrahigh-resolution broadband mass spectra of natural organic matter, the van Krevelen diagram. Anal. Chem. 75, 5336-5344 (2003).
312 Hemmler, D. et al. Insights into the chemistry of non-enzymatic browning reactions in different ribose-amino acid model systems. Sci. Rep. 8, 1-9 (2018).
313 Yu, X., Zhao, M., Hu, J., Zeng, S. & Bai, X. Correspondence analysis of antioxidant activity and UV-Vis absorbance of Maillard reaction products as related to reactants. Food Sci. Technol. 46, 1-9 (2012).
314 Otter, G. E. & Taylor, L. The determination of amino acids in wort, beer and brewing materials using gas chromatography. J. Inst. Brew. 82, 264-269 (1976).
315 Friedman, M. & Molnar-Perl, I. Inhibition of browning by sulfur amino acids. 1. Heated amino acid-glucose systems. J. Agric. Food Chem. 38, 1642-1167 (1990).
316 Hollnagel, A. K., L. W. Degradation of oligosaccharides in nonenzymatic browning by formation of α-dicarbonyl compounds via a “Peeling Off” mechanism. J. Agric. Food Chem. 48, 6219-6226 (2000).
317 Yaylayan, V. A. Recent advances in the chemistry of Strecker degradation and Amadori rearrangement: Implications to aroma and color formation. Food Sci. Technol. 9, 1-6 (2003).
318 Bagdonaite, K., Derler, K. & Murkovic, M. Determination of acrylamide during roasting of coffee. J. Agric. Food Chem. 56, 6081-6086 (2008).
319 Guillén-Sans, R. & Guzmán-Chozas, M. The thiobarbituric acid (TBA) reaction in foods: A review. Crit. Rev. Food Sci. Nutr. 38, 315-330 (1998).
320 EuGH. Urteil v. 12.3.1987, Rs. 178/84, Slg. 1987, 1227. (1987).
321 Faltermeier, A., Waters, D., Becker, T., Arendt, E. K. & Gastl, M. Common wheat (Triticum aestivum L.) and its use as a brewing cereal - a review. J. Inst. Brew. 102, 1-15 (2014).
322 Teramoto, Y., Yoshida, S. & Ueda, S. Characteristics of a rice beer (zutho) and a yeast isolated from the fermented product in Nagaland, India. World J. Microbiol. Biotechnol. 18, 813-816 (2002).
323 Ceccaroni, D. et al. Specialty rice malt optimization and improvement of rice malt beer aspect and aroma. Food Sci. Technol. 99, 299-305 (2019).
324 Mayer, H., O., M., Regnicoli, G. F., Perretti, G. & Fantozzi, P. Production of a saccharifying rice malt for brewing using different rice varieties and malting parameters. J. Agric. Food Chem. 62, 5369-5377 (2014).
325 Mayer, H. et al. Development of an all rice malt beer: A gluten free alternative. Food Sci. Technol. 67, 67-73 (2016).
326 Bailly, R. et al. An economically viable way to produce beer from the maize malt. Chem. Eng. Trans. 38 (2014).
327 Santana, J. C. C., Araujo, S. A., Librantz, A. F. H. & Tambourgi, E. B. Optimization of corn malt drying by use of a genetic algorithm. Drying Technol. 28, 1236-1244 (2010).
328 Eneje, L. O. et al. Effect of steeping and germination time on malting performance of Nigerian white and yellow maize varieties. Process Biochem. 39, 1013-1016 (2004).

329 Zarnkow, M. & Back, W. Problems producing raw grain beers using high percentages of rice. Brauwelt 23, 50-53 (2005).
330 Hager, A.-S., Taylor, J. P., Waters, D. M. & Arendt, E. K. Gluten free beer - a review. Trends Food Sci. Technol. 36, 44-54 (2014).
331 Meußdoerffer, F. & Zarnkow, M. Starchy raw materials in Handbook of brewing: Processes, technology, markets (ed H. M. Esslinger) Ch. 2, (Wiley-VCH, 2009).
332 Zarnkow, M., Kessler, M., Burgerg, F., Kreisz, S. & Back, W. Gluten-free beer from malted cereals and pseudocereals in 30th EBC Congress. (Hans Carl).
333 Esslinger, H. M. Handbook of brewing: Processes, technology, markets. (Wiley-VCH, 2009).
334 O'Rourke, T. Adjuncts and their use in the brewing process. Brewers' Guardian 128, 32-36 (1999).
335 Zhuang, S. et al. Brewing with 100 % unmalted grains: barley, wheat, oat and rye. Eur. Food Res. Technol. 243, 447-454 (2016).
336 Le Van, V. M., Strehaiano, P., Nguyen, D. L. & Taillandier, P. Microbial protease or yeast extract-alternative additions for improvement of fermentation performance and quality of beer brewed with a high rice content. J. Am. Soc. Brew. Chem. 59, 10-16 (2001).
337 Schmitt, T. Zur Frage der Mitverwendung von Rohfrucht bei der Bierbereitung, PhD thesis, Dr. rer. nat., Technische Hochschule München (1961).
338 Schmitt, H. L., Kunder, H., Winkler, F.-J. & Binder, H. Möglichkeiten des Nachweises von Rohfrucht-Verwendung zur Bierbereitung durch Kohlenstoff-Isotopenbestimmung. Brauwiss. 33, 124-126 (1980).
339 Wagner, N., Krüger, E. & Rubach, K. Einfluss der Hochtemperaturwürzekochung auf den Nachweis von Rohfruchtzusätzen aus Mais und Reis. Monatsschr. Brauwiss. 4, 151-154 (1986).
340 Offizorz, P., Krüger, E. & Rubach, K. Immunochemischer Nachweis von Rohfrucht in Bier. Teil 2: Einsatz spezifischer Antiseren beim Nachweis von Mais und Reiszusätzen. Monatsschr. Brauwiss. 8, 319-323 (1988).
341 Iimure, T. & Sato, K. Beer proteomics analysis for beer quality control and malting barley breeding. Food Res. Int. 54, 1013-1020 (2012).
342 Fenz, R. Entwicklung einer HPLC-Methode zum Maisnachweis in Bier, PhD thesis, Dr. rer. nat., Technische Universität zu Braunschweig (1991).
343 Fenz, R., Ernst, L. & Galensa, R. Phenolcarbonsäuren und ihre Glycerinester in Maisgrits. Z. Lebensm. Unters. Forsch. 194, 252-258 (1992).
344 Pätzold, R. D. Untersuchungen an Bier, Rohfrüchten und Hopfen zum "Deutschen Reinheitsgebot" und zur Sortenunterscheidung mittels HPLC, PhD thesis, Dr. rer. nat., Technische Universität zu Braunschweig (1999).
345 Tsugawa, H. et al. MS-DIAL: Data independent MS/MS deconvolution for comprehensive metabolome analysis. Nat. Methods 12, 523-526 (2015).
346 Kai, K., Wakasa, K. & Miyagawa, H. Metabolism of indole-3-acetic acid in rice: Identification and characterization of N-β-D-glucopyranosyl indole-3-acetic acid and its conjugates. Phytochemistry 68, 2512-2522 (2007).
347 Lai, Z. et al. Identifying metabolites by integrating metabolome databases with mass spectrometry cheminformatics. Nat. Methods 15, 53-56 (2018).
348 Kinashi, H., Suzuki, Y., Takeuchi, S. & Kawarada, A. Possible metabolic intermediates from IAA to β-acid in rice bran. Agr. Biol. Chem. 40, 2465-2470 (1976).

349 Bonnington, L. S., Cercelo, D. & Knepper, T. P. Utilisation of electrospray time-of-flight mass spectrometry for solving complex fragmentation patterns: application to benzoxazinone derivatives. J. Mass Spectrom. 38, 1054-1066 (2003).

350 Wheelan, P., Zirrolli, J. A. & Murphy, R. C. Electrospray ionization and low energy tandem mass spectrometry of polyhydroxy unsaturated fatty acids. J. Am. Soc. Mass. Spectrom. 7, 140-149 (1996).

351 Ferreiros, N. et al. Lipoxin A4: Problems with its determination using reversed phase chromatography–tandem mass spectrometry and confirmation with chiral chromatography. Talanta 127, 82-87 (2014).

352 Roullier-Gall, C. et al. Integrating analytical resolutions in non-targeted wine metabolomics. Tetrahedron 71, 2983-2990 (2015).

353 Adams, K. L. & Wendel, J. F. Polyploidy and genome evolution in plants. Curr. Opin. Plant Biol. 8, 135-141 (2005).

354 Ahn, S. & Tanksley, S. D. Comparative linkage maps of the rice and maize genomes. PNAS 90, 7980-7984 (1993).

355 Van Deynze, A. E. et al. Comparative mapping in grasses. Oat relationships. Mol. Gen. Genet. 249, 349-356 (1995).

356 Nomura, T. et al. Structures of the three homoeologous loci of wheat benzoxazinone biosynthetic genes TaBx3 and TaBx4 and characterization of their promoter sequences. Theor. Appl. Genet., 373-381 (2008).

357 Koistinen, V. M. et al. Side-stream products of malting: a neglected source of phytochemicals. NPJ Sci. Food 4, 1-21 (2020).

358 Mogensen, B. B., Krongaard, T., Mathiassen, S. K. & Kudsk, P. Quantification of benzoxazinone derivatives in wheat (Triticum aestivum) varieties grown under contrasting conditions in Denmark. J. Agric. Food Chem. 54, 1023-1030 (2006).

359 Tang, Y., Zhu, Y. & Sang, S. A novel LC-MS based targeted metabolomic approach to study the biomarkers of food intake. Mol. Nutr. Food Res. 64, 1-13 (2020).

360 Liu, L. et al. Activation of Big Grain1 significantly improves grain size by regulating auxin transport in rice. PNAS 112, 11102-11107 (2015).

361 Ljung, K., Bhalerao, R. P. & Sandberg, G. Sites and homeostatic control of auxin biosynthesis in Arabidopsis during vegetative growth. Plant J. 28, 465-474 (2001).

362 McGovern, P. E. Ancient Brews. Rediscovered and re-created. Reprint edn, (WW Norton & Co., 2018).

363 Shalaby, N. et al. The Lost Papers: Rewriting the Narrative of Early Egyptology with the Abydos Temple Paper Archive, <https://www.arce.org/abydos-paper-archive> accessed

364 Pasteur, L. Études sur le vin ses maladies, causes qui le provoquent. Procédés nouveaux pour le conserver et pour le vieillir in Œuvres de Pasteur (ed V.-R. Pasteur) Ch. Études sur le vinaigre et sur le vin, 352 (Masson, 1924).

365 McGovern, P. E., Hartung, U., Badler, V. R., SGlusker, D. L. & Exner, L. J. The beginnings of winemaking and viniculture in the ancient Near East and Egypt. Expedition 39, 3-21 (1997).

366 McGovern, P. E. et al. Beginning of viniculture in France. PNAS 110, 10147-10152 (2013).

367 Ault, R. G. Spoilage bacteria in brewing - a review. J. Inst. Brew. 71, 376-391 (1965).

368 Walther, A., Hasselbart, A. & Wendland, J. Genome Sequence of Saccharomyces carlsbergensis, the World's First Pure Culture Lager Yeast. G3 (Bethesda) 4, 783-793 (2014).
369 Walther, A., Ravasio, D., Qin, F., Wendland, J. & Meier, S. Development of brewing science in (and since) the late 19th century: Molecular profiles of 110–130 year old beers. Food Chem. 183, 227-234 (2015).
370 Jeandet, P. et al. Chemical messages in 170-year-old champagne bottles from the Baltic Sea: Revealing tastes from the past. PNAS 112, 5893-5898 (2015).
371 Roullier-Gall, C., Heinzmann, S. S., Garcia, J.-P., Schmitt-Kopplin, P. & Gougeon, R. D. Chemical messages from an ancient buried bottle: metabolomics for wine archeochemistry. npj Science of Food 1 (2017).
372 Scholtes, C., Nizet, S. & Collin, S. How sotolon can impart a Madeira off-flavor to aged beers. J. Agric. Food Chem. 53, 2886-2892 (2015).
373 Thausing, J. E. Die Theorie und Praxis der Malzbereitung und Bierfabrikation. 946 (Gebhardt's, 1888).
374 Delchier, N. et al. Thermal degradation of folates under varying oxygen conditions. Food Chem. 165, 85-91 (2014).
375 Pferdmenges, L. E. et al. Characterization of the nutrient composition of German beer styles for the German nutrient database. J. Food Compos. Anal. (2021, accepted manuscript).
376 Thomas, K., Ironside, K., Clark, L. & Bingle, L. Preliminary microbiological and chemical analysis of two historical stock ales from Victorian and Edwardian brewing. J. Inst. Brew. 127 (2021).
377 Hutzler, M. Yeast biodiversity of traditional and modern hop beer fermentations and their targeted expansion via developed yeast hunting Methods, Habilitation, Habilitation Thesis, Technical University Berlin (2021).
378 Enzinger, L. E. Apparat mit Filterböden aus Papier zum Filtrieren von trüben Flüssigkeiten. Germany patent (1879).
379 Peterson, B. O., Nilsson, M. B., M., Hindsgaul, O. & Meier, S. 1H NMR spectroscopy for profiling complex carbohydrate mixtures in non-fractionated beer. Food Chem. 150, 65-72 (2014).
380 Avila, M. A., Garcia-Trevijano, E. R., Lu, S. C., Corrales, F. J. & Mato, J. M. Methylthioadenosine. Int. J. Biochem. Cell Biol. 36, 2125-2130 (2004).
381 Norris, F. W. Nicotinic acid in brewing materials. J. Inst. Brew. 51, 38-38 (1945).
382 Barton-Wright, E. C. The microbiological assay of nicotinic acid in cereals and other products. Biochem. J. 38, 314-319 (1944).
383 Younger, M. & Harvey, E. H. Stability of added vitamins in beer. Food Res. 10, 397-400 (1945).
384 Stringer, W. J. Vitamins in beer. J. Inst. Brew. 51, 81-97 (1946).
385 Punčochářová, L., Pořízka, J., Diviš, P. & Štursa, V. Study of the influence of brewing water on selected analytes in beer. Potr. S. J. F. Sci. 13, 1-8 (2019).
386 Ward, C. M. & Trennerry, V. C. The determination of niacin in cereals, meat and selected foods by capillary electrophoresis and high performance liquid chromatography. Food Chem. 60, 667-674 (1997).
387 Davis, C. F., Laotee, S. & Sealetan, L. A study of some of the vitamin B complex factors in malted and unmalted barley and wheat of the 1941 crop. Cereal Chem. 20, 109-113 (1943).
388 Ball, G. F. M. Vitamins in Foods. 1st edn, (CRC Press, 2005).

389 Qureshi, A. A., Burger, W. C. & Prentice, N. Polyphenols and pyrazines in beer during aging. J. Am. Soc. Brew. Chem. 37, 161-163 (1978).
390 Vanderhaegen, B., Neven, H., Verachtert, H. & Derdelinckx, G. The chemistry of beer aging - a critical review. Food Chemistry 95, 357-381 (2006).
391 Saucier, C., Bourgeois, G., Vitry, C., Roux, D. & Glories, Y. Characterization of (+)-catechin-acetaldehyde polymers: a model for colloidal state of wine polyphenols. J. Agric. Food Chem. 45, 1045-1049 (1997).
392 Vanderhaegen, B., Delvaux, F., Daenen, L., Verachtert, H. & Delvaux, F. R. Aging characteristics of different beer types. Food Chem. 103, 404-412 (2007).
393 Narziss, L., Back, W., Gastl, M. & Zarnkow, M. Abriss der Bierbrauerei. Vol. 8th rev. and enl. edition (Wiley-VCH, 2017).
394 Simpson, R. F. Aroma and compositional changes in wine with oxidation, storage and ageing. Vitis 17, 274-287 (1978).
395 Viegas, O., Prucha, M., Gökmen, V. & Ferreira, I. M. P. L. V. O. Parameters affecting 5-hydroxymethylfurfural exposure from beer. Food Addit. Contam. 35, 1464-1471 (2018).
396 Madigan, D., Perez, A. & Clements, M. Furanic Aldehyde Analysis by HPLC as a Method to Determine Heat-Induced Flavor Damage to Beer. J. Am. Soc. Brew. Chem. 56, 146-151 (2018).
397 Malfliet, S. et al. Flavour instability of pale lager beers: Determination of analytical markers in relation to sensory ageing. J. Inst. Brew. 114, 180-192 (2008).
398 Meilgaard, M. C. Flavor chemistry of beer. II. Flavour and threshold of 239 aroma volatiles. Tech. Q. Master Brew. Assoc. Am. 12, 151-168 (1975).
399 Li, M., Yang, Z., Yang, M., Shan, L. & Dong, J. Determination of furfural in beer by high-performance liquid chromatography with solid-phase extraction. J. Inst. Brew. 115, 226-231 (2009).
400 Karbowiak, T. et al. Wine aging: a bottleneck story. NPJ Sci. Food 3, 1-14 (2019).
401 Jamieson, A. M. & Van Gheluwe, J. E. A. Identification of a compound responsible for cardboard flavor in beer. Proc. Am. Soc. Brew. Chem., 192-197 (1970).
402 Drost, B. W., van den Berg, R., Freijee, F. J. M., van der Velde, E. G. & Hollemans, M. Flavor Stability. J. Am. Soc. Brew. Chem. 48, 124-131 (1990).
403 Liégeois, C., Meurens, N., Badot, C. & Collin, S. Release of deuterated (E)-2-nonenal during beer aging from labeled precursors synthesized before boiling. J. Agric. Food Chem. 50, 7634-7638 (2002).
404 Lermusieau, G., Noël, S., Liégeois, C. & Collin, S. Nonoxidative mechanism for development of trans-2-nonenal in beer. J. Am. Soc. Brew. Chem. 57, 29-33 (1999).
405 Noël, S. et al. The use of Oxygen 18 in appraising the impact of oxidation process during beer storage. J. Inst. Brew. 105, 269-274 (1999).
406 Hashimoto, N. & Eshima, T. Oxidative degradation of isohumulones in relation to flavour stability of beer. J. Inst. Brew. 85, 136-140 (1979).
407 Williams, R. S. & Wagner, H. P. Contribution of hop bitter substances to beer staling mechanisms. J. Am. Soc. Brew. Chem. 37, 13-19 (1979).
408 Hashimoto, N. & Kuroiwa, Y. Proposed pathways for the formation of volatile aldehydes during storage of bottled beer. Proc. Am. Soc. Brew. Chem. 33, 104-111 (1975).

409 Intelmann, D. et al. Structures of storage-induced transformation products of the beer's bitter principles, revealed by sophisticated NMR spectroscopic and LC-MS techniques. Chem. Eur. J. 15, 13047-13058 (2009).
410 Dresel, M., Vogt, C., Dunkel, A. & Hofmann, T. The bitter chemodiversity of hops (Humulus lupulus L.). J. Agric. Food Chem. 64, 7789-7799 (2016).
411 Nikolantonaki, M. et al. Impact of Glutathione on Wines Oxidative Stability: A Combined Sensory and Metabolomic Study. Front. Chem. 6, 1-9 (2018).
412 Coghe, S., Benoot, K., Delvaux, F., Vanderhaegen, B. & Delvaux, F. R. Ferulic Acid Release and 4-Vinylguaiacol Formation during Brewing and Fermentation: Indications for Feruloyl Esterase Activity in Saccharomyces cerevisiae. J. Agric. Food Chem. 52, 602-608 (3004).
413 Meußdoerffer, F. G. A comprehensive history of beer brewing. (WILEY-VCH, 2009).
414 Mattner, W. 150 Jahre Barre Bräu 1842-1992. Eine Festschrift. Ch. 4, 10-11 (Ernst Barre Privatbrauerei, 1992).
415 Back, W. Colour Atlas and Handbook of Beverage Biology. (Hans Carl, 2006).
416 Back, W. Farbatlas und Handbuch der Getrankemikrobiologie. Vol. 2 (Hans Carl, 1994).
417 Brandl, A. Entwicklung und Optimierung von PCR-Methoden zur Detektion und Identifizierung von brauereirelevanten Mikroorganismen zur Routine-Anwendung in Brauereien, Dissertation, PhD, Technical University of Munich (2006).
418 Hutzler, M. Entwicklung und Optimierung von Methoden zur Identifizierung und Differenzierung von getränkerelevanten Hefen, Dissertation, PhD, Technical University of Munich (2009).
419 Hutzler, M. Getränkerelevante Hefen - Identifizierung und Differenzierung. (SVH, 2010).
420 Koob, J., Jacob, F., Wenning, M. & Hutzler, M. Lactobacillus cerevisiae sp. nov., isolated from a spoiled brewery sample. Int. J. Syst. Evol 76, 3452-3457 (2017).
421 Riedl, R., Goderbauer, P., Brandl, A., Jacob, F. & Hutzler, M. Bavarian wheat beer process, a special microbe habitat – cultivation, detection, biofilm formation characterization of selected lactic acid bacteria spoilers and hygiene indicators. BrewingScience 70, 39-50 (2017).
422 Riedl, R., Fütterer, J., Goderbauer, P., Jacob, F. & Hutzler, M. Combined yeast biofilm screening – characterization and validation of yeast related biofilms in a brewing environment with combined cultivation and specific real-time PCR screening of selected indicator species. J. Am. Soc. Brew. Chem. (2019).
423 Sampaio, J. P., Pontes, A., Libkind, D. & Hutzler, M. Taxonomy, diversity, and typing of brewing yeasts in Brewing Microbiology: Current Research, Omics and Microbial Ecology Ch. Chapter 2, (Horizon Press, 2017).
424 Schneiderbanger, J., Jacob, F. & Hutzler, M. Genotypic and phenotypic diversity of Lactobacillus rossiae isolated from beer. J. Appl. Microbiol. (2019).
425 Cavanagh, J. & Rance, M. Sensitivity Improvement in Isotropic Mixing (TOCSY) Experiments. J. Magn. Reson. 88, 72-85 (1990).
426 Sklenar, V., Piotto, M., Leppik, R. & Saudek, V. Gradient-tailored water suppression for 1H-15N HSQC experiments optimized to retain full sensitivity. J. Magn. Reson. 102, 241-245 (1993).

427 Piotto, M., Saudek, V. & Sklenar, V. Gradient-tailored excitation for single-quantum NMR spectroscopy of aqueous solutions. J. Biomol. NMR 2, 661-665 (1992).
428 Palmer, A. G., Cavanagh, J., Wright, P. E. & Rance, M. Sensitivity improvement in proton-detected two-dimensional heteronuclear correlation NMR spectroscopy. J. Magn. Reson. 93, 151-170 (1991).
429 Kay, L. E., Keifer, P. & Saarinen, T. Pure absorption gradient enhanced heteronuclear single quantum correlation spectroscopy with improved sensitivity. J. Am. Chem. Soc. 114, 10663-10665 (1992).
430 Schleucher, J. et al. A general enhancement scheme in heteronuclear multidimensional NMR employing pulsed field gradients. J. Biomol. NMR 4, 301-306 (1994).
431 Schieberle, P. The Carbon Module Labeling (CAMOLA) technique. A useful tool for identifying transient intermediates in the formation of Maillard-type target molecules. Ann. N.Y. Acad. Sci. 1043, 236-248 (2005).
432 Hemmler, D., Heinzmann, S., Wöhr, K., Schmitt-Kopplin, P. & Witting, M. Tandem HILIC-RP liquid chromatography for increased polarity coverage in food analysis. Electrophoresis 39, 1645-1653 (2018).
433 Bostan, I., Onofrei, M., Gavrilută, A. F., Toderas, C. & Lazăr, C. M. An integrated approach to current trends in organic food in the EU. Foods 8, 1-17 (2019).
434 Hempel, C. & Hamm, U. Local and/or organic: a study on consumer preferences for organic food and food from different origins. Int. J. Consum. Stud. 40, 732-741 (2016).
435 Mie, A. et al. Discrimination of conventional and organic white cabbage from a long-term field trial study using untargeted LC-MS-based metabolomics. Anal. Bioanal. Chem. 406, 2885-2897 (2014).
436 Cubero-Leon, E., De Rudder, O. & Maquet, A. Metabolomics for organic food authentication: Results from a long-term field study in carrots. Food Chem. 239, 760-770 (2018).
437 Kessler, N. et al. Learning to classify organic and conventional wheat – a machine learning driven approach using the MeltDB 2.0 metabolomics analysis platform. Front. bioeng. biotechnol. 3, 1-10 (2015).
438 Röhlig, R. M. & Engel, K.-H. Influence of the input system (conventional versus organic farming) on metabolite profiles of maize (Zea mays) kernels. J. Agric. Food Chem. 58, 3022-2030 (2010).
439 Mihailova, A. et al. High-resolution mass spectrometry-based metabolomics for the discrimination between organic and conventional crops: A review. Trends Food Sci. Technol. 110, 142-154 (2021).
440 Zörb, C., Langenkämper, G., Betsche, T., Niehaus, K. & Barsch, A. Metabolite Profiling of Wheat Grains (Triticum aestivum L.) from Organic and Conventional Agriculture. J. Agric. Food Chem. 54, 8301-8306 (2006).
441 Roullier-Gall, C. et al. Usage of FT-ICR-MS metabolomics for characterizing the chemical signatures of barrel-aged whisky. Front. Chem. 6, 1-11 (2018).
442 Hertkorn, N. et al. High-precision frequency measurements: indispensable tools at the core of the molecular-level analysis of complex systems. Anal. Bioanal. Chem. 389, 1311-1327 (2007).
443 Borremans, F., De Potter, M. & De Keukeleire, D. Carbon-13 NMR spectroscopy of hop bitter substances. Org. Magn. Reson. 7, 415-417 (1975).

444 Vogt, C. Strukturanalytische Studien zu bitteren, antimikrobiellen und schaumstabilisierenden Hopfeninhaltsstoffen und Oxidationsprodukten in Bier, PhD thesis, Dr. rer. nat., Technischen Universität München (2015).
445 Intelmann, D. Molekulare, psychophysikalische und rezeptorbasierte Studien zum Bittergeschmack von Bier, PhD thesis, Technical University of Munich (TUM) (2010).
446 Haseleu, G. Sensorische, strukturanalytische und quantitative Studien zu Bitterstoffen aus Hopfen (Humulus lupulus L.) und deren Beitrag zum Bittergeschmack von Bier, PhD thesis, Technical University of Munich (TUM) (2010).
447 Kowaka, M., Kokubo, E. & Kuroiwa, Y. New bitter substances of beer: lupoxes c and lupdoxes b. Proc. Am. Soc. Brew. Chem. 30, 42-46 (1972).
448 Hanhineva, K. et al. Qualitative characterization of benzoxazinoid derivatives in whole grain rye and wheat by LC-MS metabolite profiling. J. Agric. Food Chem. 59, 921-927 (2001).
449 Frommberger, M. unpublished.
450 Donhauser, S., Wagner, S. & Wagner, D. Zucker und Endvergärungsgradbestimmung mittels der HPLC. Monatsschr. Brauwiss. 43, 296-305 (1990).
451 Jacob, F. Collection of brewing analysis methods. (MEBAK, 2012).
452 Striegel, L., Chebib, S., Netzel, M. E. & Rychlik, M. Improved Stable Isotope Dilution Assay for Dietary Folates Using LC-MS/MS and Its Application to Strawberries. Front. Chem. 6, 1-10 (2018).

List of Tables

List of Figures

Figures 1.1 and 1.2 were created with adapted transcription and protein templates provided by BioRender.com. All figures were illustrated utilizing the inkscape vector graphic environment (Inkscape Community Projekt).

Curriculum Vitae

Stefan Alexander Pieczonka

stefan.pieczonka[at]tum.de

ACADEMIC AND PROFESSIONAL EDUCATION

11/2020 - today	Research Associate at the Chair of Analytical Food Chemistry, Technical University of Munich and at the Research Unit Analytical BioGeoChemistry, Helmholtz Munich.
11/2017 – 10/2020	PhD Candidate at the Chair of Analytical Food Chemistry, Technical University of Munich and at the Research Unit Analytical BioGeoChemistry, Helmholtz Munich.
10/2015 – 10/2017	Master of Science (M. Sc.) in Food Chemistry at the Technical University of Munich (TUM). Master's Thesis: "Molecular characterization of biomarkers in biotically stressed potatoes", Chair of Food Chemistry and Molecular Sensory Science, TUM, Freising.
10/2012 – 09/2015	Bachelor of Science (B. Sc.) in Food Chemistry at the Technical University of Munich (TUM).

Voluntary commitment, memberships and additional activities during the academic and professional education

04/2017 – today	Member of the Gesellschaft Deutscher Chemiker (GDCh).
11/2017 – today	Supervision of students‘ practical courses, research internships and Master’s theses.
11/2017 – 10/2020	Member of the Graduate School of the TUM School of Life Sciences.
04/2019 – 10/2019	Appointed external student assessor for the accreditation of the degree program Analytical and Bioanalytical Chemistry, Bachelor of Science (B. Sc.) and Master of Science (M. Sc.), at Aalen University.
10/2016 – 08/2017	Scientific assistant at the Faculty of Chemistry, tutor in undergraduate courses (General Food Chemistry I and II), Technical University of Munich.

AWARDS AND CERTIFICATES

2018	„Johannes B. Ortner Preis“ for outstanding academic work as a young scientist for the Master’s thesis.
2018	„Preis des Oberbügermeisters der Stadt Freising“ for the best Master’s thesis in the field of nutritional sciences within the TUM School of Life Sciences.
2017	Certificate “Quality Management in the Food Industry“ (DIN EN ISO 9001 and 22000), in the course of the lecture Quality Management, Technical University of Munich, by Dr. Gunter Fricke (Director Quality Management Nestlé Deutschland AG).